NRC·CNRC

Technical Report

Low to Zero-Emission Heavy Logistics Vehicle Feasibility Report

Prepared for: Department of National Defence Canada
Canadian Armed Forces
101 Colonel By Drive
Ottawa, Ontario K1A 0K2

Prepared by: Stephanie Girard[1], Nathan Rues[2], Christopher Rabbitt[1], David Chuang[1]

National Research Council of Canada
Automotive and Surface Transportation

March 23, 2026

Project: A1-026014

Report number: AST-2026-0012

[1] National Research Council of Canada
[2] Drive System Design

Change Control

Version	Date	Description	Authors
0.1	March 03, 2026	Initial draft report	Stephanie Girard, Nathan Rues, Christopher Rabbit, David Chuang
0.2	March 17, 2026	Revised draft	Stephanie Girard
1.0	March 23, 2026	Initial release	Stephanie Girard

Prepared by:

Girard, Stephanie Digitally signed by Girard, Stephanie
Date: 2026.03.26 09:47:10 -04'00'

Stephanie Girard, MASc., P. Eng.
Research Officer, Hydrogen Systems Engineer, NRC

Chuang, David Digitally signed by Chuang, David
Date: 2026.03.24 10:54:34 -05'00'

David Chuang
Research Council Officer, NRC

Rabbitt, Christopher Digitally signed by Rabbitt, Christopher
Date: 2026.03.24 09:34:16 -04'00'

Christopher Rabbitt, P. Eng.
Research Officer, Vehicle Systems Engineer, NRC

Nathan G Rues

Nathan Rues
Seniors Controls Engineer, DSD

Reviewed by:

Hussein, Hussein A Digitally signed by Hussein, Hussein A
DN: cn=Hussein, Hussein A, o=GC, ou=NRC-CNRC, email=hussein.hussein@cnrc-nrc.gc.ca
Date: 2026.03.26 09:56:54 -04'00'

Hussein A. Hussein, PhD., P. Eng.
Research Associate, Intelligent Transportation System, NRC

Approved by:

Poole, Gordon Digitally signed by Poole, Gordon
Date: 2026.03.26 14:02:56 -04'00'

Gordon Poole
Director R&D, Transportation Engineering Centre

NRC.CANADA.CA

Contributors and Affiliations

Further to the list of authors on the title page, who directly prepared this document, were additional contributors that provided supporting documentation or analysis that was pertinent in preparing this report. Table 1 is the full list of authors and supporting contributors to this project. Section 2.1 further describes the consultant support contributions.

Table 1: List of report contributors and their affiliations

Name	Affiliation
Stephanie Girard	National Research Council Canada
David Chuang	National Research Council Canada
Christopher Rabbitt	National Research Council Canada
David Poisson	National Research Council Canada
Nathan Rues	Drive System Design
Capt. Besmir Shurdha	Canadian Armed Forces
Tibor Bak	Bak Motors
Paul Smith	Plasma Kinetics
Stacey Smith	Plasma Kinetics
Jonathan Hall	MAHLE
Paul Etheridge	MAHLE
Mike Bassett	MAHLE
Dr. Godfrey Udeh	MAHLE
Dan Walmsley	ESOX Group
Neil Patterson	ESOX Group
Devan Roberts	ESOX Group
Henry Hodges	Nevada Automotive Test Center (NATC)
Ryan De Backere	General Dynamics Land Systems (GDLS)
Josh Underwood	General Dynamics Land Systems (GDLS)

Table of Contents

List of Tables

List of Figures

Foreword

In April 1924, the Canadian Defence Quarterly published an article titled “The Mechanicalization of Cavalry” written by Capt. E.L.M. (Tommy) Burns. Burns argued that the Canadian cavalry regiments should replace their horses with tanks suggesting that Canada would be well placed to give birth to the “new cavalry”. This idea faced immediate and fierce opposition from the cavalry officers at the time, which included an article written by Major George S. Patton in 1930, where he surmised that tanks could not replace horses due to complex logistics and poor cross-country performance. We now find ourselves a century after these arguments took place, and with the power of hindsight are facing another major paradigm shift that could even rival mechanization. This paradigm shift has been triggered by the war in Ukraine and the clear demonstration of the vulnerability of fossil fuel supply chains. While the complex logistics of mechanized warfare were recognized even in its infancy, today, the proliferation of sensors from satellites to individual people with cellphones, the advances of long-range precision fires and missiles, and the complete reliance of military forces on liquid fuels, have exacerbated these logistical challenges even further. The linear nature of fossil fuel supply chains, their reliance on critical infrastructure such as refineries, and their length which can range in the thousands of kilometers have turned fossil fuel supply chains into a tactical, operational, strategic, and political risk that can no longer be ignored. This risk is further exacerbated by the expansion of renewable energy sources, new platforms such as electric vehicles, and the constant pressure of environmental damage, which have all worked to reduce the demand for fossil fuels and therefore the number of refineries that can sustain military forces in large-scale combat operations. It is clear today that a military must have devise another way to sustain itself that does not rely on fossil fuels.

Under these new threats, hydrogen has emerged as a unique tool in the military toolbox to address the above problems. Unlike fossil fuels, hydrogen is extremely abundant and has multiple methods and feedstocks from which it can be produced. Unlike fossil fuels, which are a mix of different hydrocarbons, hydrogen exists as a single molecule, which would greatly alleviate the inter-operability requirements. And finally, hydrogen is a unique molecule that is highly energetic and can act as a logistics vector by transporting energy and water at the same time, as one kg of hydrogen is able to produce nine litres of water. Combining energy and water into a single molecule would provide a significant logistics advantage during military operations. However, to fully leverage hydrogen’s advantages, three major challenges must be overcome. First, the production of hydrogen must increase by a few orders of magnitude. Second, a safer storage system than gas or liquid needs to be identified so that it can be incorporated in operational platforms. Finally, more efficient hybrid powertrains must be created to overcome hydrogen’s much lower volumetric energy density. This feasibility study is an attempt to address the second and third problem by analyzing different hybrid power trains and determining if they would be capable of meeting operational requirements.

Capt. Besmir Shurdha
Project Director ACSV (DLR 3-2-2)
Canadian Army Headquarters / Directorate of Land Requirements
Canadian Armed Forces

1.0 Executive Summary

The purpose of this project was to begin with a baseline diesel-combustion military heavy logistics vehicle and evaluate the technical feasibility of changing the fuel supply to solid-state hydrogen, moving towards a hybrid electrified configuration, and additionally understand the implications to the overall powertrain mass and volume. Towards that end five vehicle concepts were proposed and analyzed. The concepts were (1) conventional H_2-internal combustion engine (ICE), (2) H_2-ICE parallel-hybrid, (3) H_2-ICE series-hybrid, (4) power dense fuel cell and (5) efficiency optimized fuel cell.

Prior to analyzing the vehicle concepts, a set of high-level vehicle requirements was established as well as two drive cycles; one a simplified flat-road cycle and the other modelled on a logistics vehicle mission profile. The high-level vehicle requirements presented the concept of peak, continuous and average power demand. Combustion engines and fuel cells can sustain power output continuously, while batteries provide shorter bursts of high power; creating trade-offs in system sizing and powertrain mass.

The logistics vehicle mission drive cycle was derived from aggregate real-world vehicle performance and validated by subject matter experts. The aim in using two such disparate drive cycles was to demonstrate the impact requirements and drive cycles have on vehicle components power rating, mass and volume. The average power demand of the flat-road cycle was higher than the logistics cycle. The flat-road cycle produced vehicles with larger engines, smaller batteries, larger fuel tanks and overall larger mass powertrains while the logistics drive cycle produced powertrains with smaller engines, larger batteries, smaller fuel tanks and overall smaller mass powertrains. Using “today” technology values, and the logistics drive cycle, even in a best-case scenario, the efficiency optimized fuel cell powertrain mass was still 200 kg greater than the diesel-baseline.

Two vehicle concepts, H_2-ICE series-hybrid and efficiency optimized fuel cell, were selected to extrapolate out their designs for tomorrow (~10 years) and future (~15 to 20 years) technology values. As the technologies evolve, and system efficiencies increase, and both volumetric and gravimetric power and energy densities improve, the two concepts were comparable or better than the diesel-ICE baseline. On-board hydrogen storage energy density and energy release penalty are the parameters which need the largest improvements. Hydrogen storage dominates the mass and volume of the concept powertrains, with battery size and efficiency assumptions also contributing significantly.

This project demonstrates that, depending on requirements and drive cycle, a heavy logistics hydrogen-fueled vehicle using today’s technology assumptions, can be designed to a mass of no more than 10% of the diesel-ICE baseline. A detailed design phase is recommended to refine these concepts further.

2.0 Introduction

Through the Greening Government Strategy, the government of Canada has signaled its intent for government operations emissions to be net-zero by 2050 [1]. Canada's National Safety and Security Fleet (NSSF) is composed of aircraft, marine vessels and tactical land vehicles operated by National Defence, the Royal Canadian Mounted Police (RCMP) and the Canadian Coast Guard, and their emissions are counted in the government of Canada operations. In 2024, Canada established interim objectives including that by 2040, the average net-emission intensity of all NSSF operations will be reduced by at least 50% on the path to net-zero emissions by 2050; this will be achieved through measures such as low-carbon fuels, low and zero-emission platforms, and permanent carbon dioxide removal [2]. Actions towards that end include transitioning 100% of the RCMP light duty fleet to zero-emission vehicle (ZEV) by 2035, improving marine and air energy efficiency through operational measures, switching to low-carbon fuels, and carbon removal of any remaining greenhouse gas emissions [2].

In the National Defence Climate and Sustainability Strategy 2023-2027, there is a commitment to reduce fleet emissions on land, which will include evaluating options to reduce emissions, such as fleet upgrades, alternative technologies, and improvements to training activities, all while maintaining operational effectiveness and commitments [3]. Decarbonization plans for the military marine and air fleets are to be finalized by 2024, with land fleets to follow by 2027. The Canadian Army, under Target 11, is tasked with drafting the Land Operational Fleet Decarbonization Plan by 2025 and finalizing it by 2027

Alongside the Greening Government Strategy, there is a project by the Canadian Armed Forces (CAF) to modernize the logistics vehicles through acquisition of new fleets of light and heavy logistics vehicles, trailers, vehicle modules, and armour protection kits [4]. These vehicles cover a range of types but can include light trucks, cargo/troop carriers, command post-light, as well as heavy load handling systems for delivering trailers and equipment [5].

This project focuses on the heavy load-handling system vehicle [6]. The overall vehicle is an 8x8 truck that is capable of transporting a 20-foot ISO container. Figure 1 is an example of a heavy-load truck, with a trailer connected, based on the Mercedes Benz Zetros platform by the Marshall Group [7]. In a joint venture, the Marshall Group and General Dynamics Land Systems (GDLS) were awarded the logistics vehicle modernization (LVM) project. The baseline vehicle powertrain is a diesel internal combustion (ICE) engine. Traditional diesel-ICE engines contribute to greenhouse gas (GHGs) emissions and are not classified as low- or zero-emission vehicles.

Figure 1: Photo of Marshall Group heavy-logistics truck [7]

At present, the majority of commercial military vehicles in Canada are based on gasoline-combustion or diesel-combustion engines. There are several low- to zero-emissions technologies, existing today, which may be suitable in the design and build of a heavy logistics military vehicle. As a first step towards the design of a low- to zero-emission heavy logistics vehicle, this project aims to perform a technical feasibility study to examine the heavy logistics vehicle mission profile, define the high-level vehicle requirements, assess available low- to zero-emission technologies (e.g., fuel cell, H_2-ICE), and evaluate fuel vehicle storage options (e.g., solid-state hydrogen) to work towards establishing a vehicle envelope and determine the appropriate sizing of major system components for a low- to zero-emissions heavy logistic military vehicle. Out of scope for this project is cost of manufacturing and fuel delivery; these are items which would need to be addressed by a follow-up study.

2.1 Consultant Support

This project was performed on a co-operative basis, whereby commercial industry technology experts were invited to attend monthly progress meetings and asked to provide expertise for their respective technologies. Drive System Design (DSD) and MAHLE were contracted through the NRC, while Bak Motors / Plasma Kinetics and Donut Defence / ESOX group were contracted through DND.

DSD is an engineering consultant firm that specializes in the rapid development of next-generation electric and hybrid powertrains, internal combustion engines (ICE), and associated technologies. ZeBeyond, as a spinoff of DSD, has developed a modelling tool, Electrified Powertrain Optimization Process (ePOP), that synthesizes many powertrain combinations, comparing their cost, mass, range and efficiency, across multiple vehicles drive cycles to down-select the best powertrain candidates [8, 9]. Figure 2 provides a screenshot of the ePOP tool interface and example output screen. Further details about the ePOP tool and its deployment in this project can be found in Section 4.2.

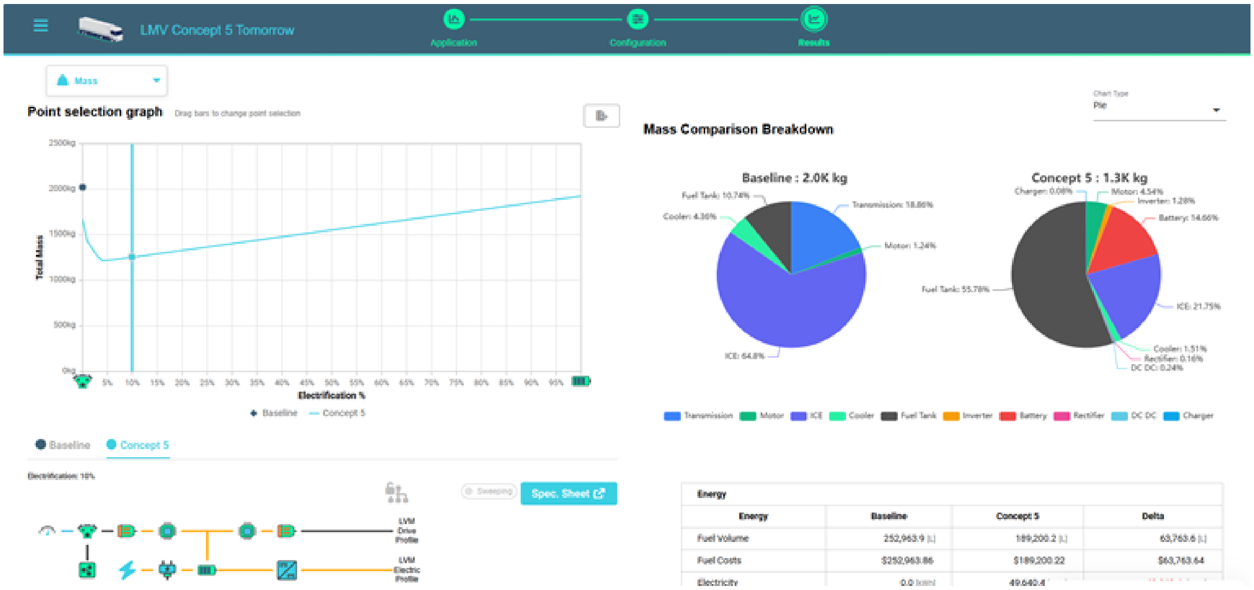

Figure 2: Screenshot of ePOP tool post-processing interface [9]

MAHLE is a leading global technology partner and supplier to the automotive industry with customers in both passenger car and commercial vehicle sectors. Founded in 1920, the technology group is working on the climate-neutral mobility of tomorrow, with a focus on the strategic areas of electrification and thermal management as well as further technologies to reduce CO_2 emissions, such as fuel cells or highly efficient, clean combustion engines that also operate on renewable fuels such as hydrogen. MAHLE has expertise in hydrogen combustion engines (H_2-ICE), having developed a powertrain for heavy-duty operation, along with project partners PHINIA, BorgWarner, Cambustion, and Hartridge. As of February 2025, MAHLE has entered the test-phase of Project Cavendish, a UK government backed initiative, in the MAHLE hydrogen test facility located in Northampton, England [10, 11]. Figure 3 is a heavy duty H_2-ICE truck from Project Cavendish. In addition to providing expertise with respect to H_2-ICE engines, MAHLE also examined the feasibility, through a system design and 1-D simulation, of a water recovery system from both a fuel cell powertrain and H_2-ICE engine. The full analysis is provided in Appendix A.

Figure 3: Heavy duty H_2-ICE truck from Project Cavendish [11]

Bak Motors is an engineering consulting firm in Ottawa, Canada, which has licensed solid-state hydrogen technology from Plasma Kinetics, for specialized applications such as the automotive industry and defence land systems. Plasma Kinetics has developed the idea for a solid-state hydrogen storage system, which stores hydrogen on light-activated nano-structured thin films. Hydrogen is adsorbed onto the thin films at atmospheric pressure and ambient temperature and then reeled onto rolls, and stored into canisters. To discharge the hydrogen, a system composed of take-up canister, tension rollers, motors, housing, lasers, radiator, pump, hose, coolant, wiring harness and controllers releases the hydrogen through light-activation to feed the hydrogen supply required by the hydrogen engine (e.g., fuel cell or H_2-ICE). A pilot hydrogen-release system has been conceived but not yet fabricated [12, 13]. Figure 4 depicts renderings for a hydrogen solid-state vehicle system. Figure 4a illustrates the take-up canister and main canisters, along with laser and H_2 manifold, while Figure 4b shows the hydrogen canister storage being installed on a heavy-duty truck. The Plasma Kinetics solid-state hydrogen system was used as a reference for this project to determine a theoretical on-board hydrogen delivery system volumetric and gravimetric energy density, as well as release power.

a) b)

Figure 4: Hydrogen solid-state storage visual renderings [13]
a) Take-up, main canister and roller, and b) Vehicle hydrogen storage placement and installation

Donut Motor, now part of the ESOX group, focuses on in-wheel motor design for electric vehicles that combines maximum torque and power density with a lightweight design, eliminating the need for traditional drivetrain components [14]. The ESOX group's focus is on re-defining electric mobility for the defence industry, examples of their work include examining fleet electrification, enhancing mission-critical artificial intelligence (AI) capabilities, or simplifying vehicle architectures for greater efficiency [15]. Figure 5a and Figure 5b shows Donut Lab 21-inch in-wheel hub motor designs, for automotive and heavy-trucking applications, respectively. For this project, Donut Motor provided generic power density, as a function of volume and weight, as well as motor efficiency, as inputs for the analysis.

a)

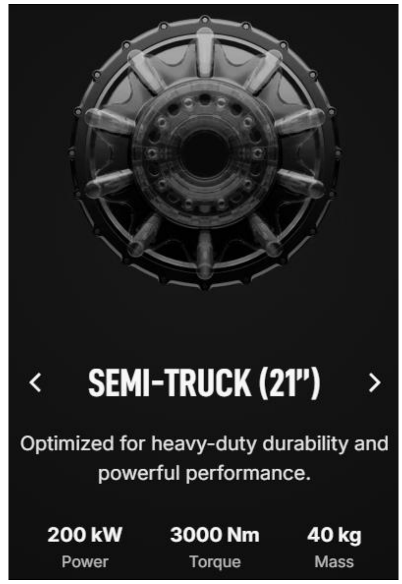

b)

Figure 5: Example Donut Lab motors and their fundamental performance
a) Automotive 21-inch design focusing on high performance, low mass, and b) Semi-truck 21-inch design designed for durability and power.

Report section contributions from the consultants and partners are summarized in Table 2.

Table 2: Report section partner contributions

Contributor affiliation	Report sections
Drive System Design	Section 3.1, Section 4.0, Section 5.0
Canadian Armed Forces	Section 3.3, Section 4.1
Bak Motors	Section 3.7, Section 4.3, Appendix B
Plasma Kinetics	Section 3.7, Section 4.3, Appendix B
MAHLE	Section 3.3, Section 3.4, Section 3.6, Section 4.3, Appendix A
ESOX Group	Section 3.9, Section 4.3, Appendix C
Nevada Automotive Test Center (NATC)	Section 4.1.3
General Dynamics Land Systems (GDLS)	Section 3.3, Section 4.1.3

3.0 Background

In this section, background information is provided as it relates to hybrid powertrain architecture design, fundamental vehicle design, as well as highlighting the various vehicle technologies examined for this study.

3.1 Hybrid Powertrain Architecture

In a conventional internal combustion engine (ICE) vehicle, the propulsion energy is provided solely by the engine. With an electric hybrid architecture, the tractive power may come from the engine (ICE or fuel cell or other), the batteries, or a combination thereof. In a series hybrid configuration, the internal combustion engine is coupled to a generator rather than the drivetrain, and mechanical propulsion is supplied exclusively by the electric motor. In a parallel hybrid configuration, the internal combustion engine and electric motor are both mechanically linked to the drivetrain, enabling either or both power sources to provide torque to the wheels [16].

A conventional ICE drives the wheels through the transmission. The technology is mature, simple, and low cost. Overall, it has lower efficiency than hybrids and does not offer the benefit of recovery energy through regenerative braking. In a series hybrid architecture, the engine drives a generator to produce electricity, which powers an electric motor that drives the wheels. In this way, the engine can run at optimal efficiency, no multi-gear transmission is needed. However, since additional components are required, generator and motor, it can be heavier and more expensive. In a parallel hybrid architecture, both the engine and the electric motor can drive the wheels directly (mechanically connected). This architecture is a mix between conventional and series-hybrid; it can improve acceleration and fuel efficiency during acceleration by sharing the load between the engine and the electric motors, while still recovering energy through regenerative braking. Drawbacks to this architecture are its higher complexity mechanically and more complicated control strategy.

There is also a trade-off in efficiency, whereas a conventional ICE architecture typically has moderate and low efficiency under highway and city driving conditions respectively, a series hybrid has moderate and high efficiency under highway and city driving conditions, and a parallel hybrid has high and moderate efficiency under highway and city driving conditions. In a study performed by Ganji et al., two drive cycles were modeled, highway fuel economy driving schedule (HWFET) and urban dynamometer driving cycle (UDDS), for different powertrain configurations (conventional, series-hybrid, parallel-hybrid, series-parallel hybrid) and their powertrain bidirectional efficiency was compared. The conventional vehicle had the lowest efficiency under both drive cycles, while the series-hybrid performed well for the urban drive cycle and the parallel-hybrid performed better than the conventional under both cycles, but not as high as the series-hybrid [17].

Figure 6 illustrates a simplified block diagram for the major systems in a conventional ICE powertrain. The fuel tank supplies fuel to the engine. The cooler provides cooling to the engine. The motor provides start-up electricity to crank the engine. The transmission transfers and modulates engine power to the wheels by adjusting torque and speed to suit driving conditions. Overall, it is a very simple architecture. This block diagram represents the architecture for the baseline diesel ICE vehicle as well as the hydrogen-ICE (H_2-ICE) vehicle.

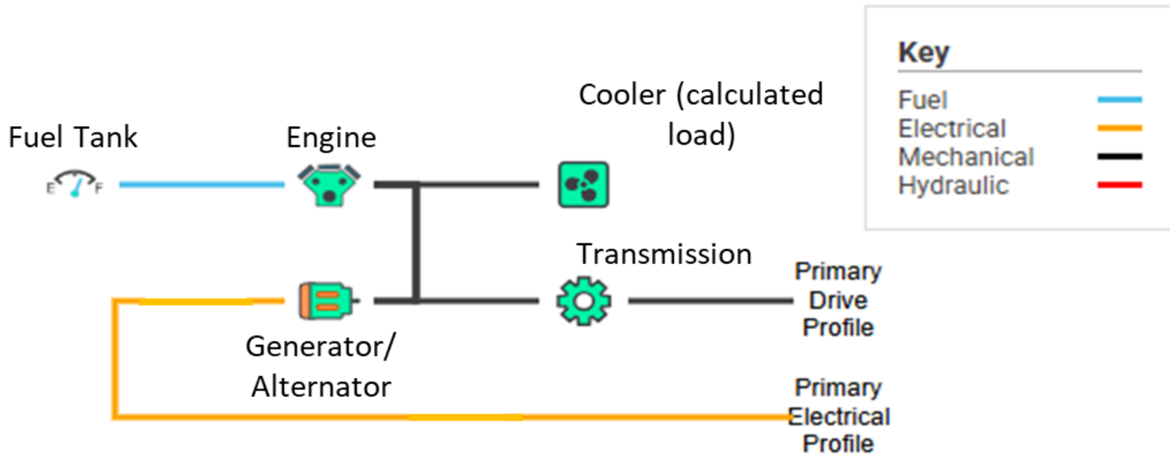

Figure 6: Conventional ICE powertrain architecture

Figure 7 illustrates a block diagram for a parallel-hybrid architecture. In a parallel architecture, both the electric motor and the engine can provide tractive power. There is additional complexity in this architecture, as compared with conventional, including the addition of an on-board charger, battery, inverter, and DC-DC converter. Batteries can be charged by operating the motor as a generator by the engine or through an electrical outlet. This block diagram represents the architecture of the H_2-ICE parallel-hybrid vehicle.

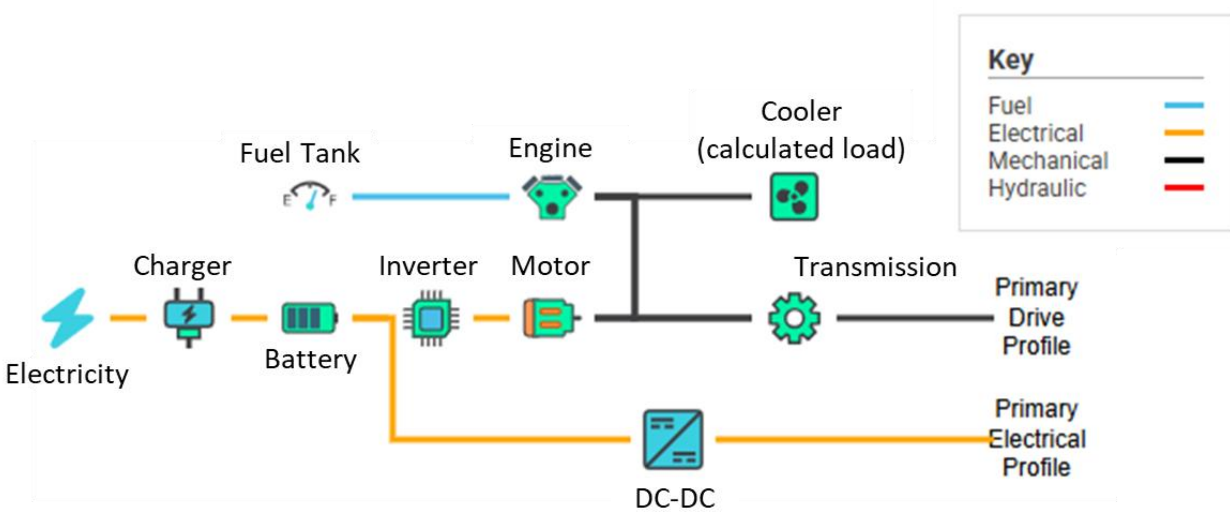

Figure 7: Parallel-hybrid plug-in powertrain architecture

Figure 8 illustrates a block diagram for a series-hybrid architecture. In the series architecture, the engine is mechanically de-coupled from the wheels. Here, the engine (H_2-ICE or fuel cell) powers a generator, which operates the motor. The motor can be powered by the engine alone, the battery alone, or a combination of both, in high power demand scenarios. This block diagram represents the architecture of H_2-ICE series-hybrid and the fuel cell vehicle concepts. In the case of the fuel cell vehicle, there is no generator between the engine and the rectifier; the energy output from the fuel cell is direct-current.

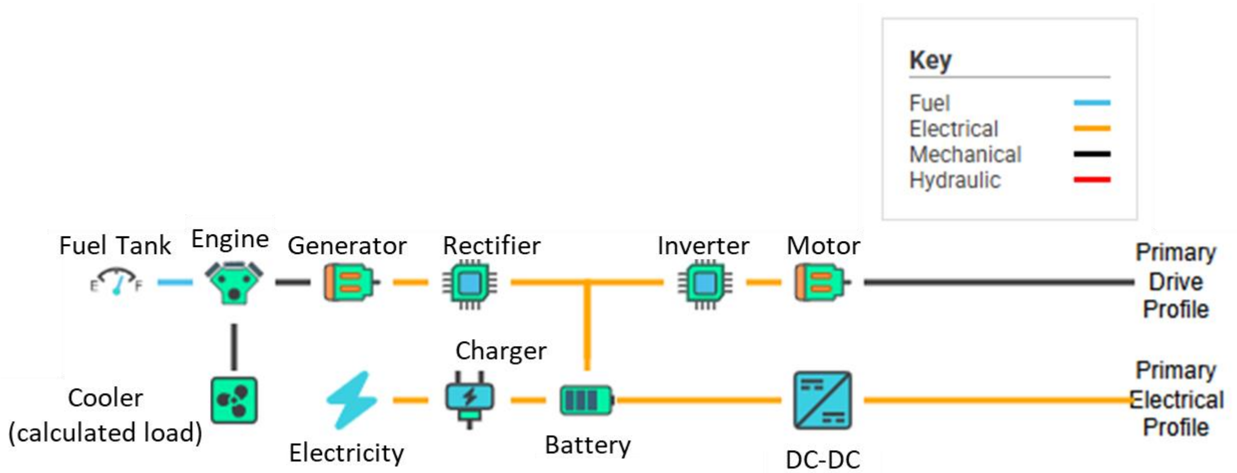

Figure 8: Series-hybrid plug-in powertrain architecture

3.2 Vehicle Model

The tractive force of a vehicle, that is the force at the wheels, is a sum of forces; including rolling resistance (Fr), aerodynamic drag (Fd), climbing resistance (Fg), and the acceleration force (Fa). The equation to describe tractive vehicle force (Fte) can be found in Equation 1:

$$Fte = Fr + Fd + Fg + Fa \qquad \text{Equation 1}$$

Rolling resistance is the force required to keep a wheel or tire rolling at a constant speed on a surface. Softer surfaces, like mud or sand, have higher rolling resistance. Rolling resistance can change with road surface, tire inflation pressure, vehicle speed, and vehicle load. Aerodynamic drag force is the force from the air in front of the vehicle opposing motion. It can depend on air density, coefficient of drag, frontal area of the vehicle, and vehicle speed. Climbing resistance force is the force required to overcome gravity when a vehicle is climbing up a slope with angle ϴ; the steeper the grade, the higher the climbing force. The force due to acceleration is the force required to accelerate the vehicle, based on Newton's second law; force is mass times acceleration. Figure 9 is an illustration of a vehicle model with the various forces described.

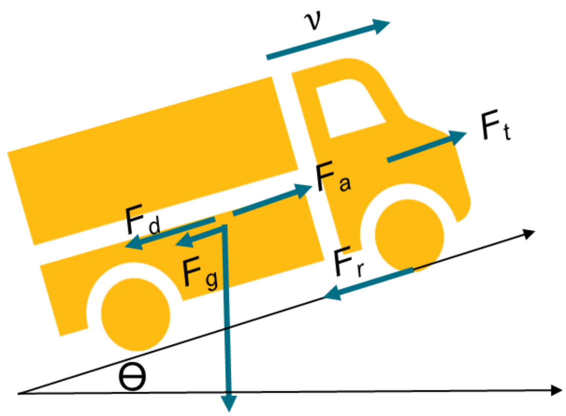

Figure 9: Vehicle model with acting forces

To determine component sizes for each powertrain system, first the high-level vehicle requirements and drive cycle must be defined. Typical vehicle requirements might include initial acceleration, average speed, maximum speed, gradeability, driving range, etc. A drive cycle is a vehicle speed versus time profile for verifying vehicle performance. There are standard drive cycles which exist to evaluate all different types of vehicles. Different drive cycles will elicit different performance, fuel economy and emissions for the same vehicle. Figure 10 illustrates an example of a drive cycle derived by MIT researchers based on analyzing 58,000 miles of real-world data for Class 8 long-haul trucking in the United States [18]. Combined with fundamental parameters, such as vehicle mass, rolling friction, frontal area, wheel radius, air density, etc., the drive cycle and the vehicle requirements can be used to derive overall vehicle power requirements. These vehicle power requirements can then be cascaded to individual components to determine component power and sizing. It’s important to include efficiency in component sizing as well.

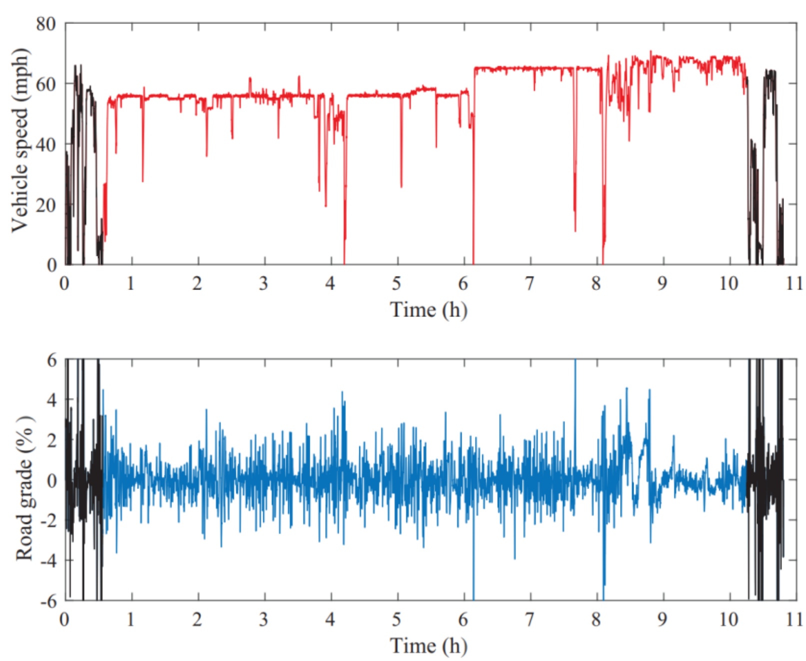

Figure 10: Example long-haul Class 8 drive cycle (USLHC8) [18]

When specifying vehicle requirements, it’s important to distinguish between the types of requirements; namely:

- peak,
- continuous, and
- average requirements.

A peak requirement would be a requirement that’s needed for only a short time (e.g., a rapid acceleration), a continuous requirement would be a requirement for a longer time (e.g., a 10-min dynamic hill climb), and an average requirement would be a requirement that a powertrain must meet over the course of an entire drive cycle (e.g., minimum highway cruise speed for 5-hrs). There is no common definition for a continuous requirement; they are defined for each project individually according to the vehicle’s needs.

Conventional ICE powertrains can produce peak power continually so long as fuel is available, whereas battery systems can produce peak power for short durations. ICE peak power is limited by the engine size, whereas battery electric peak power is determined by a combination of factors, including voltage, current, inverter size, electric motor(s) size, battery capacity, discharge rate (C-rate), and environmental temperature. This means that an electric powertrain can provide much higher peak power than traditional ICE for short durations but is not capable of sustaining the power because the peak power will drop as battery energy capacity is consumed. The other advantage with batteries is the ability to respond rapidly to increased or decreased power and torque demands, while ICE engines have longer response times. Understanding the vehicle operational drive cycle, gives an opportunity to downsize the vehicle engine and take advantage of this unique battery feature to meet all the drive cycle requirements. This highlights the criticality of determining the precise vehicle drive cycle. If improperly set, components may be oversized or undersized for the required application. In moving from traditional powertrain design to hybrid design, it’s important to understand technological limitations (e.g., battery energy density), as compared to diesel combustion, and look for opportunities to leverage other characteristics (e.g., greater energy conversion efficiency, short-term higher peak power output, reduced engine idling time during silent watch) to achieve the desired requirements.

3.3 Baseline Diesel-based Vehicle

The baseline vehicle for this study was taken to be the Mercedes-Benz Zetros, as selected through the ongoing Logistics Vehicle Modernization Project [4]. In particular, the 8x8 heavy variant was selected as the most energy intensive option; this is a four-axle vehicle with all eight wheels receiving motive power. This vehicle was chosen as the reference platform against which all the other configurations were measured. Figure 11 is a photo of a Mercedes-Benz Zetros 8x8 vehicle.

Figure 11: Mercedes-Benz Zetros 8x8 [19]

The vehicle's 6-cylinder heavy-duty diesel engine, producing 375 kW [20], is representative of a mature, stable technology, widely deployed in this type of application today. The drivetrain is likewise typical for vehicles of this type, consisting of an automatic gearbox with a hydrodynamic torque converter as part of a fully mechanical transmission driving all four axles [20]. Refuelling would be expected to take under 10 minutes. Again, this technology is mature, robust, and widely supported, with well supported supply chains. However, it does produce greenhouse gases, as well as other pollutants.

When armoured, the curb weight is expected to be approximately 22,000 kg [21]. Outfitting with standard equipment, crew, and cargo brings the operating weight up to nearly 38,000 kg, while the gross vehicle weight rating (GVWR) is over 40,000 kg [21].

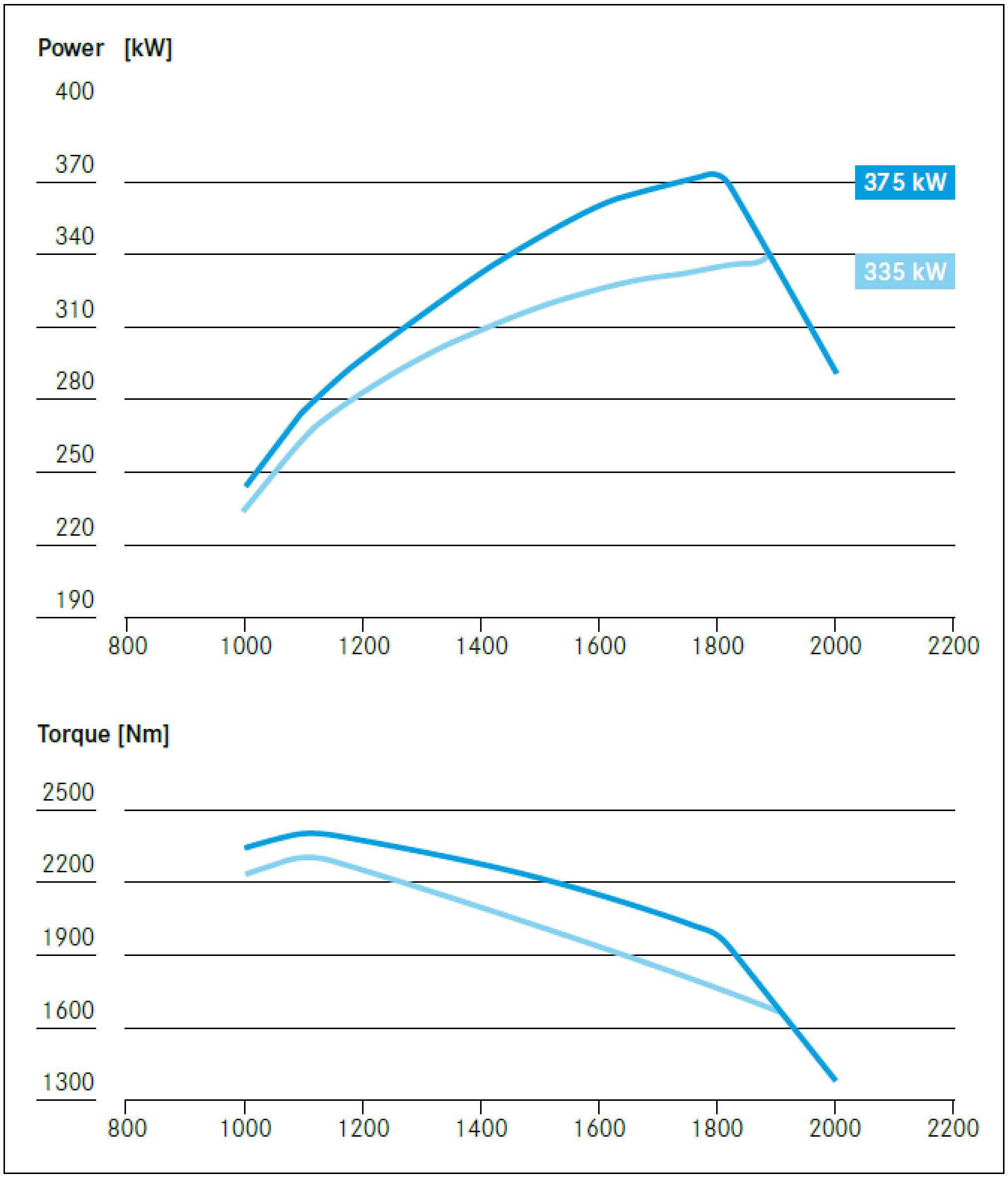

Figure 12: Power and torque versus engine speed for selected engine [22]

In common with all internal combustion engines, torque and power output varies strongly with engine speed; coupled with action of the gearbox, this results in the overall fuel efficiency being highly sensitive to the drive cycle, as is illustrated in Section 4.1 below. Figure 12 is a plot of power and torque as a function of engine speed; the light blue line is a 335 kW engine while the darker blue line is a 375 kW engine. Both are OM 460 EURO V model engines from Mercedes-Benz. Peak diesel efficiency was estimated to be 37%, based on engines employing similar technology [23] as shown in the fuel map in Figure 13. Figure 13 is based on a 12.6 L heavy duty diesel truck engine; it is a plot of engine pressure, and output power, as a function of engine speed; the contour lines are fuel flow rate. At 150 kW and 1500 rpm, the fuel consumption rate is 34 kg/hr. Based on the lower heating value of diesel (42.6 MJ/kg), this is a fuel flow power of 402 kW. The efficiency is calculated as 150 divided by 402; for a value of 37%. This efficiency implies a cooling requirement of approximately 236 kW, which is provided through a liquid cooling loop with a radiator and fan assembly, sized for continuous operation between -45°C and +50°C [20].

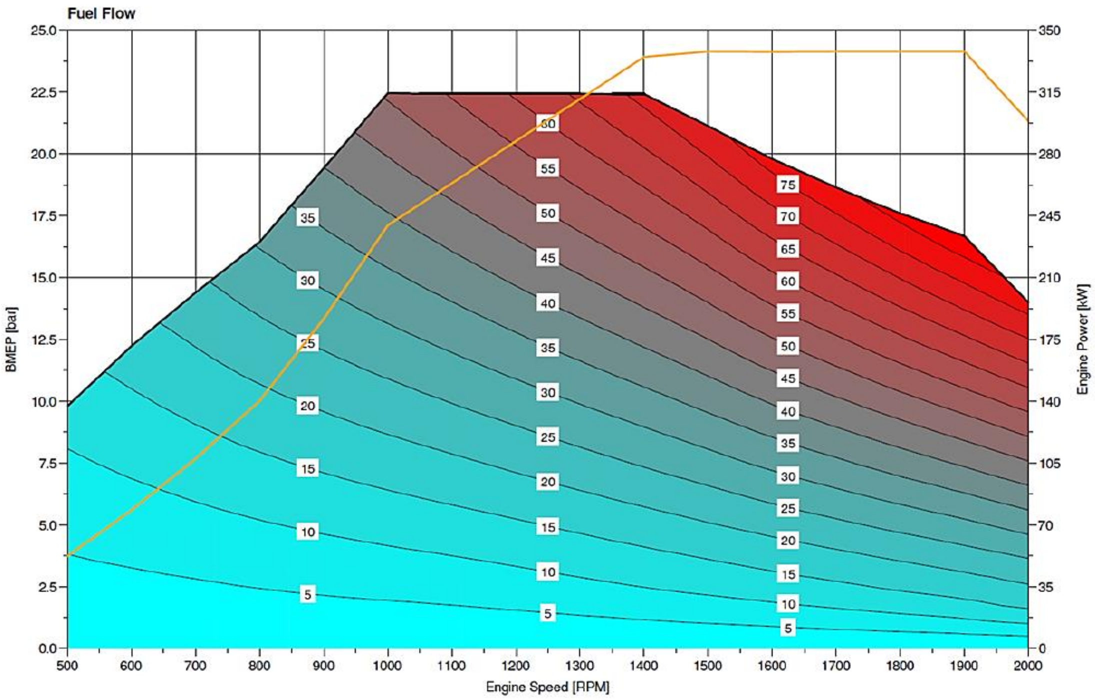

Figure 13: Engine speed, power, and fuel flow rate map for representative diesel engine [23]

These numbers all relate to engine output; like all powertrains, they are then affected by efficiency of the transmission and auxiliary power systems, which were assumed to be 91% and 70% efficient respectively [23]. The continuous driving cycle profile, discussed later on in Section 4.1.2, can take advantage of the ICE's optimal operating band by reducing throttling, idling, and hard acceleration which provides a good energy conversion efficiency. The logistics vehicle mission profile, presented in Section 4.1.3, which has low, medium, high-speed driving; cross-country, trails, secondary and primary roads, as well as an idling period, consistently pushes the engine efficiency outside of its optimal band, and represents the critical area for improvement using a hybrid system.

3.4 H_2-ICE

The hydrogen internal combustion engine (H_2-ICE) represents a possible near-term solution to decarbonization of heavy-duty vehicles, adapting existing diesel platforms to use hydrogen as a fuel for combustion. While hydrogen has very different physical and chemical properties to the diesel fuel it is replacing, the overall mode of operation remains the same as the baseline case, and therefore all the components outside of the engine itself and the fuel storage remain largely as previously described.

MAHLE Powertrain (MAHLE) estimated properties of a H_2-ICE based on a version of the engine used in the baseline vehicle modified to run on hydrogen [23]. The current technology is assumed to be port injection, with future technology taken as high-pressure direct injection (HPDI). In 2024, Cummins demonstrated an experimental engine achieving peak efficiency of 41% [24], with a recent review finding efficiencies in the 42%-45% range [25], both of which align in the estimate provided by MAHLE. At the efficiency targeted, performance is slightly below the diesel baseline, which is again consistent with finding from literature [26]. As in the baseline case, power, torque, and efficiency are strongly affected by engine speed, with the impacts of drivetrain and auxiliary power loads being largely unchanged. Figure 14 is a plot of brake mean effective pressure (BMEP) as a function of engine speed with efficiency contours for H_2-ICE.

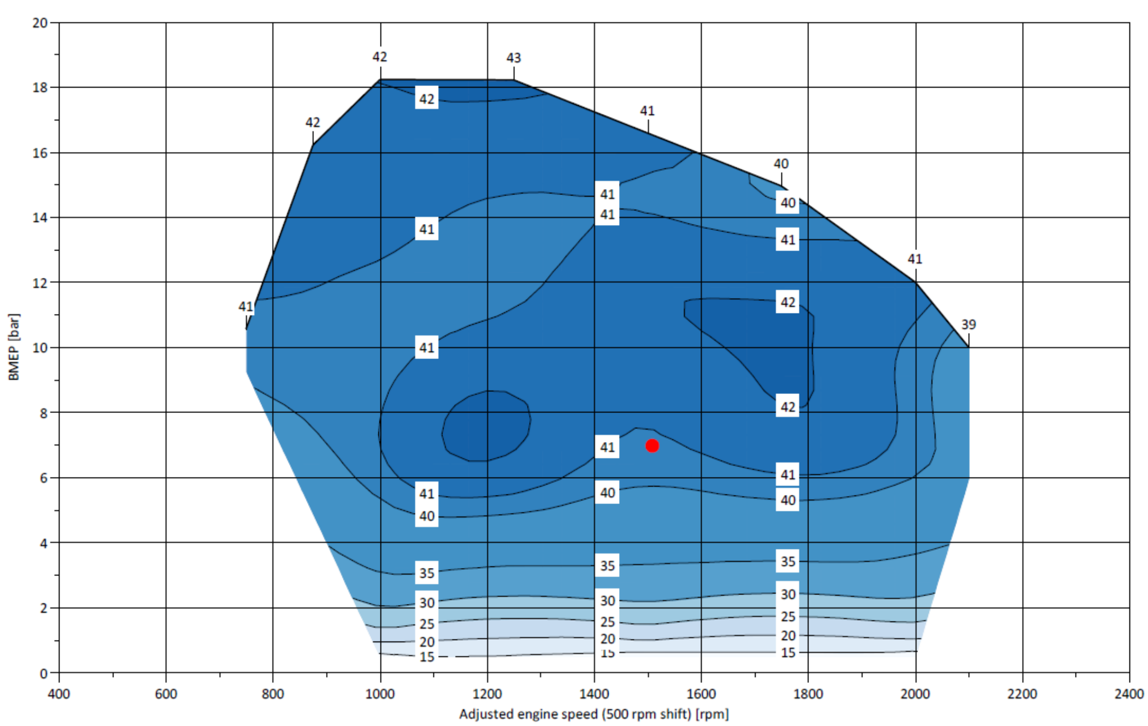

Figure 14: Brake mean effective pressure (BMEP) vs. engine speed for H_2-ICE with eff. contours [23]

While the use of hydrogen eliminates the carbon dioxide and particulate emissions from diesel combustion, nitrogen oxides are still emitted due to the high temperatures involved, albeit at lower intensity [24].

The hydrogen combustion engine also suffers from the lower volumetric energy density of hydrogen fuel which requires larger cylinder sizes to generate the same amount of power as diesel. Hydrogen's higher combustion temperature, poor lubricity (ability to reduce friction between surfaces in relative motion), and small molecular size create challenges for pre-ignition and knock. Thermal management for hydrogen ICE may require injecting produced water into pistons during combustion to reduce temperature and NOx production, which adds complexity to the system [27].

3.5 Hydrogen Fuel Cells

Hydrogen fuel cell systems transform chemical energy into electrical energy through the hydrogen oxidation reaction at the anode and the oxygen reduction reaction at the cathode to produce water. The inputs to a fuel cell system are hydrogen, oxygen (or typically air), water or glycol for cooling, and a small voltage and current on start-up. The fuel cell system includes the fuel cell stack, the cathode circuit for the air, including air compressor or turbo-pump, and humidifier, the coolant circuit including coolant pump, radiator fans, and heat exchanger, and the anode system includes the interface to the fuel cell, an injector, ejector, and possibly a hydrogen recirculation blower. Figure 15 is an illustration of a fuel cell system. Not illustrated here is the battery power required to start-up the fuel cell system; namely the air compressor and the coolant pump and heater, prior to the fuel cell system exporting power. This input power is captured as a reduced system efficiency for the fuel cell system. The powertrain configuration for the fuel cell system must always be a series-hybrid design with a battery for specifically this reason; the battery size depends on this required start-up power as well as the drive cycle requirements.

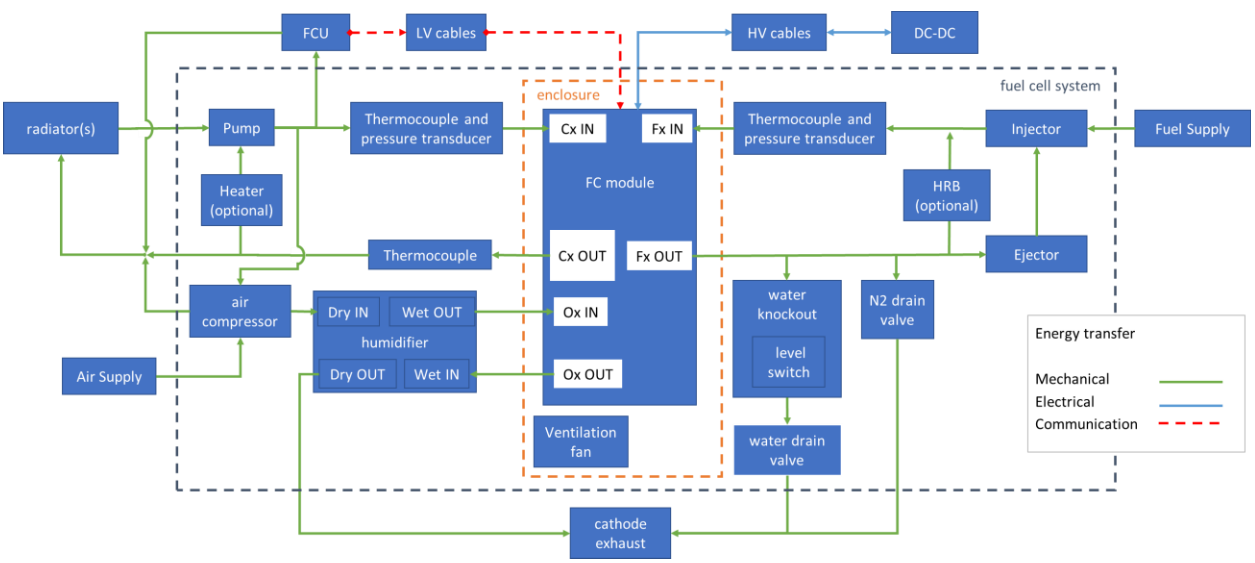

Figure 15: Boundary diagram for fuel cell system

The fuel cell stack consists of repeated layers of bipolar plates and membrane electrode frame assembly (MEFA). Hydrogen enters the anode, the anode catalyst on the MEFA causes a hydrogen oxidation reaction separating the hydrogen into a hydrogen proton and electron. The hydrogen proton travels through the MEFA while the electron travels through the conductive plate to supply the load. On the cathode side, the air enters the cathode and combines with the hydrogen proton and the electron from the neighboring plate, to produce water and waste heat. Figure 16 demonstrates the cross-section of a single anode plate, MEFA, and cathode plate. A single cell produces between about 0.65 V to 1.2 V of voltage, at different currents. These cells are stacked together to increase power to an overall desired level.

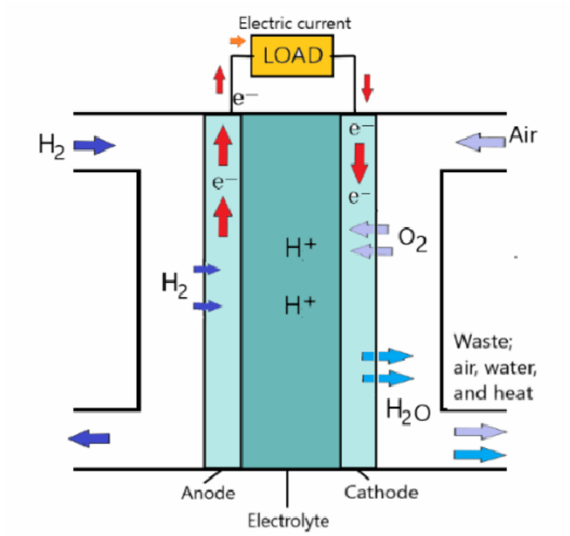

Figure 16: Working principle of hydrogen fuel cell stack [28]

Similar, to conventional combustion engines, a fuel cell can operate at continuous rated power so long as fuel is being supplied. Hydrogen fuel cell system efficiency varies at different load points. At rated power, typically 0.65 V/cell, the system efficiency is about 40%; whereas at lower power, the system efficiency can be as high as 60%. This is because of the voltage-current relationship of the fuel cell. At low load, or low current, the voltage is high, the losses are minimal and efficiency is highest but power output is low. Whereas at high current, the voltage drops due to losses, efficiency is lower but power output is highest. A fuel cell experiences activation losses, losses from the electrochemical reaction, ohmic losses, these are resistive losses, and mass transport losses, these are losses due to reactants not being able to reach reactants sites. Activation losses dominate low current density, ohmic losses occur linearly throughout the polarization curve, and mass transport losses occur most significantly at high loads. Further, at higher loads, more air flow is required to supply the fuel cell reaction, the pump is operated at higher speed, higher power, and therefore net efficiency decreases. Figure 17 is a plot of fuel cell stack and system output power, as a function of efficiency, for the Toyota Mirai vehicle as tested by Argonne National Laboratory [29]. The Toyota Mirai is a sedan-sized fuel cell vehicle. The fuel cell stack design is a proton exchange membrane (PEM) type with one stack of 114 kW size, test weight was 4,250 lbs. Nominal hydrogen tank pressure is 10,000 PSI with 5 kg of hydrogen storage. From the plot, it can be observed that at rated power, 110 kW, the system efficiency is 40% while at 25% of power, 27.5 kW, the system efficiency is much higher, at 58%. Compared with the logistics vehicle, the Mirai will exhibit lower volumetric and gravimetric energy densities for both the fuel cell engine and the hydrogen storage system; this is because, in the Mirai, the balance-of-plant components occupy a greater fraction of the total system volume and mass relative to the electrochemically active components, whereas in higher-power fuel cell systems, the auxiliary subsystem scales less significantly than the stack itself, resulting in higher overall energy density. However, the efficiency relationship will hold true between the Mirai and the logistics vehicle.

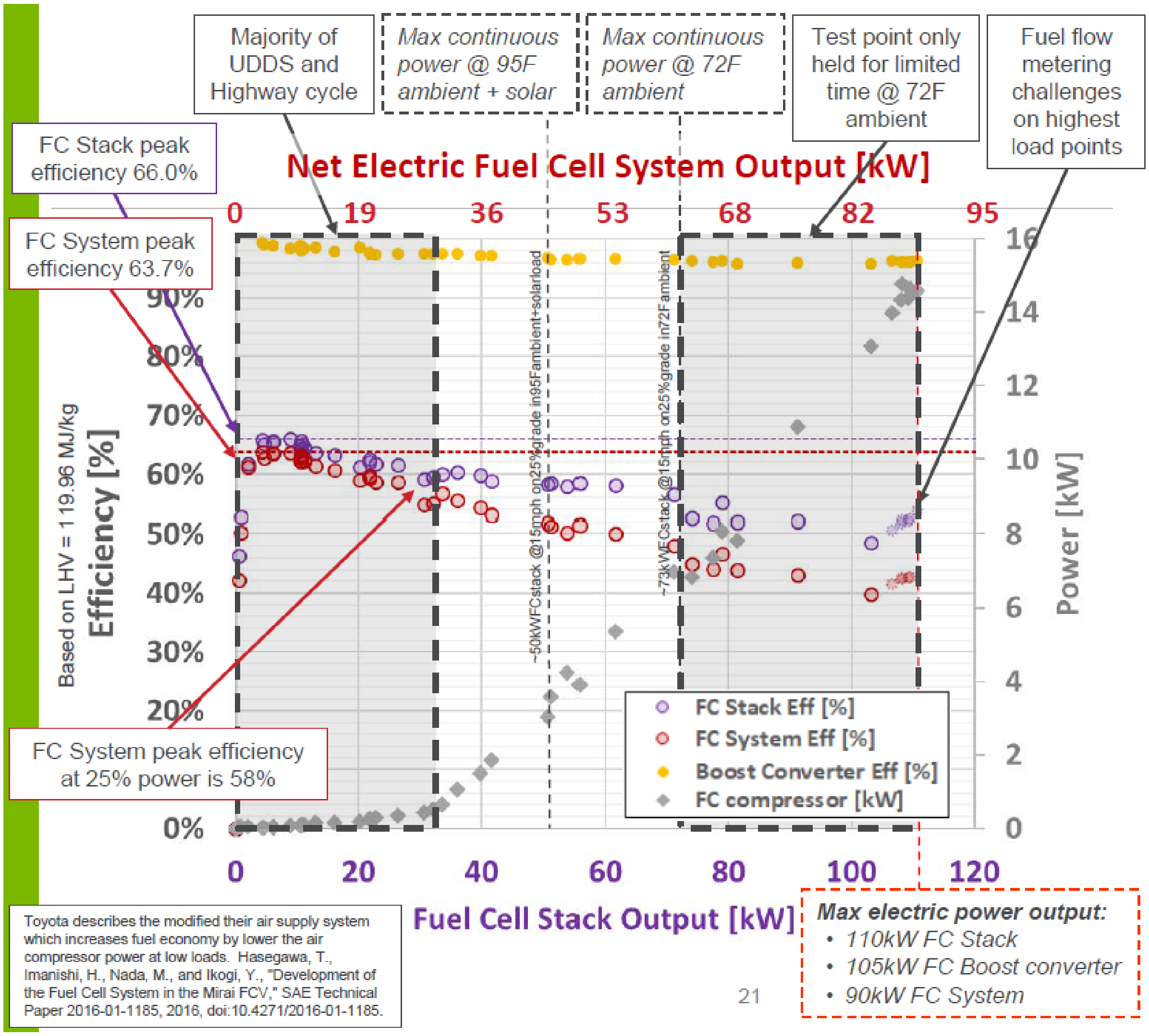

Figure 17: Fuel cell stack and system output power vs. efficiency for Toyota Mirai 2017 [29]

Some of the challenges with hydrogen fuel cell systems as vehicle powertrain technologies include the availability and accessibility of hydrogen fuel, the lower system efficiency (as compared with battery technology but higher than traditional combustion engines), the maturity of the technology, the low volumetric power density (kW/L), the potential risks associated with hydrogen as a fuel [30], and the ability to start-up at ambient temperatures less than -25°C [31, 32].

The fuel cell produces water from the hydrogen oxidation and oxygen reduction reaction during normal operation; at shutdown in sub-zero conditions, this water freezes and upon re-start can inhibit reactants reaching reactant sites, cause a voltage reversal, and prevent the fuel cell system from starting up. To better start-up from sub-zero conditions, special shutdown procedures are enacted to remove liquid water from the fuel cell stack, additionally a catalyst is added to the anode that allows water evolution to enable the hydrogen oxidation reaction until the anode sites are clear. In Section 4.1.1, the basic vehicle requirements are discussed including the ability for the vehicle to operate from -45°C to +50°C. Current fuel cell systems cannot start-up at -45°C. However, each fuel cell system includes a battery which can discharge at -45°C, at a lower C-rate. If such a low temperature start-up is required, the battery can be designed to run the fuel cell system coolant heater and pump to heat the fuel cell to a minimum start-up temperature, such as -25°C. Once the fuel cell system is running, it generates heat, which can then be fed to the battery to warm it up and recharge it from the fuel cell system. This requirement would be incorporated into the battery and fuel cell system design; such that the battery would be selected to have the lowest possible internal resistance. The impact on the specifications would be a delay in start-up to perform this heating phase or if no delay is required, the vehicle could keep the battery and fuel cell above a temperature limit by periodically heating the coolant such as during an overnight period.

Some of the advantages of the technology includes fast refueling, long driving range, no harmful tailpipe emissions, and scalability for larger vehicles [30].

3.6 Exhaust Water Recovery

In austere or desert conditions, or on a mission, access to drinking water can be a challenge. For every kilogram of hydrogen, an H_2-ICE or fuel cell engine has the potential to produce 9 kilograms of water, based on the combustion reaction and the molar mass of water and hydrogen. As a tangent to this vehicle component power sizing exercise, there was interest in understanding the possibility of capturing water from the exhaust system to drink or for other uses such as injection into the combustion chamber to improve efficiency. As such, MAHLE was invited to investigate what a potential water capture system would entail, the amount of water produced, the power demand required, as well as the impact on overall vehicle efficiency. The full report is inserted into Appendix A.

3.7 On-board Hydrogen Storage

In order to operate a hydrogen fuel cell or hydrogen combustion engine, hydrogen must be supplied. There are different storage formats for hydrogen, and each of them possesses their own gravimetric and volumetric energy density. Volumetric energy density is the amount of energy available per litre, and gravimetric energy density is the amount of energy per kilogram. Figure 18 is a plot of different fuel types and their densities. For comparison, diesel fuel has relatively high gravimetric and volumetric energy densities, at 45.4 MJ/kg and 34.6 MJ/kg, respectively [33, 34]. Gaseous hydrogen, stored at 700 bar pressures, has high gravimetric energy density but low volumetric energy density. Hydrogen is the lightest and most abundant element on earth but its volumetric energy density is low. The gravimetric energy density, based on the lower heating value of hydrogen is 33.3 kWh/kg [35]. A lower heating value represents the amount of heat released during combustion excluding the energy contained in the water vapour produced. It represents the usable energy which can be extracted from a fuel under real operating conditions.

When examining the hydrogen storage tank's gravimetric energy density, both the storage container and the fuel weight are considered. The types of storage tanks required are large, thick walled, and heavy. The fuel storage system's gravimetric energy density can be calculated as the mass of hydrogen divided by the total mass of the storage system. This value is lower than the gravimetric density of hydrogen fuel alone. The major challenge with using gaseous systems for defence applications comes from the risk of jet fire or potentially delayed explosion when damaged by high explosives and projectiles. Hydrogen compressors are also a single point of failure in the gaseous hydrogen supply chain as there is no way to fill the tanks without them. Such compressors (up to 700 bar) are complex, expensive, and difficult to operate in austere operational conditions.

Liquid hydrogen has higher volumetric density than gaseous hydrogen. Liquid hydrogen is stored at -253°C and at a pressure from 1 to 10 bar. This low temperature presents challenges with storage, including boil-off losses, material selection, infrastructure limitations, and energy-intensive liquefaction during production. Liquefaction is the process of transforming gaseous hydrogen into liquid. In a military context, large liquefaction plants would represent a similar critical infrastructure problem as refineries do for fossil fuels. While there may be some applications for liquid hydrogen in civilian applications that are not at risk of being targeted, there is significant risk in using it for defence applications.

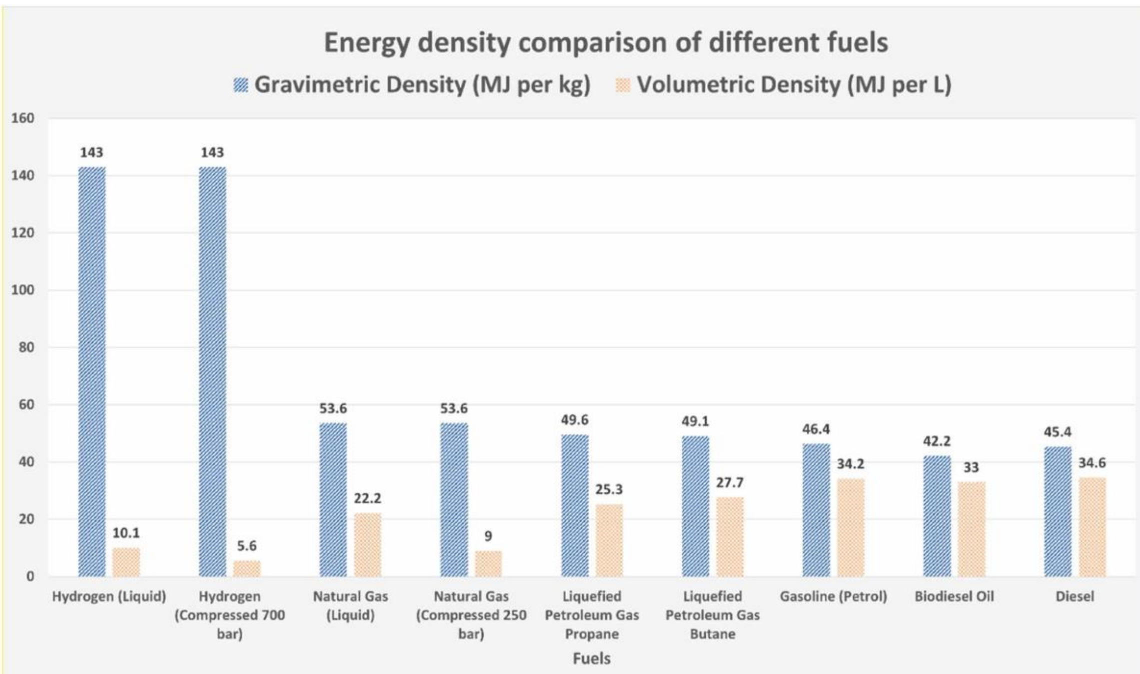

Figure 18: Comparative energy density of hydrogen and conventional fuels [33, 34]

Gaseous hydrogen has a low ignition energy (0.02 mJ), low lower flammable limit (4% in air), and wide flammability range (4 to 75% in air) [35]. Ignition energy is the energy required to ignite a substance. For comparison, gasoline vapour ignition energy is about ten times higher, at 0.2 mJ. Flammability range is the range over which a flammable mixture can occur. Hydrogen can burn at concentrations from 4 to 75% in air. Methane, or natural gas, has a flammability range of about 5 to 15% in air. To improve gaseous hydrogen volumetric density, it's stored at higher pressure, typically 350 to 700-bar. Storage at higher pressures includes risks such as containment failure, where a tank rupture or leak could lead to a jet release and / or explosion-event. A high-pressure hydrogen leak can form a high-velocity jet flame that is nearly invisible and burns very hot.

Hydrogen is also the lightest element on earth, when released it will seek the highest point. If released in an outdoor environment, it will rapidly rise and dissipate. If released in an enclosed environment, it can pool at the highest point and potentially form a flammable mixture. Diesel's weight is higher than hydrogen; if it is released, it can pool on the ground and potentially ignite if heated before it is cleaned up. Because the hydrogen molecule is so small, containing it can be challenging and care must be taken in designing systems adequately, such as reducing the number of fittings, ensuring material selection is compatible and leak free, and employing compression fittings with front and back ferrules. The storage of liquid hydrogen includes all the aforementioned challenges as well as challenges that come with sub-zero storage and delivery including boil-off and venting losses, material embrittlement, and insulation and thermal management.

There is a third category of hydrogen storage, solid-state storage, that is in addition to gaseous and liquid. It aims to reduce some of the potential risks and challenges with the other two storage methods, namely high pressure, sub-zero temperature of liquid, and low storage density. There are many different methods of hydrogen solid state storage. Figure 19 provides a breakdown of the different types. Fundamentally, hydrogen solid state refers to a method of storing hydrogen within solid materials rather than as a gas or liquid. In this approach, hydrogen is absorbed or chemically bonded to a solid substance. It can be stored at relatively low pressures and standard temperatures compared to compressed or liquid hydrogen systems.

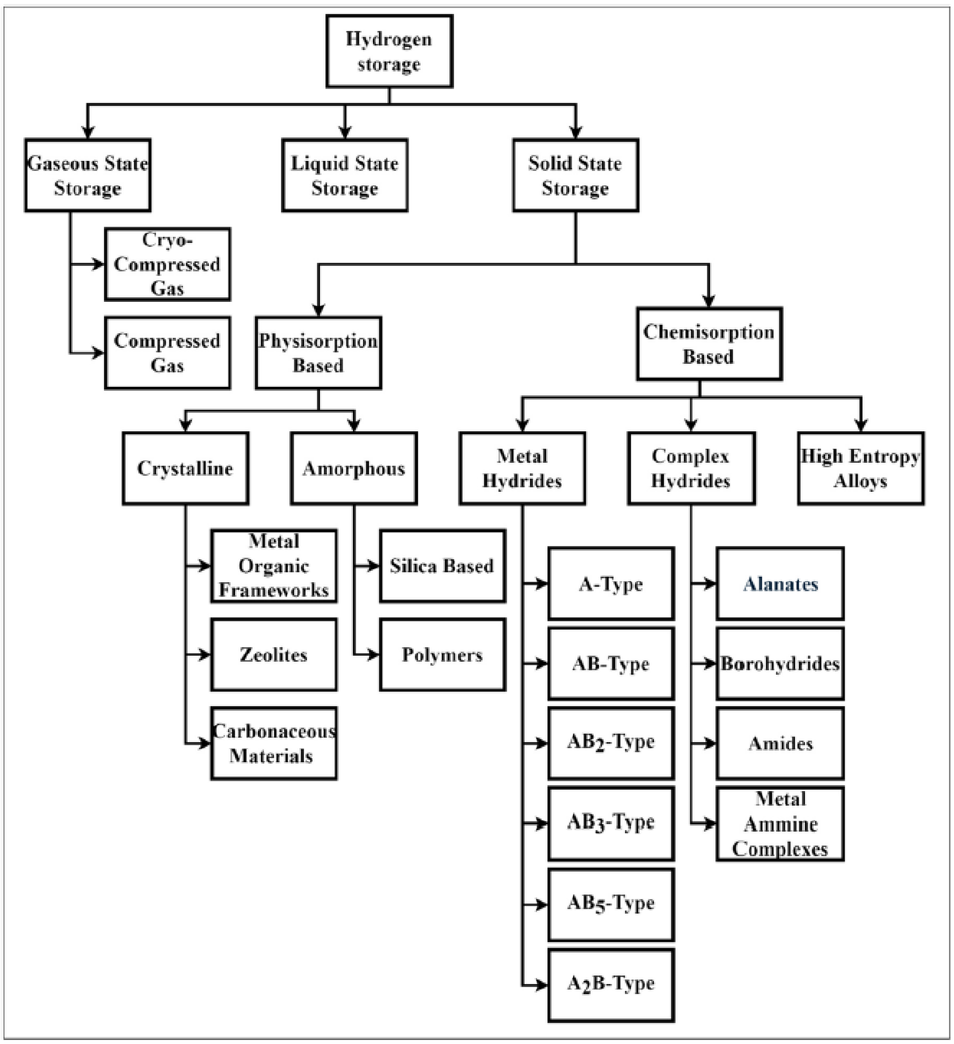

Figure 19: Categorisation of hydrogen storage technologies [34]

Figure 20 illustrates the opportunity for higher volumetric density storage that solid-state methods may provide. In this illustration, the number of hydrogen molecules per cubic cm is visually demonstrated. From left to right, the number of hydrogen molecules is increasing, nearly doubling each time. In this example, a metal hydride is the solid-state storage method. Metal hydrides are compounds created when hydrogen bonds directly with metals or metal alloys. These materials store hydrogen by forming chemical bonds through reversible reactions with the metal components. There are currently no large volume commercially available hydrogen solid-state technologies on the market. One promising technology is light-activated nano-structured thin film. As described in Section 2.1, the Plasma Kinetics solid-state hydrogen storage and release technology will be used as our demonstration hydrogen storage technology for determining fuel tank size, etc. As an input to the vehicle design, the volumetric and gravimetric energy density of this demonstration system, as well as the release energy required will be employed. The Plasma Kinetics system is endothermic during release, which increases safety by eliminating self-sustaining thermal runaway, but reduces overall conversion efficiency as some of the energy produced must be used to release the hydrogen from the thin film. This unique factor creates diminishing returns when designing platforms as adding more hydrogen to the vehicle requires more energy to release. Not considered in this analysis is the energy required to refill the canisters [36]. The flow rate is variable and precisely controlled by integrated manifold control, laser, and motor systems. The anticipated nominal flow is 1 kg per hour at 2.5 bar. But can be varied from 0.1 kg to 14 kg per hour at a pressure between 1.1 bar and 60 bar. The higher release rate pressure requires enhanced control systems which are optional. Additionally, the power demand is a linear function of the hydrogen required per unit time. In general, 30% of the energy content of the released hydrogen is required by the motor and laser system [37]. A full discussion on the current status of solid-state technology by Bak Motors Inc. is provided in Appendix B.

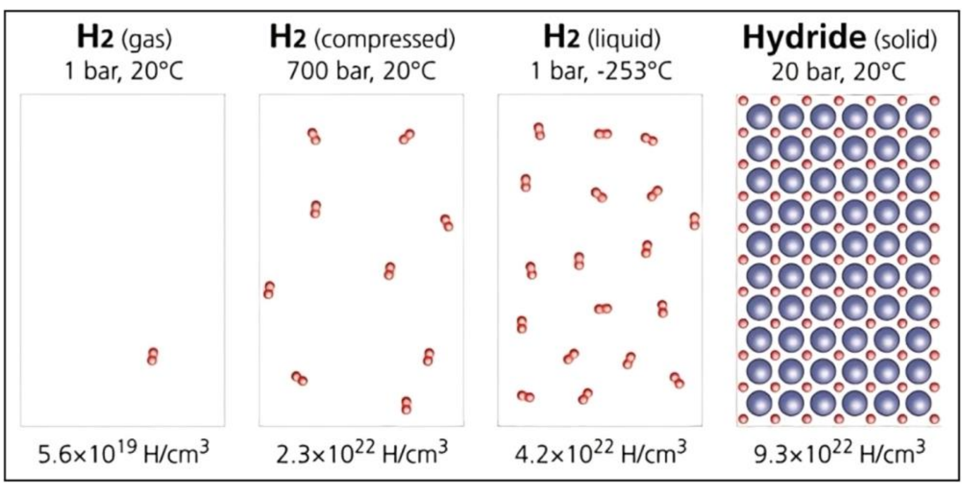

Figure 20: Number of hydrogen molecules per cubic cm in different storage techniques [38]

3.8 Batteries

The most common battery technology used for mobility applications is the lithium-ion battery (LiB) chemistry. Lithium-ion batteries have high energy and power density compared to other common battery chemistries (e.g., lead-acid, nickel metal-hydride, etc.), LiB retain more charge during storage than other non lithium-based chemistries, and have relatively high charge/discharge cycle life. This makes LiB the best available battery technology for mobility applications. However, LiB are very sensitive to being overcharged, which can create safety issues in the form of thermal runaway. For this reason, the use of battery management systems (BMS) is necessary for the batteries to maintain consistent performance over the life of the battery, detecting faults, and preventing runaway [39].

In most LiB chemistries, the anode is typically made of graphite; though lithium titanium oxide has also been used. Lithium titanium oxide as an anode can improve the battery's cycle life, power output, low-temperature performance, and safety [40]. However, the tradeoff for those improvements is a 50% reduction of the energy capacity compared to a more conventional graphite anode.

As a result, the key differentiator for the different chemistries is the cathode material which includes lithium-nickel-cobalt-aluminum oxide (NCA), lithium-nickel-manganese-cobalt oxide (NMC), lithium manganese oxide (LMO), lithium-titanate-oxide (LTO), and lithium iron phosphate (LFP).

Batteries based on NMC chemistry consist of a cathode composed of lithium, nickel, manganese, and cobalt [41], with a conventional graphite anode. Altering the percentages of the constituent compounds changes the properties and performance of the battery. Batteries based on NCA chemistry, are made with 80% nickel, 15% cobalt, and 5% aluminum. Both NMC and NCA chemistries have relatively high energy densities and cycle life, but are more costly and have reduced safety margins.

Batteries based on LFP and LTO chemistries typically have lower energy density compared to NMC and/or NCA, but have increased lifespan and safety. Batteries based on LTO chemistry perform very well in terms of efficiency, but are very expensive. Batteries based on LFP chemistry are thermally stable, do not produce toxic chemicals during a runaway, and have the lowest cost of the all of the chemistries. They (LFP batteries) also do not require any strategically important minerals in their manufacture, which adds to the sustainability of using these batteries [40].

For this reason, LFP batteries are generally considered to be one of the more promising battery technologies, but some sources claim that LTO batteries are preferable due to their advantages over LFP batteries [42]. This is despite the fact that both LTO and LFP batteries have a lower energy density than other LiB chemistries. Furthermore, LFP batteries present challenges in operation at sub-zero ambient conditions, important for operation in Canada. Below zero degrees, their energy capacity is lower and their C-rate is reduced from its peak value. This adds limitations to the amount of power available from the batteries at low temperatures. Furthermore, to charge the batteries, the temperature should be in the range of +5°C to +45°C [43]. Figure 21 provides some general performance characteristics of Li-on cells. In Figure 21, $LiFePO_4$ are LFP cell type, and $Li_{4/3}Ti_{5/3}O_4$ are LTO cell type.

Characteristic	$LiCoO_2$/graphite NMC/graphite NCA/graphite Energy cells	NMC/graphite LMO/graphite Power cells	$LiFePO_4$/ graphite Power cells	LMO/$Li_{4/3}Ti_{5/3}O_4$
Voltage range (V)	2.5–4.2 typ. 2.5–4.35 for some cells	2.5–4.2	2.5–3.6	2.8–1.5
Avg. Voltage	3.7	3.7	3.3	2.3
Specific energy (Wh/kg)	175–240 cylinder 130–200 polymer	100–150	60–110	70
Energy density (Wh/L)	400–640 cylinder 250–450 polymer	250–350	125–250	120
Continuous rate capability (C)	2–3	Over 30	10–125	10
Pulse-rate capability (C)	5	Over 100	Up to 250	20
Cycle life at 100% DOD (to 80% capacity)	500+	500+	1000+	4000+
Calendar life (yr)	>5	>5	>5	>5
Self-discharge rate (%/month)	2–10 %/mo	2–10 %/mo	2–10 %/mo	2–10 %/mo
Charge temperature range (°C)	0–45 Some cells have wider range	0–45 Some cells have wider range	0–45 Some cells have wider range	–20–45 Some cells have wider range
Discharge temperature range (°C)	–20–60	–30–60	–30–60	–30–60
Memory effect	None	None	None	None
Power density (W/L) (pulse)	~2000	~10000	~10000	~2000
Specific power (W/kg) (pulse)	~1000	~4000	~4000	~1100

NMC = $LiNi_{1/3}Mn_{1/3}Co_{1/3}O_2$, $LiNi_{0.5}Mn_{0.3}Co_{0.2}O_2$ or $LiNi_{0.42}Mn_{0.42}Co_{0.16}$, etc.
NCA = $LiNi_{0.8}Co_{0.15}Al_{0.05}O_2$, etc.
LMO = $Li_{1+x}Mn_{2-x}O_4$, etc.

Figure 21: General performance characteristics of representative Li-ion cells [44]

Another battery technology that is currently under development is solid-state batteries (SSBs). SSBs replace the flammable liquid electrolyte found in conventional lithium-ion cells with a solid material (ceramic, sulfide, or polymer) [45]. This design greatly improves safety, energy density, and thermal stability, and enables the use of lithium-metal anodes for higher capacity. Some advantages include high energy density, excellent safety, wide operating temperature range, and long cycle life potential. Some disadvantages include manufacturing complexity, high cost, interface resistance between solid layers, and challenges with scaling up to large-format cells [46]. These technologies are currently in the advanced development stage for a few companies but are not yet widely adopted or mass produced.

There are many different national and international standards that cover safety and performance specifications for battery cells, packs, and systems including electrical and mechanical requirements. In particular, MIL-PRF-32383 includes a section that outlines a cell-level nail penetration test whereby a stainless-steel nail is driven at a right angle two-thirds of the way into the centre of a cell, and left for 24-hours, with voltage and temperature monitoring. The cell must not react violently when penetrated by a sharp object [47]. In addition to designing cells which meet this standard, furthermore, a component, system and vehicle level risk assessment / hazard and operability study (HAZOP) should be performed during the design phase to consider the potential hazard causes, their likely effects, and potential outcomes.

For this study, the battery chemistry was limited to LFP chemistries. This chemistry was selected on the basis of safety; LFP batteries are significantly less susceptible to runaway events from over-charging or physical damage; which is a significant advantage for military applications despite their lower power and energy density.

Battery-only concepts were not considered for this study. There were many factors that influenced this choice and they all revolved around the unique challenges found in military expeditionary applications. Chief among those considerations were the charging infrastructure requirements and charging time. Expeditionary operations by their very nature mean that available charging infrastructure such as facilities or even just the availability of electricity in some form is unknown. This would require that any operations must bring their own charging capabilities. Even if charging facilities were available in-theatre, charging time for such large batteries would be measured in hours. This would result in the conceptual vehicle to be stationary for hours at a time, making them both vulnerable as well as unavailable for tasking.

3.9 Electric Motors

Electrification for mobility applications has undergone considerable transformation in recent history. Over the past two decades, the automotive industry has undergone a significant transformation driven by environmental regulations, advances in power electronics, and consumer demand for cleaner and more efficient vehicles. In the early stages of electrification, the conventional ICE driveline was retained and small, low(er)-powered auxiliary motors provided transient assistance to the ICE prime mover (e.g., launch, mild-regenerative braking, engine start/stop), and/or powered auxiliary equipment such as air-conditioning to allow for engine-off operation as a fuel-consumption reduction strategy.

More recently, electrification has transitioned into performance enhancement, with electric motors providing an ever-increasing portion of the total vehicle power; in addition to increased battery capacity to sustain the electrical power delivery. The shift from auxiliary motors providing help to the ICE to electric traction motors providing significant portion of the total power and enabling substantial engine-off mobility marks a pivotal step toward full electrification [48, 49].

Electric traction motors convert electrical energy into mechanical energy through a rotating magnetic field. The most common types include induction motors, permanent magnet synchronous motors (PMSMs), and switched reluctance motors [50]. These motors rely on sophisticated motor controllers to regulate current and voltage, precisely energizing and de-energizing motor stator coils to modulate torque output and control speed. These controllers also manage the regenerative braking by operating the traction motors in reverse, recovering kinetic energy during deceleration, converting it back to electrical energy stored in batteries rather than dissipating the braking energy as heat through conventional friction brakes.

The underlying technology is based on three major advancements [48]:

1. Power electronics: High-efficiency inverters and converters using silicon carbide (SiC) and gallium nitride (GaN) materials allow compact designs and better thermal management.
2. Energy storage: Modern lithium-ion and emerging solid-state batteries provide high energy density and rapid charge/discharge capabilities.
3. Control systems: Sophisticated algorithms and sensors ensure optimal energy use, torque response, and motor protection.

Electric traction systems offer numerous advantages over combustion-based auxiliaries. They provide instant torque, higher efficiency (often above 90%), lower maintenance requirements due to fewer moving parts, and zero tailpipe emissions. Regenerative braking extends range and reduces energy waste, and the compact design of electric motors allows more flexible vehicle architecture [50].

However, disadvantages remain. Electric traction systems depend heavily on battery technology, which faces limitations in energy density, cost, and charging infrastructure. The production of batteries and rare-earth magnets (used in PMSMs) raises concerns about resource availability and environmental impact [51]. Furthermore, thermal management and electromagnetic interference are engineering challenges that require continuous innovation.

The transition faces technical and economic challenges. Scaling up manufacturing while minimizing environmental footprint, improving battery recycling, and ensuring grid stability as electric vehicle adoption grows are key priorities. Researchers are exploring new motor designs, such as magnet-free synchronous motors and advanced cooling techniques, to enhance sustainability and performance [51, 52].

Similar to batteries, there were many different types of electric motor architectures to choose from for this study. Most passenger automotive applications place the traction motor(s) in-chassis, with conventional driveshafts to the driven wheels. In-chassis motors reduces the unsprung mass as well as centralizing the mass distribution; two factors which are important for passenger vehicle ride quality, comfort, and performance.

However, for this application of a heavy wheeled logistics vehicle, the unsprung mass is a less important factor, and with an 8x8 drive, there exists and opportunity to use in-wheel motors to leverage the flexibility advantages of electrical power distribution since no driveshafts, reduction gearboxes, or transmissions are required. An electric motor's bi-directional rotation ability lets the motor spin in either direction equally effectively. This means that "forward" (the direction of vehicle travel) is independent of motor rotation. For an 8x8 drive vehicle, the bi-directional rotation ability of an electric motor on paper means that the electric motor itself can be configured as "left" or "right" in software, making the motors of all eight-wheel positions identical, which can provide positive impacts to military logistics as well.

For this project, all the concept vehicles electric motors were in-wheel motors as designed by Donut Defense (ESOX Group). The primary rationale for this was the availability of accurate, fine-grained information regarding the various performance metrics such as power density, volume, peak/continuous power, and other important variables for this study. A detailed analysis by ESOX Group can be found in Appendix C.

4.0 Methodology

This section describes the vehicle parameters and requirements, the mission profile, the technology inputs, and the vehicle concepts selected for analysis.

4.1 Vehicle Requirements

This section discusses the fundamental vehicle requirements that are constant across both drive cycles; as well as describing the specific drive cycles in details and how they were derived.

4.1.1 Basic Vehicle Requirements

As described in Section 3.3, the diesel-ICE 8x8 heavy logistics vehicle was used as a starting point for this study; it is the baseline vehicle and powertrain against which all other parameters are compared. For this study, the diesel-ICE vehicle weight and fundamental parameters are used as a starting point to determine the minimum concept vehicle requirements. Table 3 lists these parameters. Weight compensation was employed when analyzing the concepts. The powertrain increased or decreased, from the baseline concept, based on weight compared to the baseline powertrain.

There are many different LVM configurations and corresponding GVWs. The version selected for this evaluation is the 38,000 kg GVW with 15,000 kg payload. This is the largest of the LVM vehicles and therefore the most challenging to electrify.

Rolling resistance is the counter force applied to the wheels when the vehicle is in motion. Sources of rolling resistance include tire deformation, friction between tire and road surface, wheel friction with surrounding air, friction in the wheel hub and surrounding, and road surface deformation. The coefficient of rolling resistance (Crr) is a static term for which tables of values have been determined for some common road surface and wheel types [53]. The Mercedes Zetros uses off-road tires on asphalt. The Crr for asphalt road with pneumatic tires is 0.011; the Crr for the vehicle parameters was set just above this value.

The aerodynamic drag force is the force of the area acting counter to the vehicle. Sources of aerodynamic drag include pressure drag (due differences in air pressure between the front and back of the vehicle), skin friction drag (due to surface roughness of the vehicle), interference drag (due where components meet), induced drag (due to lift generation), and wave drag (due to compressibility at high speeds). Similarly, to rolling resistance, a coefficient of drag (Cd) can be developed for standard vehicle design and sizes. A semi-trailer truck was analyzed to have a Cd value between 0.5 to 0.9 [54]. For the LVM vehicle, a middle value of 0.75 was selected as a starting point.

The frontal area of the diesel-baseline vehicle was calculated by multiplying the Zetros vehicle width (2.477 m) by its height (2.925 m) [55] and by an empirically determined form factor for heavy trucks of 0.84 [56] for a value of ~6m^2.

Table 3: Diesel-ICE 8x8 heavy logistics vehicle parameters [53-57]

Parameter	Unit	Value
Unladed mass	kg	23,000
Payload	kg	15,000
Gross vehicle weight (GVW)	kg	38,000
Coefficient of rolling resistance (Crr)	N/A	0.011
Coefficient of drag (Cd)	N/A	0.75
Frontal area	m^2	6

In this project, two different drive cycles will be explored in order to compare and contrast the impact of the cycle on vehicle peak and continuous power demand, total power demand, and their influence on component sizing and degree of electrification. Common to both cycles were standard minimum vehicle performance requirements determined from the logistics vehicle modernization statement of work [6] and those presented as high-level requirements in the initial project briefing [57].

The high-level requirements were the following [57]:

4. 15,000 kg payload for the prime mover
5. 500 km range on flat road with both prime mover and trailer at gross vehicle weight (GVW)
6. Able to maintain 80 km/h at 2% grade
7. Able to handle 20-foot ISO container
8. Able to fit in C-17
9. Vehicle-to grid capability
10. Collect and store water for crew
11. Able to operate between -45°C to + 50°C, etc.

These high-level requirements were categorized by the authors of this report as “need to have” and “nice to have”. The 15,000 kg payload for the prime move is a need to have requirement. The 500 km range is used as the requirement for the primary road cycle. The 80 km/hr at 2% grade is an incomplete requirement as it does not provide a duration. In real operation, a vehicle will not climb a hill indefinitely. The vehicle will ultimately reach the top of the incline and begin descending. The power needed to sustain this climb is considered a continuous requirement within the context of this project, as it represents the steady-state power necessary to maintain that speed under load. For this project, the hill-climb required time was assumed to be 10-minutes, based on subject matter experts. The critical challenge with identifying platform requirements for hybrid military vehicles is the lack of understanding in the differences between ICE and hybrid powertrains. Current requirements have been refined over eighty years of ICE platform development and have been optimized for its capability. The above requirements were not fully validated and represent a paradigm shift in future requirements.

Nice to have requirements are the vehicle to grid capability, and collect and store water for the crew. Able to fit into a C-17 will be an output from this work as this early report will give an indication of total system mass and volume. Able to handle 20-foot ISO container, and able to operate between -45°C and +50°C are requirements that should be evaluated in a subsequent more in-depth study; but fundamentally a technology shouldn’t be examined if it cannot operate within this temperature window.

In addition, it was important to define a speed and acceleration requirement. For the acceleration requirement, a 30-second acceleration was selected based on the assumption of the baseline vehicle. Wheel power is calculated by inputting the vehicle parameters from Table 3, and these vehicle performance requirements into Equation 1. The average duration requirement was set based on a vehicle range of 500 km at 80 km/hr, which is 6.25 hours. Table 4 outlines the wheel power from these different fundamental requirements; which were calculated using the ePOP concept tool.

Table 4: Minimum concept vehicle performance requirements

Requirement	Wheel power (kW)	Requirement type	Duration
Speed: 80 km/hr, dry level paved road, no headwind	125	Average	6.25-hours
Dynamic hill-climb: 80km/hr at 2% grade	290	Continuous	10-minutes
Acceleration: 0 to 80km/hr, shortest acceleration time	320	Peak	30-seconds
Distance: 500km at 80km/hr	6.25 hours		

4.1.2 Primary Road Cycle

One of the outcomes of this project is a better understanding of how vehicle drive cycles affect power demand, overall energy demand, sizing of components, as well as fuel quantity. When the project began, no specific heavy logistics drive cycle was provided; as such, the authors selected a very simplistic flat road cycle as a starting point; set to a logistics vehicle modernization (LVM) speed and distance where duration was calculated; as described in Table 4 [6]. This primary road cycle is fundamentally a very long continuous requirement. Traditional combustion engines, with adequate cooling, are able to sustain a long continuous power output, so long as fuel input is available but no braking regeneration energy is possible; whereas, battery technologies are able to deliver short high-power output and then regain energy through regenerative braking. The primary road cycle described below is more favourable for traditional combustion technologies, whereas the more intricate drive cycle described in Section 4.1.3 is more favourable to electrified technologies.

Figure 22 is a plot of the primary road cycle demand mechanical energy. The peak power is 320 kW and the average power is a sustained 125 kW. The cycle duration is 6.25 hours long.

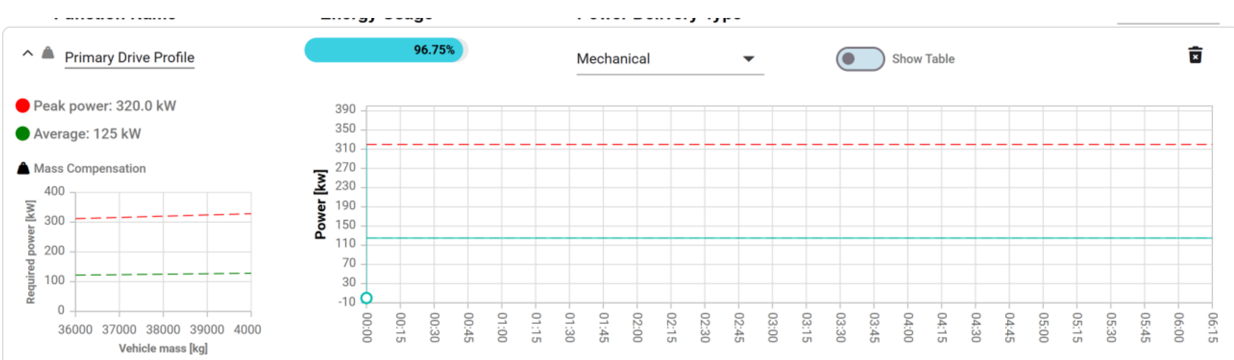

Figure 22: Primary road demand mechanical energy drive profile

Figure 23 is a plot of the primary road cycle auxiliary's electrical energy. This electrical energy peak and average is derived based on real-world diesel-ICE idle vehicle data operation. The same value is used for the primary road cycle and the logistics vehicle mission profile. The peak power is 8.4 kW and the average power is 4.2 kW.

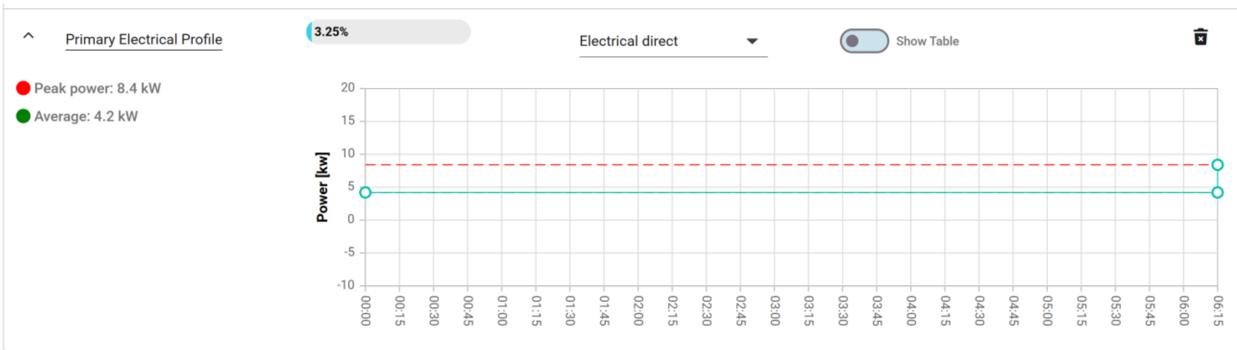

Figure 23: Primary road auxiliary electrical energy drive profile

Figure 24 is a plot of the primary road cycle combined mechanical and electrical energy. These values are added together to form a combined cycle.

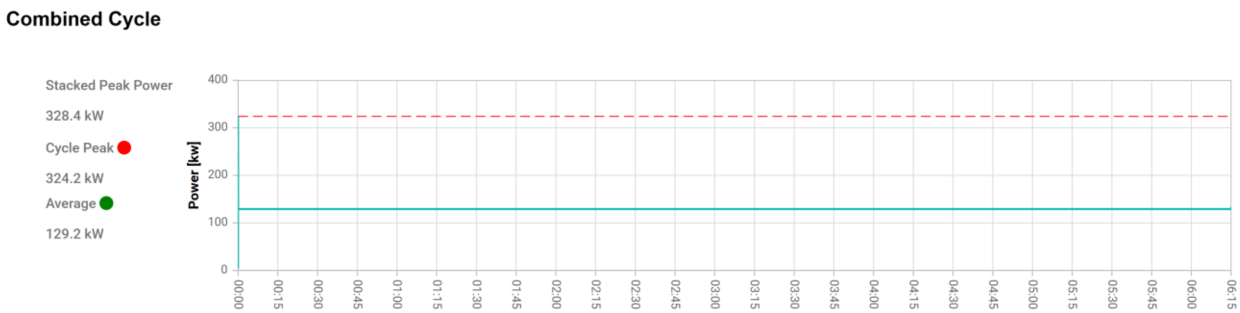

Figure 24: Primary road combined demand drive profile

4.1.3 Logistics Vehicle Mission Profile

As stated above, no drive cycle data was provided as input for this project. Rather, a set of high-level requirements, and a logistics vehicle heavy mission profile were provided, along with aggregated real-world operational data from a diesel-ICE baseline vehicle. The lack of drive cycle data was a challenge for the project and it required additional unplanned project time and resources to construct using indirect methods. Having this drive cycle data available, and validated for future platform designs is a critical component to accelerating future studies.

The mission profile gives information of the mission total duration, the approximate total distance, the breakdown of terrain types excluding elevation, grade, braking energy, or terrain rolling resistance, which are required to calculate the vehicle forces, and determine vehicle energy and power requirements. The current definition of mission profiles for military platforms is not suitable for assessing hybrid vehicles due to a lack of specificity. Parameters such as elevation, grade, braking energy etc. do not have as large of an impact on ICE vehicle performance, but are critical in determining hybrid vehicle architecture to determine potential for downsizing, regeneration, and peak power demands during hill climbs. Therefore, a more detailed mission profile format that assesses power and duration should be created for future hybrid vehicle studies. Table 5 is a reproduced copy of the LVM heavy mission profile [5].

Table 5: LVM heavy mission profile [5]

Mission	Unit of measure	Quantity	Comments
a. Time	duration in hours	10	
b. Length	distance in kilometers	200	
c. Idling time	hours	2	
d. Driving Primary Roads	% of distance	20	Approximately 90-100 km/h
e. Driving Secondary Roads	% of distance	50	Approximately 60 km/h
f. Driving Trails	% of distance	25	Approximately 20-25 km/h, the ground conditions and drivers experience will dictate the appropriate speed, DLR representatives will determine if route meets definition of trail
g. Driving Cross Country	% of distance	5	Approximately 3-15 km/h, the ground conditions and drivers experience will dictate the appropriate speed, DLR representatives will determine if route meets definition of cross country.
h. Night Driving	% of time	40	including both Black Out Drive and with headlights
i. Driving in Reverse	times per mission	10	
j. Max Speed	times per mission	2	Dash or unstained speed, up to vehicles maximum speed
k. Fording	times per mission	1	
l. Trailer Towing	% of time	45	
m. Shutdown, Start-up	times per mission	4	
n. Hard Breaking	times per mission	20	Vehicle makes its maximum braking application
o. Hard Acceleration	times per mission	50	Vehicle makes its maximum acceleration
p. Hard Turns	times per mission	4	Steering limiter hit, conducted at slow speed (2-10 km/h)
q. LHS Loading cycles	times per mission	6	only for LHS vehicles and trailers
r. Crane Operation	hours per mission	1	only for vehicles with crane
s. Crane Operation	cycles per mission	12	at maximum capacity
t. All wheel drive	distance in km per mission	20	
u. Differential locks engaged (where applicable)	distance in km per mission	1	
v. Self Recovery	dimes per mission	0.01	Vehicles with Winch
w. Self Recovery	distance in meters per event	30	Vehicles with winch only
x. Suspended tow	times per mission	0.02	At GVW
y. Suspended tow	distance in km per event	80	At GVW
z. Driving with tire chains	max. occurrence per mission	0.05	note: occurs in winter or marginal traction condition
aa. Driving with Tire Chains	distance in km per event	50	note: vehicle speed reduced as per OEM and chain manufactures specifications
ab. Camouflaging Vehicle	times per mission	1	2 soldiers climbing on vehicle. Only applies to the tractor.

Working closely with contributors to this project, aggregated diesel-ICE baseline real-world operational data was provided, from which the authors, with input and feedback from experts, were able to adapt and break down into the necessary information to properly characterize the LVM profile. Should this drive cycle data and vehicle requirements be available beforehand it can reduce the time to conduct the study significantly. 11 operational runs of real-world data were provided to the NRC which stated the terrain type (pavement, secondary, trails, cross country, transit, discrete, and idle), the duration of each terrain segment, and the combined overall fuel usage, in kg of diesel. These 11 runs were not meant to be representative of the mission profile but were simply operational runs for validating different metrics for the vehicles. To determine the tractive power for each terrain segment, the authors selected six of these runs and reverse-engineered from fuel usage, to fuel energy, assumed an engine efficiency, added in accessory power, assumed a transmission efficiency, and assumed a brake power. By combining the six runs together, it was possible to solve for each terrain power individually. The powers were confirmed by verifying that the summed fuel usage for each terrain and each run was within ±15% of the actual fuel usage. For future studies, it is recommended that much more accurate data sets be created through physical testing of different hybrid powertrains to confirm simulation results.

Table 6 is an abbreviated version of the aggregate fuel economy data provided for the diesel-ICE baseline 8x8 vehicle. Each test run is a combination of different terrains; 5079ah and 5079ap are predominantly secondary roads and trails with some grade operations, 5079bi is predominantly trails with some grade operations, 5079bl is predominantly low motion resistance pavement and secondary on level ground with short grade exposure, and DLC involved conduct of paved road test. For this test, speeds ranged from about 15 km to a maximum of approximately 55 km. Vehicle would perform a double lane change maneuver at the required speed on the skid pad then continue around the 1.8-mile oval at speeds of 35 to 50 km/hr and then perform the next speed increment double lane change. Transit distance was not considered part of the official mission; for example, if a vehicle broke down and it had to be returned at a reduced speed. Discrete events were terrains that were performed at low speed such as a river crossing or low speed obstacles or through mud. B1H GVW was a combined terrain test. No retarding or braking energy was captured for this testing; however, through email communications it was confirmed that the vehicles start and end at the same elevation, the vehicles run up and down the same grade and the vehicle retarders were on “full” for about 70% of the down grade operations. The feedback from the project contributors is that there is significant opportunity for regeneration in these profiles. Identifying these regeneration opportunities will require physical testing of hybrid platforms in the future. This testing should be standardized and a common database needs to be established so future studies can use it without having to re-do the physical testing.

Table 6: LVM fuel economy data

		Duration (min)					
Run name		**B1H GVW**	**J5079ah_sec**	**J5079ap_sec**	**J5079bi_trails**	**J5079bl**	**DLC**
Terrain	Pavement	33.0	--	--	--	13.5	190.0
	Secondary	256.8	47.0	13.9	16.2	18.2	--
	Trails	258.9	62.4	23.0	55.3	--	--
	Cross country	267.0	14.7	--	5.1	--	--
	Transit	28.7	10.3	3.0	4.9	1.6	--
	Discrete	210	1.8	0.8	2.3	4.6	--
	Idle	260.1	28.3	44.1	20.7	26.0	6
Fuel weight (kg)		327.2	60.0	25.3	31.3	24.4	103.8

To simplify reporting, only the B1H GVW is broken down in detail but the same practice was applied to all runs. As a starting point, 125 kW was assumed to be the tractive power for the pavement terrain; this value comes for the 80 km/hr requirement calculated in Table 4. Suitable tractive power values were assumed for the other terrains. Output power was calculated as tractive power multiplied by one plus brake power. Brake power was assumed based on subject matter experts; 10% for pavement and trails; 20% for secondary, transit, and discrete; and 0% for cross-country. ICE power was calculated as output power divided by transmission efficiency plus accessory power. Transmission efficiency was assumed to be 91%, based on subject matter experts, and accessory power was set at 7 kW during operation and 9 kW during idle. ICE output energy is ICE power multiplied by duration. ICE fuel energy is ICE output energy divided by ICE engine efficiency. Fuel amount is ICE fuel energy divided by fuel density (11.94 kWh/kg). The sum of the calculated fuel values is 361.5 kg, whereas the actual fuel amount used for this test run was 327.2 kg; a percent error of 10.5%. This analysis was repeated for the other five runs; all the characterized fuel values were within ±12% of the measured fuel amount.

Once the tractive power values were established for the different terrains, it was possible to build a time-normalized LVM profile. From the mission profile, the overall duration is 10-hours and the duration for each terrain type can be calculated from the percentage of distance, distance, and speed. Table 7 provides the LVM terrain type distance, speed and duration.

Table 7: LVM terrain type distance, speed, and duration

Terrain type	% of distance	Distance (km)	Speed (km/hr)	Approx. duration (hr)
Primary	20	40	90	0.44
Secondary	50	100	60	1.67
Trails	25	50	20	2.50
Cross country	5	10	3	3.33
Idle	--	--	--	2
TOTAL		**200**		**9.94**

The project contributors were invited to provide feedback for the time-normalized LVM profile. The feedback provided was that the brake power was underestimated and that the engine efficiency varied for each terrain and was over-estimated. Table 8 provides an example of the analysis of run B1H GVW, which was executed for all of the six runs above.

Table 8: B1H GVW run tractive power and fuel economy assessment

Terrain	Time (min)	Tractive power (kW)	Brake power (% of tractive power)	Output power (kW)	Transmission efficiency (%)	Accessory power (kW)	ICE power (kW)	ICE output energy (kWh)	ICE efficiency (%)	ICE fuel energy (kWh)	Fuel (kg)
Pavement	33.0	125	10%	137.5	91%	7	158.1	87.0	37%	235.0	19.7
Secondary	256.8	72	20%	86.4	91%	7	101.9	436.3	37%	1179.3	98.8
Trails	258.9	72	10%	79.2	91%	7	94.0	405.8	37%	1096.6	91.8
Cross country	267.0	72	0%	72.0	91%	7	86.1	383.2	37%	1035.8	86.7
Transit	28.7	90	20%	108.0	91%	7	125.7	60.1	37%	162.5	13.6
Discrete	21.0	90	20%	108.0	91%	7	125.7	44.0	37%	118.9	10.0
Idle	260.1	N/A	N/A	N/A	100%	9	9.0	39.0	8%	487.7	40.8
										GROSS TOTAL characterized	361.5
										GROSS TOTAL measured	327.2

Table 9 provides a breakdown of the updated LVM defined profile. For the pavement terrain, tractive power is estimated as 114 kW, with 20% brake power (as a function of tractive power), and the engine efficiency is the highest, at 37%. For the secondary terrain, the tractive power is 53.1 kW with 25% brake power, and engine efficiency is 29%. For trails and cross-country, the tractive power is 41.2 kW and 37.3 kW, respectively. Brake power is 25% and engine efficiency is 25%. For the idle operation, accessory power is assumed to be 9 kW and operating at an engine efficiency of 8%. These values were confirmed by the project contributors. While the transit and discrete terrains were included for the fuel economy analysis, they were not included in the final LVM characterization as they were not included in the mission profile.

Table 9: LVM defined profile

Terrain	Time (min)	Tractive power (kW)	Brake power (% of tractive power)	Output power (kW)	Transmission efficiency (%)	Accessory power (kW)	ICE power (kW)	ICE output energy (kWh)	ICE efficiency (%)	ICE fuel energy (kWh)	Fuel (kg)
Pavement	26.7	114.0	20%	136.8	91%	7	157.3	69.9	37%	189.0	15.8
Secondary	100.0	53.1	25%	66.4	91%	7	79.9	133.2	29%	459.4	38.5
Trails	150.0	41.2	25%	51.5	91%	7	63.6	159.0	25%	635.9	53.3
Cross country	200.0	37.3	25%	46.6	91%	7	58.2	194.1	25%	776.5	65.0
Idle	120.0	N/A	N/A	N/A	100%	9	9.0	18.0	8%	225.0	18.8
GROSS TOTAL characterized											191.4

In order to input the LVM profile into ePOP as a cycle, tractive and braking energy, power and duration must be calculated for each terrain type. Traction energy is output power multiplied by total terrain duration. Traction duration is time allocated to tractive effort, not braking; 80% for pavement terrain, for example. Traction power is energy divided by duration, in hours. For brake energy, it is the brake percentage multiplied by traction energy. Brake duration is the time allocated to braking; 20% for pavement terrain. And similarly, brake power is brake energy divided by braking time. Table 10 outlines the values calculated for each terrain.

Table 10: LVM defined profile – energy, power, duration

Terrain	Traction energy (kWh)	Tractive duration (hr)	Traction power (kW)	Brake energy (kWh)	Brake time (hr)	Brake power (kW)
Pavement	60.8	0.36	171.0	12.2	0.09	136.8
Secondary	110.6	1.25	88.5	27.7	0.42	66.4
Trails	128.8	1.88	68.7	32.2	0.63	51.5
Cross country	155.4	2.50	62.2	38.9	0.83	46.6

Figure 25 is a plot of the LVM characterization profile. There are four different terrain sections in the profile; pavement, secondary, trails, and cross-country. The tractive power is positive while the braking energy is negative. The peak power is 320 kW while the average power is 34.6 kW. This is a much smaller average power than the primary road cycle; which was 125 kW.

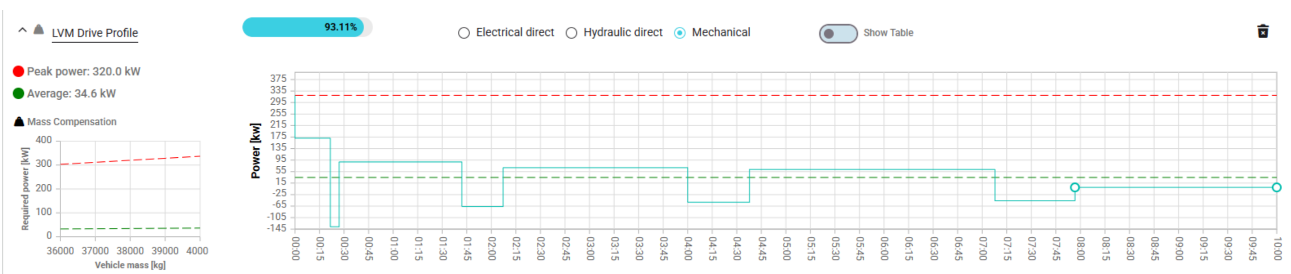

Figure 25: LVM characterization mechanical energy drive profile

Figure 26 is a plot of the combined LVM characterization profile, including auxiliaries and the same electrical energy as in Figure 23, from the primary road cycle.

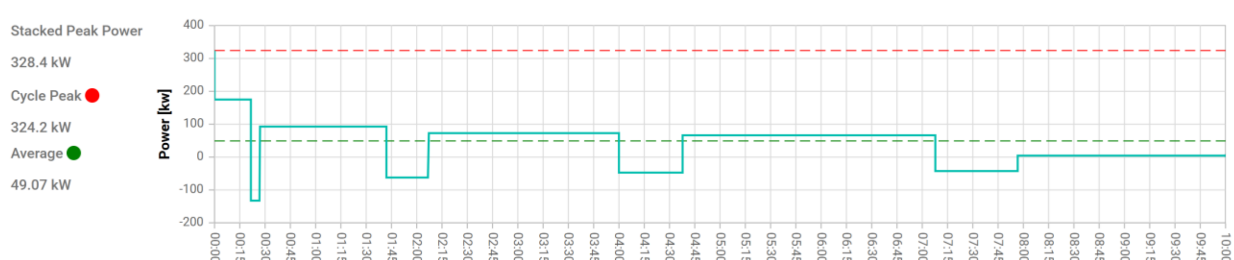

Figure 26: LVM characterization combined drive profile

4.2 ePOP Concept Tool

In 2025, ZeBeyond developed the Electrified Propulsion Optimization Process (ePOP) concept tool, a software platform designed to estimate the cost, efficiency, mass, volume, and power duration of various electrified powertrain configurations [58]. The tool employs a system-level modeling approach to assess complex trade-offs among powertrain architectures, component technologies, fuel types, and degrees of electrification. Using ePOP, powertrain concepts can be optimized across multiple key performance indicators (KPIs) tailored to specific vehicle types and operational applications. The tool scales powertrain component technologies along the electrification spectrum, ranging from internal combustion engine (ICE)-only systems (0% electrification) to fully battery electric vehicles (BEVs) (100% electrification), including all hybrid configurations in between.

Unlike many traditional industry tools, which develop powertrain concepts prior to cycle evaluation, ePOP adopts a cycle-driven methodology that generates powertrain concepts based on a specific drive cycle. This approach ensures that each design is inherently optimized for the intended duty cycle and operational requirements. By embedding the drive cycle within the concept-generation process, ePOP enables more efficient design-space exploration and facilitates early identification of optimal trade-offs in cost, energy efficiency, and overall performance.

Drive System Design applies ePOP in its powertrain consulting and accelerated concept development activities, utilizing its capabilities to identify effective configurations across a wide range of electrification levels and vehicle applications. As the transportation sector progresses toward greater electrification and data-driven design, tools such as ePOP exemplify the shift toward integrated, model-based engineering practices that support informed decision-making, improved development timelines, and the advancement of sustainable vehicle technologies.

4.3 Technology Inputs and Vehicle Concepts

Six vehicle concepts were analyzed for this project. The vehicle concepts were the following:

- Baseline diesel-ICE
- Concept 1: H_2-ICE (no electrification)
- Concept 2: H_2-ICE parallel-hybrid
- Concept 3: H_2-ICE series-hybrid
- Concept 4: Fuel cell power dense (PD), series-hybrid
- Concept 5: Fuel cell efficiency optimized (EF), series-hybrid

The baseline concept is the current diesel-ICE conventional vehicle. This is the vehicle against which all other concepts will be analyzed. It is the current benchmark design. The first concept is a straight H_2-ICE vehicle. For this concept, the engine is replaced with a hydrogen combustion engine, and the fuel is replaced with solid-state hydrogen. The purpose of this concept is to understand how changing the fuel source to hydrogen, without electrical hybridization, impacts the vehicle design in terms of mass and volume. For all the concepts evaluated, solid-state hydrogen is the fuel source of choice. As discussed in Section 3.7, while the commercialization of solid-state hydrogen storage is relatively low, the opportunity for higher density storage with solid-state over gaseous or liquid hydrogen storage exists. Furthermore, due to its low pressure and higher relative storage temperature, there are fewer potential safety risks. A follow-on study is recommended to examine the potential risks of solid-state hydrogen for military vehicles as fuel for in-combat and non-combat missions.

The second and third concepts are an H_2-ICE parallel-hybrid and an H_2-ICE series-hybrid. There are differences in engine efficiency between parallel and series operation. There are additionally differences in number of components and complexity of design between parallel and series. In a series-design with a combustion engine, the energy is transformed from mechanical into electrical before being fed into the electrical motor and driving the wheels.

The fourth and fifth concepts are hydrogen fuel cell designs. The fourth concept is optimized for power while the fifth concept is optimized for efficiency. As stated in Figure 17, the fuel cell outputs its highest power at high current density but the overall system efficiency is lower in this region. At lower output power, around 25%, the system efficiency is the highest, at 60%. By analyzing both concepts, it's possible to understand what is the trade-off between fuel cell power and weight and fuel tank size and weight. This analysis was critical to determine the effect of efficiency improvements in platform-level energy requirements. Due to the diminishing returns from having more hydrogen on the platform, efficiency increases of the conversion process can have significant effects at the platform level.

After all five concepts are evaluated, two concepts are then promoted and extrapolated out using "tomorrow" and "future" technology values. These are potentially commercially predicted values or target values from governing body organizations. Tomorrow values are expected in the next 10 years and future values are expected in 15 to ~20 years, approximately.

The approach for this project was to use generic volumetric power and energy density and generic gravimetric power and energy values for each technology as inputs. Using the ePOP tool, the components were then right-sized for the desired drive cycle and basic vehicle level requirements. These components do not necessarily exist commercially; but their volumetric and gravimetric power and energy density values are derived or based on today's existing commercial products. Volumetric power density is the power per unit volume, typically kW per litre. Gravimetric power density is the power per unit mass, typically kW per kilogram; also called specific power. Volumetric and gravimetric energy density is energy per unit volume or mass, typically kWh per litre or kilogram.

Table 11 contains all the technology input values. Starting with prime power, or engine power, there are many different efficiency values defined, which were provided by the different subject matter experts or from literature. Here also the ICE term is used to interchangeably to apply to the hydrogen combustion engine and fuel cell designs. For the combustion engine powertrains, the efficiency values will change based on the configuration (series, parallel) as well as the drive cycle (primary, LVM). MAHLE performed some analysis to predict torque as a function of engine speed, overlayed with efficiency [23], to estimate efficiency. For the tomorrow and future efficiency of the H_2-ICE series hybrid, it's assumed the efficiency will increase by +3% for both tomorrow and future. For the fuel cell, the efficiency increase is based on the US Department of Energy (DOE) hydrogen and fuel cell technologies office multi-year program plan targets [59].

One disadvantage of the hydrogen solid-state storage is the energy penalty when the hydrogen is released for use on the vehicle. This technology is in its commercial infancy and it's currently predicted that as much as 30% of the energy content of the released hydrogen is required by the release system. This energy penalty is captured under the "fuel" section of Table 11, but ultimately impacts the overall engine efficiency. Effective H_2 release adjusted efficiency numbers are calculated for all engines by taking the original engine efficiency and multiplying it by one minus 30% to get a new reduced overall engine efficiency. It's assumed that for the tomorrow and future values, this release energy will be reduced to 25% and then 20%, respectively.

For the volumetric and gravimetric engine power density, the diesel value is based on the current engine density. The H_2-ICE values were provided by MAHLE. The fuel cell today power dense value is based on the median value of commercially available higher power (150 to 300 kW) fuel cell systems from well-known manufacturers and suppliers (e.g., Ballard, Bosch, Cummins, Plug Power, REFIRE, Symbio, and Toyota Motor). For the efficiency optimized fuel cell, the volumetric and gravimetric engine power density is set at one fourth of the power of the power dense value but the efficiency increases from 40 to 60% here. The waste heat rejection to the coolant for the combustion engine is assumed to be 60% and reduced to 55% and 50% for tomorrow and future. The fuel cell heat rejection is assumed to be 100%.

The gravimetric energy density of hydrogen alone is 33.3 kWh/kg while diesel is 11.94 kWh/kg. The volumetric and gravimetric energy density of the hydrogen and storage and release system is provided from calculations by BAK Motors and Plasma Kinetics [36]. The tomorrow and future values are based on storage targets from the US DOE [60]. It must be noted that the overall powertrain weight for hydrogen includes the weight of the storage system, not just the hydrogen fuel being used. In the case of the Plasma Kinetics system, the gravimetric storage capacity is in the vicinity of 3.5% by weight. This means that efficiency increases that reduce the amount of hydrogen required can have large effects on the weight of the storage system required to carry it on board.

Only the diesel baseline, H_2-ICE and H_2-ICE parallel hybrid use a transmission. It is based off the 4500 SP transmission manufactured by Allison, who make automatic gearboxes for commercial and military vehicles. The other concepts use an electric drive unit (EDU), which is an integrated assembly that contains the motor, transmission, power electronics, housing and cooling system.

For batteries, the chemistry is not specified and left open; but these values are based on lithium iron phosphate (LFP) as the technology for today. The energy density values are derived from the Advanced Propulsion Centre UK electrical energy storage technical roadmap [61]. This decision was made based on NATO standards for T6 batteries and current qualification requirements to use batteries in military platforms. The battery technology of tomorrow is chemistry agnostic and presupposes that such batteries would be capable of operating in extreme environments required by military platforms.

The ESOX group provided motor power density numbers, based on their in-wheel hub technology, as well as efficiency values [62]. In-wheel hub motors were selected for this analysis to eliminate as much volume and weight as possible from the chassis to make room for battery and hydrogen storage.

The power electronics values, namely inverter, DCDC, and onboard charger density values come from a report by the Automotive Council UK on the technology indicators for heavy-duty vehicles [63].

And finally, the cooling system coefficient of performance (COP) is provided based on the baseline diesel vehicle. All of these values are used as inputs into the ePOP component library to define the vehicle concepts.

Table 11: Technology inputs

Tech. era	**Today**	**Today**	**Today**	**Today**	**Today**	**Today**	**Tomorrow**	**Future**	**Tomorrow**	**Future**
Parameter / Vehicle	Diesel baseline	H_2-ICE	H_2-ICE, parallel hybrid	H_2-ICE, series hybrid	Fuel cell power dense, series hybrid	Fuel cell eff. optimized, series hybrid	H_2-ICE, series hybrid	H_2-ICE, series hybrid	Fuel cell eff. optimized, series hybrid	Fuel cell eff. optimized, series hybrid
Prime power (engine)										
Eff. – ICE only, primary [23]	37%	39%	39%	39%	--	--	39%	41%	--	--
Eff. – ICE only, LVM [23]	25%	27%	27%	27%	--	--	27%	29%	--	--
Eff. – Series [23, 59]	--	--	--	43%	40%	60%	47%	50%	65%	70%
Eff. – Parallel [23]			41%	--	--	--	--	--	--	--
Eff., H_2 release adj. – ICE only, primary	--	27.3%	27.3%	27.3%	--	--	29.3%	32.8%	--	--
Eff., H_2 release adj. – ICE only, LVM	--	18.9%	18.9%	18.9%	--	--	20.3%	23.2%	--	--
Eff., H_2 release adj. – Series	--	--	--	30.1%	28%	42%	35.3%	40%	48.8%	56%
Eff. H_2 release adj. – Parallel	--	--	28.7%	--	--	--	--	--	--	--
Vol. power density (kW/L)	0.362	0.210	0.321	0.187	0.280	0.070	0.321	0.321	0.163	0.213
Grav. power density (kW/kg)	0.300	0.265	0.265	0.211	0.420	0.105	0.265	0.265	0.163	0.163
Waste heat rejection to cooler (%)	60%	60%	60%	60%	100%	100%	55%	50%	100%	100%
Fuel										
Grav. energy density (kWh/kg), fuel only	11.94	33.3	33.3	33.3	33.3	33.3	33.3	33.3	33.3	33.3
Type	Diesel	Solid-state H_2	Solid-state H_2	Solid-state H_2	Solid-state H_2	Solid-state H_2	Solid-state H_2	Solid-state H_2	Solid-state H_2	Solid-state H_2
Vol. power density (kW/L) [36, 60]	9.70	0.68	0.68	0.68	0.68	0.68	1.80	2.20	1.80	2.20
Grav. energy density (kWh/kg) [36, 60]	11.4	1.06	1.06	1.06	1.06	1.06	1.30	1.70	1.30	1.70
Release energy eff.	--	30%	30%	30%	30%	30%	25%	20%	25%	20%
Transmission										
Type	Allison 4500 SP	2025 Multispeed	2025 Multispeed	EDU: incl. in motor	EDU: incl. in motor	EDU: incl. in motor	EDU: incl. in motor	EDU: incl. in motor	EDU: incl. in motor	EDU: incl. in motor
Vol. power density (kW/L)	1.49	1.49	1.49	--	--	--	--	--	--	--
Grav. power density (kW/kg)	0.84	0.84	0.84	--	--	--	--	--	--	--

Tech. era	Today	Today	Today	Today	Today	Today	Tomorrow	Future	Tomorrow	Future
Parameter / Vehicle	Diesel baseline	H_2-ICE	H_2-ICE, parallel hybrid	H_2-ICE, series hybrid	Fuel cell power dense, series hybrid	Fuel cell eff. optimized, series hybrid	H_2-ICE, series hybrid	H_2-ICE, series hybrid	Fuel cell eff. optimized, series hybrid	Fuel cell eff. optimized, series hybrid
Batteries [61]										
Peak C-rating	--	5	5	5	5	5	10	15	10	15
Continuous C-rating	--	3	3	3	3	3	5	7	5	7
Vol. energy density (Wh/L)	--	260	260	260	260	260	500	800	500	800
Grav. specific energy (Wh/kg)	--	140	140	140	140	140	280	420	280	420
Motors / Generators [62]										
Efficiency (%)	70%	70%	85%	85%	85%	85%	90%	93%	90%	93%
Vol. power density (kW/L)	0.21	0.21	11.6	11.6	11.6	11.6	5.8	6.0	5.8	6.0
Grav. power density (kW/kg)	0.34	0.34	10.2	10.2	10.2	10.2	5.6	5.8	5.6	5.8
Power electronics (inverters) [63]										
Efficiency (%)	--	--	97%	97%	97%	97%	98%	98.5%	98%	98.5%
Vol. power density (kW/L)	--	--	36	36	36	36	36.7	40	36.7	40
Grav. power density (kW/kg)	--	--	22	22	22	22	22	30	22	30
Power electronics (DCDC converters) [63]										
Efficiency (%)	--	--	98%	98%	98%	98%	98.5%	99%	98.5%	99%
Vol. power density (kW/L)	--	--	3.5	3.5	3.5	3.5	4	5	4	5
Grav. power density (kW/kg)	--	--	2.5	2.5	2.5	2.5	3.25	4	3.25	4
Power electronics (onboard chargers) [63]										
Efficiency (%)	--	--	98%	98%	98%	98%	98.5%	99%	98.5%	99%
Vol. power density (kW/L)	--	--	3	3	3	3	4	5	4	5
Grav. power density (kW/kg)	--	--	3.5	3.5	3.5	3.5	4.5	5.5	4.5	5.5
Cooling system										
COP (kW rejected / kW cooling fan)	20	20	20	20	20	20	25	35	25	35
Vol. power density, reject. heat (reject. kW/L)	28	28	28	28	28	28	32	36	32	36
Grav. power density, reject. heat (reject. kW/kg)	8	8	8	8	8	8	10	12	10	12
Vol. power density, fan power (fan kW/L)	1.4	1.4	1.4	1.4	1.4	1.4	1.28	1.03	1.28	1.03
Grav. power density, fan power (fan kW/kg)	0.4	0.4	0.4	0.4	0.4	0.4	0.4	0.34	0.4	0.34

5.0 Analysis

In this section each vehicle concept is presented and analyzed. In total 18 vehicle concepts are evaluated; five powertrain configurations (H_2-ICE, H_2-ICE parallel-hybrid, H_2-ICE series-hybrid, fuel cell power dense and fuel cell efficiency optimized), two sets of drive cycles (primary and logistics vehicle mission), and three technology eras (today, tomorrow, and future). Table 12 summarizes the vehicle concept definitions.

Table 12: Vehicle concept definitions

Count	Duty cycle type	Powertrain	Technology values
1	Primary, flat road	H_2-ICE	Today
2	Primary, flat road	Parallel hybrid, H_2-ICE	Today
3	Primary, flat road	Series hybrid, H_2-ICE	Today
4	Primary, flat road	Series hybrid, power dense fuel cell	Today
5	Primary, flat road	Series hybrid, efficiency optimized fuel cell	Today
6	Primary, flat road	Series hybrid, H_2-ICE	Tomorrow
7	Primary, flat road	Series hybrid, efficiency optimized fuel cell	Tomorrow
8	Primary, flat road	Series hybrid, H_2-ICE	Future
9	Primary, flat road	Series hybrid, efficiency optimized fuel cell	Future
10	Logistics vehicle characterization profile	H_2-ICE	Today
11	Logistics vehicle characterization profile	Parallel hybrid, H_2-ICE	Today
12	Logistics vehicle characterization profile	Series hybrid, H_2-ICE	Today
13	Logistics vehicle characterization profile	Series hybrid, power dense fuel cell	Today
14	Logistics vehicle characterization profile	Series hybrid, efficiency optimized fuel cell	Today
15	Logistics vehicle characterization profile	Series hybrid, H_2-ICE	Tomorrow
16	Logistics vehicle characterization profile	Series hybrid, efficiency optimized fuel cell	Tomorrow
17	Logistics vehicle characterization profile	Series hybrid, H_2-ICE	Future
18	Logistics vehicle characterization profile	Series hybrid, efficiency optimized fuel cell	Future

5.1 Primary Road Cycle

For this section, the vehicle concepts drive cycle is the primary road cycle, as outlined in Section 4.1.2.

5.1.1 Today Technology Values

For this section, the vehicle concepts technology values are based on “today” numbers. The prime power engine efficiency, volumetric and gravimetric power density varied for each technology concept. The hydrogen fuel volumetric power density was 0.68 kW/L while the gravimetric energy density was 1.06 kWh/kg. The H_2-ICE and H_2-ICE parallel-hybrid concepts include a transmission while all others do not. The battery gravimetric and volumetric energy density are 140 Wh/kg and 260 Wh/L, respectively while the continuous C-rating is 3 and the peak C-rating is 5. The H_2-ICE motor is the same as the diesel-baseline configuration while all other vehicle concept motors are 85% efficient, with 11.6 kW/L and 10.2 kW/kg, volumetric and gravimetric power density, respectively. Power electronics, including inverters, DCDC converters, and onboard chargers, are 97%, 98%, and 98% efficient, respectively. Their gravimetric power densities are 22 kW/kg, 2.5 kW/kg, and 3.5 kW/kg, respectively. Lastly the cooling system assumes the same parameters as the diesel-baseline, such as a volumetric cooling system fan power density of 1.4 kW/L.

5.1.1.1 Concept 1: H_2-ICE Conventional

Recall that concept 1 is a straight H_2-ICE conventional vehicle, no electric hybridization. Our continuous power requirement was 320 kW for 10-minutes. Figure 27 is a waterfall plot of the components which contribute to the overall power calculation. Starting from the left-side of Figure 27, the first bar is the continuous power output of the baseline-diesel engine, at 285.9 kW. The next bar would be the contribution to power by the battery, however, since this concept is H_2-ICE, no traction battery is included and therefore, the contribution is 0 kW. Next bar is the required additional contribution to the engine power due to the lower power density of the H_2-ICE engine; this value is 22.5kW. Next, is the power required by the coolant system to maintain the engine and battery temperature; this is a reduction in power of 10.4kW. The net continuous power output from the H_2-ICE concept is therefore 298 kW. It is undersized for our requirements and can only be increased by increasing the size of the overall engine. Furthermore, the baseline diesel-ICE vehicle power is also undersized for this requirement; which was a fundamental observation from a project contributor.

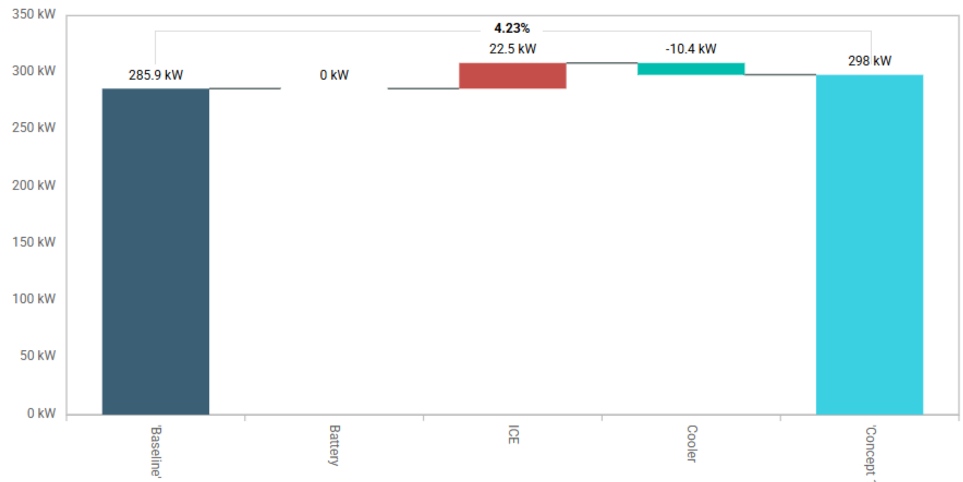

Figure 27: H_2-ICE, primary cycle, today values, component power

Figure 28 is a waterfall plot of the major vehicle components and the amount of mass they add, or subtract, as compared with the baseline diesel-ICE vehicle. The diesel baseline power train mass is composed of the motor, the generator, the engine, the fuel tank, the transmission, and the cooler. Overall, there is a 178% increase in mass from the diesel-ICE vehicle, the majority of which is due to the fuel tank and the engine size increase to provide the necessary power with the hydrogen fuel system's lower gravimetric energy density, as compared with diesel.

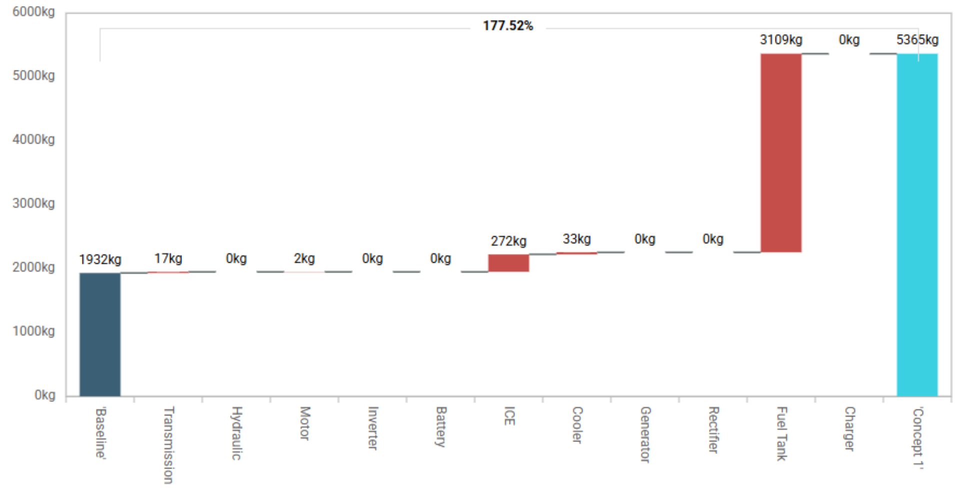

Figure 28: H_2-ICE, primary cycle, today values, component mass

More significant than the mass increase is the overall volume increase for the H_2-ICE concept. Figure 29 is a plot of the major system component volume breakdown. An increase in the fuel tank of 4,932 L is required to shift from diesel to H_2 solid-state storage.

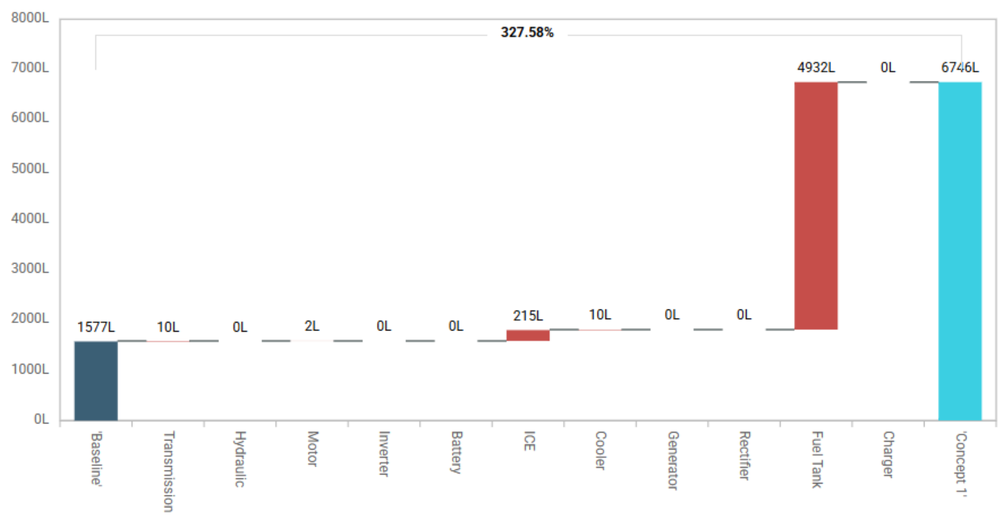

Figure 29: H_2-ICE, primary cycle, today values, component volume

5.1.1.2 Concept 2: H_2-ICE Parallel-Hybrid

Figure 30 is a plot of the component power source duration breakdown. This is for a continuous power requirement of 10-minutes, assuming the starting state of charge (SOC) of the battery is 100%. This design is optimized for minimum mass while still achieving the 320 kW continuous power requirement.

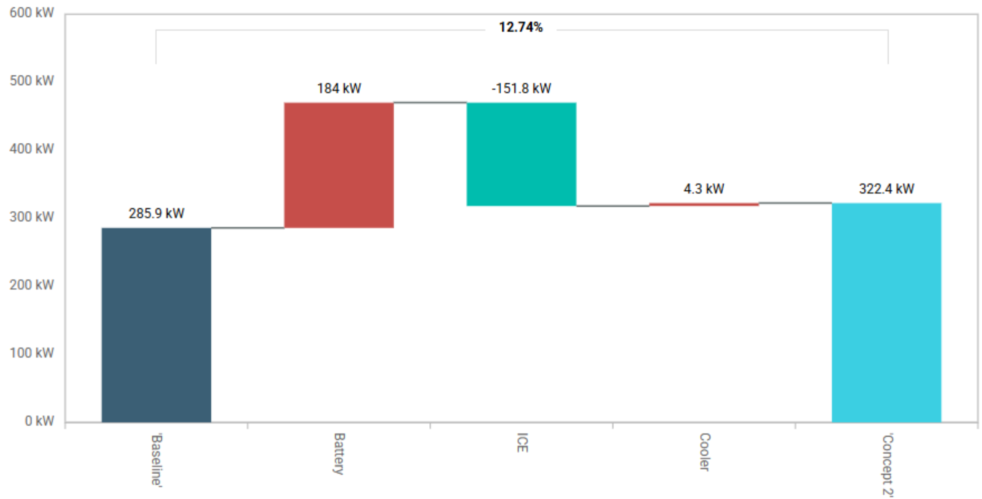

Figure 30: H_2-ICE parallel-hybrid, primary cycle, today values, component power

Figure 31 is a plot of powertrain total mass as a function of electrification (battery size). The baseline diesel vehicle is non-electrified and is therefore on the y-axis. The H_2-ICE parallel-hybrid vehicle is 5% electrified. The cursor has been placed to the right of the minimum vehicle mass. If placed at the minimum vehicle mass, the total continuous power for the vehicle is only 294.1 kW and does not meet the minimum continuous power requirement. To meet the minimum power requirement, an engineer could increase the battery size or increase the engine size, as desired. Here the battery size was increased.

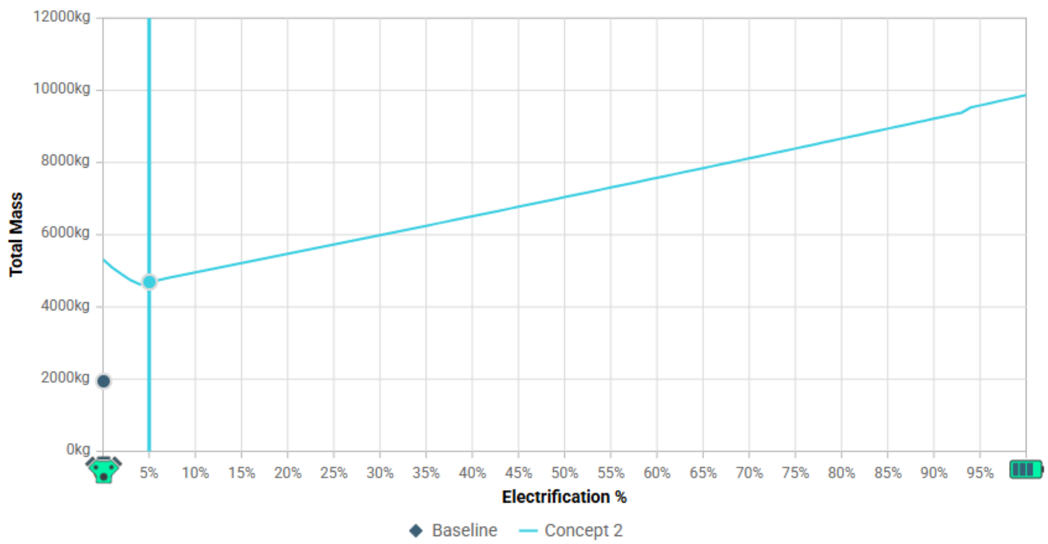

Figure 31: H_2-ICE parallel-hybrid, primary cycle, today values, electrification vs. total mass

Figure 32 is a plot of H_2-ICE parallel-hybrid component mass breakdown with the primary road cycle, and with today’s technology values. There is an increase in vehicle mass of 2,751 kg; predominantly from the fuel and the battery.

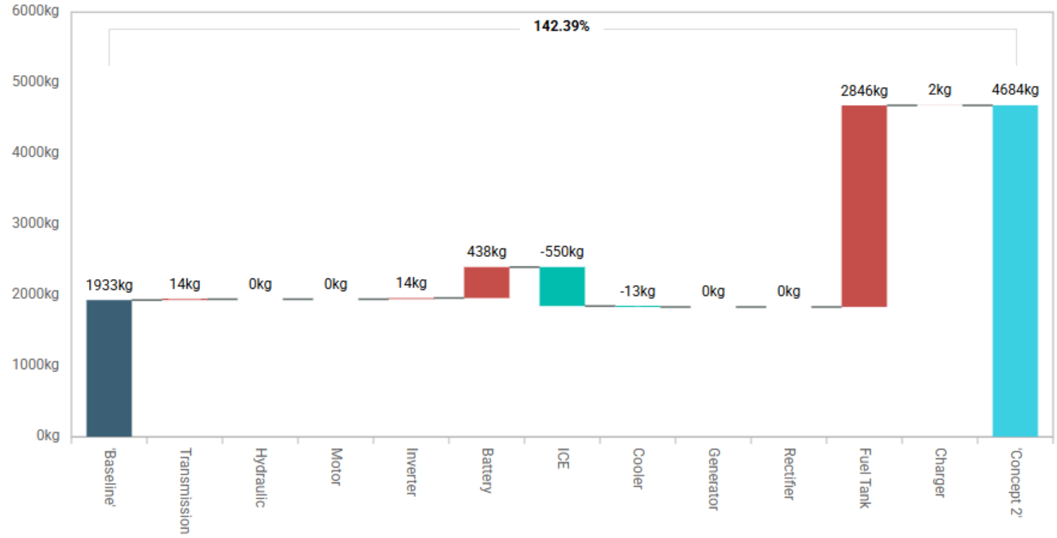

Figure 32: H_2-ICE parallel-hybrid, primary cycle, today values, component mass

Figure 33 is a plot of the H2-ICE parallel-hybrid component volume comparison breakdown under the primary road cycle with today's technology values. Overall, this powertrain has a 272% volume increase over the diesel baseline vehicle.

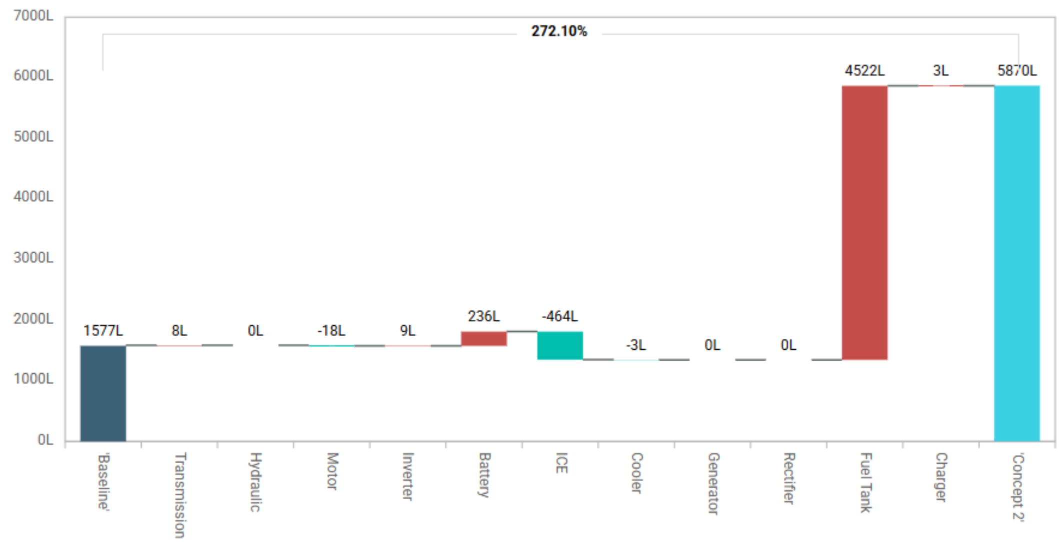

Figure 33: H_2-ICE parallel-hybrid, primary cycle, today values, component volume

5.1.1.3 Concept 3: H_2-ICE Series-Hybrid

Figure 34 is a plot of the H_2-ICE series-hybrid component power source duration comparison breakdown for a 10-minute continuous power requirement with a starting battery SOC of 100%. Overall, the engine power is downsized from the diesel-baseline and the battery is able to make up for the 10-minute power requirement.

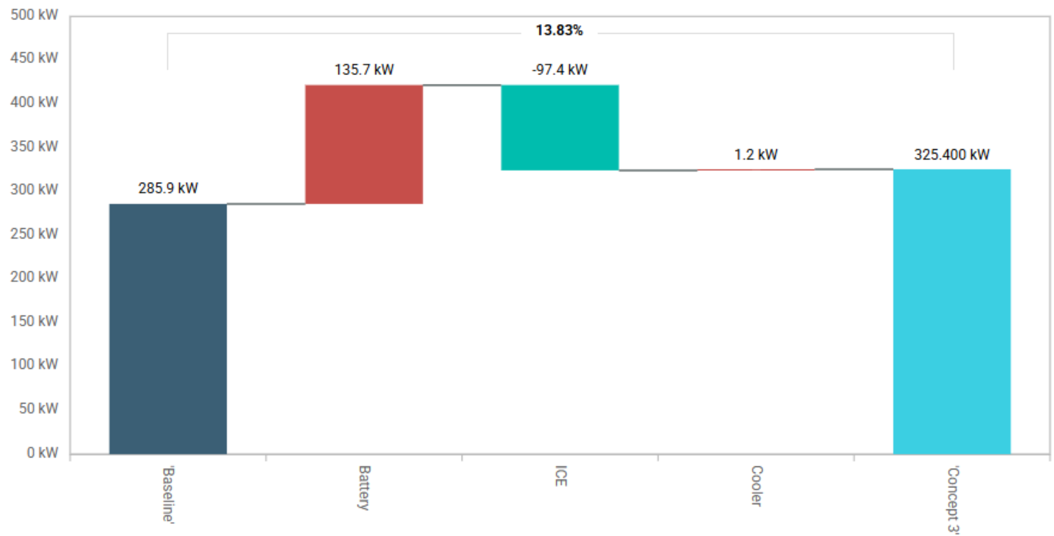

Figure 34: H_2-ICE series-hybrid, primary cycle, today values, component power

Figure 35 is a plot of the H_2-ICE series-hybrid component mass breakdown under the primary road cycle using today's technology values. Overall, this design has similar mass to the H_2-ICE conventional design but higher than the H_2-ICE parallel hybrid.

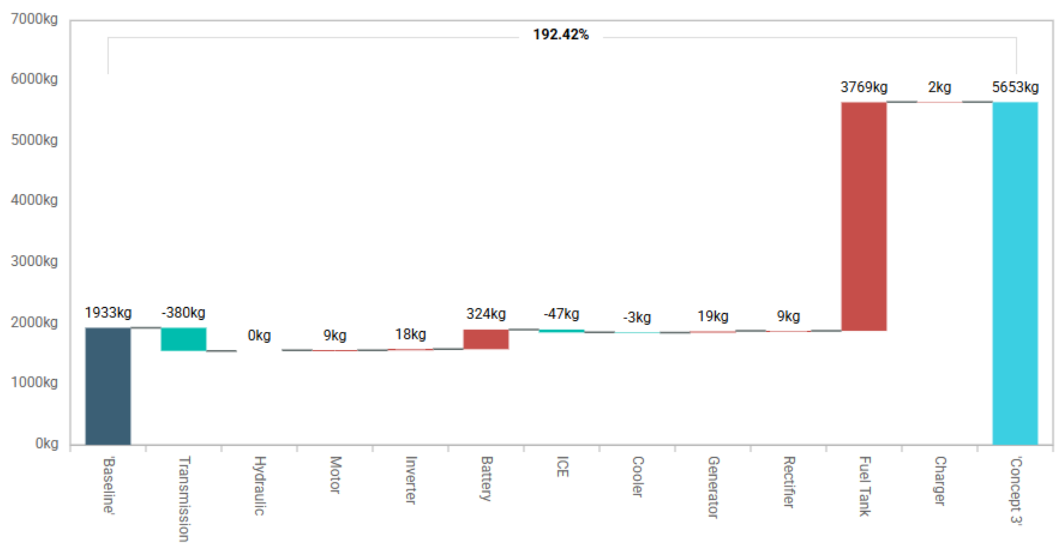

Figure 35: H_2-ICE series-hybrid, primary cycle, today values, component mass

Figure 36 is a plot of the H_2-ICE series-hybrid component volume breakdown for the primary road cycle and today technology values. For this design, by increasing the degree of electrification (becoming more of a battery electric vehicle), the overall volume will decrease but the mass will increase; this is due to volumetric battery capacity. This is different than the previous two vehicles, whose mass and volume were increasing with increasing electrification.

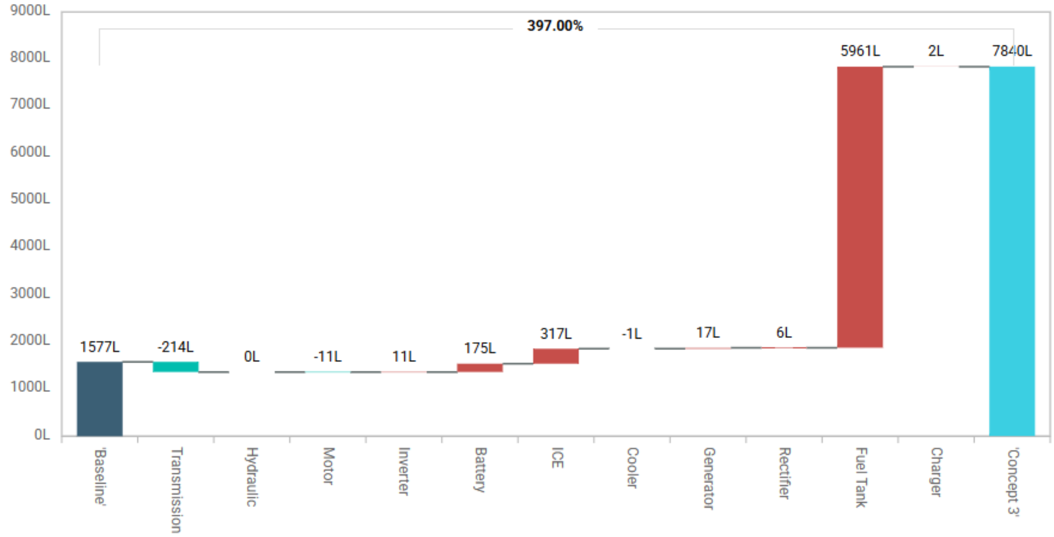

Figure 36: H_2-ICE series-hybrid, primary cycle, today values, component volume

5.1.1.4 Concept 4: Power Dense Fuel Cell Series-Hybrid

Figure 37 is a plot of the power dense fuel cell series-hybrid component power for a 10-minute continuous power duration when the starting battery SOC is 100%. As compared with the diesel-baseline, the engine is downsized overall while the battery is able to make-up the remaining required power for this continuous power requirement.

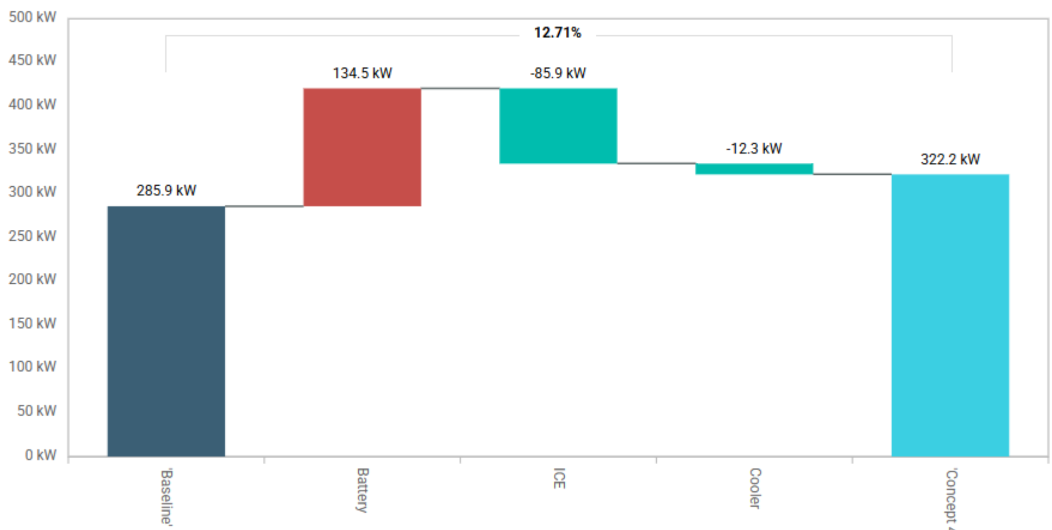

Figure 37: Power dense fuel cell series-hybrid, primary cycle, today values, component power

Figure 38 is a plot of the power dense fuel cell component mass for the primary road cycle under today technology values. The total powertrain mass is smaller than the H_2-ICE conventional or the H_2-ICE series-hybrid and similar to the H_2-ICE parallel-hybrid. The majority of weight comes from the fuel and fuel tank components.

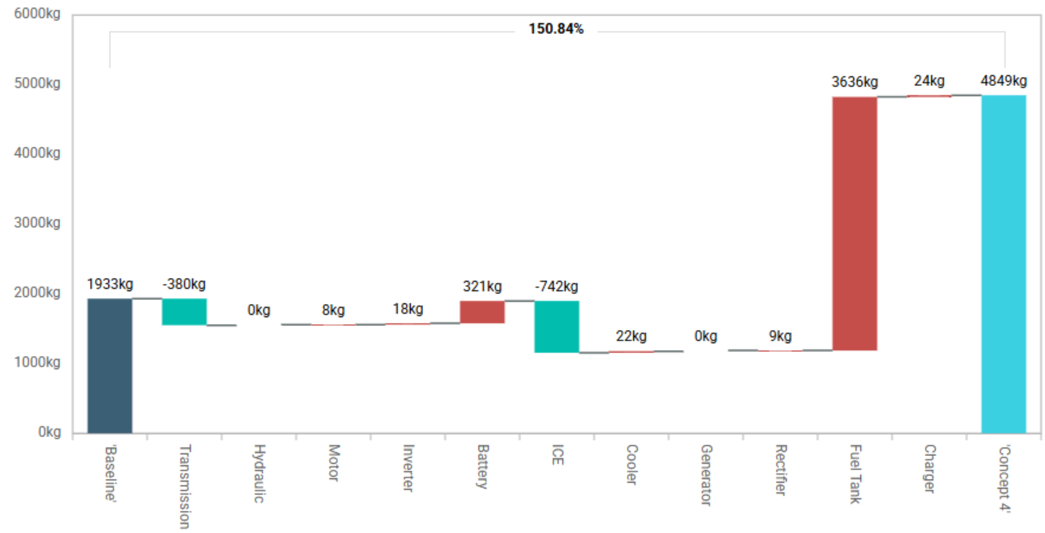

Figure 38: Power dense fuel cell series-hybrid, primary cycle, today values, component mass

Figure 39 is a plot of the power dense fuel cell series-hybrid component volume breakdown for the primary road cycle and today's technology values. The total powertrain volume is slightly above the H_2-ICE conventional powertrain. The predominant volume comes from the fuel tank and fuel.

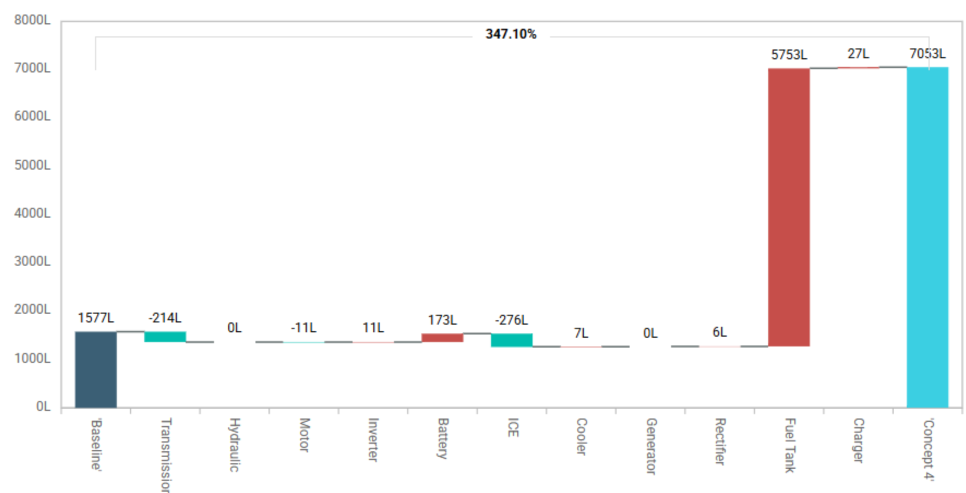

Figure 39: Power dense fuel cell series-hybrid, primary cycle, today values, component volume

5.1.1.5 Concept 5: Efficiency Optimized Fuel Cell Series-Hybrid

Figure 40 is a plot of the efficiency optimized fuel cell series-hybrid component power over a 10-minute duration. Recall that this efficiency optimized fuel cell operates nominally at one-quarter power, to take advantage of the higher efficiency, but can operate at full power continuously, assuming fuel is provided. Because of the oversized fuel cell, its able to meet all the drive cycle requirements and the continuous power requirement without additional battery power to the prime mover. The power calculation in Figure 40 assumes peak fuel cell operation. This analysis does not factor in that a small battery is required to start-up the fuel cell.

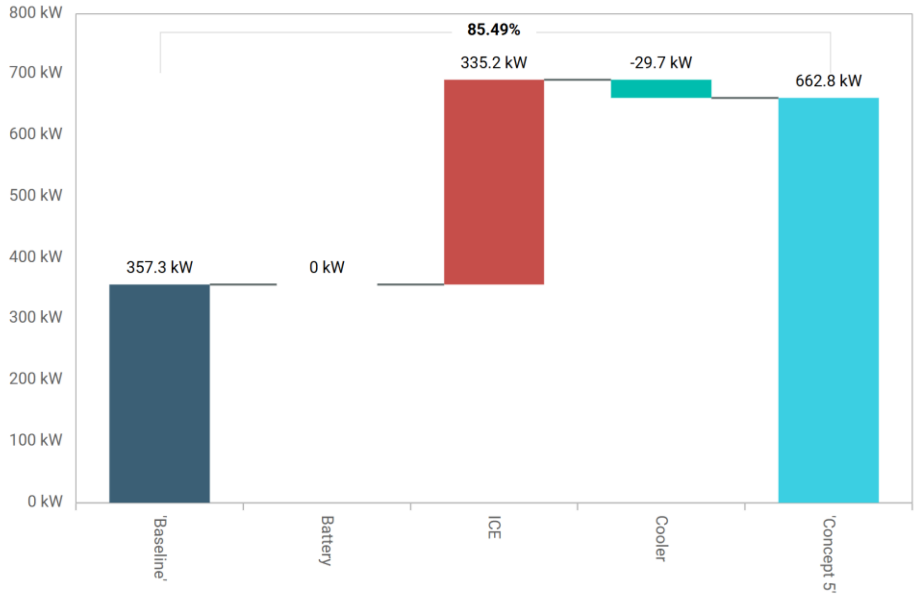

Figure 40: Eff. optimized fuel cell series-hybrid, primary cycle, today values, component power

Figure 41 is a plot of the efficiency optimized fuel cell series-hybrid component mass breakdown for the primary road cycle and today technology values. To date, this concept has the lowest powertrain mass but still much higher than the diesel-baseline.

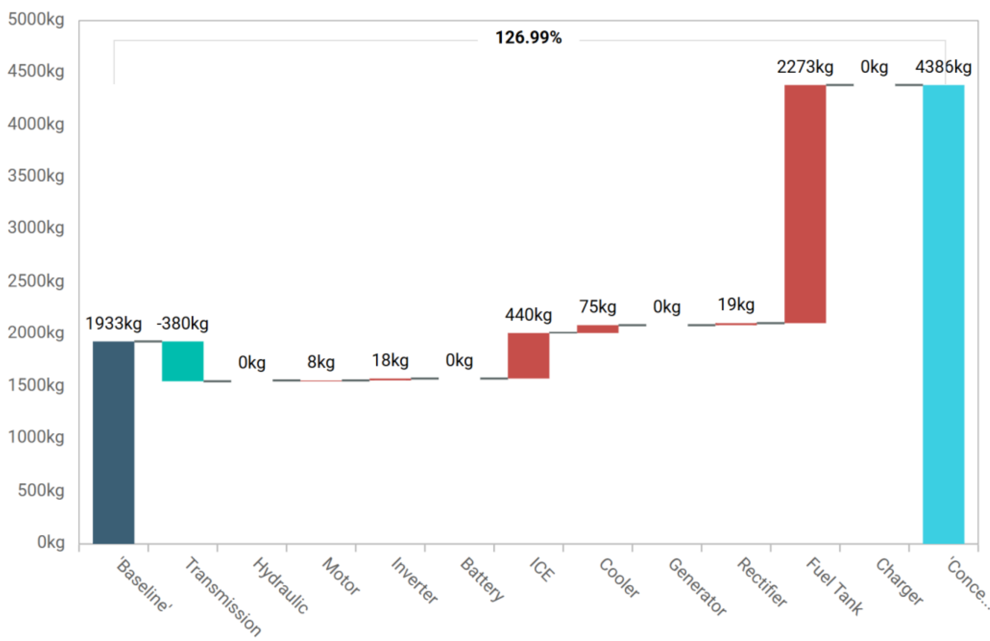

Figure 41: Eff. optimized fuel cell series-hybrid, primary cycle, today values, component mass

Figure 42 is a plot of the efficiency optimized fuel cell series-hybrid component volume breakdown for the primary road cycle and today technology values. This concept has the second smallest volume, after the H_2-ICE parallel-hybrid but is still much higher volume than the diesel-baseline.

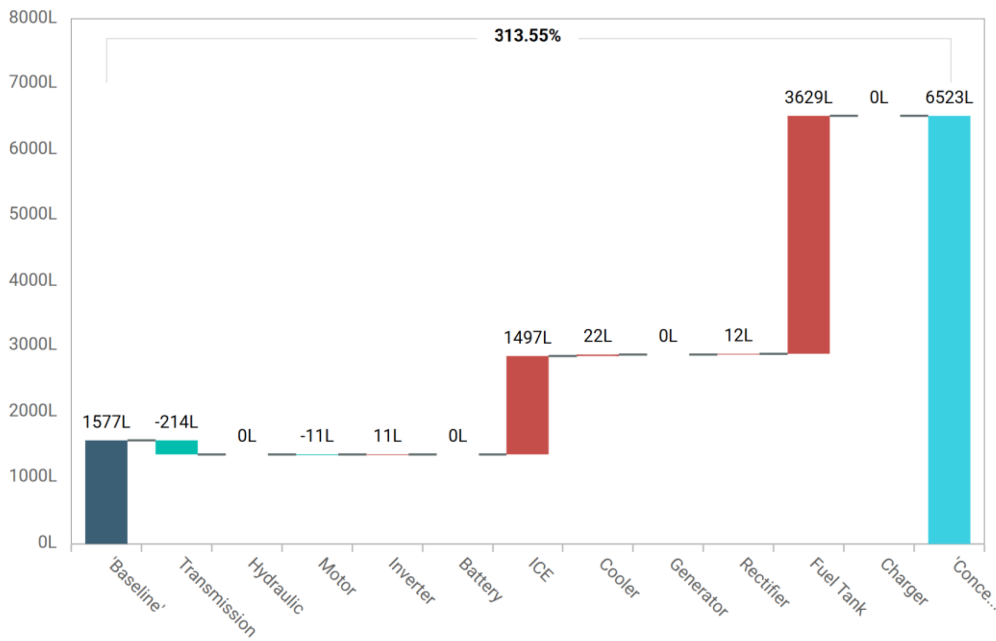

Figure 42: Eff. optimized fuel cell series-hybrid, primary cycle, today values, component volume

5.1.2 Tomorrow Technology Values

In this section the tomorrow technology values are applied to two concepts; the H_2-ICE series-hybrid and the efficiency optimized fuel cell series-hybrid design. For the H_2-ICE series-hybrid, the engine efficiency is 47% and the volumetric and gravimetric power density are 0.321 kW/L and 0.265 kW/kg, respectively. For the efficiency optimized fuel cell, the engine efficiency is 65% and the volumetric and gravimetric power density are the same; both 0.163 kW/L and 0.613 kW/kg. For hydrogen fuel, the release energy efficiency is reduced from 30% to 25%. The volumetric power density and gravimetric energy density are 1.80 kW/L and 1.30 kWh/kg. The battery volumetric and gravimetry energy density are 500 Wh/L and 280 Wh/kg, respectively; while the continuous C-rating is 5 and the peak C-rating is 10. The motor efficiency is increased to 90% and the volumetric and gravimetric power density is reduced to 5.8 kW/L and 5.6 kW/kg, respectively. For the power electronics, there is a slight increase of efficiency by 0.5 to 1% and only a small decrease in power density. For the cooling system, there is no change to the gravimetric power density but the COP is increased to 25 kW rejected / kW cooling fan.

5.1.2.1 Concept 3: H_2-ICE Series-Hybrid

Figure 43 is a plot of the H2-ICE series-hybrid, primary road cycle power comparison for a 10-minute continuous power requirement with a battery starting SOC 100% using tomorrow technology values. To achieve the desired power value, the degree of electrification can be increased or decrease using a coarse slider in ePOP. The power steps in increments of 50 kW. In order to meet the 320 kW requirement, the power is set to 369 kW.

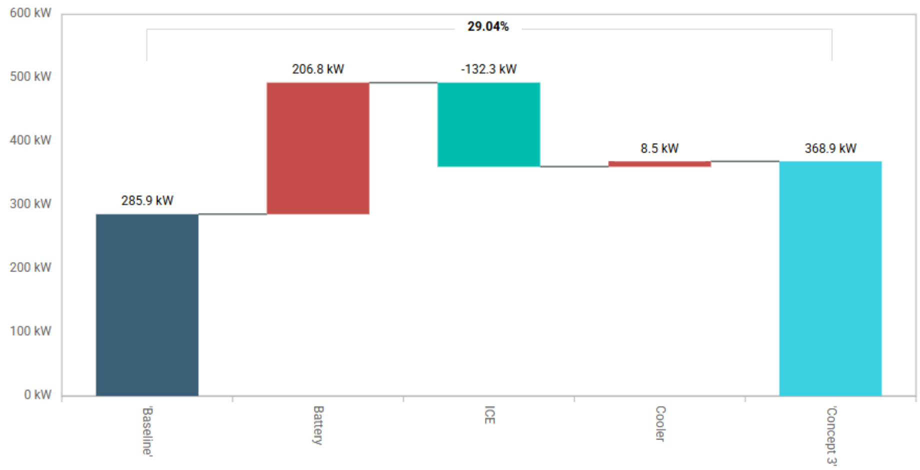

Figure 43: H_2-ICE series-hybrid, primary cycle, tomorrow values, component power

Figure 44 is a plot of the H_2-ICE series-hybrid component mass breakdown for the primary road cycle with tomorrow's technology values. Globally, a decrease in powertrain mass of 2,000 kg is observed from today technology values. The total mass is still higher than the current diesel-baseline powertrain.

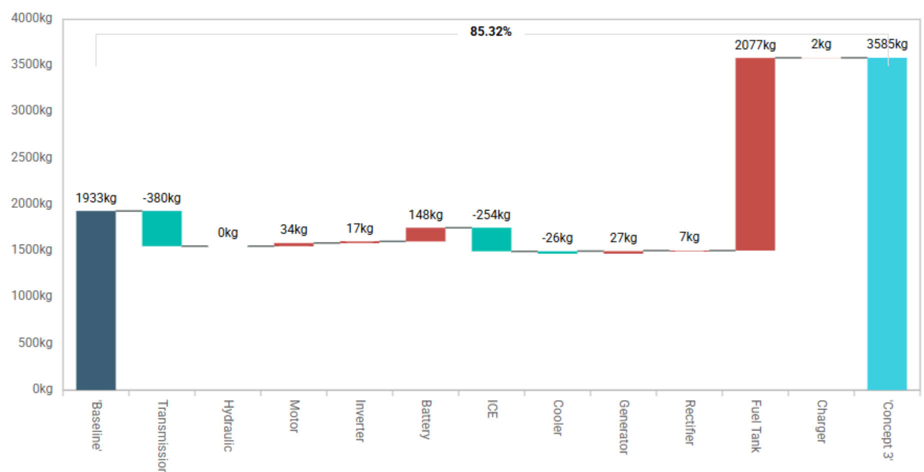

Figure 44: H_2-ICE series-hybrid, primary cycle, tomorrow values, component mass

Figure 45 is a plot of the H_2-series hybrid component volume breakdown under the primary road cycle and with tomorrow's technology values. There is a decrease in volume of almost 5,000 L from the today technology values for the same drive cycle and vehicle type. The powertrain is still 1,400 L larger than the diesel-baseline powertrain, with today technology values.

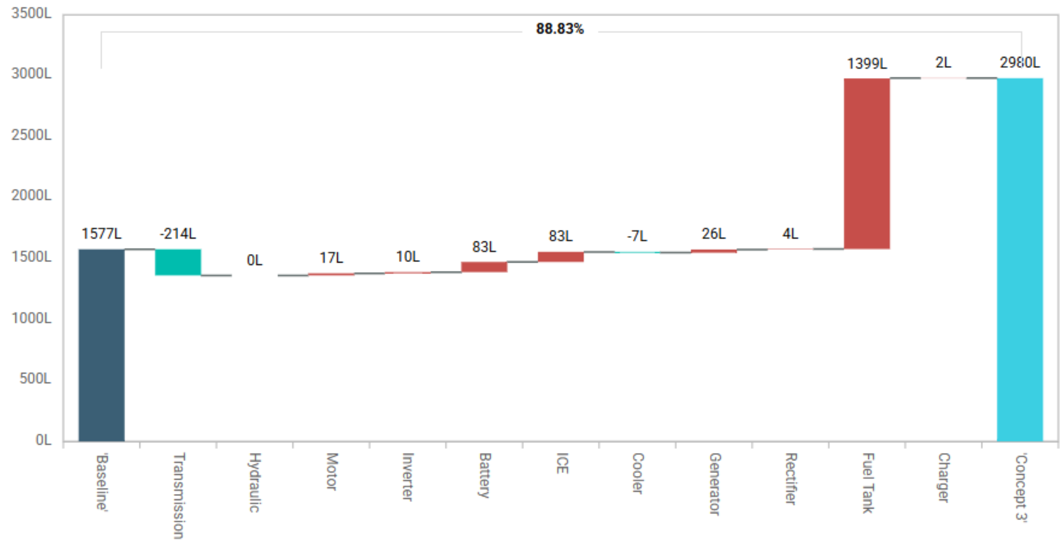

Figure 45: H_2-ICE series-hybrid, primary cycle, tomorrow values, component volume

5.1.2.2 Concept 5: Efficiency Optimized Fuel Cell Series-Hybrid

Figure 46 is a component power breakdown for the efficiency optimized fuel cell under the primary road cycle, with tomorrow technology values, for a 10-minute continuous power duration and starting battery SoC 100%.

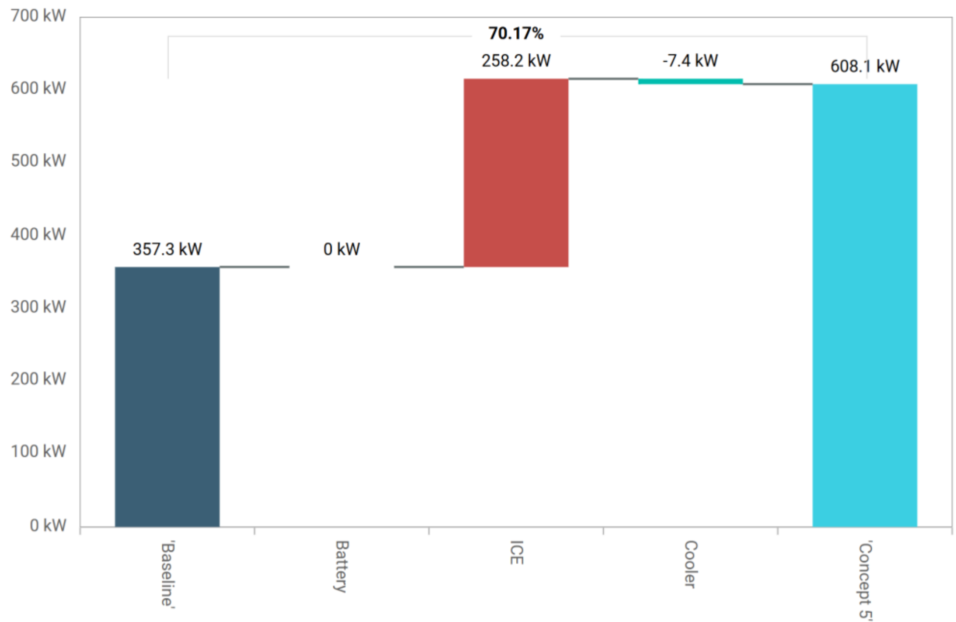

Figure 46: Eff. optimized fuel cell series-hybrid, primary cycle, tomorrow values, component power

Figure 47 is a plot of the component mass breakdown for the efficiency optimized fuel cell concept vehicle under the primary road cycle using tomorrow's technology values. There is a 1,700 kg decrease in mass from the same concept under today technology values; this concept still has larger mass than the diesel-baseline.

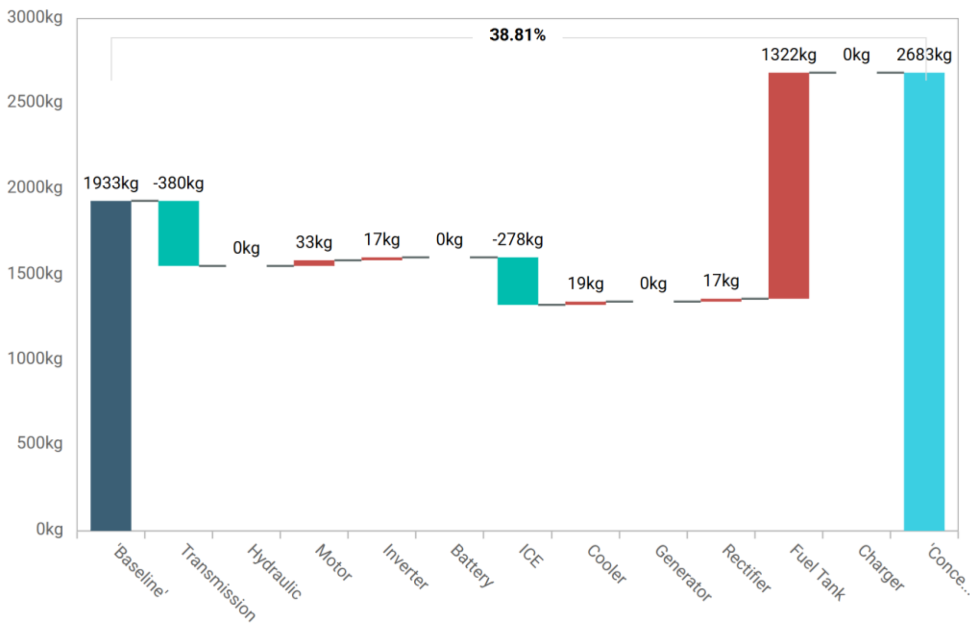

Figure 47: Eff. optimized fuel cell series-hybrid, primary cycle, tomorrow values, component mass

Figure 47 is a plot of the component volume breakdown for the efficiency optimized fuel cell concept vehicle under the primary road cycle using tomorrow's technology values. There is a decrease of 4,330 L of volume from todays technology values, for the same concept.

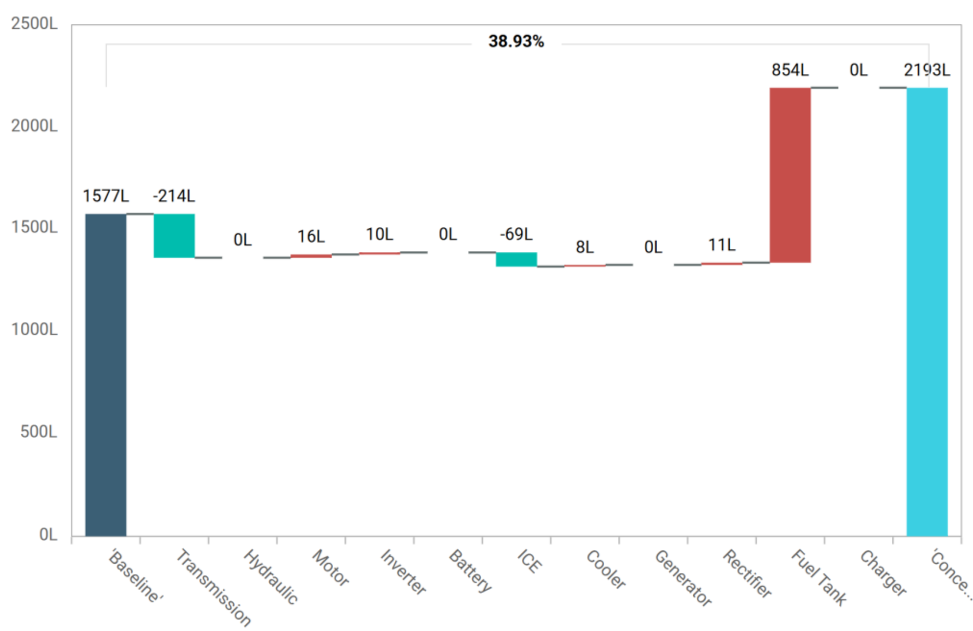

Figure 48: Eff. optimized fuel cell series-hybrid, primary cycle, tomorrow values, component volume

5.1.3 Future Technology Values

In this section the future technology values are applied to two concepts; the H_2-ICE series-hybrid and the efficiency optimized fuel cell series-hybrid design. For the H_2-ICE concept, the engine efficiency is increased to 50% while there is no change in the power density from tomorrow values. For the efficiency optimized fuel cell, the engine efficiency is increased to 70% and the volumetric and gravimetric power density are 0.213 kW/L and 0.163 kW/kg, respectively. For the hydrogen fuel, the release energy efficiency is further reduced to 20%. The volumetric power density is 2.20 kW/L while the gravimetric energy density is 1.70 kWh/kg. For the battery, the continuous C-rate is 7 while the peak C-rate is 15. The volumetric and gravimetric energy density are 800 Wh/L and 420 Wh/kg, respectively. For the motors, the efficiency increases to 93% and there is a slight increase of 0.2 in both volumetric and gravimetric power density. For the power electronic components; inverters, DCDC, and onboard charger, a small increase in power density is observed. For the cooling circuit, the gravimetric power density of the fan decreases to 0.34 kW/kg and the COP is 35 kW rejected / kW cooling fan.

5.1.3.1 Concept 3: H_2-ICE Series-Hybrid

Figure 49 is a plot of the power breakdown for a 10-minute continuous power requirement with a starting battery SOC of 100% for the H_2-ICE series-hybrid concept using the primary road cycle and future technology values.

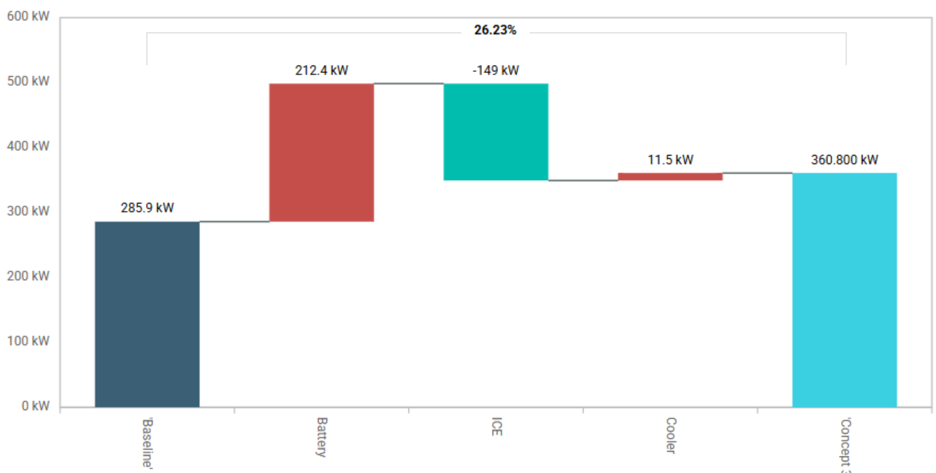

Figure 49: H_2-ICE series-hybrid, primary cycle, future values, component power

Figure 50 is a plot of the component mass breakdown for the H_2-ICE series-hybrid concept under the primary road cycle and future technology values. The most significant change is the reduction in mass for the fuel tank. This is due to increasing efficiency as well as increased gravimetric energy density of the fuel system.

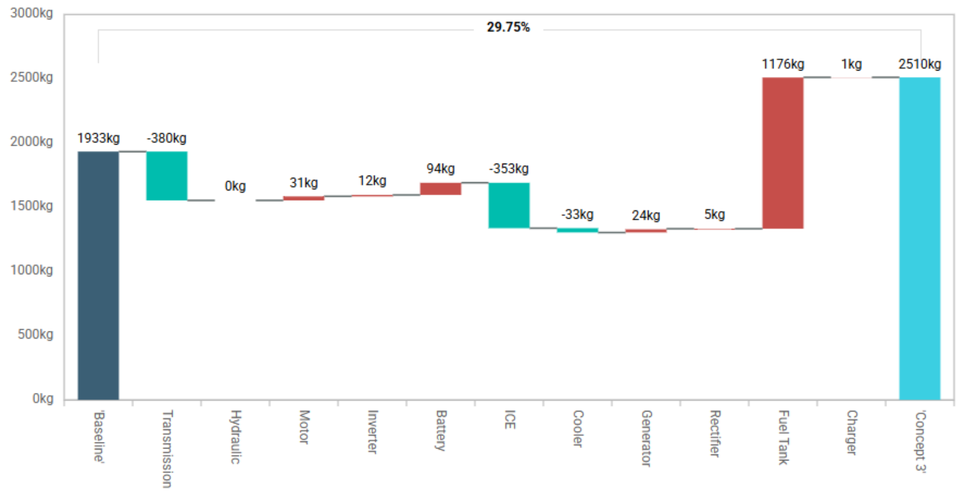

Figure 50: H_2-ICE series-hybrid, primary cycle, future values, component mass

Figure 51 is a plot of the component volume breakdown for the H_2-ICE series-hybrid concept design for the primary road cycle and future technology values.

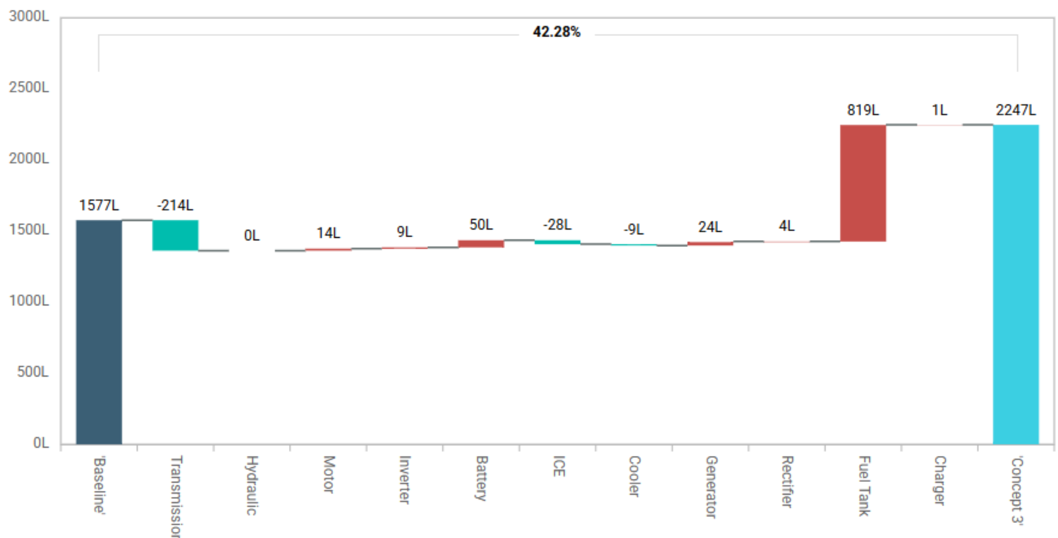

Figure 51: H_2-ICE series-hybrid, primary cycle, future values, component volume

5.1.3.2 Concept 5: Efficiency Optimized Fuel Cell Series-Hybrid

Figure 52 is a plot of the component power breakdown for the efficiency optimized fuel cell concept design under the primary road cycle and the future technology values.

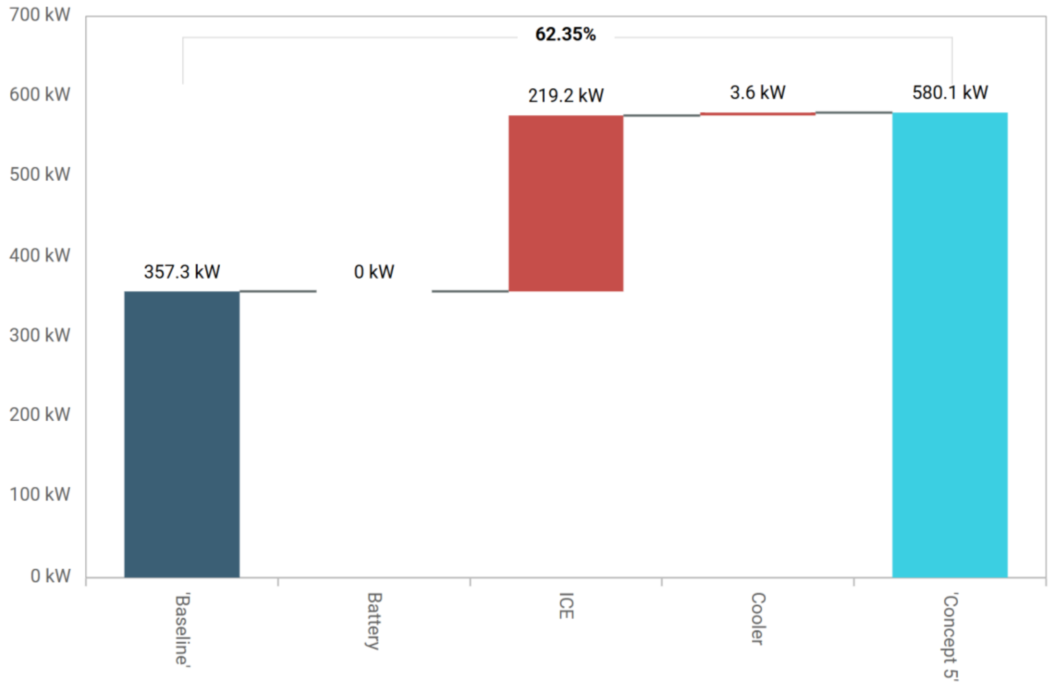

Figure 52: Eff. optimized fuel cell series-hybrid, primary cycle, future values, component power

Figure 53 is a plot of the component mass breakdown for the efficiency optimized fuel cell concept design under the primary road cycle and the future technology values. This concept mass is on-par with the baseline diesel powertrain.

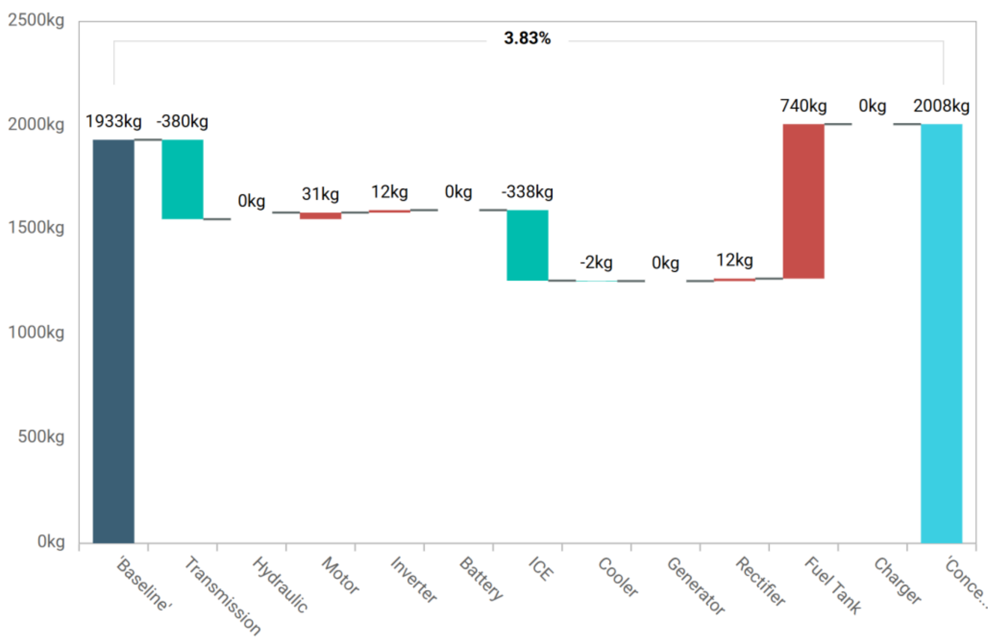

Figure 53: Eff. optimized fuel cell series-hybrid, primary cycle, future values, component mass

Figure 54 is a plot of the component volume breakdown for the efficiency optimized fuel cell concept design under the primary road cycle and the future technology values. This concept powertrain volume is slightly less than the diesel-baseline powertrain.

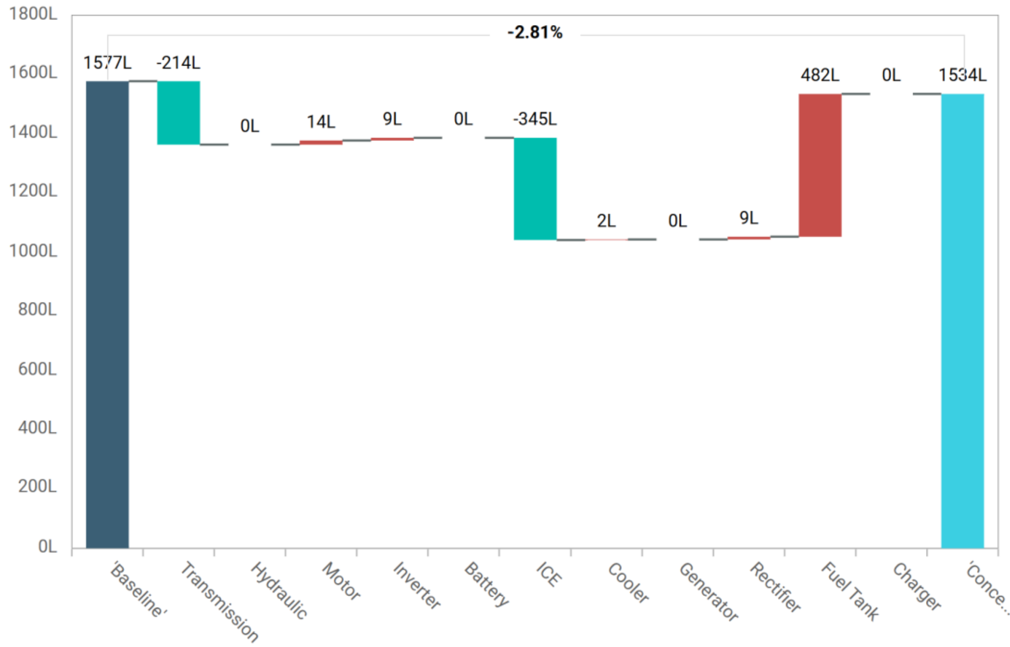

Figure 54: Eff. optimized fuel cell series-hybrid, primary cycle, future values, component volume

5.2 Logistics Vehicle Characterization Profile

For these vehicle concepts, the drive cycle is the LVM defined profile, as outlined in Section 4.1.3.

5.2.1 Today Technology Values

For this section, the vehicle concepts technology values are based on “today” numbers. The prime power engine efficiency, volumetric and gravimetric power density varied for each technology concept. The hydrogen fuel volumetric power density was 0.68 kW/L while the gravimetric energy density was 1.06 kWh/kg. The H_2-ICE and H_2-ICE parallel-hybrid concepts include a transmission while all others do not. The battery gravimetric and volumetric energy density are 140 Wh/kg and 260 Wh/L, respectively while the continuous C-rating is 3 and the peak C-rating is 5. The H_2-ICE motor is the same as the diesel-baseline configuration while all other vehicle concept motors are 85% efficient, with 11.6 kW/L and 10.2 kW/kg, volumetric and gravimetric power density, respectively. Power electronics, including inverters, DCDC converters, and onboard chargers, are 97%, 98%, and 98% efficient, respectively. Their gravimetric power densities are 22 kW/kg, 2.5 kW/kg, and 3.5 kW/kg, respectively. Lastly the cooling system assumes the same parameters as the diesel-baseline, such as a volumetric cooling system fan power density of 1.4 kW/L.

5.2.1.1 Concept 1: H_2-ICE Conventional

Figure 55 is a plot of the H_2-ICE continuous power breakdown, under the LVM profile and with today's technology values. There is no battery in this concept. The total output power is 302.7 kW, which is undersized for the 320 kW 10-minute continuous power requirement. To increase power, the engine must be upsized.

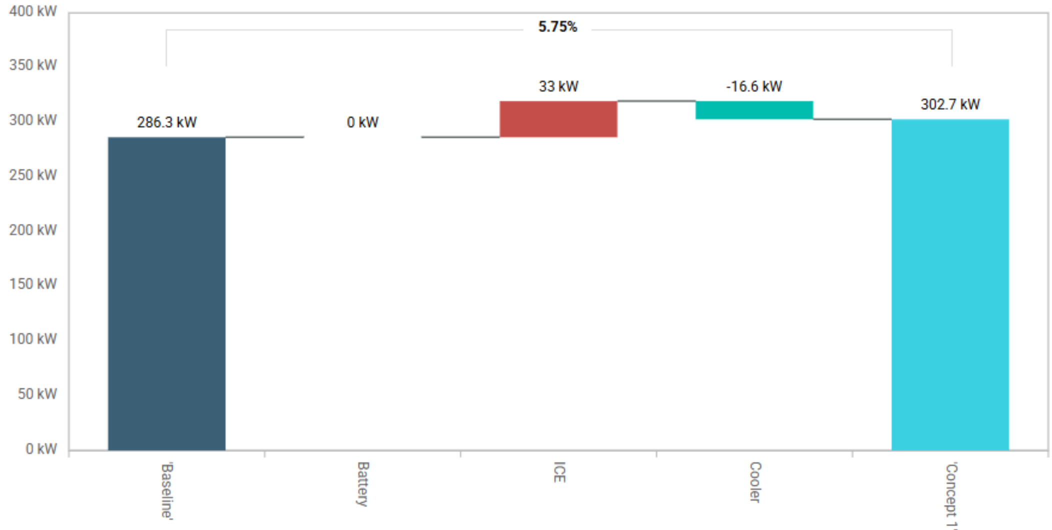

Figure 55: H_2-ICE, LVM profile, today values, component power

Figure 56 is a plot of the H_2-ICE component mass breakdown for the LVM cycle and using today technology values. The total powertrain mass is smaller than the same concept for the primary road cycle. This is because the overall energy required to complete the LVM cycle is lower than the primary road cycle.

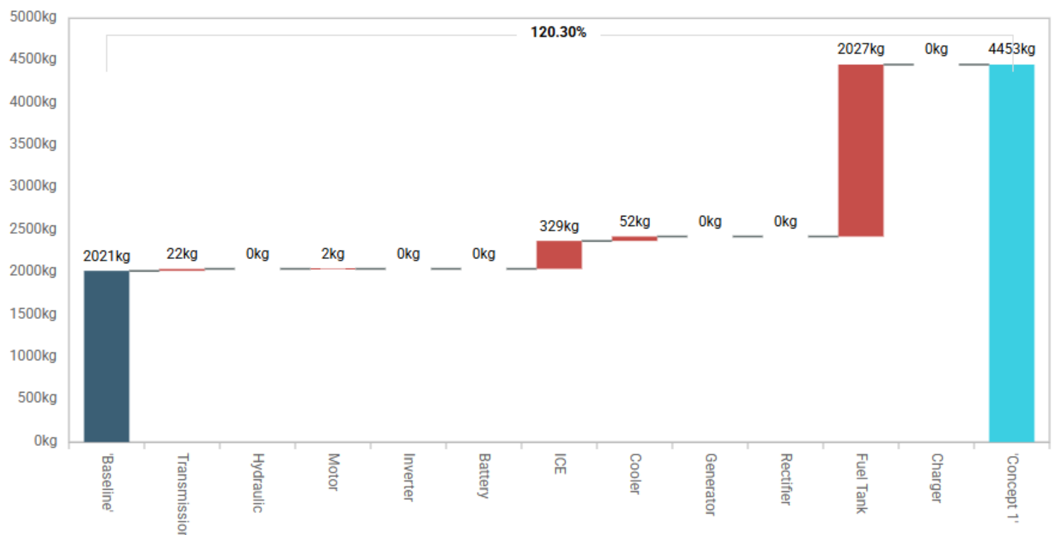

Figure 56: H_2-ICE, LVM profile, today values, component mass

Figure 57 is a plot of the H_2-ICE concept component volume breakdown for the LVM profile and today technology values.

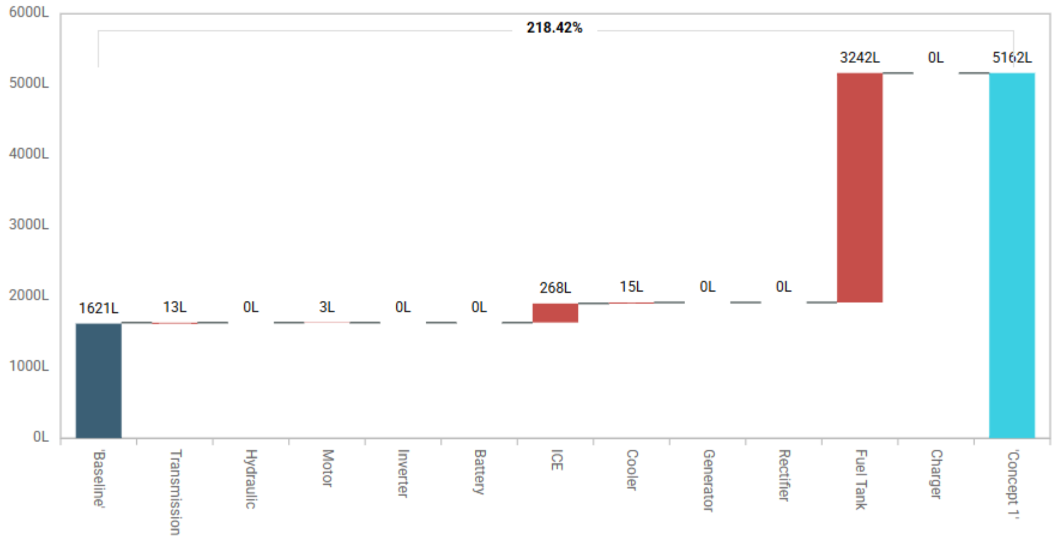

Figure 57: H_2-ICE, LVM profile, today values, component volume

5.2.1.2 Concept 2: H_2-ICE Parallel-Hybrid

Figure 58 is a plot of the power breakdown for a 10-minute continuous operation with a starting battery SOC of 100%. This design is mass optimized while still achieving the minimum continuous power target of 320kW for 10-minutes. As compared with the same concept under the primary road cycle, in this design, the engine power has been greatly downsized with the batteries able to make up the remaining necessary power.

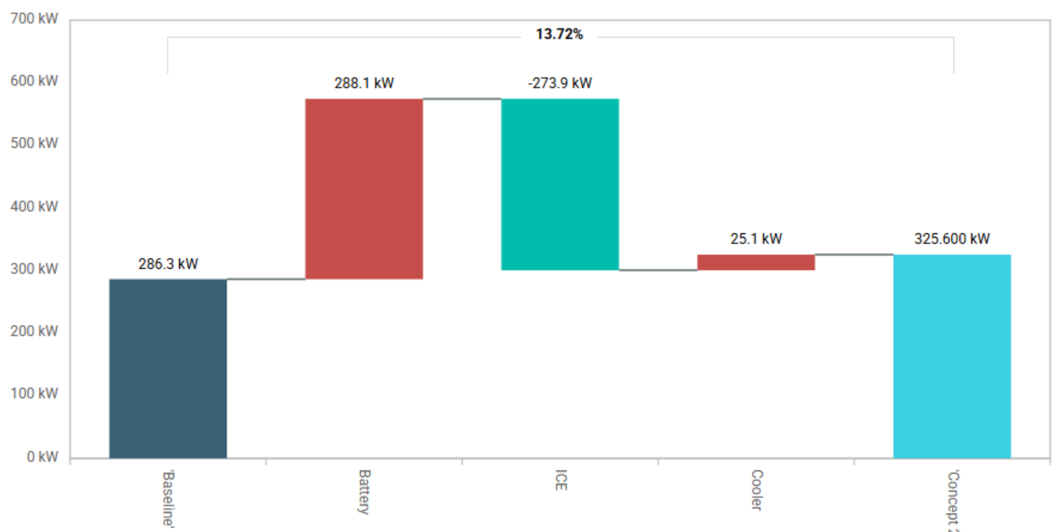

Figure 58: H_2-ICE parallel-hybrid, LVM profile, today values, component power

Figure 59 is a plot of the component mass breakdown for the H_2-ICE parallel-hybrid concept under the LVM profile and with today technology values. This concept mass is only 642 kg larger than the diesel-baseline powertrain.

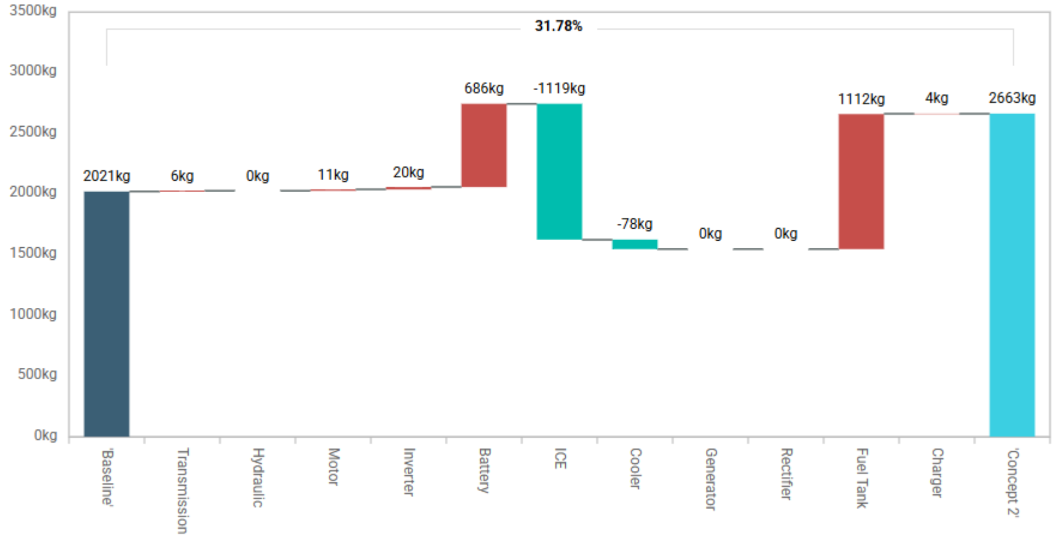

Figure 59: H_2-ICE parallel-hybrid, LVM profile, today values, component mass

Figure 60 is a plot of the component volume breakdown for the H_2-ICE parallel-hybrid concept under the LVM profile with today technology values. For this design, the engine is significantly downsized. Compared with the primary road cycle, this design fuel tank is only 2070 L, whereas the primary road cycle fuel tank was 4,785 L; a reduction of 2,715 L.

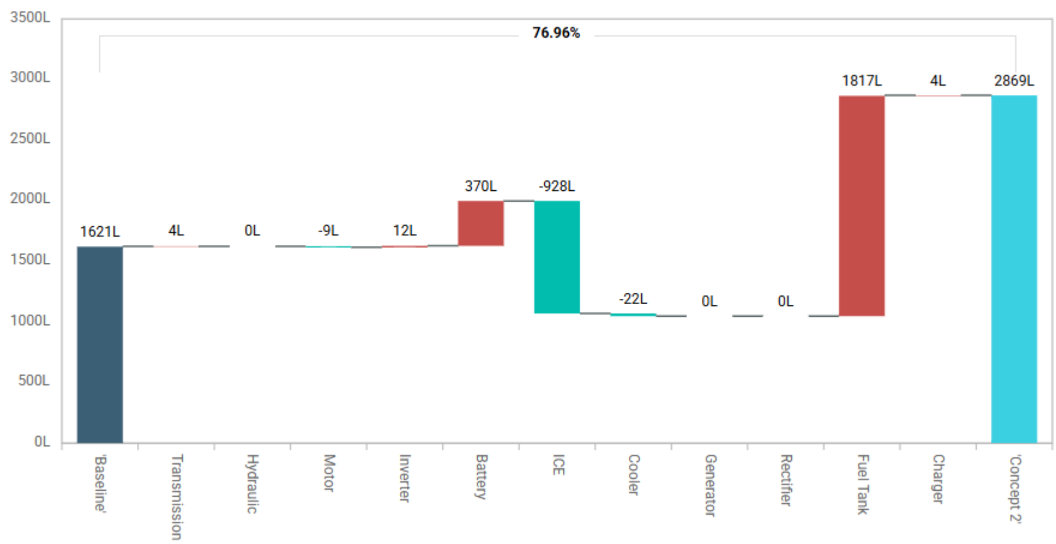

Figure 60: H_2-ICE parallel-hybrid, LVM profile, today values, component volume

5.2.1.3 Concept 3: H_2-ICE Series-Hybrid

Figure 61 is a plot of the power breakdown for the H_2-ICE series-hybrid over a 10-minute duration, assuming a starting battery SOC of 100% for the LVM profile and today technology values.

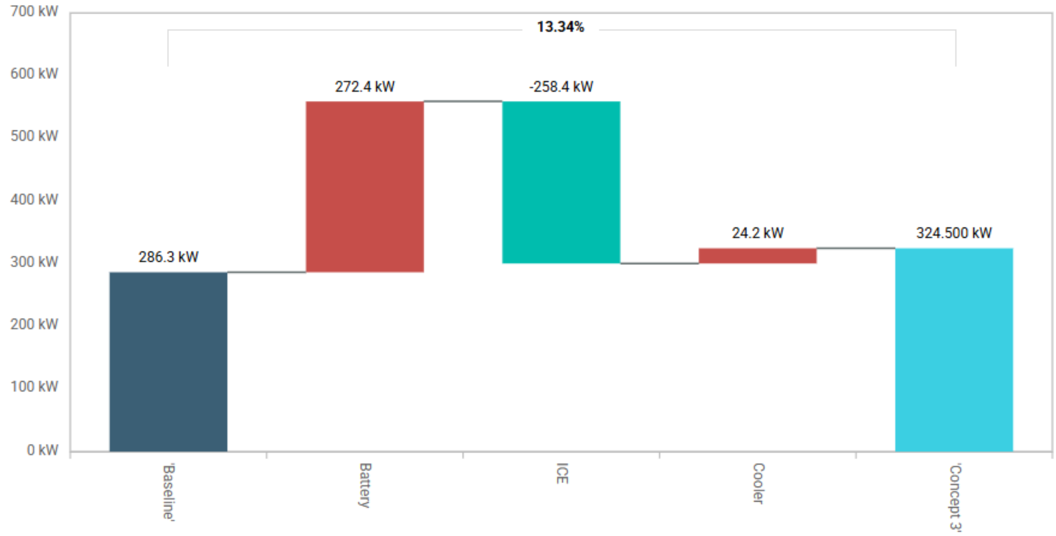

Figure 61: H_2-ICE series-hybrid, LVM profile, today values, component power

Figure 62 is a plot of the component mass for the H_2-ICE series-hybrid vehicle concept with the LVM profile and today technology values. The total powertrain mass is 2,808 kg; which is only ~800 kg larger than the diesel-baseline.

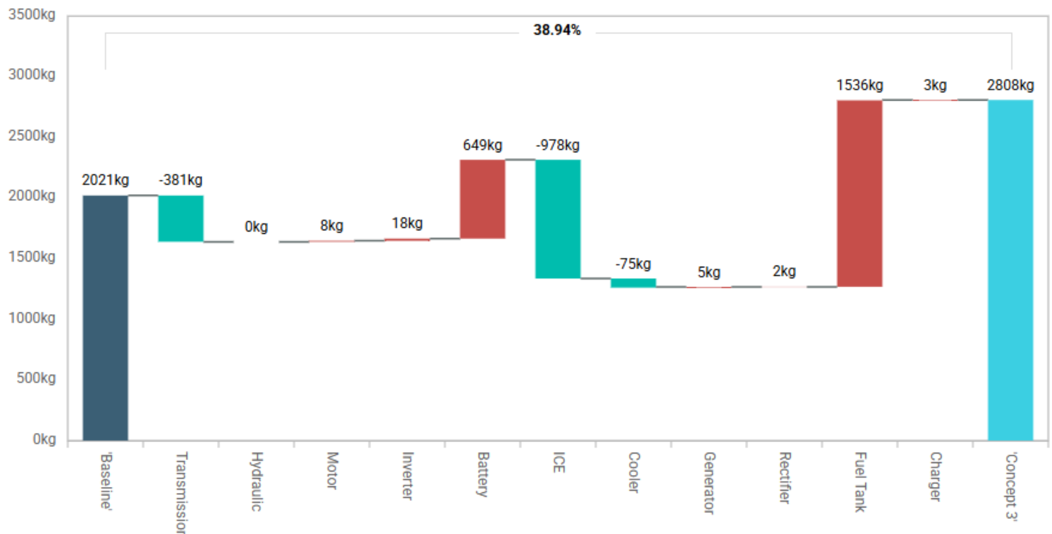

Figure 62: H_2-ICE series-hybrid, LVM profile, today values, component mass

Figure 63 is a plot of the component volume for the H_2-ICE series-hybrid vehicle concept with the LVM profile and today technology values. The total powertrain volume is 3,513 L, much larger than the diesel-baseline but much less than the same powertrain under the primary road cycle.

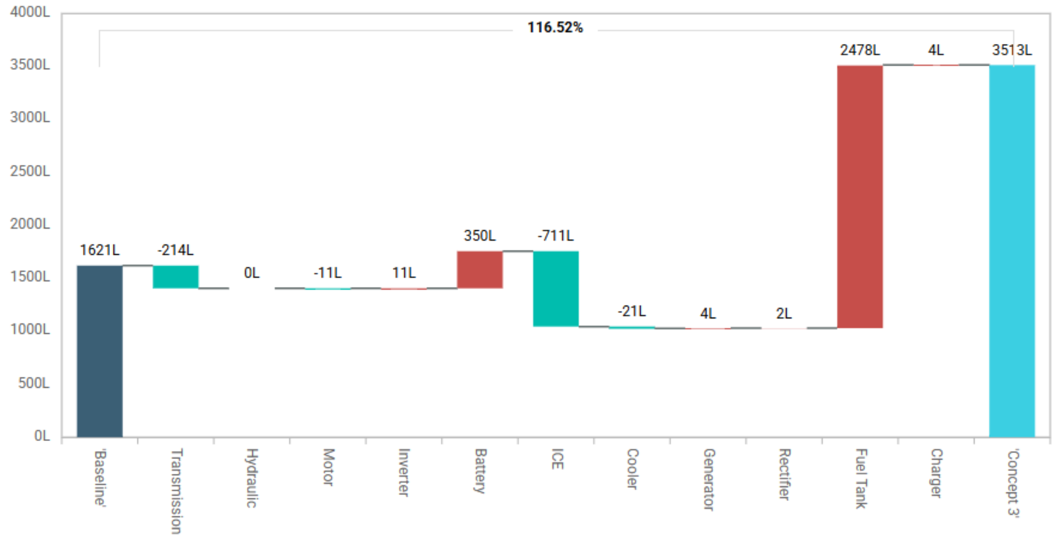

Figure 63: H_2-ICE series-hybrid, LVM profile, today values, component volume

5.2.1.4 Concept 4: Power Dense Fuel Cell Series-Hybrid

Figure 64 is a plot of the power breakdown for a 10-minute continuous power requirement with a battery starting SOC of 100% for the power dense fuel cell design with the LVM profile and today technology values.

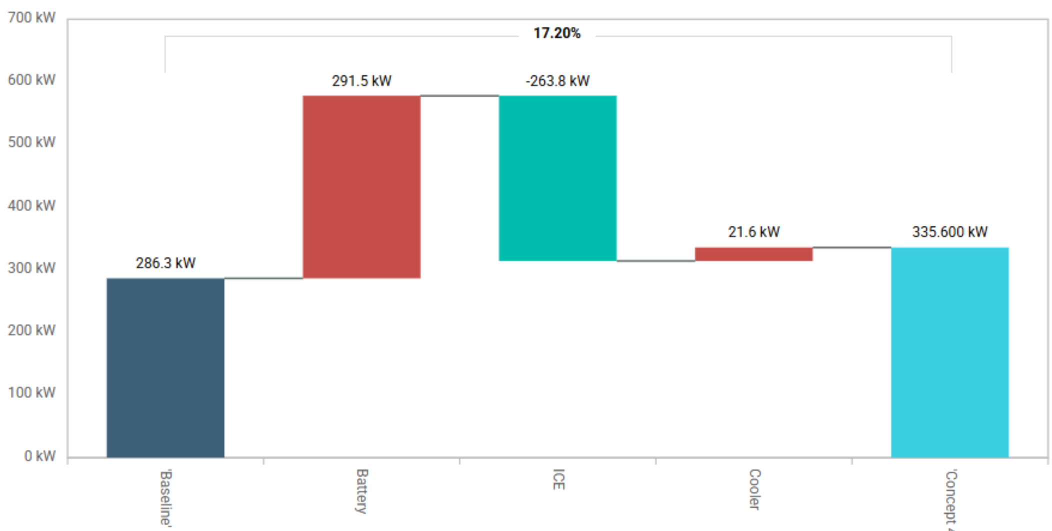

Figure 64: Power dense fuel cell series-hybrid, LVM profile, today values, component power

Figure 65 is a plot of the component mass breakdown for the power dense fuel cell concept vehicle under the LVM profile and today's technology values. This powertrain mass is similar to the H_2-ICE parallel-hybrid concept mass, both under the LVM profile.

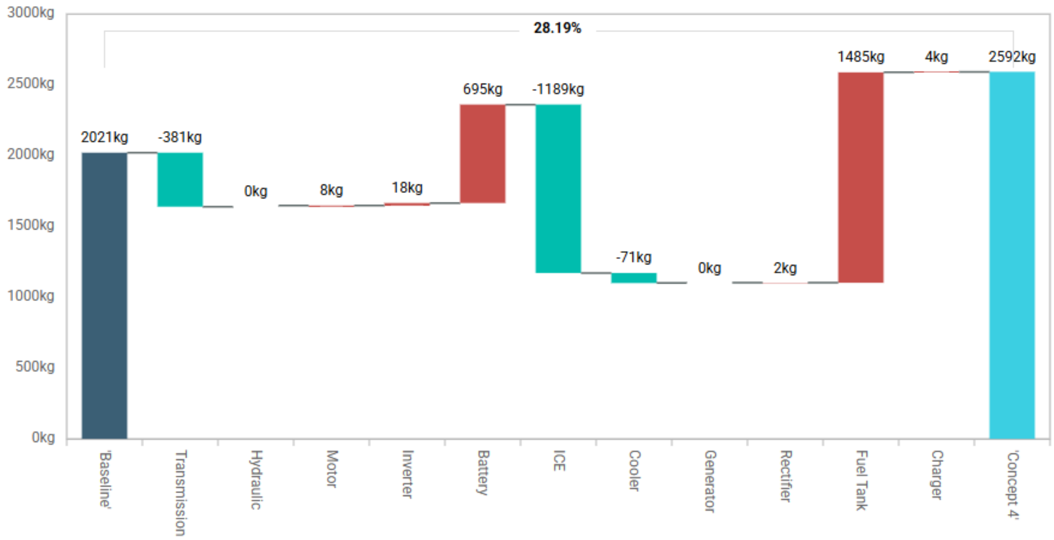

Figure 65: Power dense fuel cell series-hybrid, LVM profile, today values, component mass

Figure 66 is a plot of the component volume breakdown for the power dense fuel cell concept vehicle under the LVM profile and today's technology values. This powertrain volume is 1,637 L larger than the diesel-baseline.

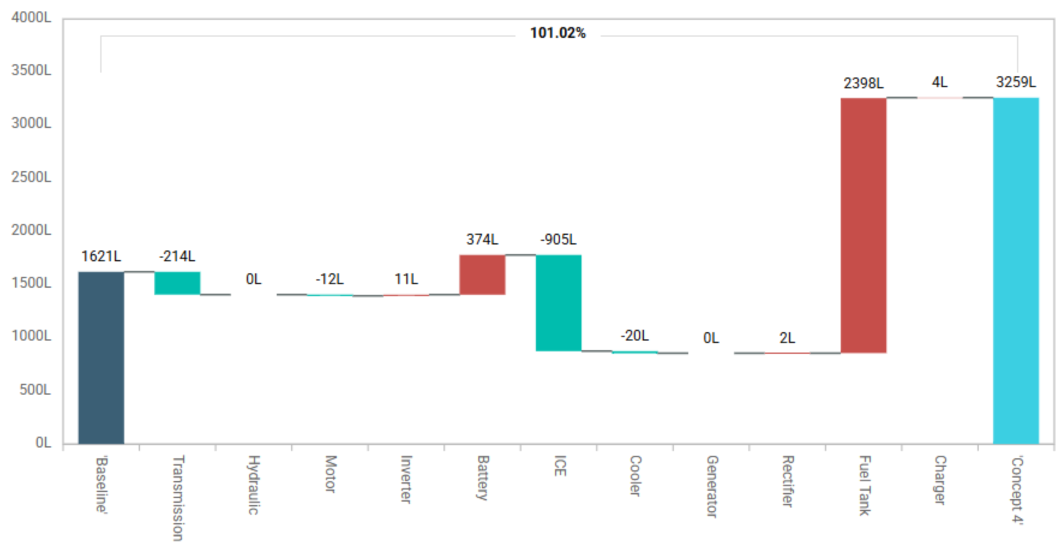

Figure 66: Power dense fuel cell series-hybrid, LVM profile, today values, component volume

5.2.1.5 Concept 5: Efficiency Optimized Fuel Cell Series-Hybrid

Figure 67 is a plot of the power breakdown for the efficiency optimized fuel cell, under the LVM profile and today technology values for a 10-minute power requirement starting with a battery SOC of 100%.

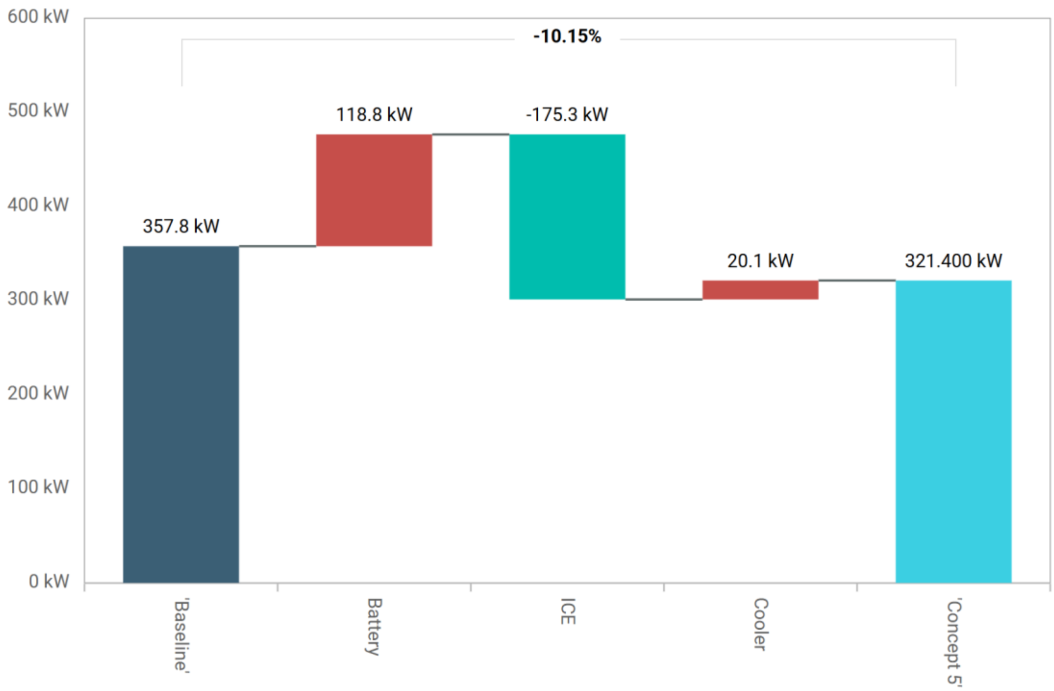

Figure 67: Eff. optimized fuel cell series-hybrid, LVM profile, today values, component power

Figure 68 is a plot of the component mass breakdown for the efficiency optimized fuel cell concept design, under the LVM profile with today's technology values. The total mass for this concept is only 200 kg larger than the diesel-baseline.

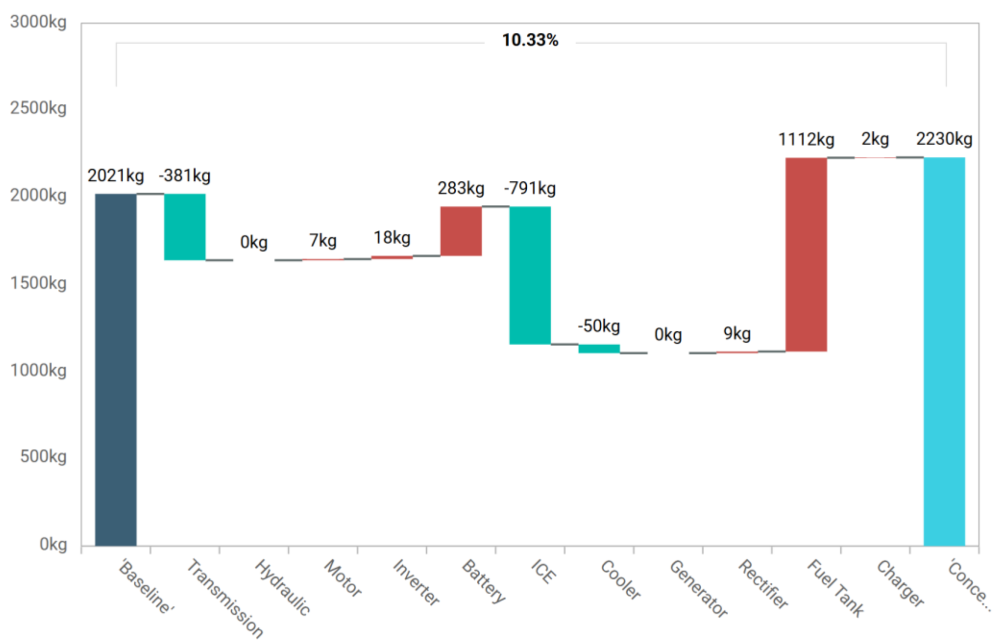

Figure 68: Eff. optimized fuel cell series-hybrid, LVM profile, today values, component mass

Figure 69 is a plot of the component volume breakdown for the efficiency optimized fuel cell vehicle concept under the LVM cycle and with today's technology values. Whereas the total mass is in-line with the diesel baseline powertrain, the total volume is still higher than the diesel baseline powertrain; about 1,679 L.

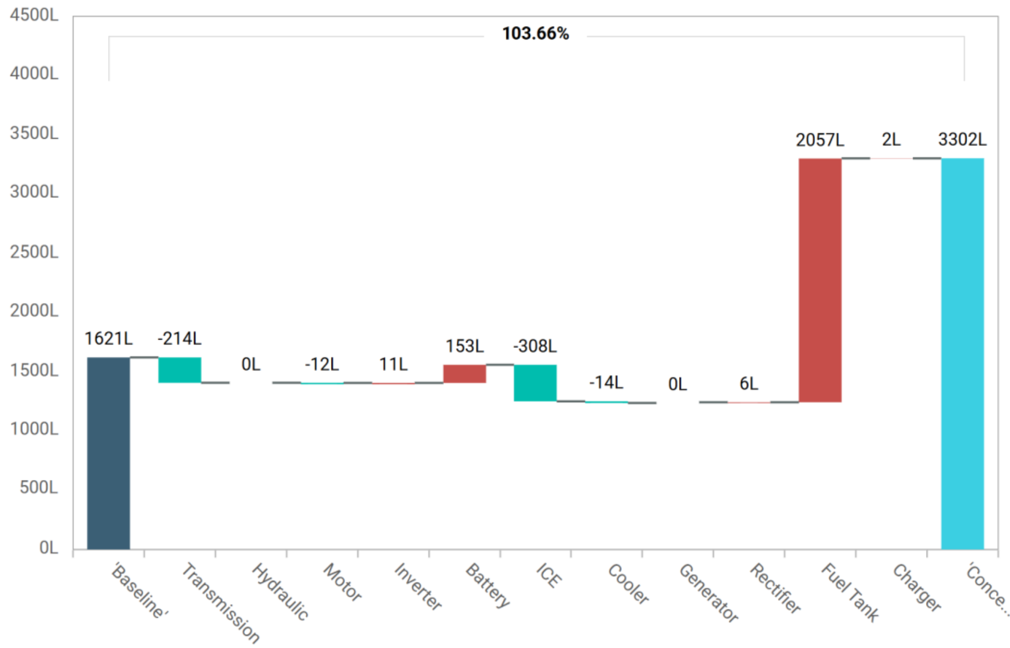

Figure 69: Eff. optimized fuel cell series-hybrid, LVM profile, today values, component volume

5.2.2 Tomorrow Technology Values

For this section, the vehicle concepts technology values are based on tomorrow's technology values. For the H_2-ICE series-hybrid, the engine efficiency is 47% and the volumetric and gravimetric power density are 0.321 kW/L and 0.265 kW/kg, respectively. For the efficiency optimized fuel cell, the engine efficiency is 65% and the volumetric and gravimetric power density are the same; both 0.163 kW/L and 0.613 kW/kg. For hydrogen fuel, the release energy efficiency is reduced from 30% to 25%. The volumetric power density and gravimetric energy density are 1.80 kW/L and 1.30 kWh/kg. The battery volumetric and gravimetry energy density are 500 Wh/L and 280 Wh/kg, respectively; while the continuous C-rating is 5 and the peak C-rating is 10. The motor efficiency is increased to 90% and the volumetric and gravimetric power density is reduced to 5.8 kW/L and 5.6 kW/kg, respectively. For the power electronics, there is a slight increase of efficiency by 0.5 to 1% and only a small decrease in power density. For the cooling system, there is no change to the gravimetric power density but the COP is increased to 25 kW rejected / kW cooling fan.

5.2.2.1 Concept 3: H_2-ICE Series-Hybrid

Figure 70 is a plot of the component power for the H_2-ICE series-hybrid under the LVM cycle and with tomorrow technology values for a continuous requirement of 10-minutes.

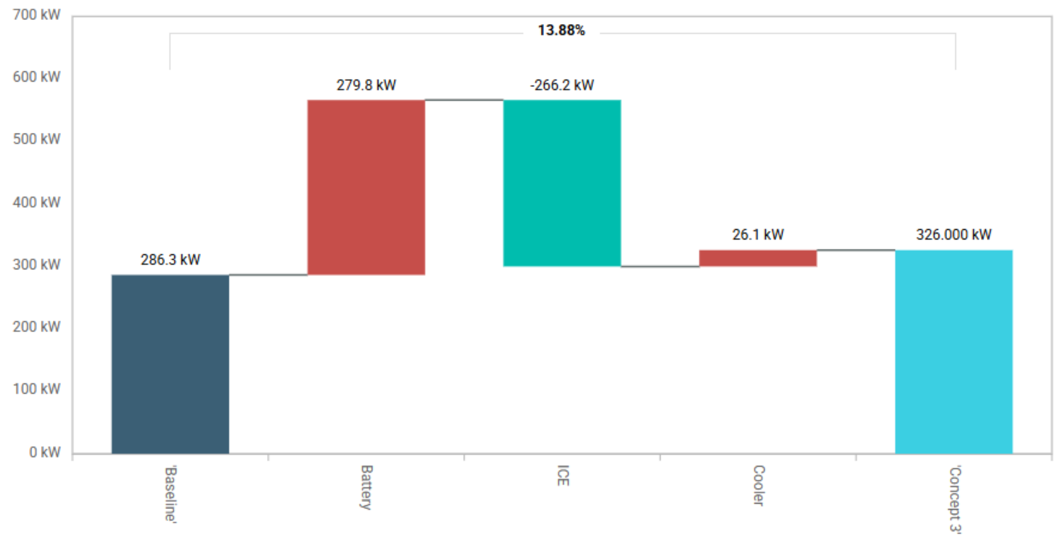

Figure 70: H_2-ICE series-hybrid, LVM profile, tomorrow values, component power

Figure 71 is a plot of the component mass for the H_2-ICE series-hybrid vehicle concept under the LVM profile and with tomorrow technology values. Using tomorrow technology values, the H_2-ICE series-hybrid concept is able to achieve a smaller mass than the baseline-diesel powertrain for the first time.

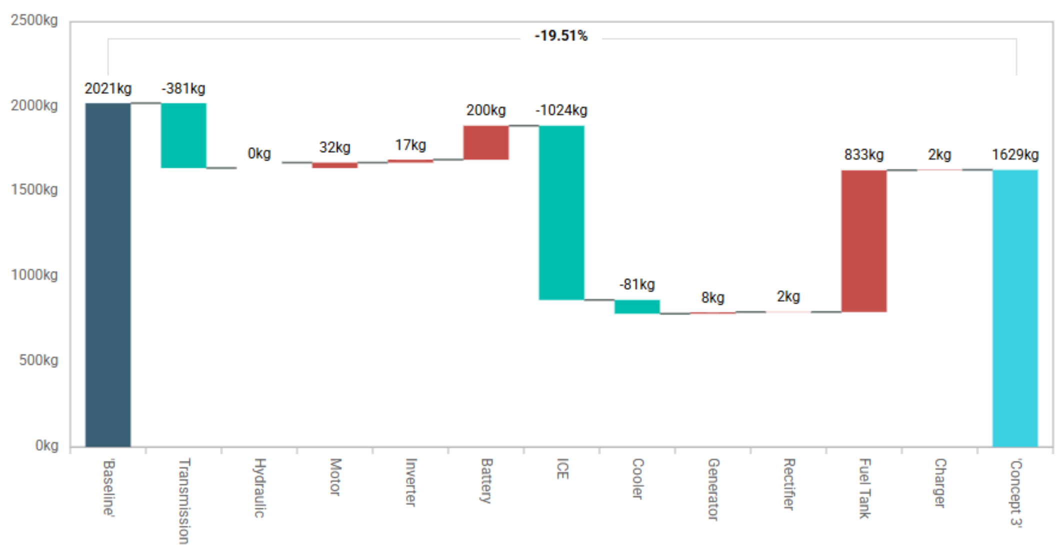

Figure 71: H_2-ICE series-hybrid, LVM profile, tomorrow values, component mass

Figure 72 is a plot of the component volume breakdown for the H_2-ICE series-hybrid vehicle design under the LVM cycle and with tomorrow technology values. Similar to mass, the volume of this concept is also less than the diesel-baseline.

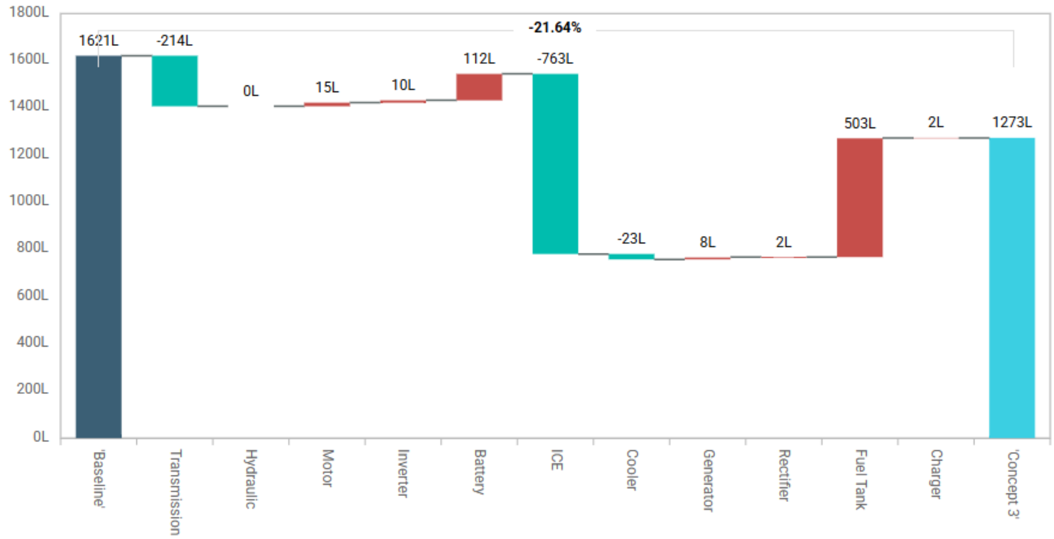

Figure 72: H_2-ICE series-hybrid, LVM profile, tomorrow values, component volume

5.2.2.2 Concept 5: Efficiency Optimized Fuel Cell Series-Hybrid

Figure 73 is a plot of the component power for the efficiency optimized fuel cell vehicle concept under the LVM cycle and with tomorrow technology values for a continuous power requirement of 10-minutes with a starting battery SOC of 100%.

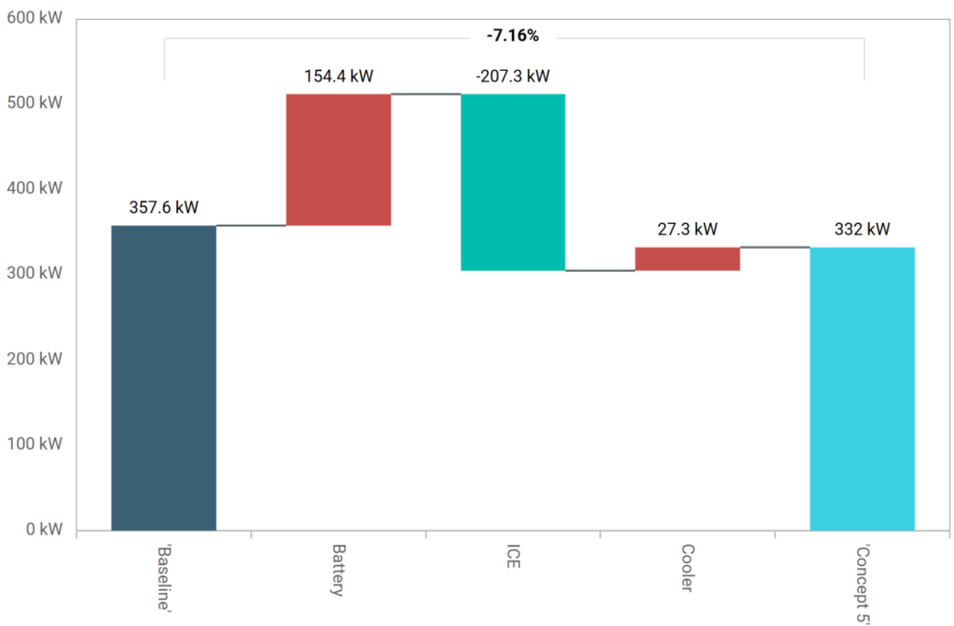

Figure 73: Eff. optimized fuel cell series-hybrid, LVM profile, tomorrow values, component power

Figure 74 is a plot of the component mass breakdown for the efficiency optimized fuel cell concept design under the LVM cycle and with tomorrow technology values. This powertrain concept mass is 707 kg less than the baseline-diesel powertrain.

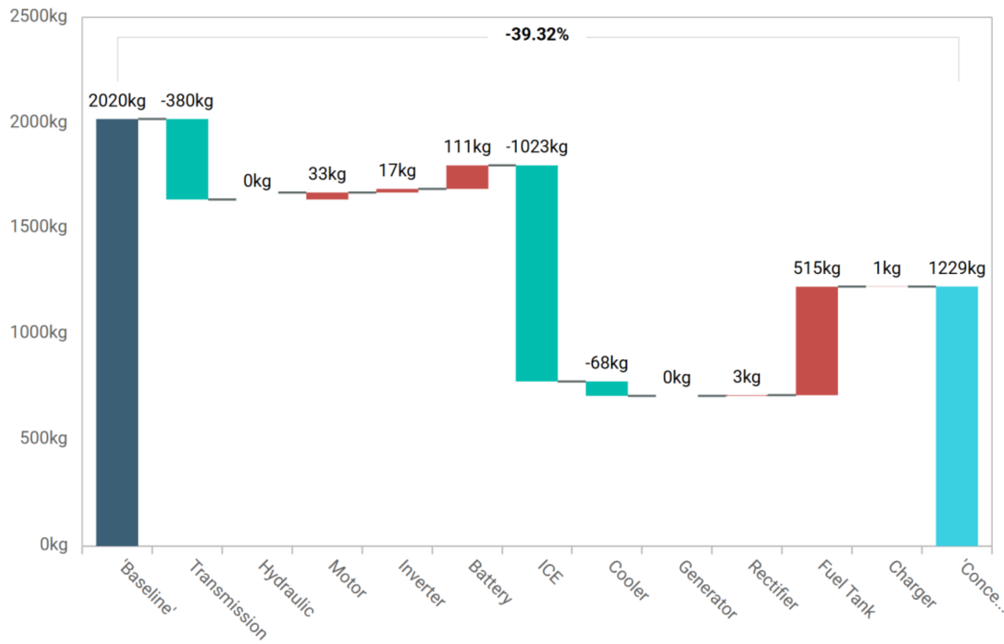

Figure 74: Eff. optimized fuel cell series-hybrid, LVM profile, tomorrow values, component mass

Figure 75 is a plot of the component volume breakdown for the efficiency optimized fuel cell concept design under the LVM cycle and with tomorrow's technology values. This powertrain volume is more than 600 L smaller than the diesel-baseline powertrain.

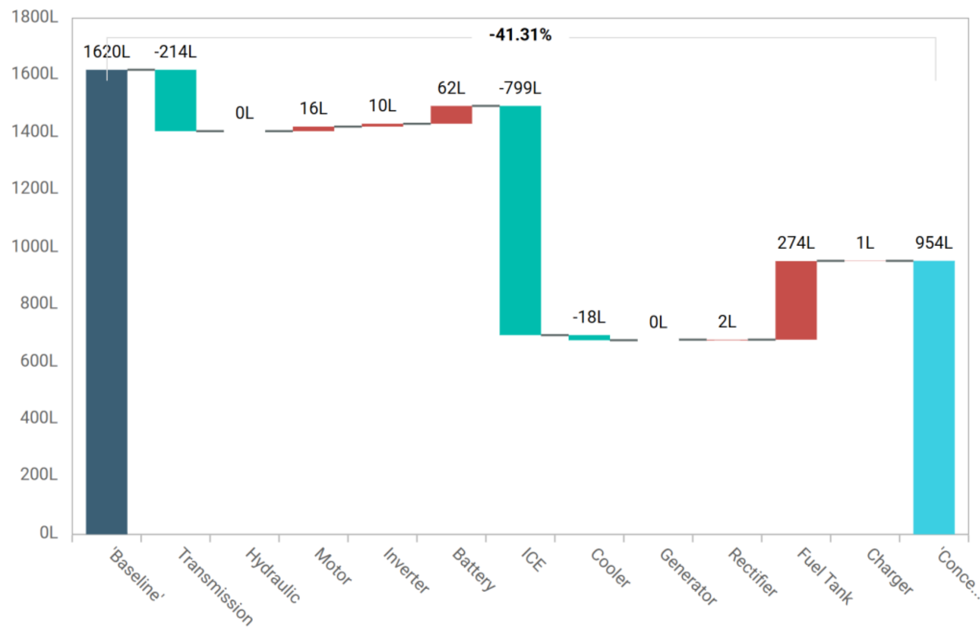

Figure 75: Eff. optimized fuel cell series-hybrid, LVM profile, tomorrow values, component volume

5.2.3 Future Technology Values

For this section, the vehicle concepts technology values are based on future technology values. For the H_2-ICE concept, the engine efficiency is increased to 50% while there is no change in the power density from tomorrow values. For the efficiency optimized fuel cell, the engine efficiency is increased to 70% and the volumetric and gravimetric power density are 0.213 kW/L and 0.163 kW/kg, respectively. For the hydrogen fuel, the release energy efficiency is further reduced to 20%. The volumetric power density is 2.20 kW/L while the gravimetric energy density is 1.70 kWh/kg. For the battery, the continuous C-rate is 7 while the peak C-rate is 15. The volumetric and gravimetric energy density are 800 Wh/L and 420 Wh/kg, respectively. For the motors, the efficiency increases to 93% and there is a slight increase of 0.2 in both volumetric and gravimetric power density. For the power electronic components; inverters, DCDC, and onboard charger, a small increase in power density is observed. For the cooling circuit, the gravimetric power density of the fan decreases to 0.34 kW/kg and the COP is 35 kW rejected / kW cooling fan.

5.2.3.1 Concept 3: H_2-ICE Series-Hybrid

Figure 76 is a plot of the component power breakdown for the H_2-ICE series-hybrid vehicle design under the LVM profile and with future technology values.

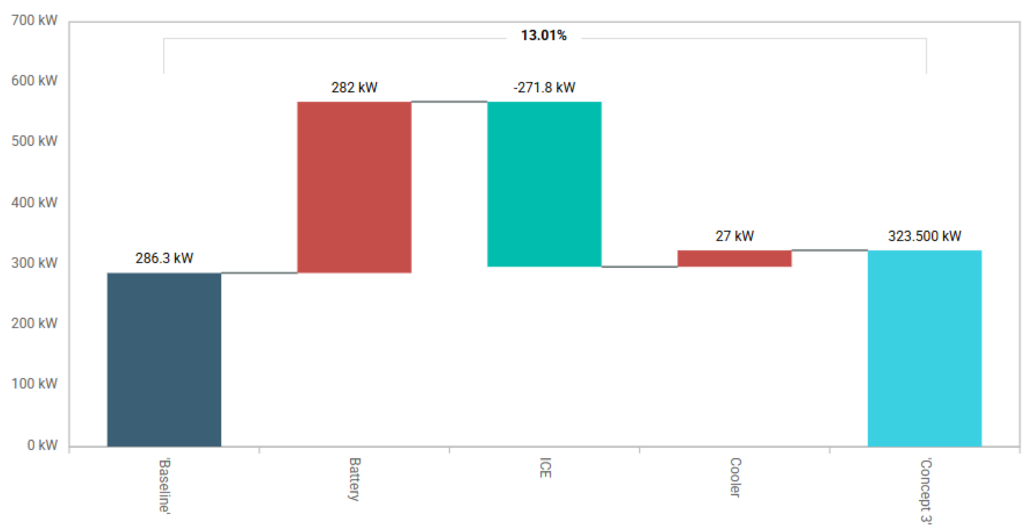

Figure 76: H_2-ICE series-hybrid, LVM profile, future values, component power

Figure 77 is a plot of the component mass breakdown for the H_2-ICE series-hybrid vehicle concept under the LVM profile and with future technology values. This concept powertrain is about half the mass of the diesel-baseline.

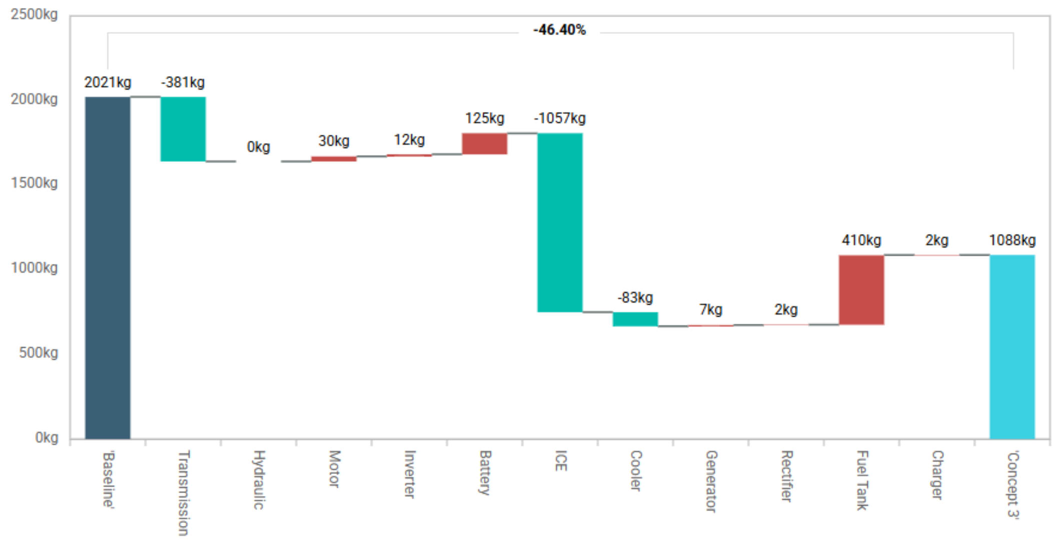

Figure 77: H_2-ICE series-hybrid, LVM profile, future values, component mass

Figure 78 is a plot of the component volume breakdown for the H_2-ICE series-hybrid vehicle concept under the LVM profile and with future technology values. Similarly, this concept powertrain volume is almost half that of the diesel-baseline.

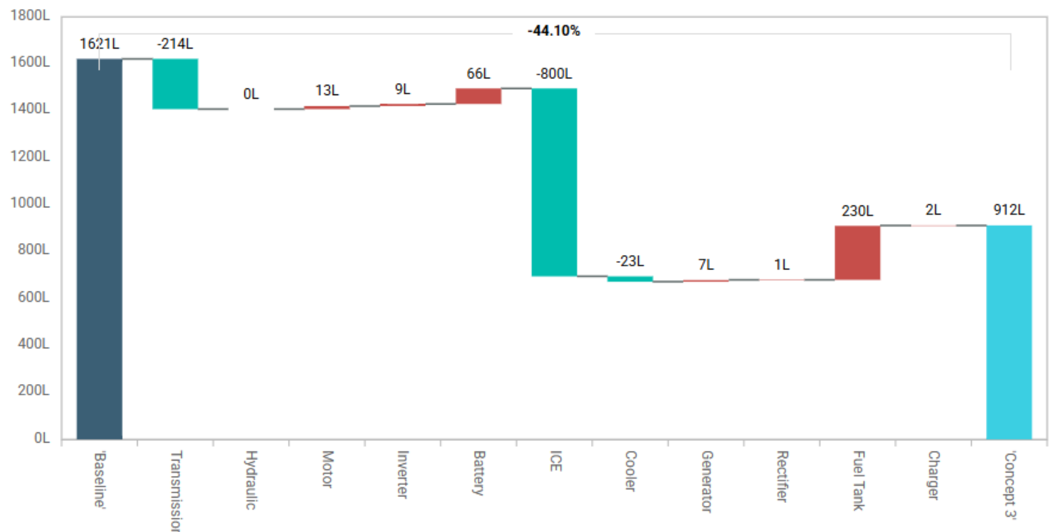

Figure 78: H_2-ICE series-hybrid, LVM profile, future values, component volume

5.2.3.2 Concept 5: Efficiency Optimized Fuel Cell Series-Hybrid

Figure 79 is a plot of the component power for the efficiency optimized fuel cell vehicle concept design under the LVM cycle and with future technology values. This power breakdown assumes a 10-minute duration and a starting battery SOC of 100%.

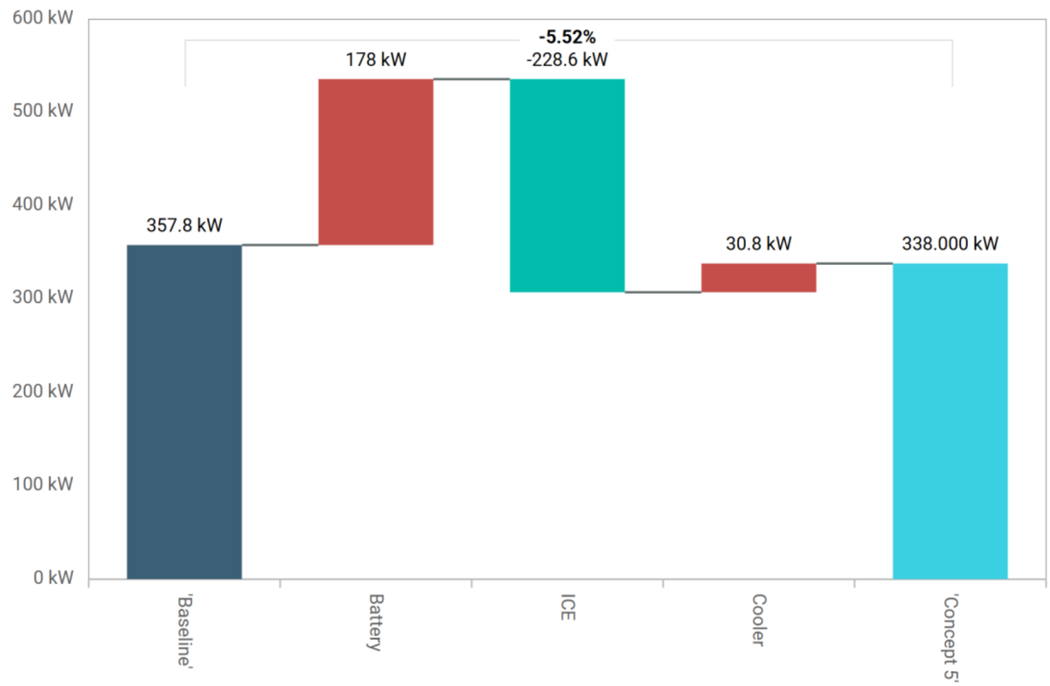

Figure 79: Eff. optimized fuel cell series-hybrid, LVM profile, future values, component power

Figure 80 is a plot of the component mass breakdown for the efficiency optimized fuel cell concept vehicle under the LVM cycle and with tomorrow's technology values. This concept powertrain is almost 60% less mass than the diesel-baseline.

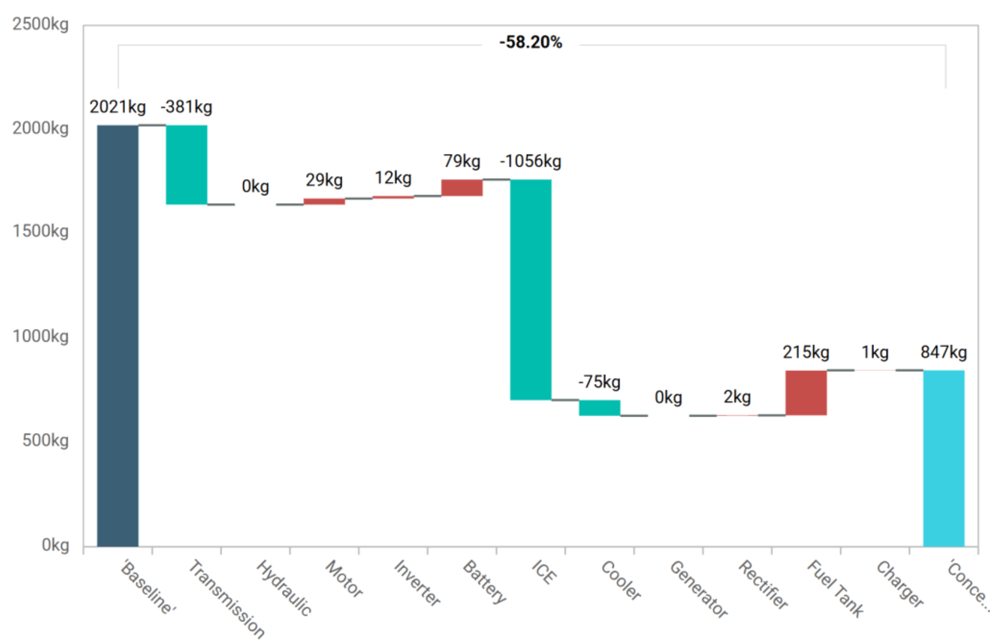

Figure 80: Eff. optimized fuel cell series-hybrid, LVM profile, future values, component mass

Figure 81 is a plot of the component volume breakdown for the efficiency optimized fuel cell concept vehicle under the LVM cycle and with tomorrow's technology values. This powertrain volume is 60% of the diesel-baseline.

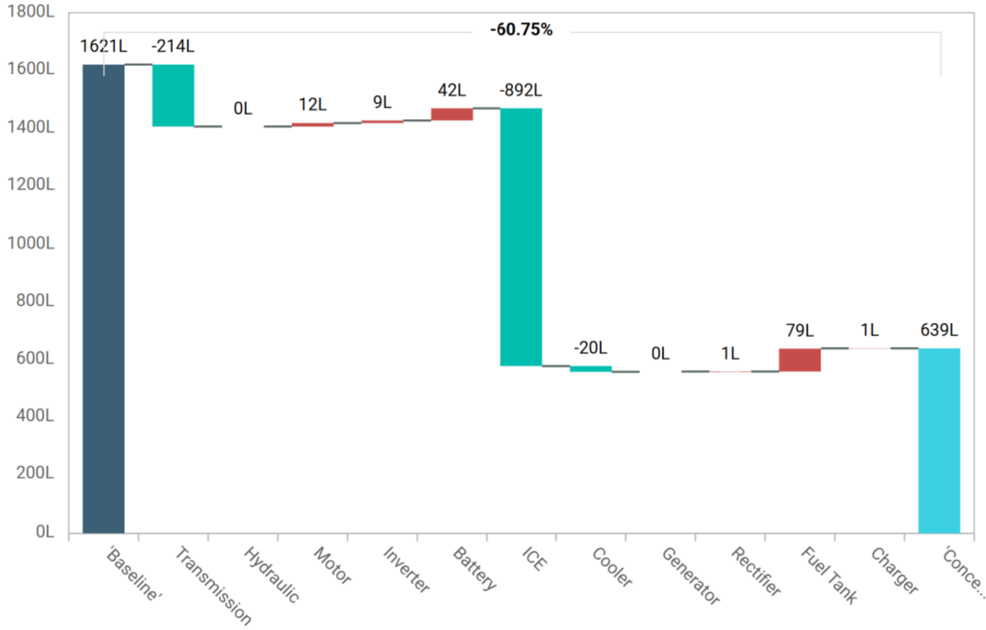

Figure 81: Eff. optimized fuel cell series-hybrid, LVM profile, future values, component volume

6.0 Discussion

In this section, the vehicle concepts, the drive cycle, and the technology values are compared with one another. Further, a detailed discussion is provided on setting the continuous power requirement and the impact it has on vehicle component sizing and overall power.

6.1 Vehicle Concept Comparison

Examining the vehicle concepts under the primary road profile and with today's technology values first, the mass of the components is compared under all the vehicle configurations. Figure 82 indicates how much mass each component contributes to the overall powertrain. For the diesel baseline powertrain, the majority of the mass comes from the ICE and then the transmission. For the remaining powertrains, with H_2 solid-state fuel supply, the majority of the mass comes from the fuel and fuel tank. All the design powertrains have significantly higher weight than the diesel-baseline. The efficiency optimized fuel cell has a large engine and no battery for prime power; this is because it nominally operates at quarter power, for better efficiency, but can operate at peak power to reach higher power demands.

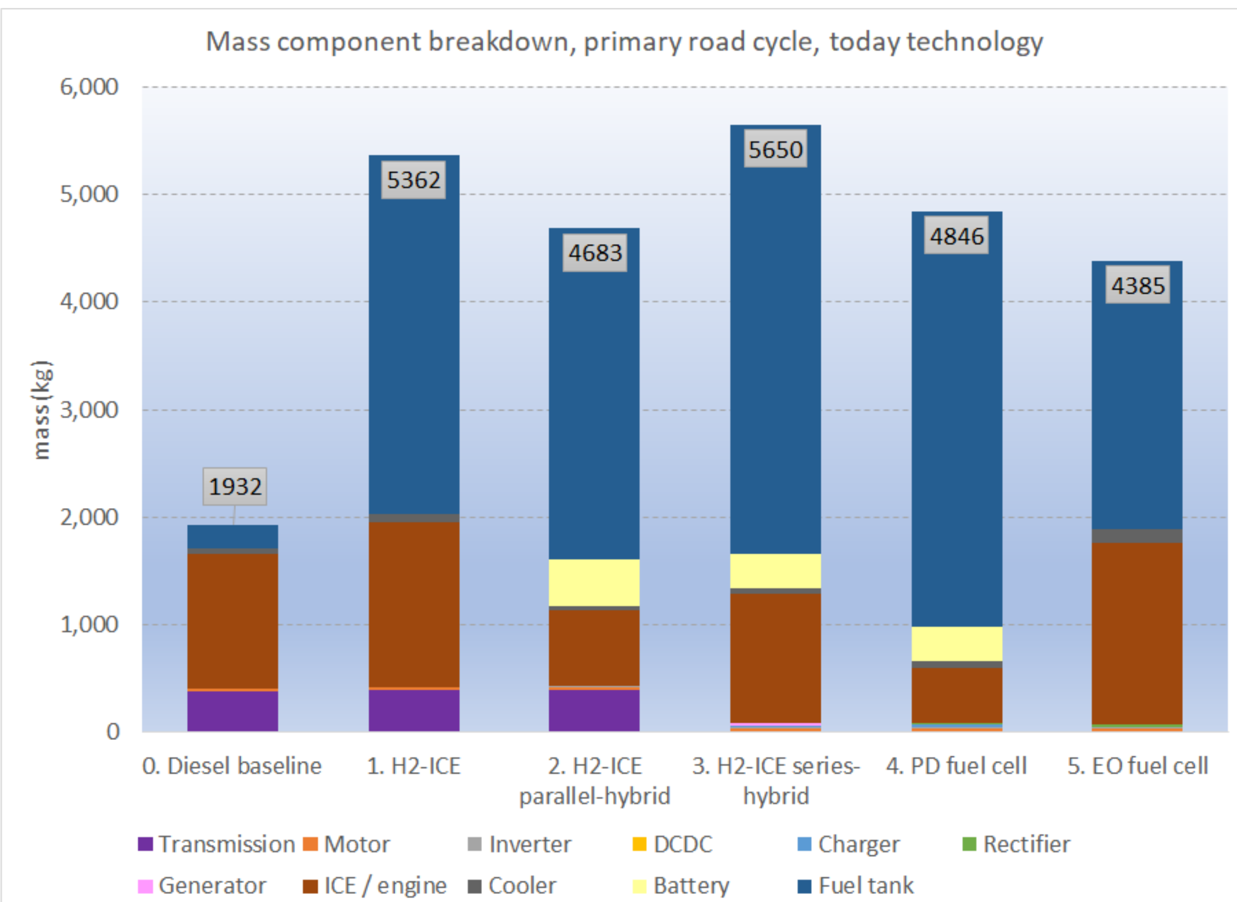

Figure 82: Mass component breakdown, primary road cycle, today technology

Figure 83 is a plot of volume component breakdown under the primary road cycle and with today's technology values. For the diesel-baseline powertrain, the ICE is the largest volume; the fuel tank is relatively small. For the concept powertrains, the fuel tank takes up by far the largest volume, with the engine / ICE taking up the second largest volume, and then battery (where present). All the concept powertrains have significantly larger volume than the diesel-baseline powertrain (2 to ~3x).

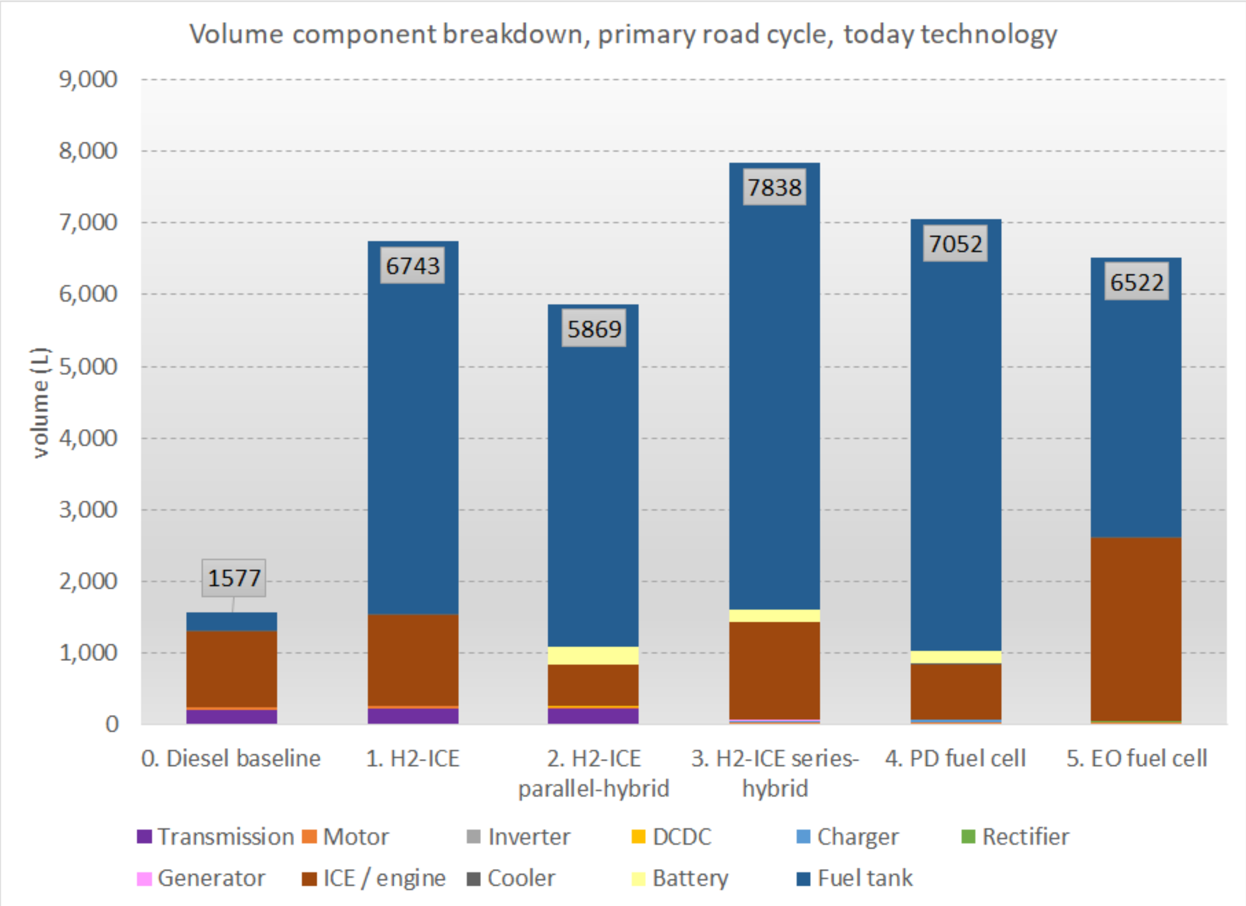

Figure 83: Volume component breakdown, primary road cycle, today technology

Examining next the vehicle concepts under the LVM cycle and with today technology values, Figure 84 is a plot of the mass component contribution to the overall powertrain. All the vehicle concepts have lower mass than those under the primary road cycle. This is because the overall power and energy for the LVM cycle is lower than the primary road cycle and the hybrid design is better adapted to the LVM cycle. For the H_2-ICE powertrain, the ICE and the fuel tank contribute equally to the powertrain mass. For the hybrid vehicles, the battery size and fuel tank contribute to the mass, whereas the ICE or engine contributes less. The efficiency optimized fuel cell has a smaller battery but larger engine, and smaller fuel tank, as compared with the power dense fuel cell. This is because the efficiency optimized fuel cell mainly operates at one-quarter power for higher efficiency and lower required fuel supply.

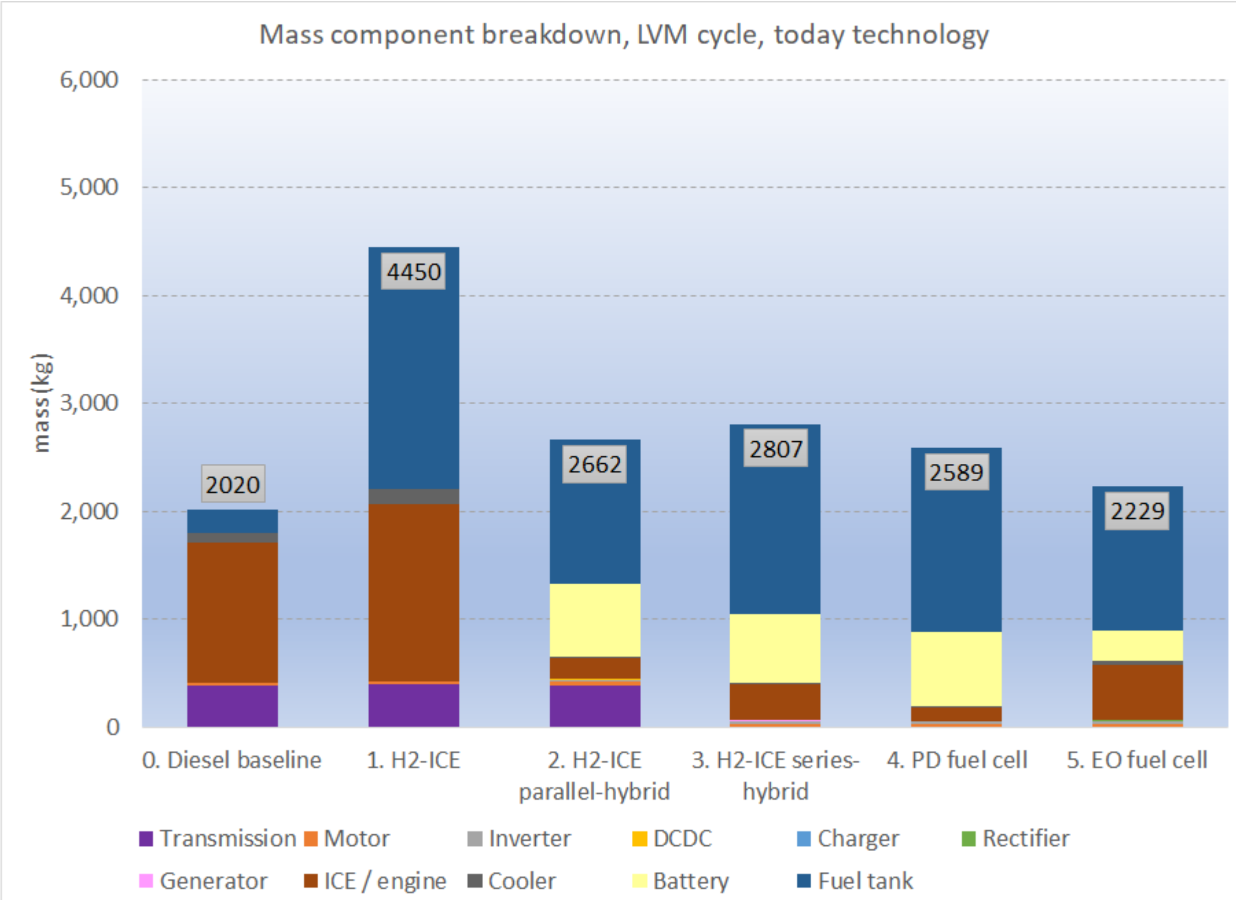

Figure 84: Mass component breakdown, LVM cycle, today technology

Figure 85 is a plot of the component volume contribution to the total powertrain volume. All of the concepts have higher volume than the diesel-baseline. The fuel tank is the largest volume contributor for all the vehicle concepts. The ICE volume is the second largest contributor to volume for the H_2-ICE whereas battery volume is for the hybrid designs, except the efficiency optimized fuel cell. None of the concept powertrains can achieve the diesel-baseline volume.

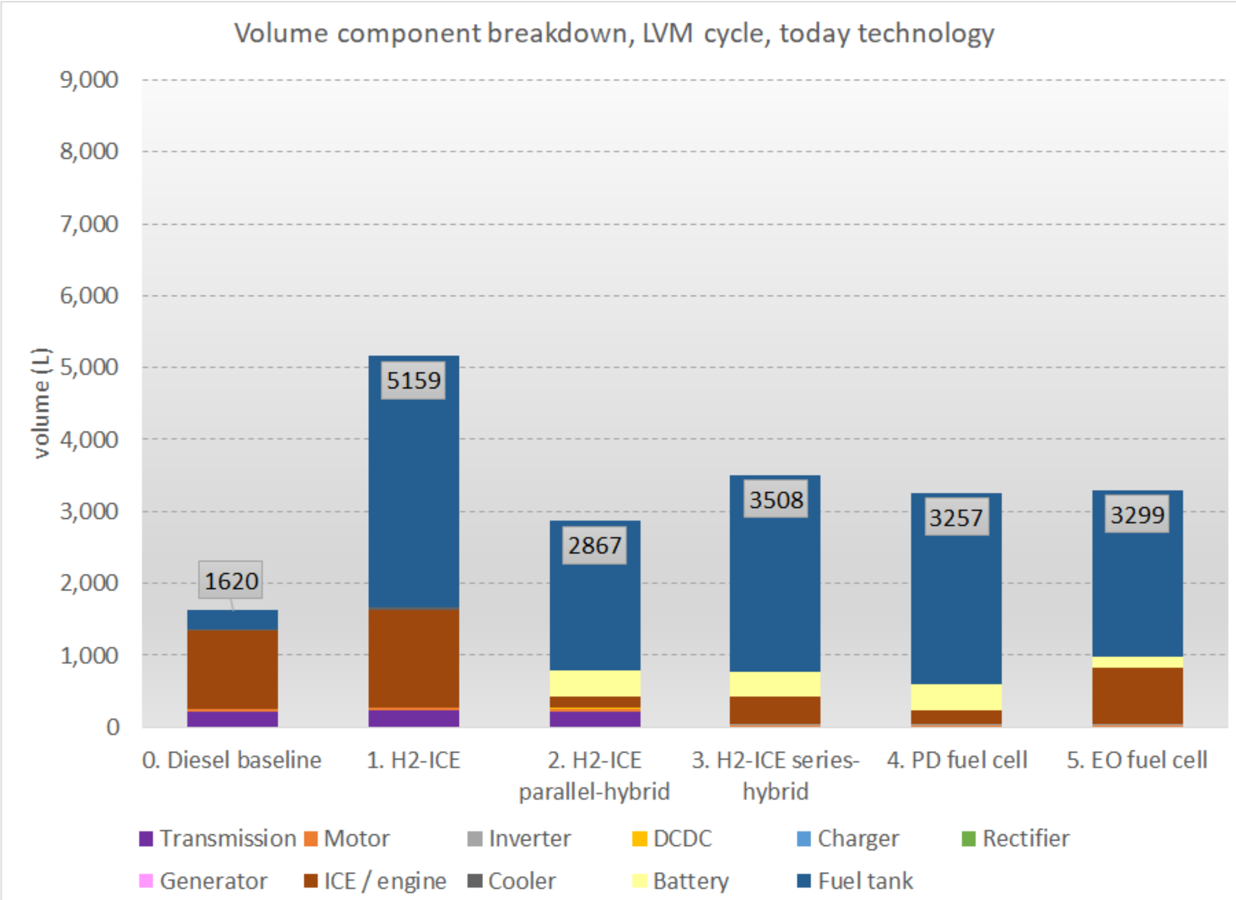

Figure 85: Volume component breakdown, LVM cycle, today technology

Figure 86 is a plot of engine size, battery, and fuel tank capacity, for today technology values, for both the primary road cycle and the LVM cycle. Overall, the primary road cycle concept powertrains have larger ICE / engines than the LVM cycle; this is because primary road cycle is essentially a long continuous requirement. The effect on engine size will be examined further in Section 6.4. The primary road cycle concept powertrains have smaller batteries than the LVM powertrains; with a smaller engine, a larger battery is required to meet the power requirements. The efficiency optimized fuel cell has the largest engine and no battery for prime power in the primary road cycle but a small battery is required to start-up the fuel cell (not illustrated here). For the LVM cycle, the efficiency optimized fuel cell has a smaller fuel cell (218 kW) and a battery with capacity 40 kWh. Next, the diesel-baseline and the H_2-ICE concepts have the second largest engines because they are conventional and do not have a secondary traction power source. The H_2-ICE parallel and series hybrids as well as the power dense fuel cell concepts have the smallest engines with batteries.

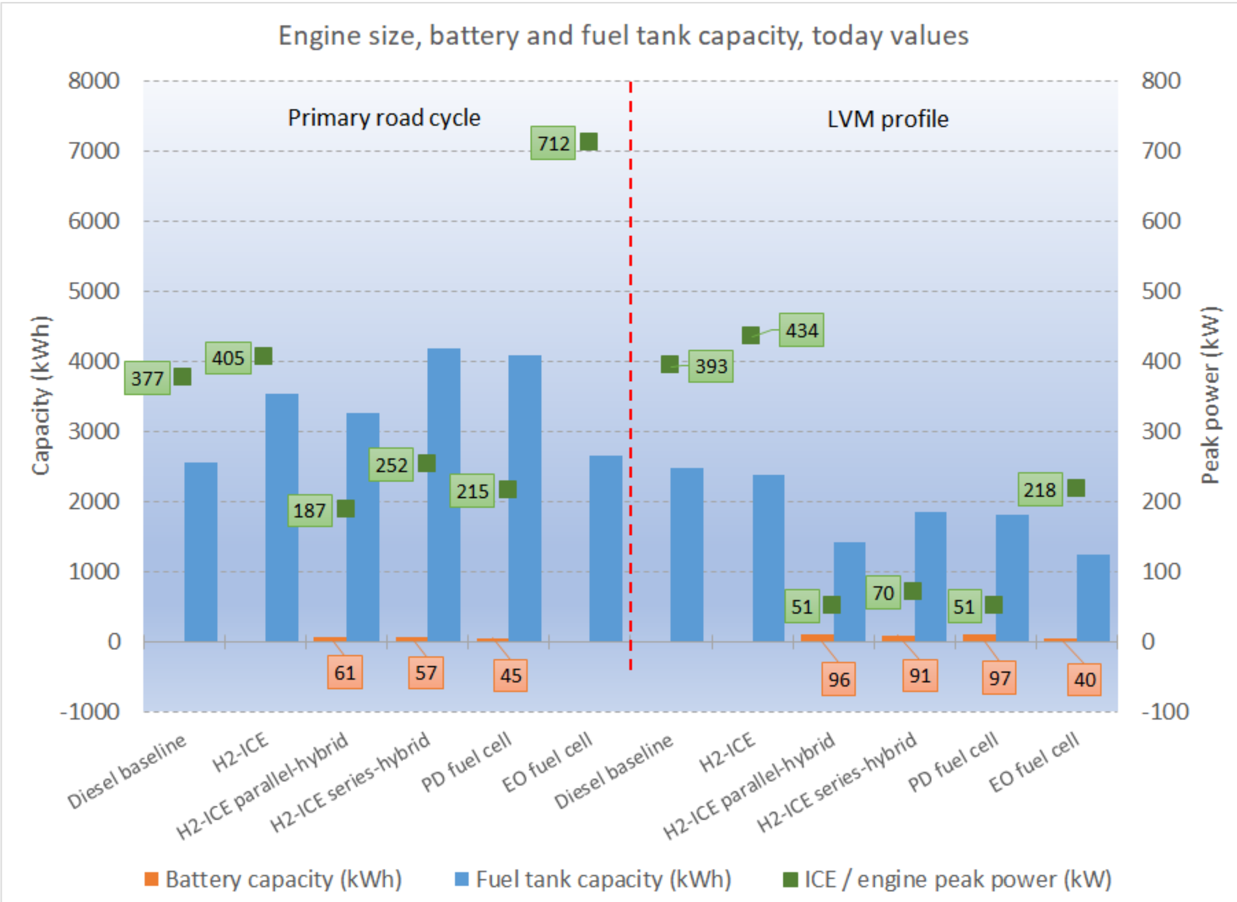

Figure 86: Engine size, battery, and fuel tank capacity, today technology values

6.2 Drive Cycle Comparison

It is evident from analyzing the two drive cycles that they are vastly different. The primary road cycle is essentially a long straight flat road, of the same terrain type, with minimal acceleration, no downhill operation and no braking. It is something akin to an oversimplified highway cycle. Whereas the LVM cycle assumes four different terrain types with different power demands, including downhill and uphill operation, and includes braking. At this time, it cannot be said that either cycle is the ideal LVM cycle but the purpose in selecting such dissimilar cycles it to demonstrate the impact the drive cycle has on component sizing, and powertrain mass. In this section, two vehicle concepts are examined to understand what impact the drive cycle had on powertrain mass, and component sizing.

Examining first the H_2-ICE parallel-hybrid vehicle concept, Figure 87 a plot of component mass and volume for both the primary and LVM cycles as well as engine size and battery capacity. The engine for the primary road cycle is 187 kW while the LVM engine is 51 kW; this is reflected in the smaller mass for the LVM concept vehicle. The battery for the primary road cycle is 61 kWh, whereas the battery for the LVM profile is 96 kWh. With a smaller engine, a larger battery is used to meet the power requirements. The fuel tank mass of the primary road cycle is 3,070 kg while the LVM cycle is only 1,328 kg. Because the engine is larger in the primary road cycle, it requires more fuel to run at its nominal operating point.

This larger engine has a compounding effect on the fuel tank size and weight. The total mass for the H_2-ICE parallel-hybrid primary road cycle powertrain is 4,683 kg where as the H_2-ICE parallel-hybrid LVM cycle powertrain is 2,662 kg; about half the weight. In this instance, the difference in drive cycle here reduced the powertrain weight by 50%. If vehicle requirements are incorrectly set, it may lead to the case where a powertrain is over-sized or under-sized in terms of power or energy.

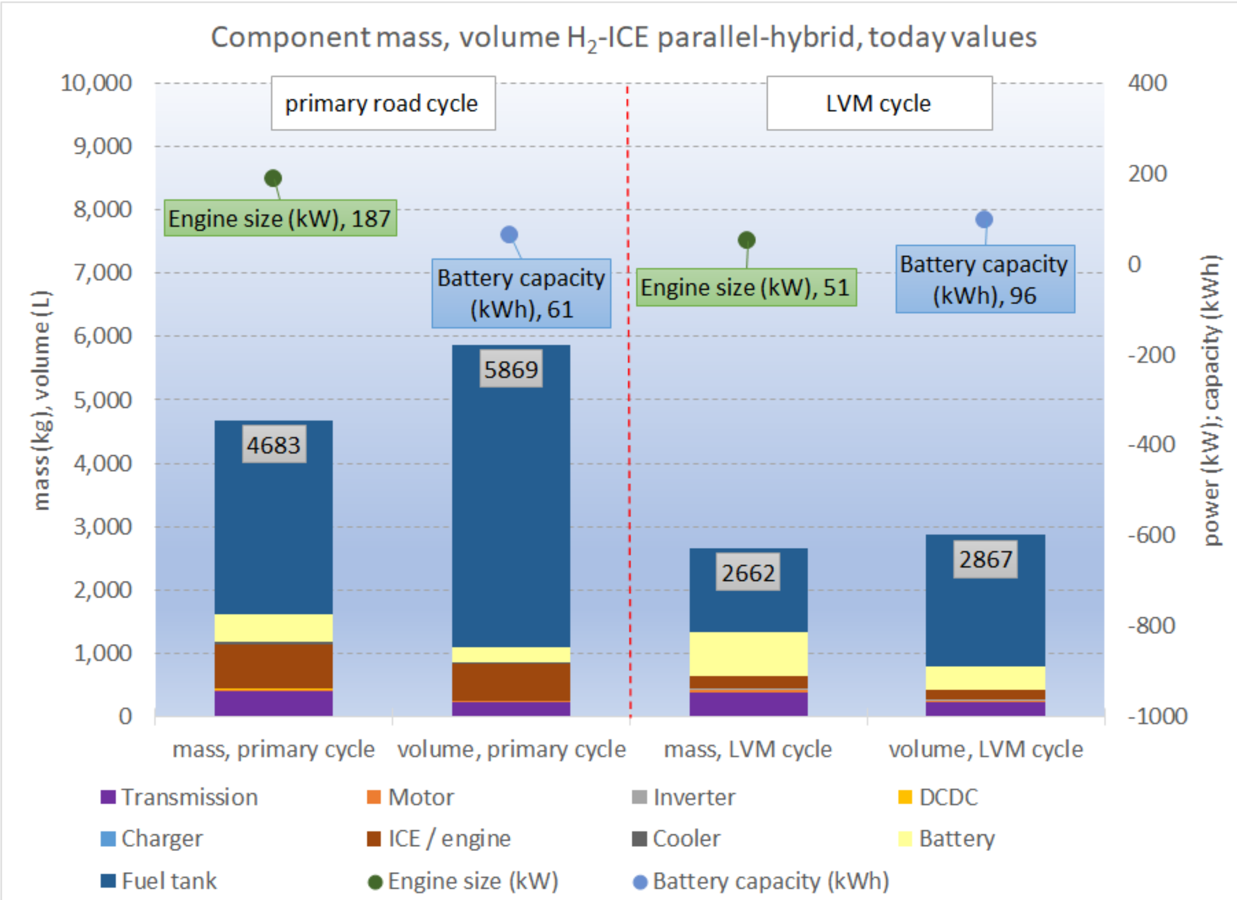

Figure 87: Mass, power, and energy H_2-ICE parallel-hybrid primary and LVM cycle, today values

The second case to be examined is the power dense fuel cell. This fuel cell operates at the lower efficiency value (40%) but at its highest power output; the engine is sized to meet the power demands exactly. Figure 88 is a plot of component mass and volume for both the primary and LVM cycles as well as engine size and battery capacity. The primary road cycle fuel cell (engine) is 215 kW while the LVM cycle is only 51 kW. The battery for the primary road cycle is 45 kWh while the LVM cycle is 97 kWh. Here again with a larger engine (fuel cell) a smaller battery is required to meet the requirements; whereas with a smaller engine, a larger battery is required. The primary road cycle fuel tank mass is 3,859 kg while the LVM cycle fuel tank mass is 1,701 kg. The total powertrain mass for the primary road cycle is 4,846 kg while the LVM road cycle total powertrain mass is 2,589 kg. Here once again the primary road cycle powertrain mass is twice that of the LVM cycle powertrain mass, demonstrating that even for different vehicle configurations the drive cycle selection has a significant impact on vehicle design.

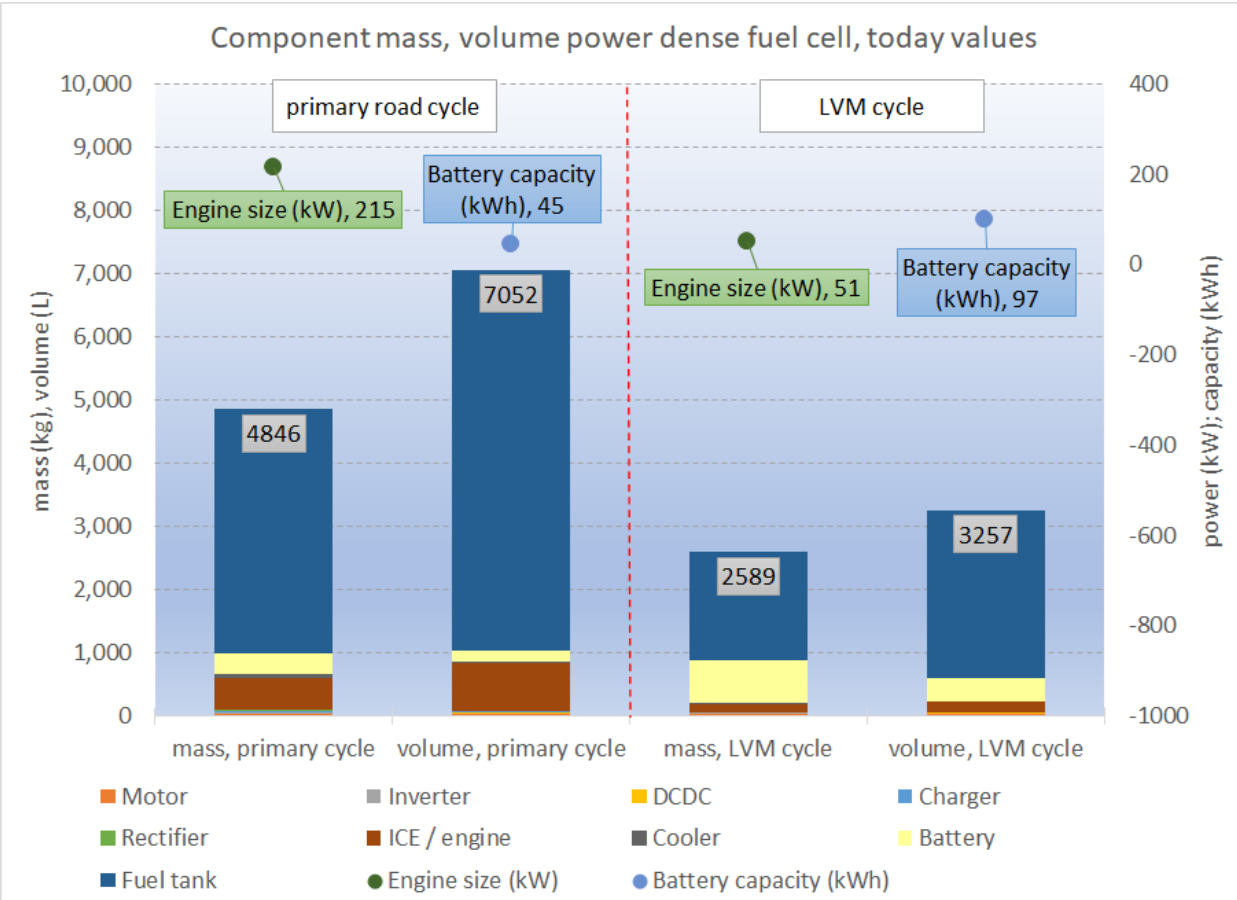

Figure 88: Mass, power, and energy PD fuel cell primary and LVM cycle, today values

6.3 Today, Tomorrow and Future Technology Comparison

To try and predict changes to mass, volume, power, and energy for tomorrow and future technologies, the contributors for this project were invited to estimate how their technologies are likely to improve in the future, in terms of efficiency, volumetric and gravimetric power and energy density. Where an expert contributor was not available, predicted values from industry or government whitepapers were selected. The values presented here are in no way conclusive and only provide an estimation of what may be possible, according to technology progress in the future.

Two vehicle concepts were analyzed under today, tomorrow and future technology values; the H_2-ICE series-hybrid and the efficiency optimized fuel cell vehicle concept designs. Tomorrow is defined as 10 years from now while future is defined as 15 to 20 years from now.

Figure 89 is a plot of the H_2-ICE series-hybrid system component mass analysis for today, tomorrow, and future technology values, for both the primary and LVM cycle. The diesel-baseline is provided for reference. There is an overall trend moving from today to future technology that the component mass, as well as the overall powertrain mass is decreasing. The most significant change is a decrease in fuel tank, followed by the battery mass. The engine mass is staying relatively constant; engine technology is mature and significant changes in power density are not anticipated in the near term. Furthermore, a certain engine size is required to achieve the power requirements so there is a limit to decreases in the size of the engine. Under the LVM cycle, this H_2-ICE series-hybrid design is able to achieve smaller total powertrain mass than the diesel-baseline with tomorrow and future technology values.

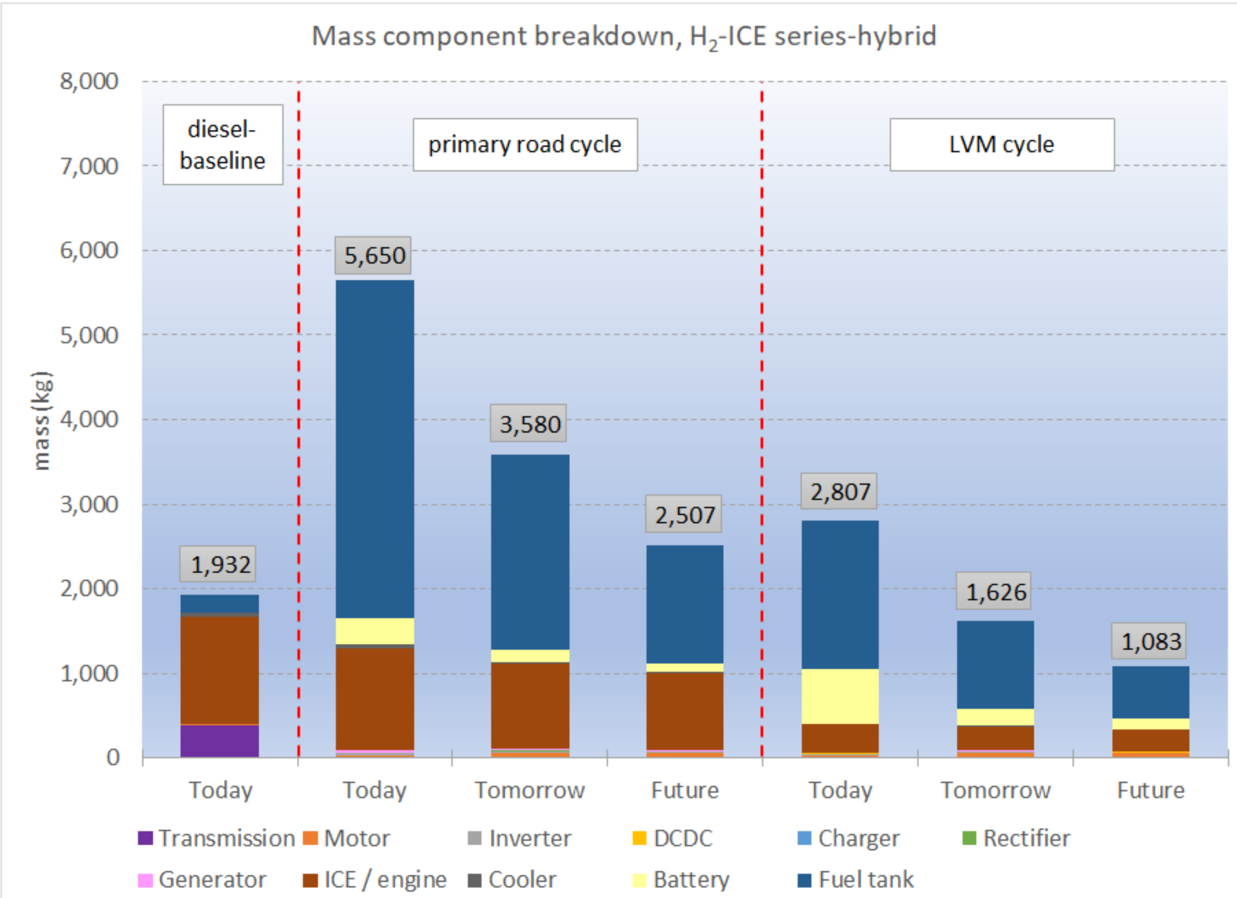

Figure 89: Mass component analysis, H_2-ICE series-hybrid for today, tomorrow, and future values

Figure 90 is a plot of the H_2-ICE series-hybrid system component volume analysis for today, tomorrow, and future technology values, for both the primary and LVM cycle. From today to tomorrow values, the decrease in volume is more than half. And then from tomorrow to future values, the decrease in volume is about 20%.

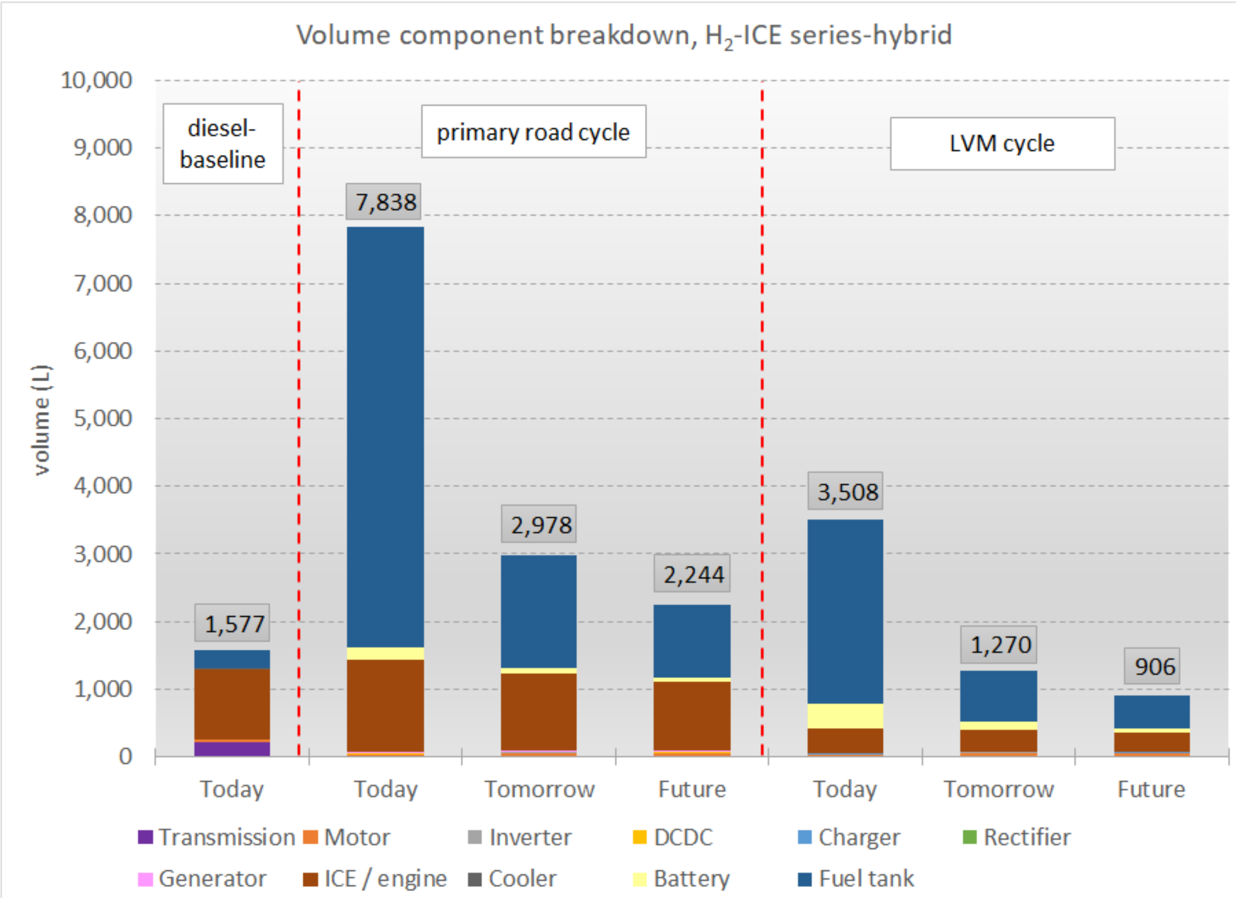

Figure 90: Volume component analysis, H_2-ICE series-hybrid for today, tomorrow, and future values

Figure 91 is a plot of system component mass for the efficiency optimized fuel cell as a function of today, tomorrow, and future technology values for the primary and LVM cycles. The total powertrain mass is lower than the H_2-ICE series-hybrid concepts. All the tomorrow and future concepts have lower powertrain mass than the diesel-baseline. Here again fuel tank and battery mass decreases with technology but engine size stays relatively constant.

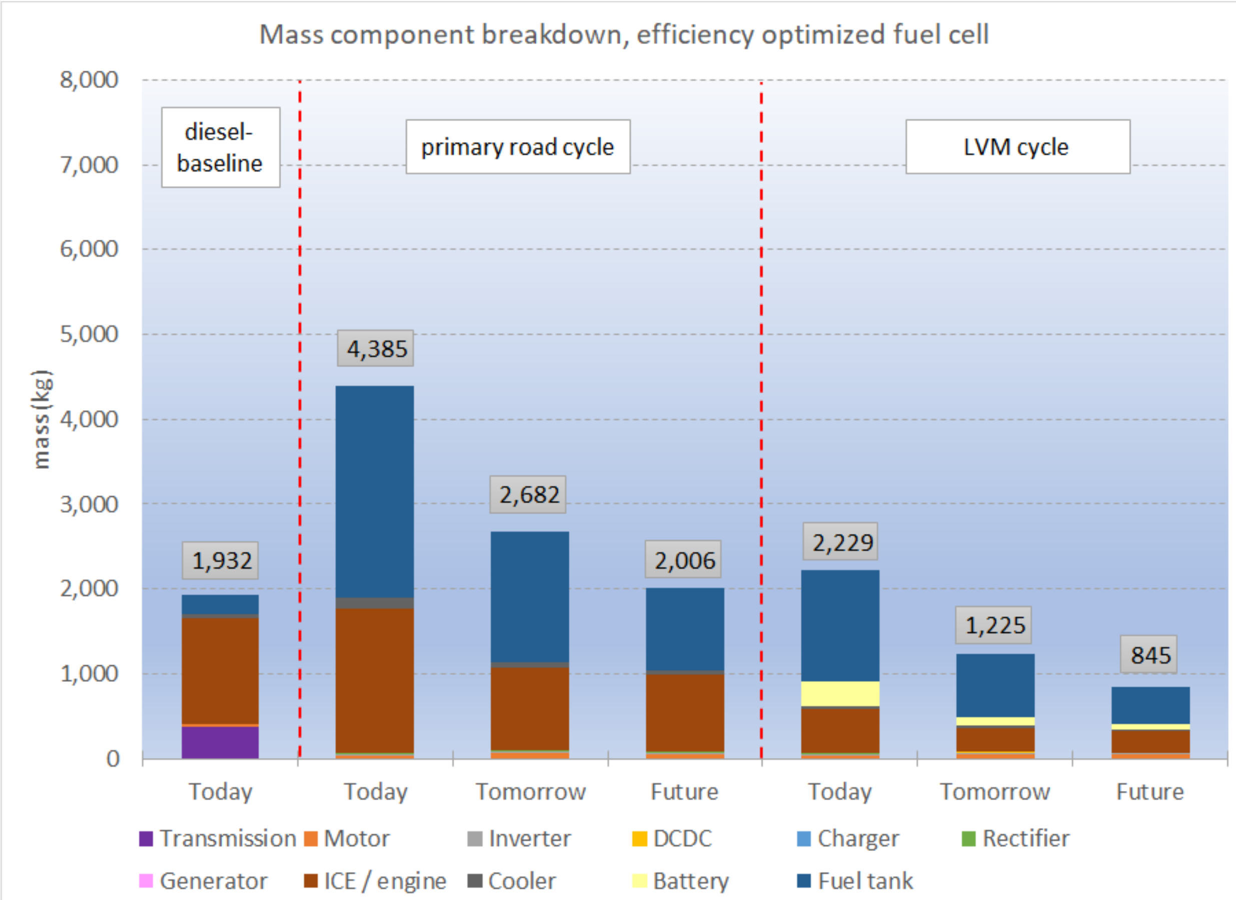

Figure 91: Mass component analysis, eff. optimized fuel cell for today, tomorrow, and future values

Figure 92 is a plot of system component volume for the efficiency optimized fuel cell as a function of today, tomorrow, and future technology values for the primary and LVM cycles. From today to tomorrow values, the reduction in volume is about 50%, while from tomorrow to future values, the reduction is another 20%.

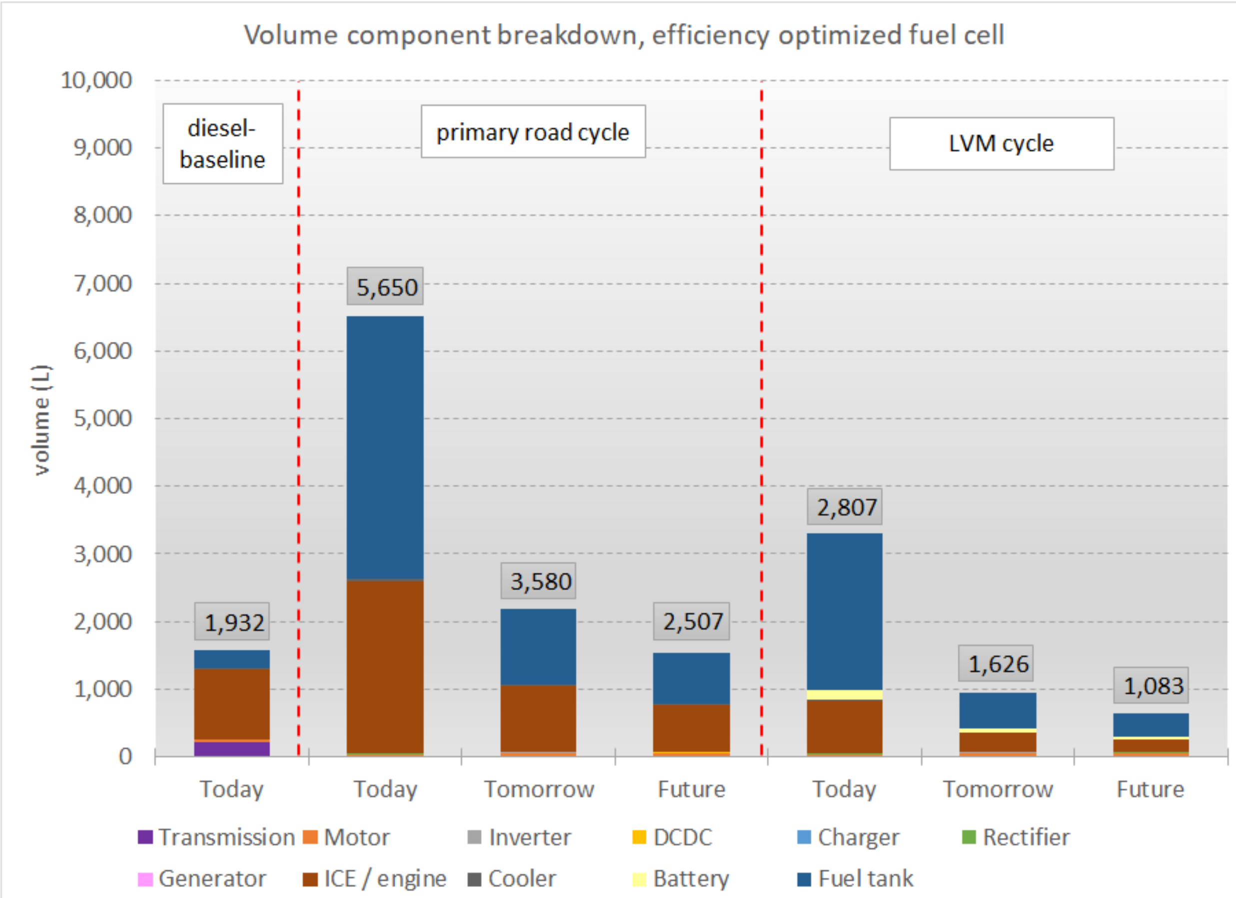

Figure 92: Volume component analysis, eff. optimized fuel cell for today, tomorrow, and future values

6.4 Continuous Power Requirement

Conventional combustion engines have a low sensitivity to duration; that is, so long as fuel supplied to the engine and heat is removed, they can operate at their peak power output. This is in contrast to batteries, which have a high sensitivity to duration. For select periods of time, and depending on the starting SOC, batteries can operate at peak power output; providing short bursts of power to the engine. There is a trade-off between engine size, battery capacity, powertrain mass, and power output as a function of time. For all the vehicle concepts in this project, the continuous power duration requirement was set at 10-minutes but it could be set longer or shorter. The example below illustrates the effect on electrification of vehicle depending on where this duration is set. The vehicle concept used for this example is the power dense fuel cell; but this example holds for any of the hybrid vehicle concepts.

Figure 93 is a plot of total power output as a function of degree of vehicle electrification for a continuous power output of 10-minutes. Recall that the continuous power output requirement is 320 kW. The cursor can be moved on the line from left to right to increase the power output. If moved towards the left, the vehicle is becoming less electrified (bigger engine); if moving to the right, the vehicle is becoming more electrified (more batteries). At the line minimum, the total power is a minimum as well as the powertrain mass (2,511 kg); however, this total power is only 268.5 kW. It does not meet the 320 kW continuous power requirement. To reach the 320 kW requirement, there are two solutions; increase the engine size or increase the battery capacity. Because the continuous power duration is short, 10-minutes only, the slope of the line to the right is steep. The maximum power output for a 100% fully electrified vehicle is very high; almost 1,800 kW. Such a vehicle would have access to 1,800 kW of power for 10-mins at a starting battery SOC of 100%. Conversely, the slope of the line to the left of the minimum is gentler; a fully non-electrified engine could produce 423 kW of power. It should be noted that by increasing engine size or battery capacity, powertrain mass is increasing. For this example, to better increase power while keeping the powertrain mass low, it’s optimal to increase battery capacity.

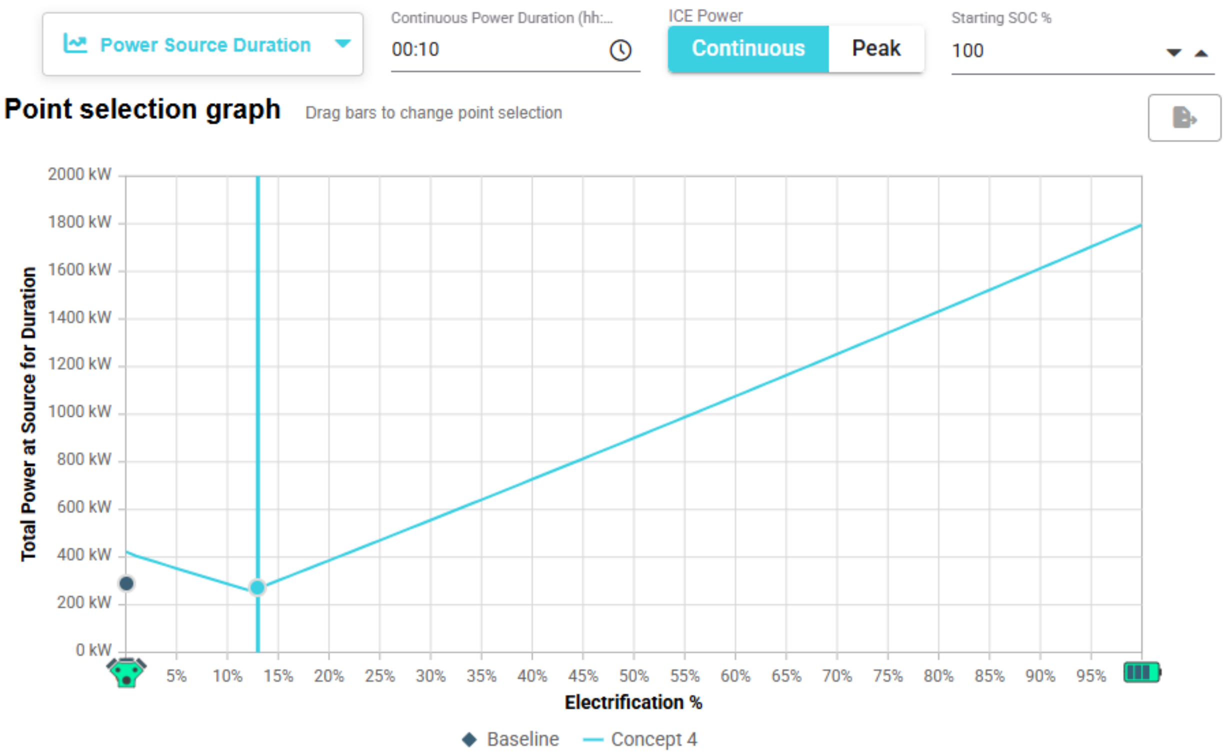

Figure 93: Power output PD fuel cell, LVM cycle, today values 10-min. continuous power

Figure 94 is a plot of total power output as a function of degree of vehicle electrification for a continuous power output of 2-hours. The power output is 79.5 kW at the minimum powertrain mass of 2,511 kg. This is the same powertrain mass as the Figure 93 but now the power output is 3.3 times less. The total power available for this powertrain is much less if the continuous power duration is 2-hours. For a fully 100% electrified powertrain, the total power is 269.4 kW, which is less than the fully non-electrified version. For this example, to get more power, while keeping powertrain mass lower; it’s more advantageous to increase engine size.

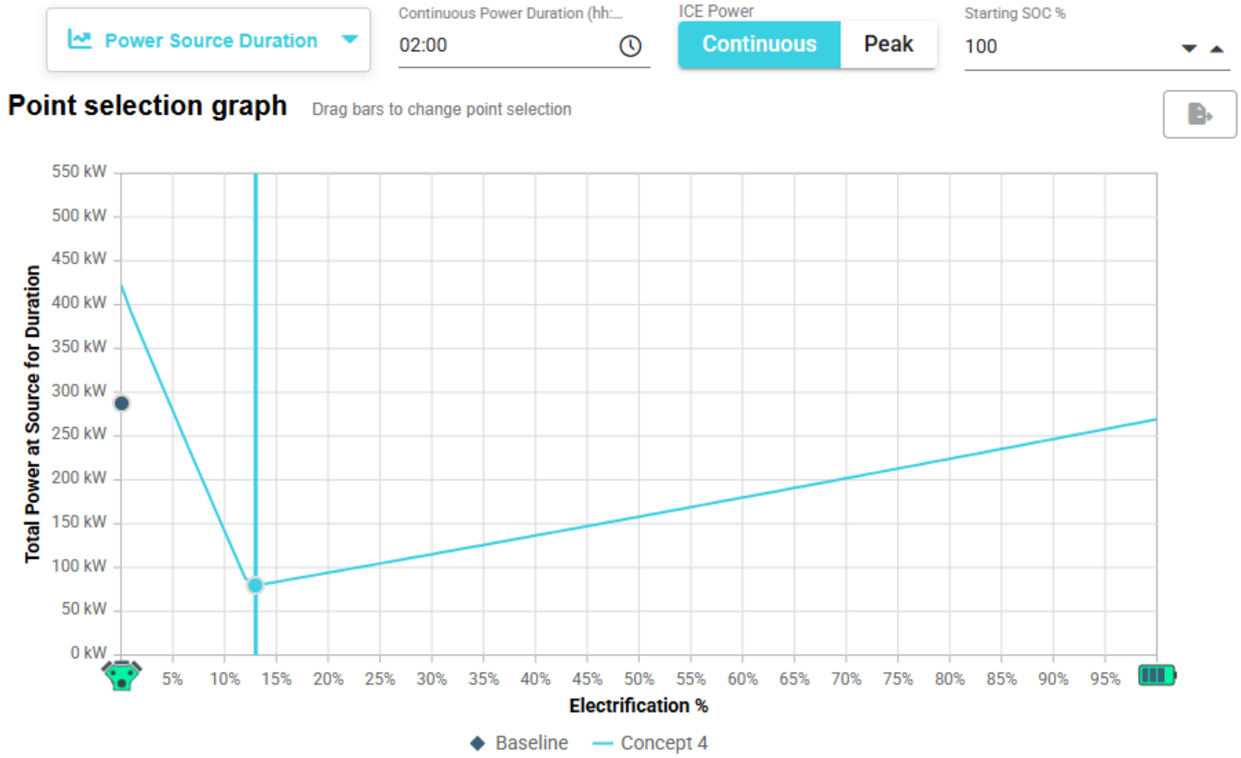

Figure 94: Power output PD fuel cell, LVM cycle, today values 2-hr continuous power

Figure 95 illustrates the trade-off between engine size, battery capacity, powertrain mass and total power output. Total power output is kept constant at around 320 to ~330 kW while continuous power duration is increased from 10-minutes to 2.5-hours. Moving from the centre axis to the left, means increasing the engine size and moving away from an electrified vehicle. Moving from the centre axis to the right, means increasing the battery capacity and moving towards an electrified vehicle. All of these vehicles meet the design requirements but their composition and overall mass changes. This plot shows that the continuous power requirement duration has a significant impact on powertrain composition and mass. For duration 40-minutes or less, the electrified vehicle has smaller powertrain mass. For duration longer than 50-minutes, the non-electrified vehicle has smaller powertrain mass. There is a transition point between 40 and 50-minutes. When setting requirements for vehicle power output, with conventional combustion engine power duration has not typically been a concern but to move towards an electrified powertrain, power duration must be considered. There can be a tendency to overestimate continuous power requirements; to want full power all the time. When transitioning to electrified powertrains, a shift in mindset is needed; actual vehicle performance requirements should be understood and applied, rather than relying on historical assumptions.

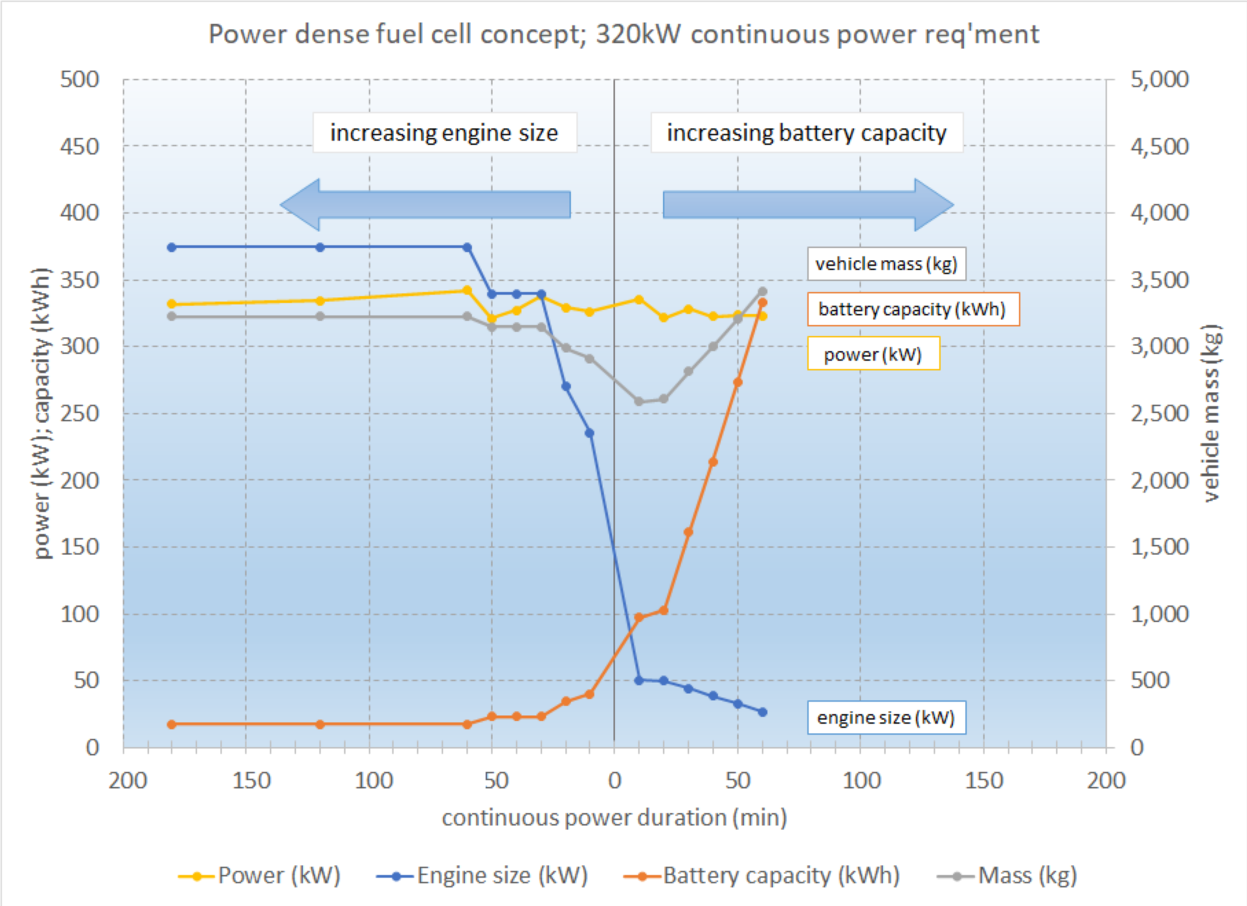

Figure 95: Engine size, battery capacity and powertrain mass vs. power duration, PD fuel cell LVM cycle today values, 320-kW continuous power

In addition to considering the continuous power duration, the battery starting SOC must also be studied. For this project, 100% battery SOC has been assumed throughout. But if the starting SOC is less than 100%, this will impact the total power available, especially for an electrified powertrain. Figure 96 and Figure 97 are examples of the impact of a lower SOC, namely 50%. For Figure 96, with 10-minute continuous duration, the minimum power has lowered from 269 kW to 224 kW and the power output for a fully electrified powertrain would be 1435 kW. Still very high but not as much as 1800 kW. For Figure 97, the 2-hour continuous duration, the minimum power has lowered from 79.5 kW to 60.9 kW. There was no change to the non-electrified slope. Once a vehicle concept has been established, it's critical to return to the drive cycle and model the power and energy usage over the cycle to understand how consumption of fuel and battery capacity will evolve; to determine if the assumptions that have been made during design are correct or need to be revised. An iterative design process is required.

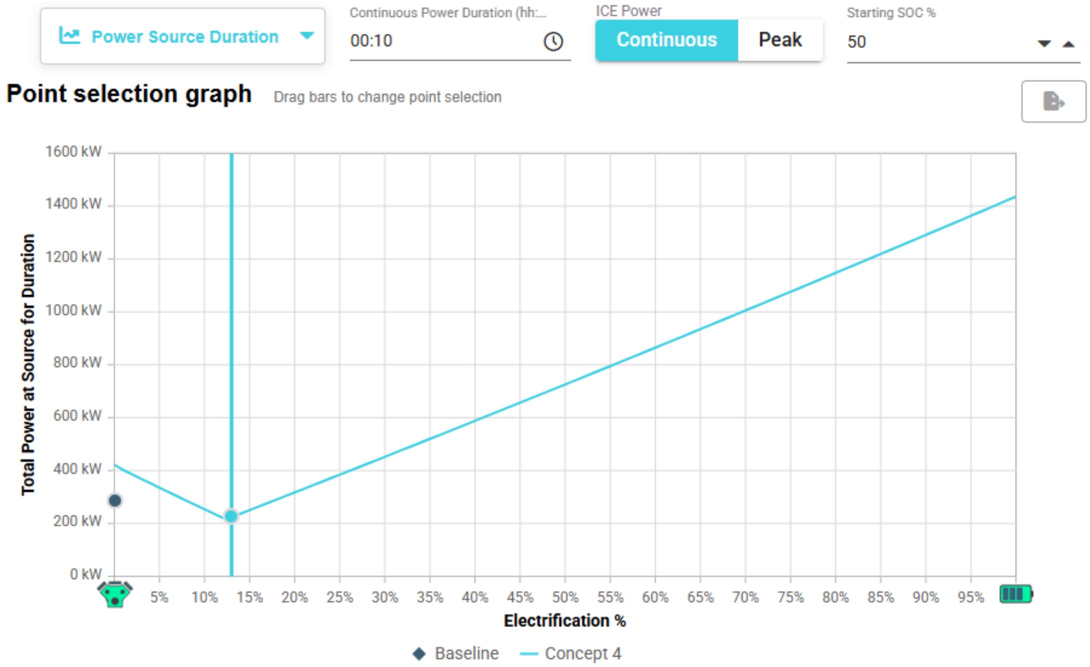

Figure 96: Power output PD fuel cell, LVM cycle, today values 10-min. cont. power, 50% batt. SOC

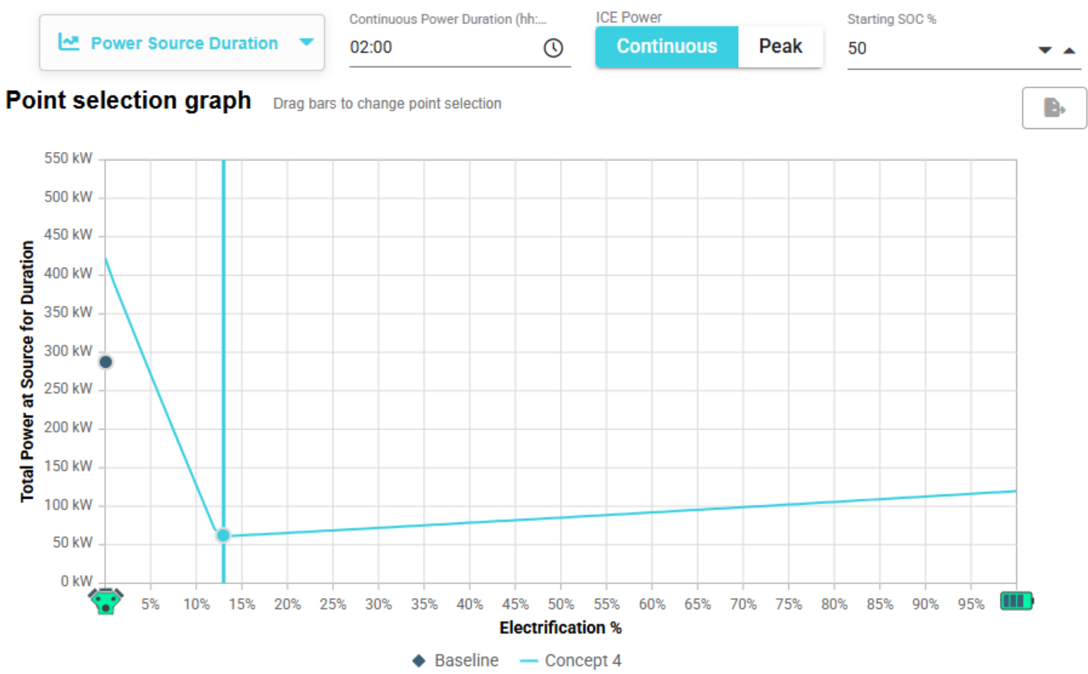

Figure 97: Power output PD fuel cell, LVM cycle, today values 2-hr cont. power, 50% batt. SOC

6.5 All Concept Vehicle Data

Table 13 and Table 14 summarize all the vehicle concept sizing, power, and energy data for the primary road and LVM cycle, respectively.

Table 13: Vehicle concepts sizing, power, and energy data for the primary road cycle

Techn.	Concept	Parameter	Trans-mission	Motor	Inverter	DCDC	Charger	Rectifier	Generator	Engine	Cooler	Parameter	Battery	Fuel Tank	TOTAL
Today	Diesel baseline	Peak power (kW)	319.7	8.4	--	--	--	--	--	376.5	192.0	Capacity (kWh)	--	2,549.6	
Today	Diesel baseline	Mass (kg)	380.6	24.7	--	--	--	--	--	1,255.1	48.0	Mass (kg)	--	223.6	**1,932**
Today	Diesel baseline	Volume (L)	214.6	40.0	--	--	--	--	--	1,045.9	13.7	Volume (L)	--	262.8	**1,577**
Today	H_2-ICE	Peak power (kW)	333.3	8.7	--	--	--	--	--	404.6	32.1	Capacity (kWh)	--	3,532.0	
Today	H_2-ICE	Mass (kg)	396.7	25.7	--	--	--	--	--	1,526.8	80.3	Mass (kg)	--	3,332.1	**5,362**
Today	H_2-ICE	Volume (L)	223.7	41.7	--	--	--	--	--	1,260.4	23.0	Volume (L)	--	5,194.1	**6,743**
Today	H_2-ICE parallel	Peak power (kW)	330.7	245.5	288.8	8.9	6.9	--	--	186.8	13.8	Capacity (kWh)	61.3	3,253.5	
Today	H_2-ICE parallel	Mass (kg)	393.6	24.1	13.1	3.5	2.0	--	--	704.7	34.6	Mass (kg)	438.0	3,069.4	**4,683**
Today	H_2-ICE parallel	Volume (L)	221.9	24.1	8.0	2.5	2.3	--	--	581.8	7.8	Volume (L)	235.8	4,784.6	**5,869**
Today	H_2-ICE series	Peak power (kW)	--	334.4	393.3	9.0	5.1	183.7	189.4	254.8	17.7	Capacity (kWh)	45.2	4,231.8	
Today	H_2-ICE series	Mass (kg)	--	32.8	17.9	3.6	1.5	8.4	18.6	1,207.4	44.2	Mass (kg)	323.2	3,992.3	**5,650**
Today	H_2-ICE series	Volume (L)	--	28.8	10.9	2.6	1.7	5.1	16.3	1,362.3	12.6	Volume (L)	174.0	6,223.2	**7,838**
Today	PD fuel cell	Peak power (kW)	--	331.3	389.8	8.9	80.7	182.1	--	215.3	276.0	Capacity (kWh)	44.8	4,090.7	
Today	PD fuel cell	Mass (kg)	--	32.5	17.7	3.5	23.1	8.3	--	512.7	69.1	Mass (kg)	320.3	3,859.2	**4,846**
Today	PD fuel cell	Volume (L)	--	28.6	10.8	2.5	26.9	5.1	--	769.9	19.7	Volume (L)	172.4	6,015.7	**7,052**
Today	EO fuel cell	Peak power (kW)	--	329.7	387.9	8.8	--	404.3	--	711.7	48.9	Capacity (kWh)	--	2,646.4	
Today	EO fuel cell	Mass (kg)	--	32.3	17.6	3.5	--	18.4	--	1,694.6	122.3	Mass (kg)	--	2,496.6	**4,385**
Today	EO fuel cell	Volume (L)	--	28.4	10.8	2.5	--	11.2	--	2,541.9	34.9	Volume (L)	--	3,891.8	**6,522**
Tomorrow	H_2-ICE series	Peak power (kW)	--	326.4	362.6	8.7	4.7	142.9	145.9	211.1	8.5	Capacity (kWh)	41.4	2,989.9	
Tomorrow	H_2-ICE series	Mass (kg)	--	58.3	16.5	2.7	1.0	6.5	26.0	1,000.4	21.2	Mass (kg)	147.7	2,299.9	**3,580**
Tomorrow	H_2-ICE series	Volume (L)	--	56.3	9.9	2.2	1.2	3.9	25.1	1,128.8	6.6	Volume (L)	82.7	1,661.1	**2,978**
Tomorrow	EO fuel cell	Peak power (kW)	--	322.8	358.7	8.6	--	370.3	--	634.7	26.6	Capacity (kWh)	--	2,009.0	
Tomorrow	EO fuel cell	Mass (kg)	--	57.6	16.3	2.6	--	16.8	--	976.4	66.5	Mass (kg)	--	1,545.4	**2,682**
Tomorrow	EO fuel cell	Volume (L)	--	55.7	9.8	2.2	--	10.2	--	976.4	20.8	Volume (L)	--	1,116.1	**2,191**
Future	H_2-ICE series	Peak power (kW)	--	322.1	346.3	8.5	4.4	136.0	138.0	190.3	4.8	Capacity (kWh)	39.2	2,378.4	
Future	H_2-ICE series	Mass (kg)	--	55.5	11.5	2.1	0.8	4.5	23.8	901.8	14.0	Mass (kg)	93.7	1,399.1	**2,507**
Future	H_2-ICE series	Volume (L)	--	53.7	8.7	1.7	0.9	3.4	23.0	1,017.5	4.6	Volume (L)	49.2	1,081.1	**2,244**
Future	EO fuel cell	Peak power (kW)	--	320.0	344.1	8.5	--	353.6	--	595.7	15.6	Capacity (kWh)	--	1,637.7	
Future	EO fuel cell	Mass (kg)	--	55.2	11.5	2.1	--	11.8	--	916.5	45.9	Mass (kg)	--	963.1	**2,006**
Future	EO fuel cell	Volume (L)	--	53.3	8.6	1.7	--	8.8	--	700.8	15.1	Volume (L)	--	744.2	**1,533**

Table 14: Vehicle concepts sizing, power, and energy data for the LVM cycle

Techn.	Concept	Parameter	Trans-mission	Motor	Inverter	DCDC	Charger	Rectifier	Generator	Engine	Cooler	Parameter	Battery	Fuel Tank	TOTAL
Today	Diesel baseline	Peak power (kW)	320.2	8.4	--	--	--	--	--	392.9	35.0	Capacity (kWh)	--	2,470.1	
Today	Diesel baseline	Mass (kg)	381.1	24.7	--	--	--	--	--	1,309.8	87.8	Mass (kg)	--	216.7	**2,020**
Today	Diesel baseline	Volume (L)	214.9	40.0	--	--	--	--	--	1,085.4	25.1	Volume (L)	--	254.6	**1,620**
Today	H_2-ICE	Peak power (kW)	338.6	8.9	--	--	--	--	--	434.2	55.8	Capacity (kWh)	--	2,377.6	
Today	H_2-ICE	Mass (kg)	403.1	26.1	--	--	--	--	--	1,638.5	139.5	Mass (kg)	--	2,243.0	**4,450**
Today	H_2-ICE	Volume (L)	227.2	42.3	--	--	--	--	--	1,352.7	39.9	Volume (L)	--	3,496.5	**5,159**
Today	H_2-ICE parallel	Peak power (kW)	325.2	357.3	420.4	8.7	10.8	--	--	50.5	3.7	Capacity (kWh)	96.0	1,408.1	
Today	H_2-ICE parallel	Mass (kg)	387.1	35.0	19.1	3.5	3.1	--	--	190.6	9.4	Mass (kg)	686.0	1,328.4	**2,662**
Today	H_2-ICE parallel	Volume (L)	218.2	30.8	11.7	2.5	3.6	--	--	157.4	2.7	Volume (L)	369.4	2,070.7	**2,867**
Today	H_2-ICE series	Peak power (kW)	--	326.3	383.8	8.7	10.2	42.9	44.2	69.9	4.8	Capacity (kWh)	90.8	1,857.7	
Today	H_2-ICE series	Mass (kg)	--	32.0	17.4	3.5	2.9	2.0	4.3	331.3	12.1	Mass (kg)	648.6	1,752.5	**2,807**
Today	H_2-ICE series	Volume (L)	--	28.1	10.5	2.5	3.4	1.2	3.8	373.8	3.5	Volume (L)	349.2	2,731.8	**3,508**
Today	PD fuel cell	Peak power (kW)	--	324.6	381.9	8.7	10.9	42.7	--	50.5	6.5	Capacity (kWh)	97.2	1,803.4	
Today	PD fuel cell	Mass (kg)	--	31.8	17.4	3.5	3.1	1.9	--	120.2	16.2	Mass (kg)	694.0	1,701.3	**2,589**
Today	PD fuel cell	Volume (L)	--	28.0	10.6	2.5	3.6	1.2	--	180.3	4.6	Volume (L)	373.7	2,652.0	**3,257**
Today	EO fuel cell	Peak power (kW)	--	321.8	378.6	8.6	4.5	196.6	--	217.6	15.0	Capacity (kWh)	39.6	1,248.1	
Today	EO fuel cell	Mass (kg)	--	31.6	17.2	3.4	1.3	8.9	--	518.2	37.4	Mass (kg)	282.9	1,327.8	**2,229**
Today	EO fuel cell	Volume (L)	--	27.7	10.5	2.5	1.5	5.5	--	777.3	10.7	Volume (L)	152.3	2,311.4	**3,299**
Tomorrow	H_2-ICE series	Peak power (kW)	--	317.0	352.2	8.4	6.3	40.7	416.0	60.2	2.4	Capacity (kWh)	56.0	1,363.7	
Tomorrow	H_2-ICE series	Mass (kg)	--	56.5	16.0	2.6	1.4	1.9	7.4	285.2	6.1	Mass (kg)	199.9	1,049.0	**1,626**
Tomorrow	H_2-ICE series	Volume (L)	--	54.7	9.6	2.1	1.6	1.1	7.2	321.8	1.9	Volume (L)	111.9	757.6	**1,270**
Tomorrow	EO fuel cell	Peak power (kW)	--	320.0	355.6	8.5	3.8	58.3	--	185.4	7.8	Capacity (kWh)	30.9	950.0	
Tomorrow	EO fuel cell	Mass (kg)	--	57.1	16.2	2.6	0.8	2.7	--	285.3	19.4	Mass (kg)	110.3	730.8	**1,225**
Tomorrow	EO fuel cell	Volume (L)	--	55.2	9.7	2.1	0.9	1.6	--	285.3	6.1	Volume (L)	61.7	527.8	**950**
Future	H_2-ICE series	Peak power (kW)	--	312.5	336.1	8.3	5.9	38.0	38.6	53.2	1.3	Capacity (kWh)	52.2	1,064.3	
Future	H_2-ICE series	Mass (kg)	--	53.9	11.2	2.1	1.1	1.3	6.7	252.2	3.9	Mass (kg)	124.3	626.1	**1,083**
Future	H_2-ICE series	Volume (L)	--	52.1	8.4	1.7	1.2	1.0	6.4	284.6	1.3	Volume (L)	65.3	483.8	**906**
Future	EO fuel cell	Peak power (kW)	--	310.5	333.9	8.2	3.7	39.4	--	164.4	4.3	Capacity (kWh)	33.0	733.8	
Future	EO fuel cell	Mass (kg)	--	53.5	11.1	2.1	0.7	1.3	--	252.9	12.7	Mass (kg)	78.5	431.7	**845**
Future	EO fuel cell	Volume (L)	--	51.8	8.3	1.6	0.7	1.3	--	193.4	4.2	Volume (L)	41.2	333.6	**636**

7.0 Conclusions

The purpose of this project was to examine the existing diesel-baseline heavy logistics vehicle, establish fundamental vehicle level requirements, generate two drive cycles, survey current, and future component technology levels, select vehicle configurations, and analyze these vehicle configurations, based on all the inputs, towards understanding the overall vehicle envelope, particularly mass and volume, of a hydrogen-fuel supplied vehicle.

The lack of vehicle level requirements as well as drive cycles posed a challenge such that assumptions were made; assumptions open the opportunity for interpretation. Leveraging the expertise of the project contributors enabled the qualification of these assumptions. After much analysis and effort, the logistics vehicle mission profile is now a useable drive cycle for the heavy logistics vehicle and can be re-used for other analyses, such as energy management or other modeling. The drive cycle should be validated with real-world data.

A clear dependency of both powertrain mass and volume on the selected drive cycle was observed across all hydrogen-based powertrain configurations. The results indicate that while the overall trends are consistent, the magnitude of the variation differs notably between the primary road cycle and the logistics vehicle drive cycle.

For the primary road cycle, total powertrain masses ranged from approximately 4,385 to 5,650 kilograms. In comparison, for the LVM cycle, the range was lower, between 2,229 and 4,450 kilograms. The wider variation in mass under the LVM cycle suggests that vehicle architecture and component sizing are more sensitive to the lower-speed, transient operating conditions typical of this drive cycle. This may reflect differences in powertrain optimization strategies, such as energy storage capacity and the relative contribution of the internal combustion engine or fuel cell. While vehicle idling time was considered in the LVM cycle, other requirements, such as silent drive and silent watch capabilities were not part of the analysis. In the future, they need to be incorporated in a more detailed platform design effort to ensure that the vehicle is optimized to meet these requirements.

Among the vehicle concepts evaluated, the H_2-ICE parallel hybrid and the two fuel cell configurations generally demonstrated lower mass and/or volume compared to other designs. This outcome aligns with expectations, as fuel cell systems typically allow for higher energy conversion efficiencies and can be integrated with lighter ancillary systems when optimized for hybrid operation.

Despite these advantages, there was no clear overall winner in terms of vehicle concept configuration under either drive cycle when using current technology assumptions. Each concept presented trade-offs between mass, volume, and performance characteristics. For example, while fuel cell systems achieved lower masses, they may involve higher system complexity and cost. Factors such as cost, durability, reliability, maintainability, availability, etc. will determine the optimal solution for platform designs going forward, but these elements were not studied in this report.

The H_2-ICE concept in particular emerged as the least competitive configuration, showing the highest total powertrain mass under the LVM cycle and the second highest mass under the primary road cycle.

This suggests that, with today's component efficiencies and packaging constraints, hydrogen internal combustion technologies may face limitations in achieving mass parity with fuel cell–based systems. Improvements in engine downsizing, light-weighting strategies, and hybridization could narrow this gap in future iterations.

From a sensitivity perspective with today technology, both power duration and SOC strongly influence vehicle mass. Shorter continuous power durations (40 minutes or less) favour electrified vehicles, which can deliver high power bursts with smaller overall mass, while longer durations (over 50 minutes) favour conventional or non-electrified vehicles, which can sustain continuous power without relying on large batteries. Moreover, a lower starting battery SOC (for example, 50% instead of 100%) significantly reduces total available power by as much as 15–20% for short durations and over 20% for extended durations, further emphasizing the need to accurately define operational power durations and model SOC changes over time.

Looking forward, it's evident that advances in technologies will have a significant impact on powertrain component sizing. Of the two concepts which were analyzed under today, tomorrow, and future technology values, both converged and then went under the diesel-baseline mass and volume at some point in the future; the speed in the conversion being a function of advances in hydrogen storage, engine efficiency, and battery energy density increases, for example.

The technology focus in the future should be on increasing the fuel tank volumetric power density and gravimetric energy density, as well as reducing the energy required to release the hydrogen on the vehicle and increasing engine efficiency. The hydrogen fuel and tank made up the most significant mass and volume for all the concepts examined. Improvements in the onboard hydrogen storage will have a vast impact on the overall vehicle design in the future.

Overall, these findings highlight the importance of considering drive-cycle characteristics when evaluating electrified vehicle designs. The results emphasize that optimal configurations may differ depending on the intended vehicle application, and that technology advances in energy storage, power density, and system integration will be key to improving competitiveness across all hydrogen powertrain concepts.

An area that wasn't highlighted in this project are the similarities and differences in understanding how vehicle engineering diverges between civilian and military applications. For example, the Mercedes-Benz Zetros is the baseline platform for the logistics military vehicle but it shares components across other civilian commercial vehicles, particularly in the heavy-duty truck range. The fundamental process of vehicle design is the same across both civilian and military applications however design priorities differ; for example, military vehicles prioritize survivability, modularity, redundancy and off-road capability while civilian vehicles prioritize cost, efficiency, comfort, and emissions. In the past, emissions haven't been a large concern for the military but increasingly both sectors must consider emissions, fuel efficiency, and sustainability. These differences in design priorities, as well as the requirements and drive cycles, discussed herein this report, are the fundamental reasons why civilian and military vehicle designs can differ so significantly. They also illustrate why electrifying the military transport sector poses unique challenges, despite the availability of advanced electrification technologies in the civilian market.

8.0 Lessons Learned

Upon completion of this project, the contributors were invited to provide feedback on key lessons learned from the activity. These were items which should be retained for future projects, as well as areas which could be improved. The areas for improvement can be broken down into the following categories:

- project planning,
- expertise,
- drive cycle and requirements, and
- tools.

In terms of project planning, both NRC and DND must abide by the Government of Canada procurement rules and guidelines. When working with other government organizations or outside contractors, it's important to communicate these rules and guidelines early. There is potential for challenges with contracting and careful planning is required at the start of each project.

Having to contract-out some of the required expertise for this project was time-consuming. NRC should examine how they can better leverage their internal expertise, expand their available expertise or review streamlining the contracting process.

In order to properly perform powertrain analysis, data is required. The ideal format for the cycle is vehicle speed and grade over time. The data provided for this project was aggregate fuel consumption data. In order to rework the data into the necessary format, assumptions were made, which leaves room for interpretation. This drive cycle data should ideally be correlated with real world fuel consumption.

Along with the drive cycle, fundamental specific requirements for vehicle level performance, which exceed the cycle performance, should be provided. These are items such as gradeability, acceleration, hill-climb, and maximum speed etc. These requirements need to be well defined; including powertrain mass (if different), grade, duration, environmental condition and temperature, etc.

For electrified powertrains, available power is highly dependent on duration. Whereas historically combustion engines can operate at continuous power, assuming fuel is available and heat is removed; electrified powertrains are specified in terms of energy capacity, rather than power. This provides a unique opportunity to downsize engine and fuel tank, while still meeting, or exceeding, all the power target requirements. This fundamental characterization of electrified powertrains must be distinctly understood when establishing requirements. Setting a continuous power requirement duration to be too long will inherently limit the design possibilities and lead down a path where conventional combustion is the only solution.

Multiple different powertrain analysis and sizing tools exist commercially, including AVL Cruise, GT-Suite, Autonomie by Argonne Labs, and CarSim / Truck Sim. For this project, the ePOP Concept tool was selected, the contributors helped validate new software features including regenerative braking and power output analysis. To carry out a full detailed powertrain analysis, it is also necessary to model the thermal (e.g., radiators, pumps, fans) and energy management systems (e.g., battery SoC, fuel level etc.) over the duration of the drive cycle; performing an iterative analysis.

8.1 Recommendations and Future Work

Recommendations for follow-on work related to this project include:

- Collecting drive cycle data in the appropriate format (vehicle speed and grade versus time, braking energy, terrain type)
- Validating modeled drive cycles against real-world fuel consumption data
- Clearly defining vehicle-level performance requirements, and limitations, including:
    - Gradeability, acceleration, hill-climb, and maximum speed
    - Vehicle mass, grade, duration, environmental conditions, terrain
    - Detailed sensitivity and uncertainty analysis for each system / operational variability (e.g., terrains, gradients etc.)
- Modeling vehicle thermal and energy management as a function of the drive cycle and component size selection
    - Compare commercially available toolsets for vehicle designing
    - Monitoring fuel economy and battery SoC and understanding their impact on system component size, performing dynamic simulations including thermal systems of the vehicle (e.g., radiators, pumps, fans, pipework)
- Efficiency analysis for each vehicle concept, including error calculations

Areas that were not in scope for this project but that should be examined in a future project include:

- Refuelling and power delivery infrastructure
- Cost modelling (fuel and electricity, vehicle cost)
- Safety assessment of solid-state hydrogen supply for military vehicles

Acronyms and Abbreviations

Table 15 provides definitions for acronyms and abbreviations from this document.

Table 15: Acronyms and abbreviations

Acronyms and abbreviations	Definition	Acronyms and abbreviations (cont'd)	Definition (cont'd)
AI	artificial intelligence	ISO	International Organization for Standardization
BEV	battery electric vehicle	LFP	lithium iron phosphate
BMEP	brake mean effective pressure	LHS	load handling system
BMS	battery management system	LiB	lithium-ion battery
CAF	Canadian Armed Forces	LMO	lithium manganese oxide
Cd	coefficient of drag	LTO	lithium-titanate-oxide
COP	coefficient of performance	LVM	logistics vehicle modernization
Crr	coefficient of rolling resistance	MEFA	membrane frame electrode assembly
DLR	Director Land Requirements	NATC	Nevada Automotive Test Center
DND	Department of National Defence	NCA	lithium-nickel-cobalt-aluminum oxide
DSD	Drive System Design	NMC	lithium-nickel-manganese-cobalt oxide
EDU	electric drive unit	NRC	National Research Council Canada
eff.	efficiency	NSSF	Canada National Safety and Security Fleet
EO	efficiency optimized	PD	power dense
ePOP	electrified powertrain optimization process	PEM	proton exchange membrane
GaN	gallium nitride	PMSM	permanent magnet synchronous motors
GDLS	General Dynamics Land Systems	RCMP	Royal Canadian Mounted Police
GHG	green-house gas	SiC	silicon carbide
grav.	gravimetric	SOC	state of charge
GVWR	gross vehicle weight rating	SSB	solid-state batteries
H2	hydrogen	tech.	technology
H2-ICE	hydrogen internal combustion engine	UDDS	urban dynamometer driving cycle
HAZOP	hazard and operability study	US DOE	U.S. Department of Energy
HWFET	highway fuel economy driving schedule	vol.	volumetric
ICE	internal combustion engine	ZEV	zero-emission vehicle
KPI	key performance indicator		

References

[1] Government of Canada. "Greening Government Strategy: A Government of Canada Directive." https://www.canada.ca/en/treasury-board-secretariat/services/innovation/greening-government/strategy.html (accessed November 18, 2025).

[2] Government of Canada. "Greening Government Strategy implementation plan and roadmap." https://www.canada.ca/en/treasury-board-secretariat/services/innovation/greening-government/implementing.html (accessed November 18, 2025).

[3] Department of National Defence Canada, "Defence Climate and Sustainability Strategy 2023-2027," 2023.

[4] Department of National Defence Canada. "Logistics Vehicle Modernization Project (LVM)." https://www.canada.ca/en/department-national-defence/services/procurement/logistics-vehicle-modernization-project.html (accessed October 22, 2024).

[5] Department of National Defence Canada, "A - Statement of Requirements Logistics Vehicle Modernization (LVM)."

[6] Department of National Defence Canada, "B - Appendix 1 to B LVM Heavy Capability."

[7] Marshall Group. "Integrated platform solutions." https://marshalllandsystems.com/capabilities/integrated-platform-solutions (accessed December 15, 2025).

[8] Drive System Design. "Drive System Design, A Hinduja Tech Company." https://www.drivesystemdesign.com/ (accessed December 23, 2025).

[9] Drive System Design, "Drive System Design Optimizes In-House Analysis Tool for E-mobility Applications," *OEM Off-Highway*. [Online]. Available: https://www.oemoffhighway.com/engineering-manufacturing/press-release/21533074/drive-system-design-dsd-drive-system-design-optimizes-inhouse-analysis-tool-for-emobility-applications

[10] MAHLE. "Hydrogen Combustion." https://www.mahle-powertrain.com/en/ic-engines/hydrogen-combustion/ (accessed December 23, 2025).

[11] MAHLE. "MAHLE Powertrain supports heavy-duty hydrogen combustion engine development." https://newsroom.mahle.com/press/en/press-releases/mahle-powertrain-supports-heavy-duty-hydrogen-combustion-engine-development-107520# (accessed December 23, 2025).

[12] Bak Motors. https://bakmotors.ch/ (accessed December 23, 2025).

[13] Plasma Kinetics. https://plasmakinetics.com/ (accessed December 23, 2025).

[14] Donut Lab. "The Donut Motors." https://www.donutlab.com/motor/ (accessed December 23, 2025).

[15] ESOX Group. "ESOX Group." https://esoxgroup.com/ (accessed December 23, 2025).

[16] Chris Mi, Abul Masrur, and D. W. Gao, *Hybrid electric vehicles : principles and applications with practical perspectives*. Hoboken, N.J.: Wiley, 2011.

[17] B. Ganji, A. Kouzani, and H. Trinh, "Drive Cycle Analysis of the Performance of Hybrid Electric Vehicles," presented at the Life System Modeling and Intelligent Computing, International Conference on Life System Modeling and Simulation, LSMS 2010, and International Conference on Intelligent Computing for Sustainable Energy and Environment, ICSEE 2010, Wuxi, China, 2010.

[18] R. Jones *et al.*, "A realistic US Long-haul Drive Cycle for Vehicle Simulations, Costing and Emissions Analysis," MIT, Transportation Research Record, 2023.

[19] M.-B. D. Trucks. "Zetros 8x8 all-rounder." https://special.mercedes-benz-trucks.com/en/mercedes-benz-defence-trucks/general/product-range/zetros-8x8-all-rounder.html (accessed 2026-02-27, 2026).

[20] General Dynamics Land Systems, "LVM-BB142-V2 Att 53," 2022.

[21] General Dynamics Land Systems, "LVM Vehicle Summary," 2025.

[22] Mercedes-Benz Powertrain. *Portfolio Truck Classic: EURO III, EURO V, and EEV*. (2021).

[23] MAHLE, "H2 ICE input data for ePop simulation tool," 2025.

[24] L. Liu, Y. Zhang, X. Qin, H. Hui, X. Min, and P. Leggott, "Development of a 6.7L Direct Injection, Lean Burn H2 Spark Ignition Engine for Medium- and Heavy-Duty Commercial Vehicles," 2025. [Online]. Available: https://doi.org/10.4271/2025-01-8393.

[25] C. Bekdemir, E. Doosje, and X. Seykens, "H2-ICE Technology Options of the Present and the Near Future," 2022. [Online]. Available: https://doi.org/10.4271/2022-01-0472.

[26] K. Singh, T. N. Verma, G. Dwivedi, and A. K. Shukla, "Hydrogen production, storage, and CI Engine utilisation: A global perspective," *Process Safety and Environmental Protection,* vol. 190, pp. 1067-1092, 2024/10/01/ 2024, doi: https://doi.org/10.1016/j.psep.2024.07.110.

[27] Z. Stępień, "A Comprehensive Overview of Hydrogen-Fueled Internal Combustion Engines: Achievements and Future Challenges," *Energies*, vol. 14, no. 20*,* p. 6504doi: 10.3390/en14206504.

[28] G. Chandrasa, Soedibyo, B. Tambunan, E. Listiani Dewi, and R. Fajar, "Developing hydrogen as energy for transportation means in Indonesia," 2023.

[29] Argonne National Laboratory, "Technology Assessment of a Fuel Cell Vehicle: 2017 Toyota Mirai," 2018.

[30] Q. Hassan, I. D. J. Azzawi, A. Z. Sameen, and H. M. Salman, "Hydrogen Fuel Cell Vehicles: Opportunities and Challenges," *Sustainability*, vol. 15, no. 15*,* p. 11501doi: 10.3390/su151511501.

[31] W. Zhu, Y. Wang, S. Gao, F. He, C. Li, and Y. Wang, "Study on cold start of fuel cell stack combined with liquid heating and fuel cell self-starting," *Case Studies in Thermal Engineering,* vol. 60, p. 104814, 2024/08/01/ 2024, doi: https://doi.org/10.1016/j.csite.2024.104814.

[32] M. Luo *et al.*, "Cold start investigation of fuel cell vehicles with coolant preheating strategy," *Applied Thermal Engineering,* vol. 201, p. 117816, 2022/01/25/ 2022, doi: https://doi.org/10.1016/j.applthermaleng.2021.117816.

[33] K. Mazloomi and C. Gomes, "Hydrogen as an energy carrier: Prospects and challenges," *Renewable and Sustainable Energy Reviews,* vol. 16, no. 5, pp. 3024-3033, 2012/06/01/ 2012, doi: https://doi.org/10.1016/j.rser.2012.02.028.

[34] M. Altaf, U. B. Demirci, and A. K. Haldar, "Review of solid-state hydrogen storage: Materials categorisation, recent developments, challenges and industrial perspectives," *Energy Reports,* vol. 13, pp. 5746-5772, 2025/06/01/ 2025, doi: https://doi.org/10.1016/j.egyr.2025.05.034.

[35] M. H. McCay and S. Shafiee, "22 - Hydrogen: An Energy Carrier," in *Future Energy (Third Edition)*, T. M. Letcher Ed.: Elsevier, 2020, pp. 475-493.

[36] Bak Motors. *Solid state hydrogen storage specification for defence land systems programs*. (2025).

[37] P. Smith, "H2 Solid State Storage," S. Girard, Ed., ed, 2025.

[38] M. Balcerzak, M. Lau, and F. Heubner, "Solid Hydrogen Carriers. Advanced metal hydride technology for hydrogen storage, purification and compression applications," Fraunhofer Institute for Manufacturing Technology and Advanced Materials IFAM, 2024.

[39] F. Coelho Barbosa, "Battery Electric Rail Technology Review - A Technical and Operational Assessment. Current Status, Challenges and Perspectives," 2022, doi: 10.1115/JRC2022-78133.

[40] R. Knibbe *et al.*, "Application and limitations of batteries and hydrogen in heavy haul rail using Australian case studies," *Journal of Energy Storage,* vol. 56, p. 105813, 2022/12/01/ 2022, doi: https://doi.org/10.1016/j.est.2022.105813.

[41] M. Li, J. Lu, Z. Chen, and K. Amine, "30 Years of Lithium-Ion Batteries," *Advanced Materials,* vol. 30, no. 33, p. 1800561, 2018/08/01 2018, doi: https://doi.org/10.1002/adma.201800561.

[42] R. Thorne, A. H. Amundsen, and I. Sundvor, "Battery Electric and Fuel Cell Trains: Maturity of Technology and Market Status," Institute of Transport Economics Norwegian Centre for Transport Research, 2019. [Online]. Available: https://www.toi.no/publications/battery-electric-and-fuel-cell-trains-maturity-of-technology-and-market-status-article35971-29.html

[43] U.S. Department of Transportation Federal Railroad Administration, "Assessment of Battery Technology for Rail Propulsion Application," 2017. [Online]. Available: https://railroads.dot.gov/elibrary/assessment-battery-technology-rail-propulsion-application

[44] T. B. Reddy and D. Linden, *Linden's handbook of batteries*, 4th ed. (no. Book, Whole). New York: McGraw-Hill (in English), 2011.

[45] E. Kazyak and R. García-Méndez, "Recent progress and challenges for manufacturing and operating solid-state batteries for electric vehicles," *MRS Bulletin,* vol. 49, no. 7, pp. 717-729, 2024/07/01 2024, doi: 10.1557/s43577-024-00740-7.
[46] R. Shah, V. Mittal, and A. M. Precilla, "Challenges and Advancements in All-Solid-State Battery Technology for Electric Vehicles," *J*, vol. 7, no. 3, pp. 204-217doi: 10.3390/j7030012.
[47] *MIL-PRF-32383 Performance specification batteries, rechargeable, sealed generation specification for*, U.S. Department of Defense, 2011.
[48] K. Rajashekara, "Present Status and Future Trends in Electric Vehicle Propulsion Technologies," *IEEE Journal of Emerging and Selected Topics in Power Electronics,* vol. 1, no. 1, pp. 3-10, 2013, doi: 10.1109/JESTPE.2013.2259614.
[49] M. Ehsani, Y. Gao, S. Longo, and K. Ebrahimi, *Modern electric, hybrid electric, and fuel cell vehicles*. CRC press, 2018.
[50] S. Krishnamoorthy and P. P. K. Panikkar, "A comprehensive review of different electric motors for electric vehicles application," *Int. J. Power Electron. Drive Syst,* vol. 15, no. 1, p. 74, 2024.
[51] Z. Wang, T. W. Ching, S. Huang, H. Wang, and T. Xu, "Challenges Faced by Electric Vehicle Motors and Their Solutions," *IEEE Access,* vol. 9, pp. 5228-5249, 2021, doi: 10.1109/ACCESS.2020.3045716.
[52] M. Khaleel, A. A. Ahmed, A. Alsharif, and M. M. Beiek, "Technology challenges and trends of electric motor and drive in electric vehicle," *Int. J. Electr. Eng. and Sustain.,* pp. 41-48, 2023.
[53] x-engineer.org. "How to calculate rolling resistance." https://x-engineer.org/rolling-resistance/ (accessed December 03, 2025).
[54] H. Chowdhury, H. Moria, A. Ali, I. Khan, F. Alam, and S. Watkins, "A Study on Aerodynamic Drag of a Semi-trailer Truck," *Procedia Engineering,* vol. 56, pp. 201-205, 2013/01/01/ 2013, doi: https://doi.org/10.1016/j.proeng.2013.03.108.
[55] P. Valpolini, "Mercedes-Benz Special Trucks Zetros 4×4 and not only," *European Defence Review Magazine*, November 11, 2021. [Online]. Available: https://www.edrmagazine.eu/mercedes-benz-special-trucks-zetros-4x4-and-not-only
[56] K. R. Cooper, "Truck Aerodynamics Reborn - Lessons from the Past," 2003. [Online]. Available: https://doi.org/10.4271/2003-01-3376.
[57] B. Shurdha, "Solid-state Hydrogen Powered Heavy Logistics Vehicle Feasibility Study Project Kick-Off Briefing," Candian Armed Forces, National Defence, May 23 2025.
[58] ZeBeyond. "Size and simulate power systems fast." https://www.zebeyond.com/ (accessed February 12, 2026).
[59] U.S. Department of Energy, "Hydrogen and Fuel Cell Technologies Office Multi-Year Program Plan," 2024. [Online]. Available: https://www.energy.gov/sites/default/files/2024-05/hfto-mypp-2024.pdf
[60] U.S. Department of Energy, "Target Explanation Document: Onboard Hydrogen Storage for Light-Duty Fuel Cell Vehicles," 2017.
[61] Advanced Propulsion Centre UK, "Electric Energy Storage Technology Roadmap," 2024. [Online]. Available: https://www.apcuk.co.uk/knowledge-base/resource/electrical-energy-storage/
[62] ESOX Group, "Performance benchmarking presentation NRC DSD logistics vehicle," December 23 2025.
[63] Advanced Propulsion Centre UK, "Power Electronics Technology Roadmpa," 2024. [Online]. Available: https://www.apcuk.co.uk/knowledge-base/resource/power-electronics/

Appendix A H_2 Powertrain Exhaust Water Recovery Feasibility Study

The following H_2 powertrain exhaust water recovery feasibility study was prepared by MAHLE for DND. Permission was granted to append it within this logistics feasibility study.

H2 Powertrain Exhaust Water Recovery feasibility study

1D Simulation

Dr. Godfrey Udeh | 2025/12/12

MAHLE Powertrain

Background

H_2 ICE or Fuel Cell and water recovery

- Hydrogen powered engines/Fuel Cells produce 9 g of H_2O per 1 g of H_2 burnt
- This amounts to over 30% by volume of water vapour in the exhaust
- In desert conditions, it is difficult to provide drinking water for troops in combat operation
- Condensation of the water vapour in the exhaust gas of hydrogen powertrains could be used to provide drinking water in these conditions
- Other uses of the water could also be considered, such as injection into the combustion chamber to improve combustion efficiency, or use in an electrolyser to enable production of more hydrogen
- The specific application for this project is to harvest water from the exhaust of a 376 kW hydrogen IC engine/Fuel Cell powertrain for the Zetros 8×8 Canadian Army truck, to provide drinking water for troops

ICE	Fuel Cell
Engine displaced volume: 12.816 L	Number of Stacks: 3
Rated power: 376 kW	Rated fuel power: 376 kW
Top Speed: 55 mph	

Objectives

H_2 ICE or Fuel Cell and water recovery

- The main goals of this study are:
  - To determine the feasibility of condensing water from the exhaust of a hydrogen fuelled internal combustion engine or Fuel cell stack(s)
  - Establish the state of the art in this technology
  - Establish the state of the art for the necessary water purification process
  - Establish whether any future technologies have been published in the public domain that may improve performance or efficiency in the future

- To establish the feasibility of the technology, MPT will also complete a short feasibility study by modelling the performance of a system that may be feasibly integrated to the target Zetros Truck with 376 kW ICE or Fuel Cell Stack

Methodology

H_2 ICE or Fuel Cell and water recovery

- A review of published works including patents on exhaust water condensation has been undertaken
- Further review of existing technologies on exhaust water treatment solutions is to be carried-out
  - This should highlight the quality of condensate extracted from exhaust water condensation
  - Reveal the combination of water treatment solutions required to purify condensate
  - Show how treated water compares to alternative drinking water solutions
- Exhaust water cooling system schematic to be formulated for the condensation of exhaust gas
- Steady state model to be developed in GT-Suite to simulate system performance and quantify exhaust water to be recovered from truck at:
  - Curb weights: 18, 30, and 40 tons
  - Vehicle speed: 20, 40, 55 mph

Background study into exhaust water condensation

01

5 | Dr. Godfrey Udeh | RS.UK.ER | 2025/12/12

MAHLE Powertrain

H2 Powertrain Exhaust Water Recovery feasibility study

Early ideas and patents

Water collection from ICE exhaust gas

- The fundamental idea of condensing the water vapour from exhaust gas of internal combustion engines dates back to at least 1944, when a patent application was filed by Harry A Mulvany (US2479766A), where he proposed the method, including water purification, to provide water for onboard airships
- Kurt Von Liide, had already proposed the idea of extracting water from ICE exhaust gas earlier, in 1934, but he proposed using sorption and regeneration process, rather than condensation (US2071868A)
- In 1985, Roderick J. Ray proposed that most prior art has focussed on condensation, which requires a lot of energy to cool the exhaust stream and refrigerate the gas to produce water condensation, leading to complex systems with efficiency penalties, and the water produced is high in contaminants, needing purification. In his patent (US4725359A), he proposed using membrane separation of water vapour, and a light vacuum to draw the water through the membrane, leaving gasses and impurities behind

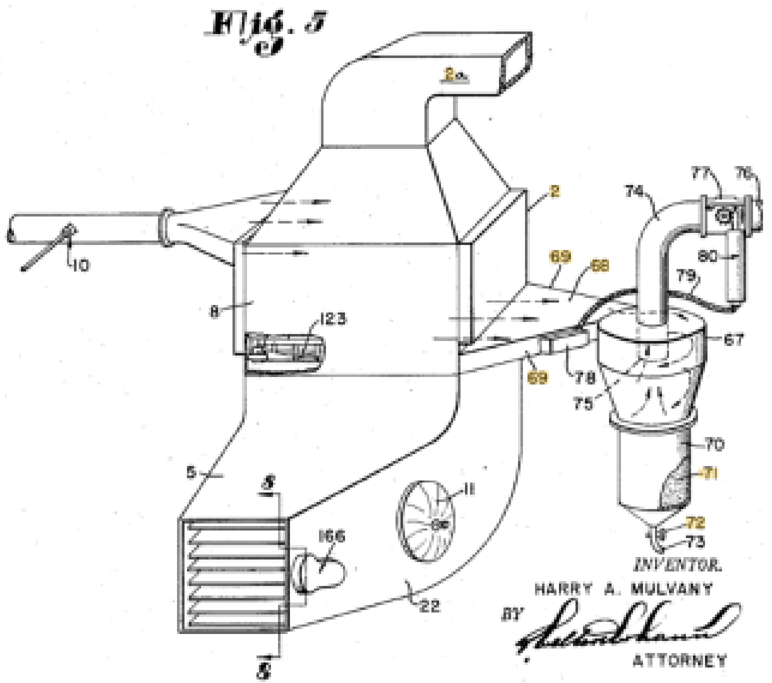

US2479766A - Recovery and purification of water from exhaust gases on aircraft - Google Patents

| Dr. Godfrey Udeh | RS.UK.ER | 2025/12/12

MAHLE internal restricted (CL2)

MAHLE Powertrain

Early ideas and patents

Water collection from ICE exhaust gas

- In 1985, Electrocom Gard Ltd, patented a system for exhaust gas aftertreatment and condensation of water from exhaust waste gasses, as can be seen, right, (US4656831).
- This carried most of the components and the essential approach which would ultimately be used by the US Army and Lexington Carbon Company in their patent in 2001 (WO2002059043A2), which focussed on the treatment of the condensed water
- The Lexington patent is particularly interesting, because it is this work that led to what appears to be the most comprehensive practical study into this technology, which resulted in a report by US Army TARDEC and LexCarb LLC, the highlights of which are summarised in this study
- Finally, KR20010034711A and DE10026695C1 were also filed around 2000/2001 but with specific uses relating to using the water for reducing the volume of diluted ammonia for aftertreatment and for water injection into an engine respectively

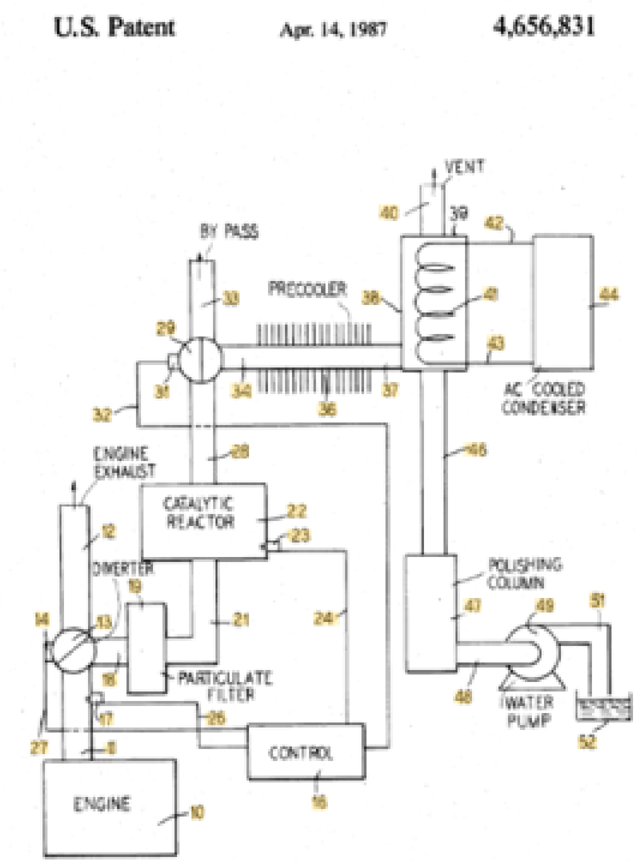

US4656831A - Apparatus and method of recovering water from engine exhaust gases - Google Patents

MAHLE Powertrain

Early ideas and patents

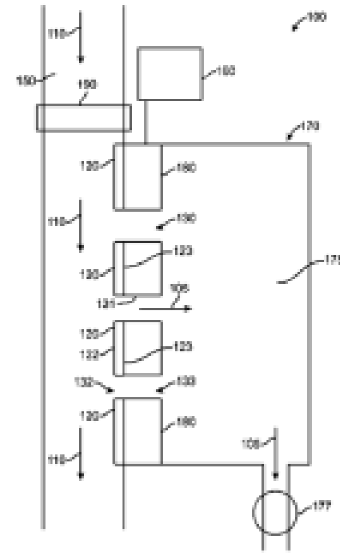

https://image-ppubs.uspto.gov/dirsearch-public/print/downloadPdf/9394672

Water collection from ICE exhaust gas

- More recently, some patents have been filed relating to capillary condensation, which has the theoretical advantage of being more efficient, avoiding the need for energy hungry cooling and refrigeration stages
- Patents have been filed by UT-Battelle, Oak Ridge (US 9,394,672 B2) and Tenneco Automotive (US 10,561,989 B1), relating to the method of removing liquid from a mixed gas stream
- The Tenneco patent relates specifically to engine exhaust
- In 2011, an NBC News article explained how the US Army were also investigating capillary condensation for engine exhaust, considering that the previously developed condensation system was big and bulky and consumed too much energy
- However, as far as can be determined, such a system has yet to be realised in a practical and successful sense, and as such condensation based systems are considered the best short-medium term solution, with capillary condensation to be considered a future technology

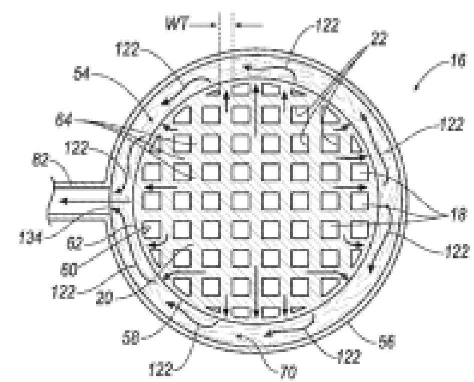

https://image-ppubs.uspto.gov/dirsearch-public/print/downloadPdf/10561989

Early ideas and patents

Water collection from ICE exhaust gas

- Only a very simple patent search has been conducted, and a more in-depth search is recommended
- However, it seems clear that the basic concept of harvesting water from the exhaust of combustion engines is not new and far beyond the time period concerned with protection of the fundamental idea
- Different options for water harvesting have been proposed, from sorption to condensation, and capillary separation a potential future technology
- Few patents appear to have been filed in recent years, leaving the landscape relatively open for new filings of specific improvements to the basic fundamental concepts

- Aside from patent applications, the most recent and comprehensive study into water harvesting from the exhaust of IC engines was conducted by the U.S. Army and Lexcarb, when they deployed a condensation system onto a HMMWV, which will now be briefly discussed

Water recovery from engine exhaust by Lexcarb LLC and U.S. Army TARDEC

MAHLE Powertrain

Early ideas and patents

U.S. Army and Lexcarb

- In 1998 a project was initiated by U.S. Army TARDEC to evaluate the feasibility of creating drinking water from the exhaust of vehicles, and a report was published in 2003 (#13951)
- Lexcarb's On-board Water Recovery Unit consists of a thin channel counter-flow heat exchanger and Chiller/demister unit, mounted on the back of a HMMWV (see prev slide and schematic, right)
- During the study, several versions and development were made, but the final demonstrator unit followed the layout shown, and used an aluminium charge air cooler with heresite (phenolic resin) coated tubes to prevent corrosion
- The vehicle was driven at series of steady speeds and also over dynamic acceleration and cruise cycles to assess the amount of water recovered
- The theoretical maximum water harvesting potential is 1 gal water to 1 gal diesel burned (1gal/gal or 1.0 yield), and the results varies from 0.58 to 0.93 depending on the driving conditions

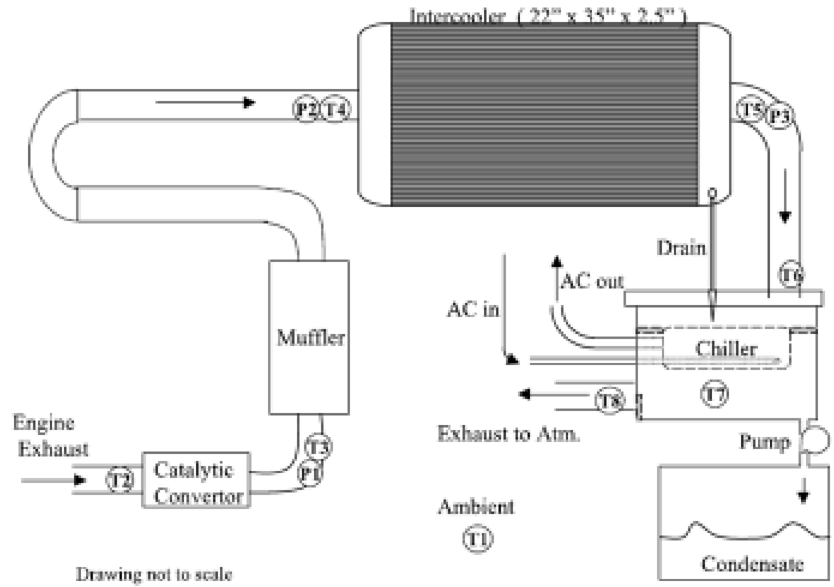

Water recovery from engine exhaust by Lexcarb LLC and U.S. Army TARDEC

MAHLE
Powertrain

Early ideas and patents

U.S. Army and Lexcarb

- The table (right) clearly shows that the yield is dependent on the final temperature achieved by the chiller. At temperatures of 70-90 F (21 – 32 Deg C), yield is around 50-60%, but when the temperature was decreased to 63 F (17 Deg C) the yield increased dramatically to 93%
- Practical results showed that typically it would be expected that the on-board water harvesting system would increase fuel consumption by 4%, from 9 mpg to 8.6 mpg
- That majority of the paper, and the patent associated with the work, is actually dedicated to the water purification system, which was needed to remove soot particles, polar and non-polar organics and heavy metals from the water and make it safe to drink according to the quality standards specified in the Technical Bulletin Med 577 Occupational and Environmental Health: Sanitary Control and Surveillance of Field Water Supplies

Run #	miles water collect.	Fuel cons (mpg)	water amounts (lbs/mile): in fuel	water amounts (lbs/mile): air in	water amounts (lbs/mile): total in	water amounts (lbs/mile): actual yield	water amounts (lbs/mile): in outlet total - yield	Yield per gal diesel (gal/gal)	Dew Point air in (°F)	Dew Point engine exh. (°F)	Temp. IC out (°F)	Calc. Dew Pt. of chiller outlet (°F)	Temp. Chiller Outlet (°F)
Steady 50mph runs													
W86	84,7	14,8	0,56	0,07	0,62	0,34	0,28	0,61	32	98	104	72	79
W90	84,9	14,1	0,58	0,18	0,76	0,35	0,41	0,59	55	105	110	84	82
W91	86,0	14,5	0,56	0,15	0,71	0,36	0,35	0,63	54	102	106	80	85
W92	86,8	14,5	0,56	0,15	0,72	0,31	0,41	0,53	53	102	113	84	80
W93	2.5	14.5	-	-		no water collected		-	54	102	95	-	-
W94	84.8	16.5	0.50	0.06	0.56	0.03	0.53	0.05	32	95	-	93	-
W95	84,8	14,7	0,56	0,10	0,66	0,34	0,32	0,61	43	95	-	76	-
W96	84,6	14,7	0,56	0,10	0,65	0,33	0,32	0,58	40	101	-	76	-
W97	84,9	14,8	0,55	0,05	0,60	0,32	0,27	0,58	<32	101	103	72	90
W10(	84,9	14,5	0,57	0,02	0,58	0,36	0,22	0,63	<32	96	100	64	83
W101	84,9	15,1	0,54	0,02	0,56	0,32	0,25	0,58	<32	94	108	68	85
5 - 50 -5 mph runs													
W87	6,5	11,0	0,74	-		no water collected		-	58	-	95	-	94
W88	6,5	12,4	0,66	-		no water collected		-	60	-	131	-	87
W89	52,2	10,8	0,76	-	-	0,59	-	0,77	60	-	127	-	70
W98	30,6	10,1	0,81	-	-	0,55	-	0,67	<32	-	79	-	70
W99	22,6	10,2	0,80	-	-	0,76	-	0,93	<32	-	80	-	63

Water recovery from engine exhaust by Lexcarb LLC and U.S. Army TARDEC

MAHLE
Powertrain

Early ideas and patents

U.S. Army and Lexcarb

- The image (right) shows the water recovered directly from the exhaust gas (black, left), and then particle filtered (centre) and Carbon/Resin purified (right)
- The water was found to be contaminated with soot, metals from the engine, exhaust and heat exchanger (incl Aluminium (HX), Boron (diesel additive), Zinc and iron (engine and exhaust)) as well as other trace metals
- Nitrates and Sulphates from the combustion process were found, and has the effect of making the water acidic, with a pH of between 2.4 and 2.9
- Phosphorous was also present
- The system used a combination of:
  - Filtration to removed solids
  - Adsorption on activated carbon monolith (ACF) to remove organics and some inorganics
  - Ion-exchange resin to remove ionic species

Water recovery from engine exhaust by Lexcarb LLC and U.S. Army TARDEC

MAHLE Powertrain

Early ideas and patents

U.S. Army and Lexcarb

Solid matter

- The soot/particle filtration step used commercially available 2 micron glass fibre papers with a few psi pressure differential to encourage flow
- The study states that only a square foot of filter area (3" dia x 8" long cylinder) is needed to process 180 gallons of condensate, at a rate of 2 gal/hr
- This removed solids down to sub-micron level (to less than 1ppm)

Total Organic Compounds (TOC)

- TOC were found to be present in higher concentration at lower water harvesting levels, and were more diluted at higher harvesting rates. This implies that the TOC are separated from the exhaust easily and have a tendency to be scrubbed by the liquid water droplets

Water recovery from engine exhaust by Lexcarb LLC and U.S. Army TARDEC

MAHLE Powertrain

Early ideas and patents

U.S. Army and Lexcarb

Total Organic Compounds (TOC)

- To filter out the TOC, the condensate was filtered through an activated carbon bed to remove non-polar organic contaminants
- A 2" dia x 5" long carbon fibre composite bed enabled a flow rate of 32 ml/min, and removed around 50% of the organic contaminants
- In this stage, the pH increased to 4.5 – 9, a wide range
- It is estimated in the paper that to treat 180 gallons of water, a 5" dia x 7-14" long canister would be required (presumably at a flow rate of 32 ml/min, or 1.9 l/hr), therefore multiple ACF tubes would be needed to process the expected volumes of water
- This process still left significant inorganic contaminants, which were dealt with using an Ion Exchange Resin

Water recovery from engine exhaust by Lexcarb LLC and U.S. Army TARDEC

| Dr. Godfrey Udeh | RS.UK.ER | 2025/12/12

MAHLE Powertrain

Early ideas and patents

U.S. Army and Lexcarb

Ion Exchange Resin

- A variety of resins were trialled, including:
  - a gel type anion exchange resin in the OH- form
  - A mixed strong acid and base gel type ion exchange resin in the H+, OH- form
  - A resin designed to increase the pH of the water
  - A resin formulated to remove nitrogen compounds
- The general approach was successful in removing metals and inorganics from the water
- The initial levels of aluminium were 97 mg/L, and the Ion Exchange process decreased these to below measurable levels
- Inorganic compounds were also reduced to below detectable levels, including chloride, fluoride, nitrates and sulphates
- The process could also be tuned to achieve pH of 6.8, which is acceptable for drinking water

Water recovery from engine exhaust by Lexcarb LLC and U.S. Army TARDEC

MAHLE Powertrain

Early ideas and patents

Proposed system – Current technology

Water condensing system

- The current state of the art is a water condensing system comprising an exhaust cooler and a refrigerant chiller, with supporting heat exchangers and fans
- This type of system has been proved to work in practice and can yield high water harvesting rates, but consumes significant energy

- **Water purification**
- A system comprising the following is state of the art and has been proven to work in practical trials:
  - Stage 1: Particle filter
  - Stage 2: Activated carbon filter
  - Stage 3: Ion-exchange resin

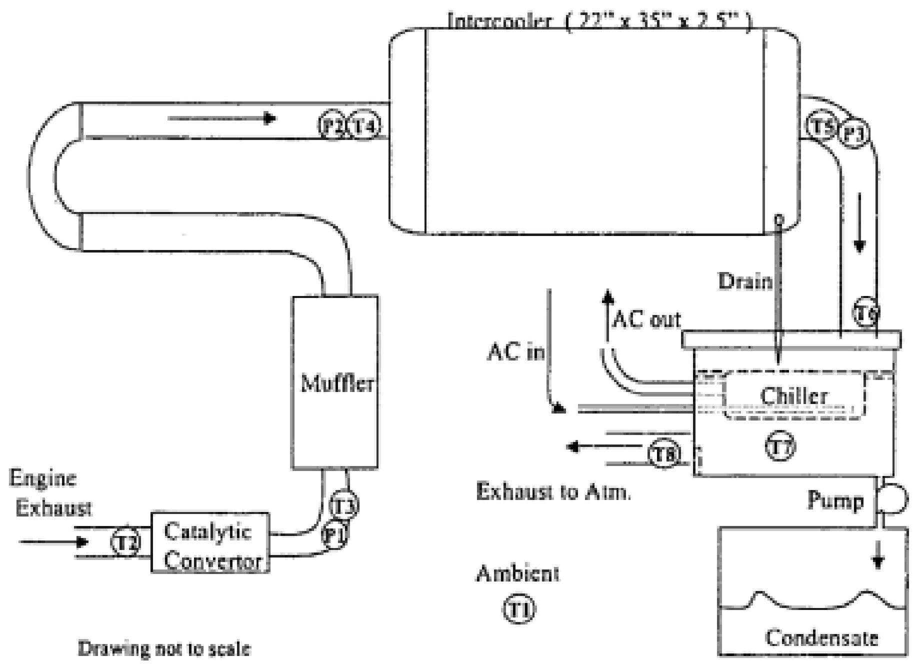

MAHLE Powertrain

Early ideas and patents

Proposed system – FUTURE technology

Capillary condensation system

- Research is ongoing into capillary condensation systems
- These types of systems should not require the energy taken for refrigeration that the condensation systems do, and should result in a more efficient solution
- However, no evidence has so far been found of successful trials on engines or vehicles, so further research is likely to be necessary to conform feasibility

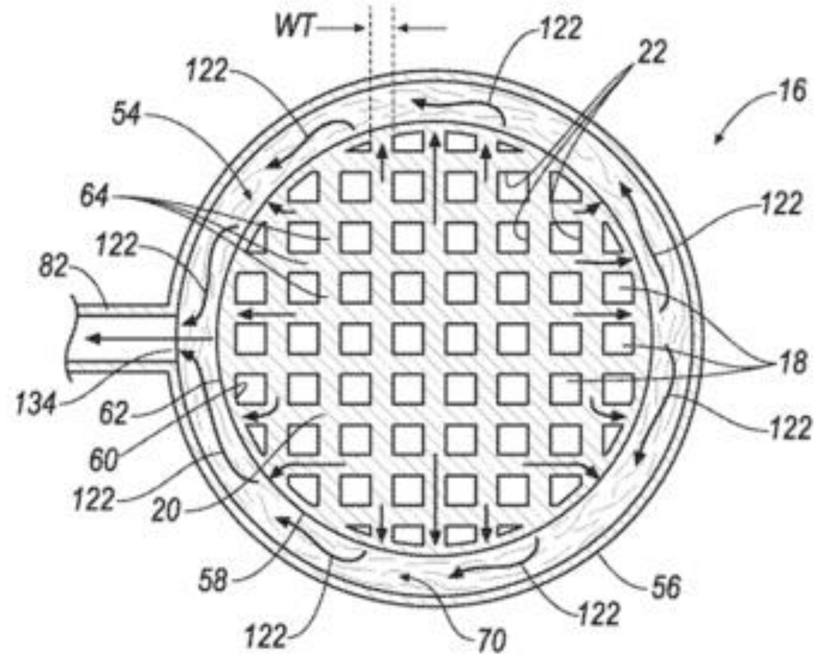

| Dr. Godfrey Udeh | RS.UK.ER | 2025/12/12

MAHLE internal restricted (CL2)

Additional information:
Overview of key patents

01

18 | Dr. Godfrey Udeh | RS.UK.ER | 2025/12/12

MAHLE
Powertrain

Exhaust Water Condensation

U.S. Army and Lexcarb – Condensation System

Water Condensation using Heat Exchangers

- Intercooler retrofitted to a vehicle to help cool engine exhaust below dew point
  - Required to condense water out of the exhaust stream
- Two stage on board cooling was proposed in a patent authored by the US Department of Defence:
  - Stage 1: counter-flow gas to gas intercooler
  - Stage 2: further cooling of exhaust gas below water dew point with vehicle chiller
- Condensed water is passed through a water purification system
- Water filtration was achieved in two stages with:
  - Activated carbon filters to reduce TOC to the EPA levels for drinking water, and
  - Ion exchange resins to buffer the pH of the condensate, soften it and eliminate dissolved ions
- Proposed system capable of producing 15 gallons of drinking water per day from 30 gallons of diesel fuel

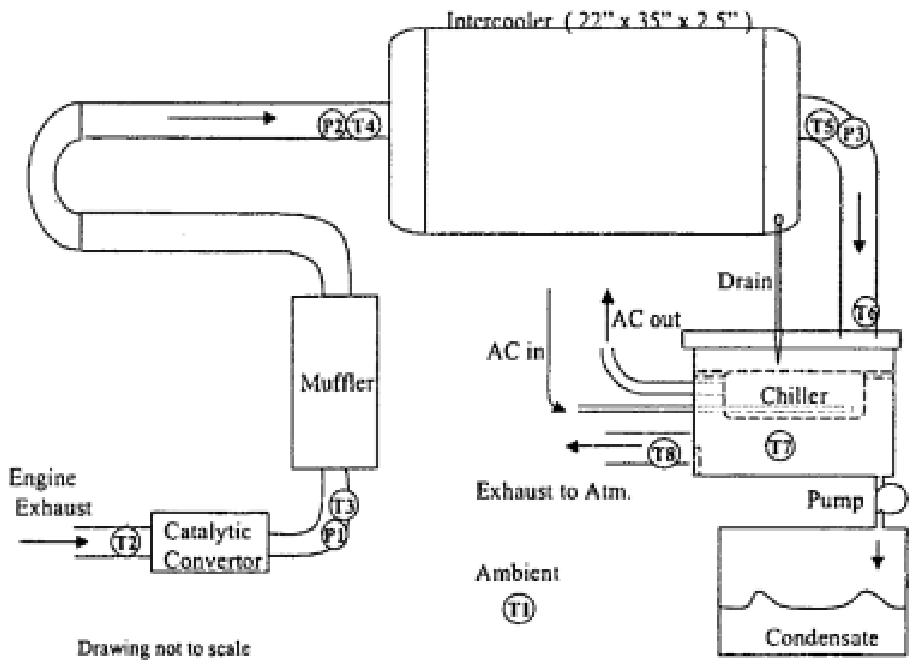

Source: https://patents.google.com/patent/WO2002059043A2/en

Exhaust Water Condensation

Water Condensation using Heat Exchangers

- Invention proposes exhaust condensation of a hydrogen-fueled engine
  - Argon (**50**) is introduced into the air/oxygen supply (**40**) to enable fuel-rich engine operation close to lambda 1
  - Inert gas helps to prevent NOx formation and other pollutants
- Cooler (**64**) is integrated to the exhaust stream for exhaust cooling to condense water vapour (**56**)
- Resulting condensate is sent into a separator (**58**) to separate condensed water (**66**) from the inert gas (**69**)
  - Inert gas is recirculated into the engine (**50**)
  - Condensed water (**27**) from the gathering tank (**68**) is sent into the electrolysis apparatus to produce hydrogen (**28**) and oxygen (**36**)
- Electrolysis apparatus (**26**) is powered by renewable energy sources
  - solar PV modules (**14**)
- This invention supports closed-cycle operation in desert and off-grid locations

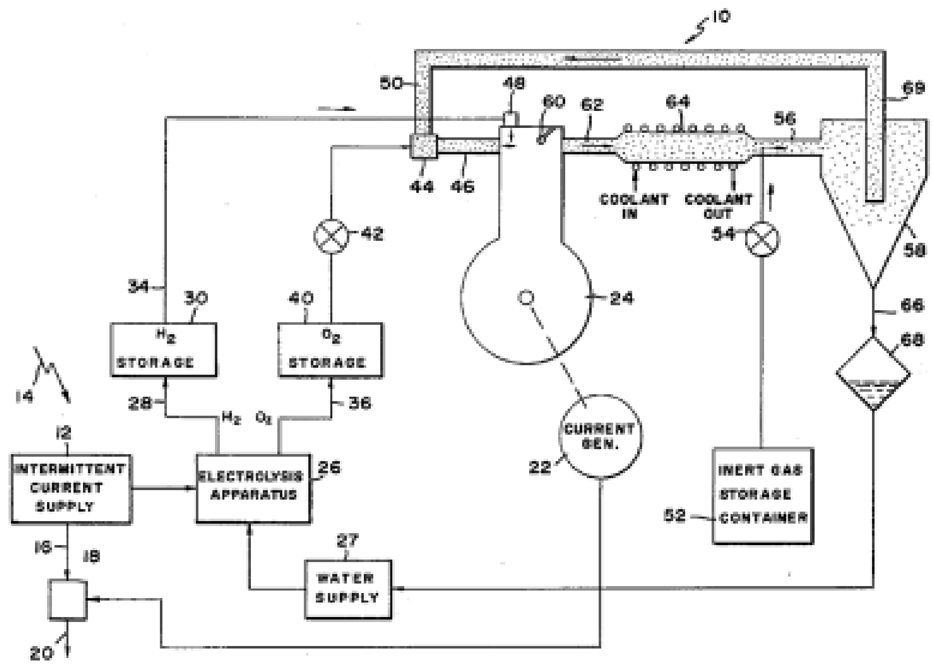

| Dr. Godfrey Udeh | RS.UK.ER | 2025/12/12

Exhaust Water Condensation

Exhaust GasIn

substrate

Tenneco Automotive – Capillary System

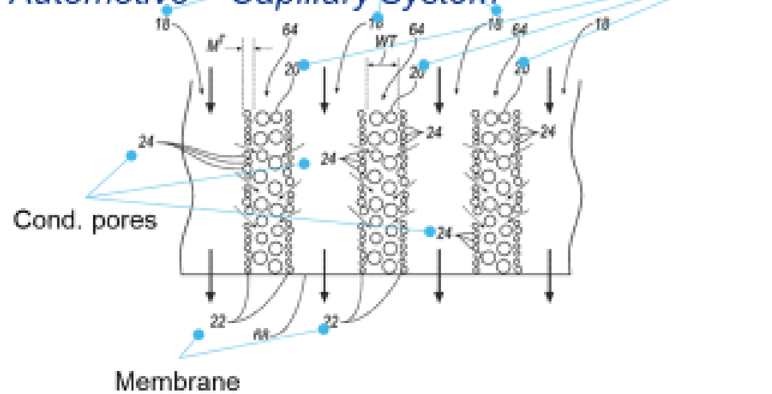

Water Condensation by Capillary Action

- Invention proposes exhaust water condensation by capillary action
  - Water vapour is condensed out of an exhaust stream with the help of a substrate (**20**) coated with a membrane (**22**)
- Water separation device (**16**) comprises a substrate (**20**), covered with membranes (**22**) that has capillary conduction pores (**24**)
- Exhaust gas from the engine is delivered to the water separation device and flows through the exhaust passage (**18**) and over the membrane (**22**)
- Water vapour condenses out of the exhaust stream by capillary action in the capillary tubes
  - Condensed water permeates the membrane and is gathered into the water flow paths (**122**) in the water collection space (**70**)
- Condensed water is removed via the water outlet (**134**)
- Heat conductive element (**120**) is introduced to cool substrate and increase efficiency

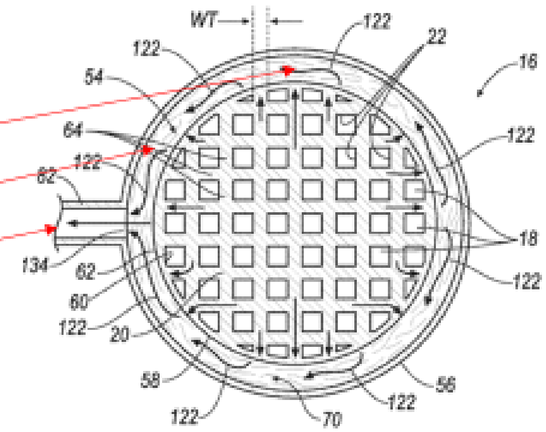

https://www.osti.gov/doepatents/biblio/1632555-water-separation-device-engine-exhaust-gas

MAHLE Powertrain

Exhaust Water Condensation

Tenneco Automotive – Capillary System

Principles of Water Condensation by Capillary Action

- Governing principles for exhaust water condensation by capillary action is presented
- According to Kelvin's Equation, narrow pores will lower vapour pressure inside the pores:

$$\ln\left(\frac{P_r}{P_0}\right) = -\frac{2\gamma V_m \cos\theta}{rRT}$$

Where: P_r = vapour pressure in the pore, P_0 = saturation vapour pressure, γ = surface tension, V_m = molar volume of liquid, r = pore radius, R = gas constant and T = temperature, θ = contact angle between liquid and capillary wall

- Small pore sizes could be blocked with increased condensation
- Absorption capacity of the walls may decline overtime
- Optimal pore sizing and material selection are required

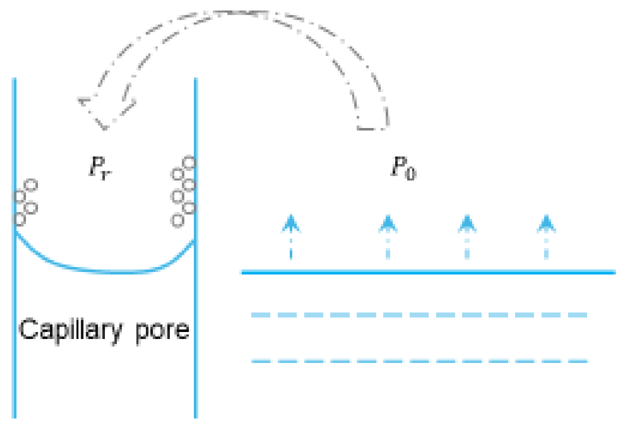

- If $P_r < P_0$, water vapour will flow into the capillary condensation pores and condense on the walls of the pores
- Increasing pore radius will increase P_r. Capillary condensation will stop if $P_r = P_0$
  - Absence of driving force to get water vapour into cond. pores

https://www.osti.gov/doepatents/biblio/1632555-water-separation-device-engine-exhaust-gas

MAHLE Powertrain


Additional information:
Condensate Purification
02
23 | Dr. Godfrey Udeh | RS.UK.ER | 2025/12/12
MAHLE internal restricted (CL2)
MAHLE
Powertrain

Exhaust Water Purification

Information taken from US Army TARDEC study

Water Treatment Solutions

- EPA (environmental protection agency) sets a limit of 2 mg/L for TOC (total organic carbon) for treated water
- Exhaust condensate of internal combustion engines contain:
  - High concentration of TOC in the range of 50 – 250[2] mg/L
    - Much higher levels possible for older vehicles
  - Low pH of about 2.8[2] which suggests the water is acidic
  - Heavy metals, and
  - Other organic and inorganic compounds
- A combination of water treatment processes are required to enhance exhaust water for human consumption as shown below:

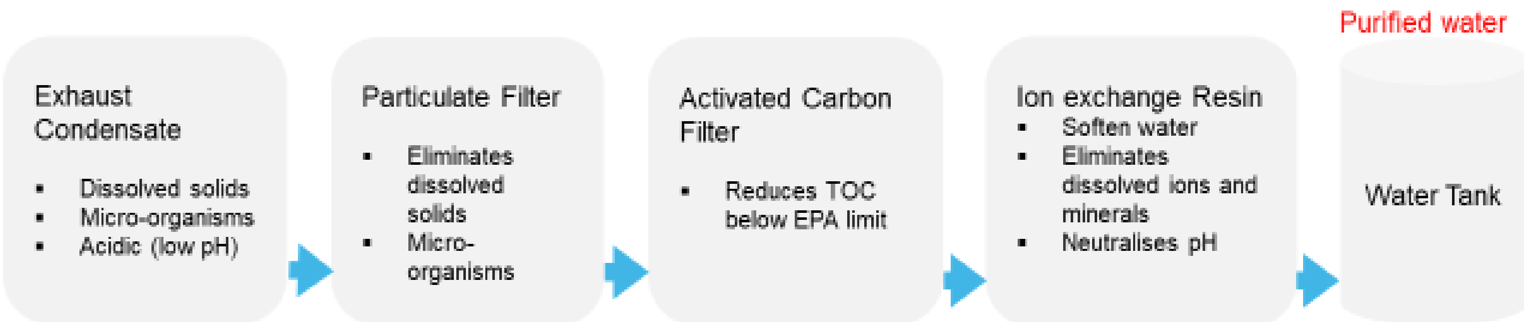

MAHLE Powertrain

Condensate Filtration

Information taken from US Army TARDEC study

- Infographic depicts condensate filtration stages

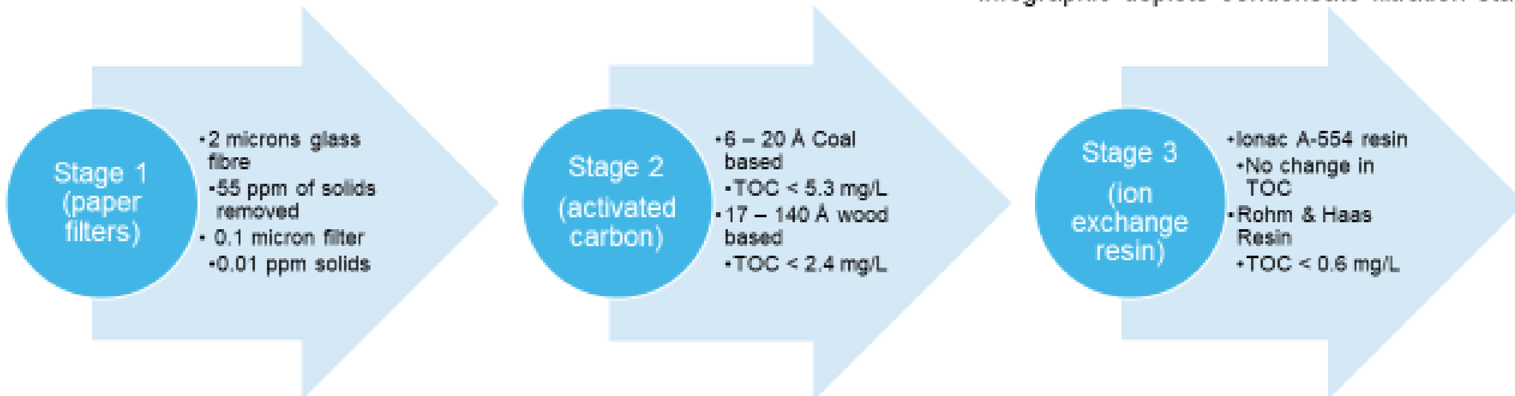

Water Condition	Condensate	Purified Water
TOC (mg/L)	65	< 2
pH (-)	3 (acidic)	6.84 (neutral)
Conductivity (µS/cm)	496.4	6.14

Source: https://patents.google.com/patent/WO2002059043A2/en

MAHLE Powertrain

Treated Water Laboratory Analysis

Information taken from US Army TARDEC study

TOC 0.1 ppm vs. TOC 2.6 ppm

- Analysis of two treated water samples obtained from exhaust gas condensation and filtration were performed
- Two lab techniques were employed to analyse collected water samples:
  - ESI/MS (Electrospray ionisation & mass spectrometry), and
  - GC/MS (Gas chromatography & mass spectrometry)
- Table compares the organic contaminants in the two water samples
- All metals in exhaust condensate were reduced below regulated levels
  - Some metals are present largely in a harmless concentration
- Treated water was compared to Kentucky drinking water and organic water purchased from an independent laboratory
  - UV scans show exhaust water contain much less organic contaminants than the benchmark

Contaminants in Purified water	Water Sample 1 (TOC = 0.1 ppm)	Water Sample 2 (TOC = 2.6 ppm)
Toluene	Trace	Trace
4-methyl-2-pentanone	Not Detectable	Not Detectable
2-ethyl-1-hexanol	Trace	Not Detectable
Small polymer	Trace	Not Detectable
Phosphoric acid, alkyl phosphates	Not Detectable	Trace
2- methyl propanoic acid	Not Detectable	Trace
Tributyrin	Not Detectable	Trace

Source: https://patents.google.com/patent/WO2002059043A2/en

MAHLE Powertrain

Exhaust Water Purification

Water Treatment Solutions – Particulate Filters

- A few particulate filters are commercially available for water purification
- Glass fibre paper are popular for removing dissolved solids
- It is essential to utilise glass fibres with maximum pore not more than 2 micron
- This should help remove fine particles up-to 55 ppm and microorganisms
- Further filtration with finer glass fibre pores (less than 0.1 micron) can be explored
  - Smaller pores may not achieve further reduction in the dissolved solids

Sample of 2 micron glass fibre filter paper

Exhaust Water Purification

Information taken from US Army TARDEC study

Water Treatment Solutions – Activated Carbon

- Next stage of water purification will require the use of granulated activated carbon
  - This helps to reduce TOC to the acceptable limit for drinking water
- Coal-based activated carbon have been explored for this purpose[2]
  - In one example, condensate was made to flow at 20 ml/min through a coal based activated carbon column
  - TOC was reported to reduce to 5.3 mg/L after 1.4 gallons of condensate
  - Coconut shell activated carbon is promising for water purification
- Further TOC reduction to below 2 mg/L will be achieved by a second layer of activated carbon
- Wood based granular activated carbon can be explored for this purpose
- It has been reported to achieve TOC reduction from 3.2 mg/L to 1.5 mg/L – 50% reduction

Activated Carbon Pore Sizes

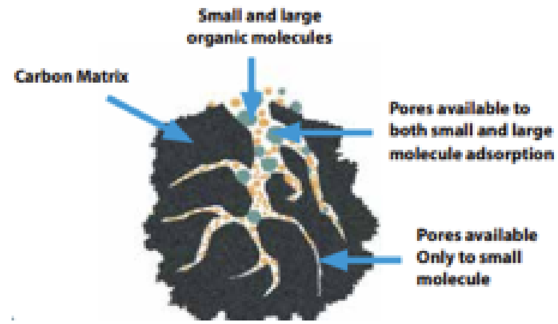

Exhaust Water Purification

Water Treatment Solutions – Ion Exchange Resins

- Flowing the condensate with low TOC through an Ion exchange resin is the final stage of water treatment
  - Helps to soften water and remove dissolved ions/minerals
  - Also helps to adjust condensate pH level
- Layered bed ion exchange resin systems are popular for industrial water treatment
- Offers the benefit of improved overall efficiency, capital cost reduction and footprint savings particularly when housed in a vessel
- Selection of right pair of layered resins is essential for optimum performance
  - Strong base anions (SBA)+ weak base anions (WBA)
  - Strong acid cations (SAC) + weak acid cations (WAC)

Sample of layered bed ion exchange resin[3]

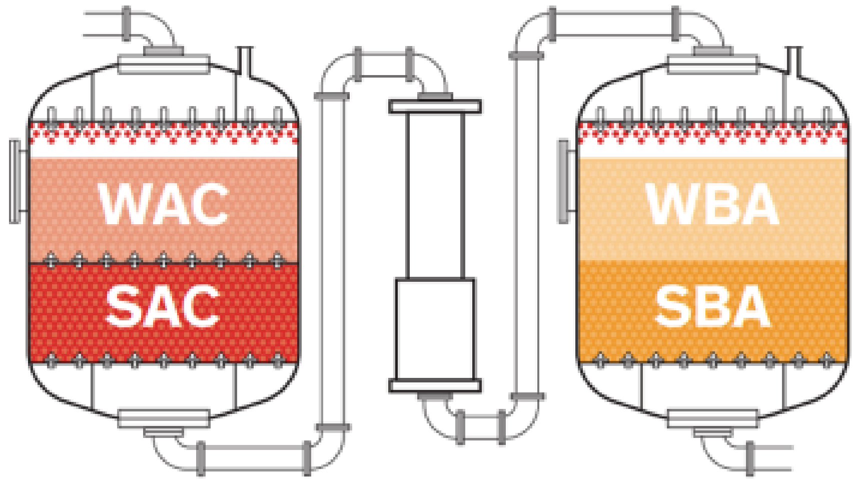

DuPont™ AmberLite™ Ion Exchange Resins for Industrial Water Treatment Product Overview

H_2ICE Feasibility study (1D simulation): Proposal for Water Condensation System

03

MAHLE Powertrain

First Principles Analysis

H_2 ICE exhaust gas needs cooling from ~400 Deg C down to <20 Deg C for good water recovery rates

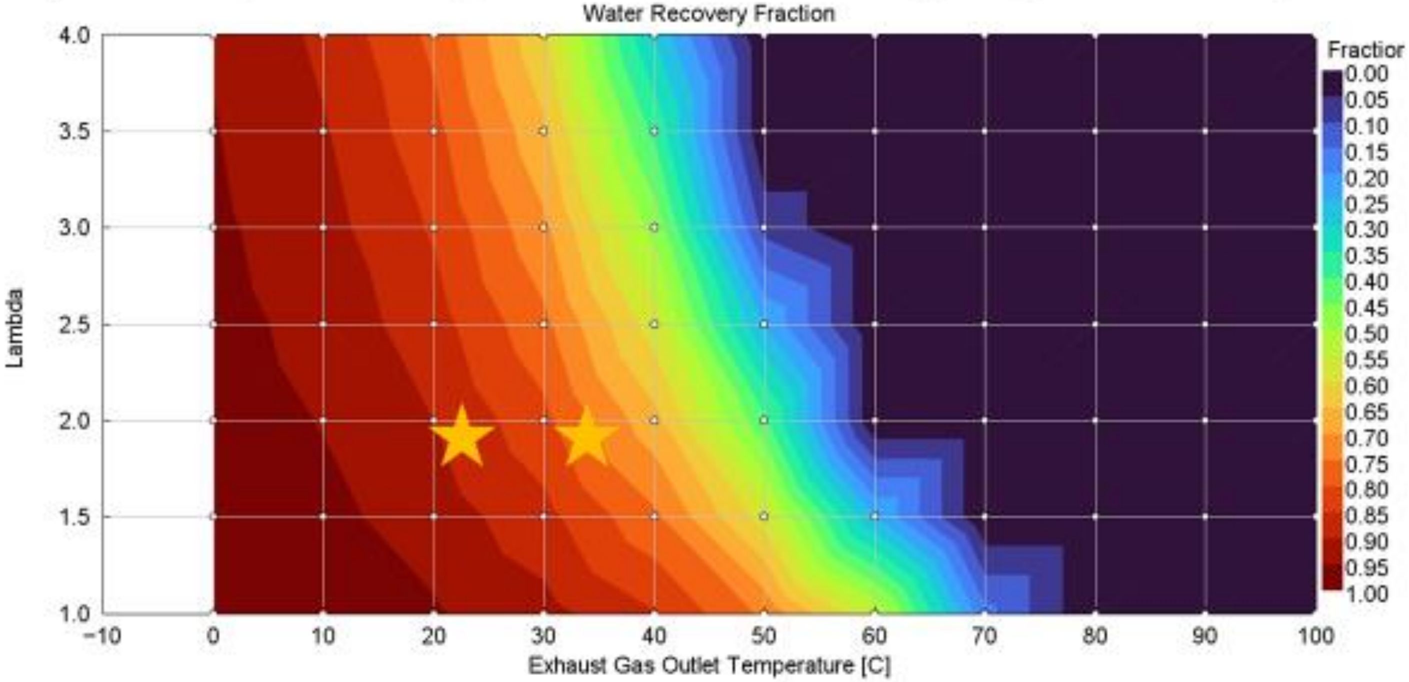

To achieve over 90% water recovery at the target air-fuel ratio of lambda = 2, the exhaust has to be cooled to less than 20°C and ideally less than 10°C (shown by the gold stars)

| Dr. Godfrey Udeh | RS.UK.ER | 2025/12/12

MAHLE Powertrain

Feasibility study:
Proposal for Water Condensation System

1D simulation

- A detailed 1D simulation model of three different configuration of the condensation system has been conducted, and the most efficient system has been identified and is taken forward for further analysis (see next page for a schematic diagram)
- This detailed 1D system model was then integrated into a longitudinal vehicle simulation model to enable assessment of the potential real-world water condensation rates when constrained by vehicle operation regimes and packaging restrictions
- The packaging restrictions for the additional heat exchangers have been considered, and the effect of airflow and the requirement for powering fans has also been quantified at different vehicle speeds
- The effect of ambient temperature on efficiency and water condensation rate has also been studied
- The detail of the necessary water purification system has not been assessed in this initial study, and will need further investigation in a follow-on work package, but is known technology

NOTE: much of the detail and results behind this simulation work has been held back due to the project requirement not to bring new intellectual Property (IP) into the project scope

The models and detailed system performance simulation work constitutes new IP generated by MAHLE Powertrain and is therefore withheld for this project

MAHLE Powertrain

H2 Powertrain Exhaust Water Recovery feasibility study

Possible Cooling System Layout

- A potential system layout is shown, which is the result of detailed 1D simulation of different layout options, and represents the most efficient system analysed
- It deploys two separate cooling loops to cool exhaust gas and engine respectively
- Two fans are driven separately to provide cooling air to the exhaust cooler radiator and engine radiator

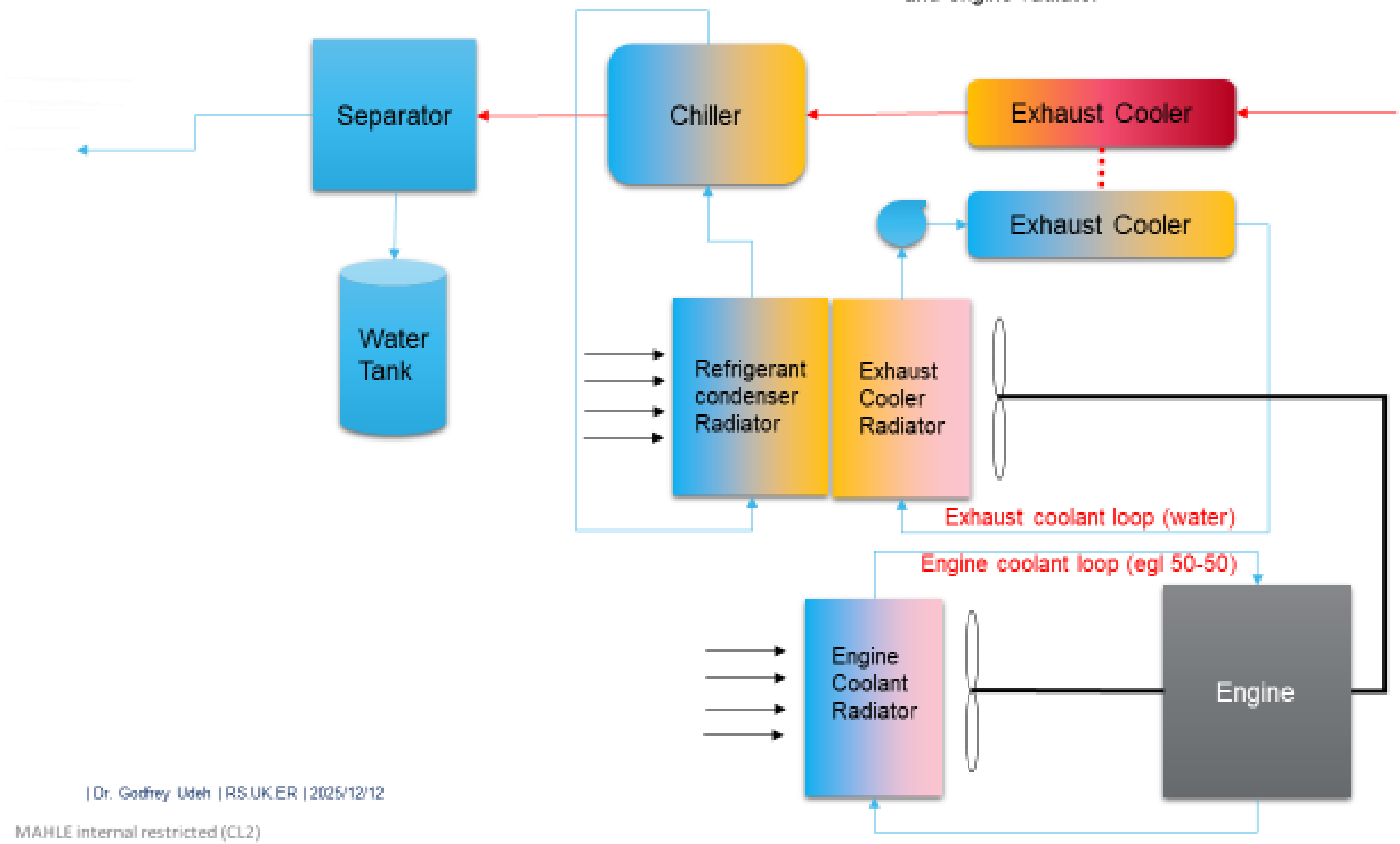

| Dr. Godfrey Udeh | RS.UK.ER | 2025/12/12

MAHLE Powertrain

Water condensation and treatment system

The vehicle system is proposed to comprise:

- Heat exchanger module (Roof-mounted)
  - 400mm x 2000mm x 150mm radiator for exhaust cooler, plus same for chiller condenser
  - Array of 5 kW fans (~5 x 400mm dia)
  - May be possible to package refrigerant compressor in same area – CAD study needed
  - Sized to keep overall vehicle height below 4.2m
- Additional coolers needing packaging elsewhere:
  - Exhaust heat exchanger (exh gas – water)
  - Exhaust chiller evaporator (cooled exh gas – refrigerant)
- Water collection tanks and H_2 storage systems also need packaging
- No consideration given at this stage for size and package of water purification:
  - Does this live on the vehicle or will the water be collected and then processed off-vehicle?

Condenser and Radiator pack, plus array of electric fans could be mounted here

MAHLE Powertrain

Input Data

Vehicle Spec

- Mercedes-Benz Zetros Tractor Unit
- 8×8 unit
- Four-axle all-wheel drive
- 11.15 metres long, 2.6 metres wide and 3.7 meters high
- Curb weight loaded: 40 tons

Powertrain

- Euro V OM 460 6-cylinder in-line engine
- Engine displacement of 12.8 litres
- Rated power 376 kW (510 hp)
- Transmission: Allison 4500 SP automatic transmission

MAHLE Powertrain

Input Data

Aero-data for model simulations

- Mercedes-Benz Zetros Tractor Unit
- 8×8 unit
- Four-axle all-wheel drive

Specification		
Mass	[kg]	18000, 30,000, 40000
Drag Coefficient	[-]	0.8*
Frontal Area	[m²]	10.42**
Tyre rolling resistance	[-]	0.007901

* Estimated
** Note the the frontal area includes area of exhaust cooler radiator to be mounted on truck cab.

MAHLE Powertrain

Road Load at Different Gross Vehicle Weights

- Vehicle road load estimated at different GVWs and assuming 0% gradient (flat road)
- Note that the vehicle is sensitive to change in curb weight particularly at high speeds

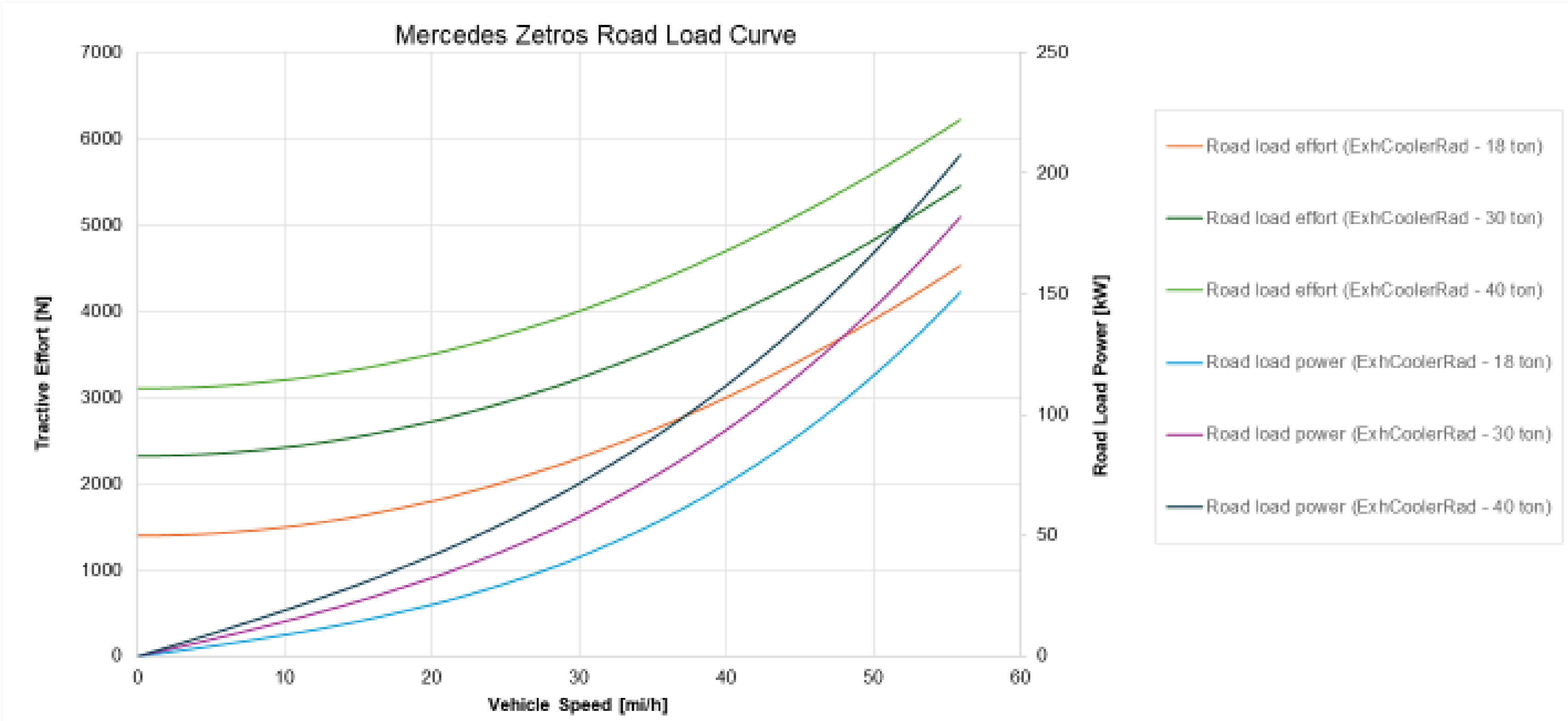

| Dr. Godfrey Udeh | RS.UK.ER | 2025/12/12

MAHLE Powertrain

Input Data

Vehicle Specification

- Engine capacity to be limited to 376 kW
  - Rated engine power for the Zetros Truck
  - Specific power $= \frac{376}{12.86} = 29.24$ [kW/lit.]
  - Hydrogen fuel combustion assumed to be at $\lambda > 2.5$
  - Below $\lambda = 2.5$, NOx levels are high with hydrogen fuel combustion although could be lowered with after treatment system
  - NOx limit target = 200 ppm
- At $\lambda > 2.0$, engine brake thermal efficiency will not exceed 42%[1]
  - Running the engine with lean fuel-air mixture will lower exhaust temperature
    - However, dew-point drops which would raise the cooling load
  - In addition, the exhaust will have lower exergy to produce water

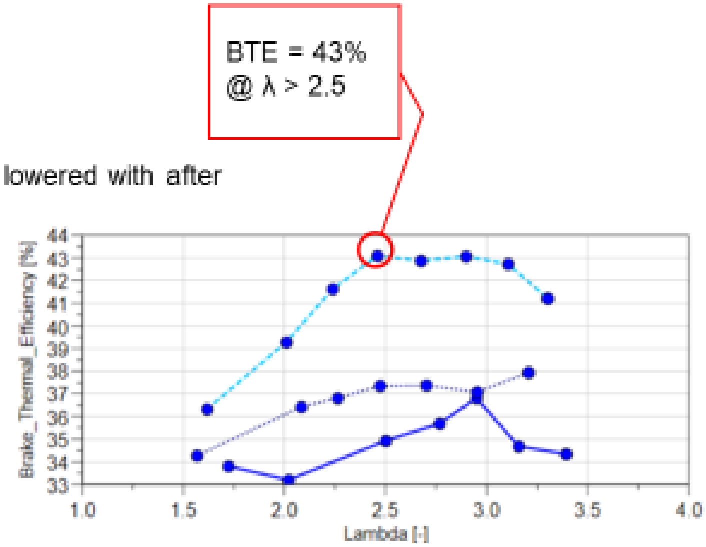

MAHLE Powertrain

Boundary conditions

Exhaust Composition (Hydrogen ICE)

- Air-fuel ratio affects exhaust composition for all fuels
  - Exhaust gas temperature affected by amount of air in fuel
    - Decreases with increase in fuel dilution
      - 550 °C @ λ = 2.0, drops to 480 °C @ λ = 3.0
    - Also affected by engine configuration
      - Single cylinder engines present lower exhaust gas temps
      - Can be 20 % higher with multi-cylinder ICEs (@ high loads)
  - Gas temperature will affect cooling load
- With high lambda (λ > 1.5), water vapour concentration in exhaust gas reduces
  - Dew-point temperature (temperature water droplets are produced from water vapour) also reduces
  - Cooling load will be impacted

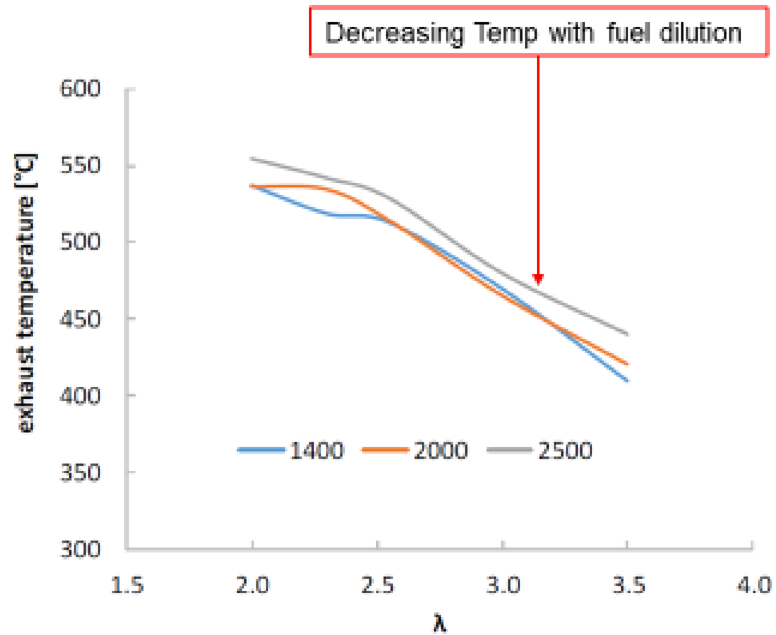

Source: S Frigo et al 2023 J. Phys.: Conf. Ser. 2648 012073

GVW and Vehicle Speed Sweep

Exhaust Temperature (Hydrogen ICE)

- Exhaust gas is admitted into cooler at 395 °C
- Cooler cools it down to below 50 °C – temperature achieved post cooler affected by truck speed and GVW
  - Effect of GVW more evident at 55 mph – exhaust temperature post cooler could change by 4 °C with increase in GVW from 18 tons to 40 tons
- Chiller cools down exhaust gas to 10 °C for all investigated cases to maximise water harvest

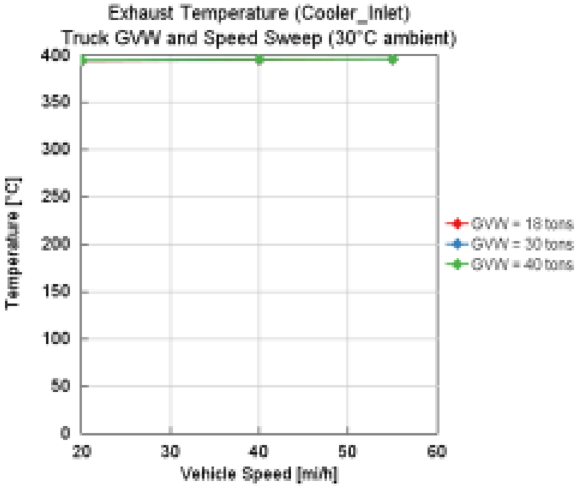

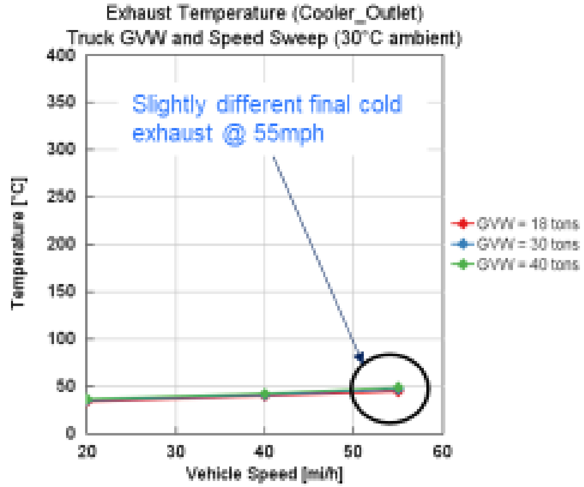

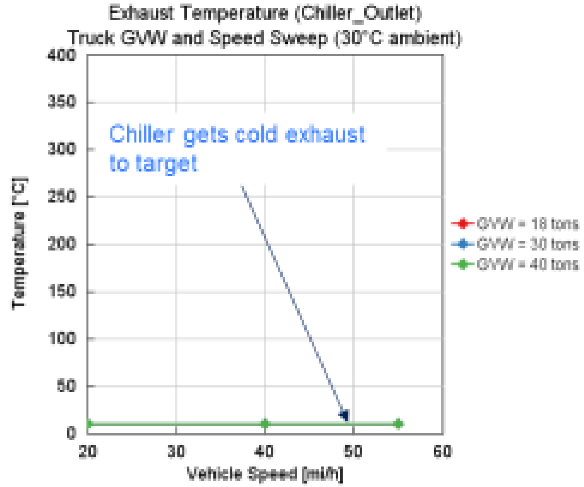

MAHLE Powertrain

GVW and Vehicle Speed Sweep

Parasitic Load on Engine

- 5 kW fan power required to remove heat from radiator – unaffected by vehicle speed and gross weight
- Compressor power increases with increase in vehicle speed and gross weight - influenced by the variation in exhaust temperature at chiller inlet
  - More pronounced at 55 mph - about 10.5 kW at truck top speed and 40 tons GVW
- Engine to provide additional power up-to 17.5 kW at top speed and full load capacity – could drop to 10 kW at 20 mph

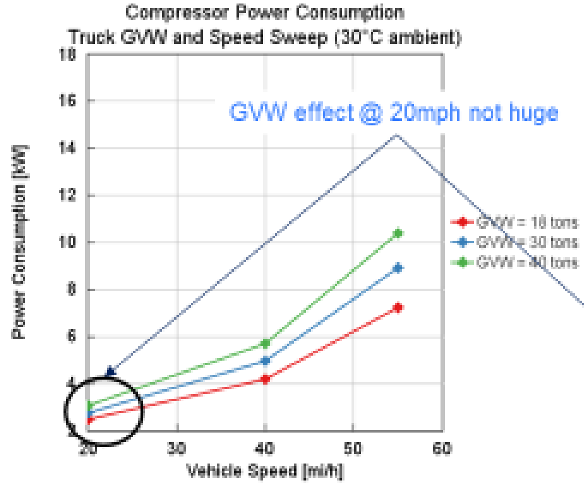

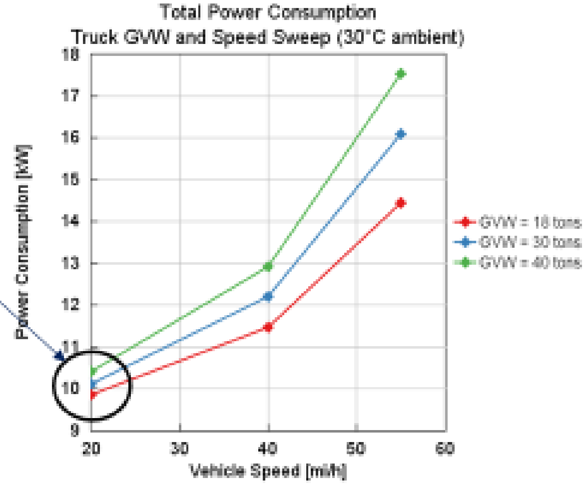

MAHLE Powertrain

GVW and Vehicle Speed Sweep

Overall System Performance (Hydrogen ICE)

- Chart A shows the power the engine needs to produce to propel the vehicle and run the water harvesting, depending on weight and vehicle speed
- The power needed to drive the water harvesting system alone is also shown (B) for the same conditions (A-B = engine power only)
- This data is shown for a 30 Deg C ambient, and as will be seen later in the report, the ambient temperature has a significant effect on the amount of power needed to drive the harvesting system. The next page shows the effect of the engine needing to provide this additional power on the system efficiency

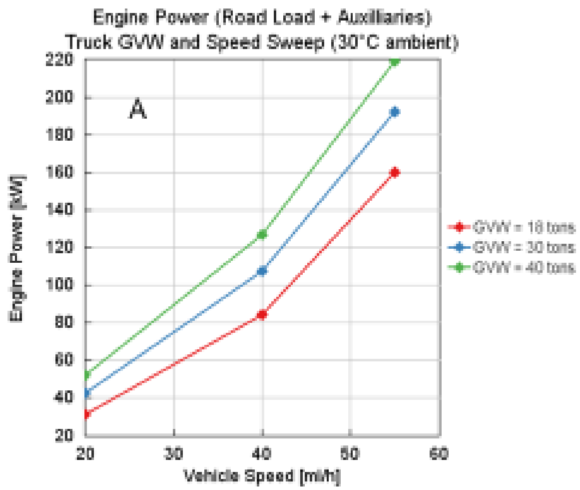

| Dr. Godfrey Udeh | RS.UK.ER | 2025/12/12

H2 Powertrain Exhaust Water Recovery feasibility study

GVW and Vehicle Speed Sweep

Overall System Performance (Hydrogen ICE)

- The charts now show the effect on overall system efficiency, considering the power required to drive the water harvesting system, against speed and weight
- Base engine efficiency is reduced from 42% to >38% at high speed, but is relatively unaffected by weight. At lower speeds, weight has a more significant effect as the proportion of power needed to run the water harvesting system becomes a bigger proportion of the overall engine power needed
- Water production increases as vehicle speed and weight (and engine power) increases, up to a max. of 132 kg/h at vehicle top speed and max GVW (40T)

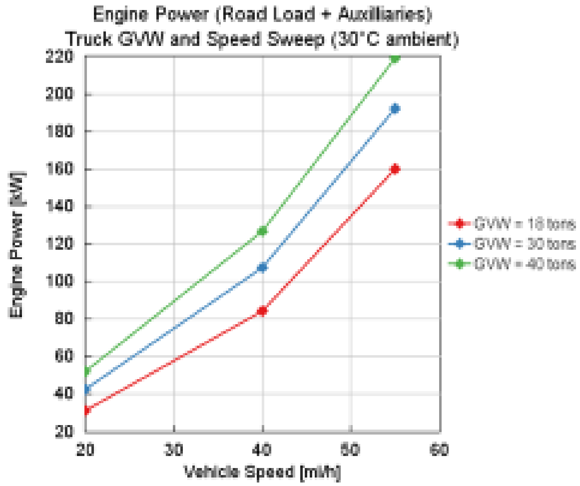

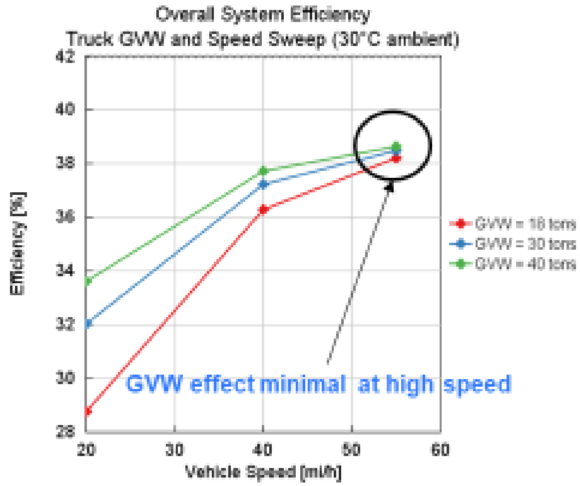

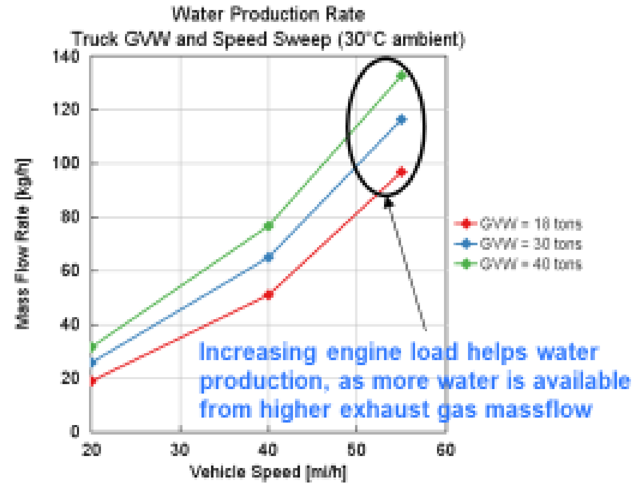

| Dr. Godfrey Udeh | RS.UK.ER | 2025/12/12

GVW and Vehicle Speed Sweep

Overall System Performance – Exhaust water recovery

- Exhaust water recovery efficiency is affected by vehicle speed and gross weight – the influence of GVW on water recovery minimized at 20 mph
- Up-to 72% of the water in the exhaust can be recovered with vehicle speed at 20 mph just from the exhaust cooler
  - Drops to 62% at 40 mph and 48% at 55 mph and 40 tons GVW due to higher massflow and energy at high engine load increasing cooling loads
- Chiller enables close to 95% water recovery from the exhaust by cooling it down to 10 °C, but consumed additional energy and reduces system efficiency

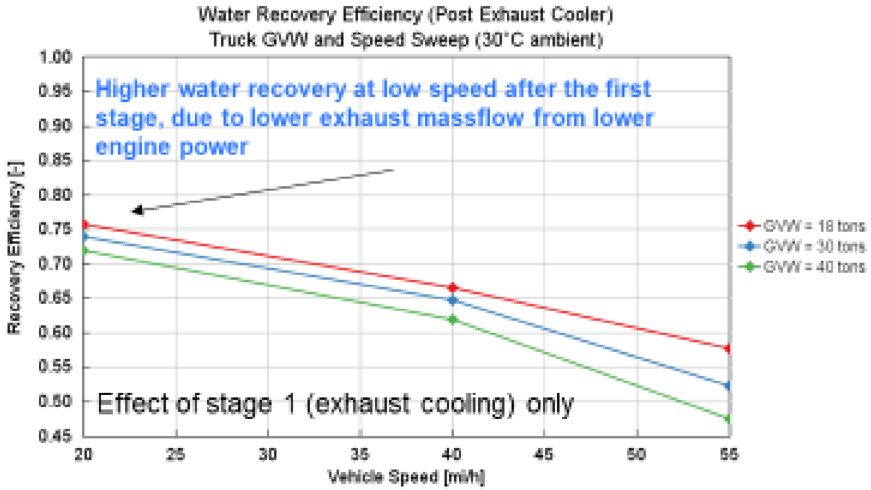

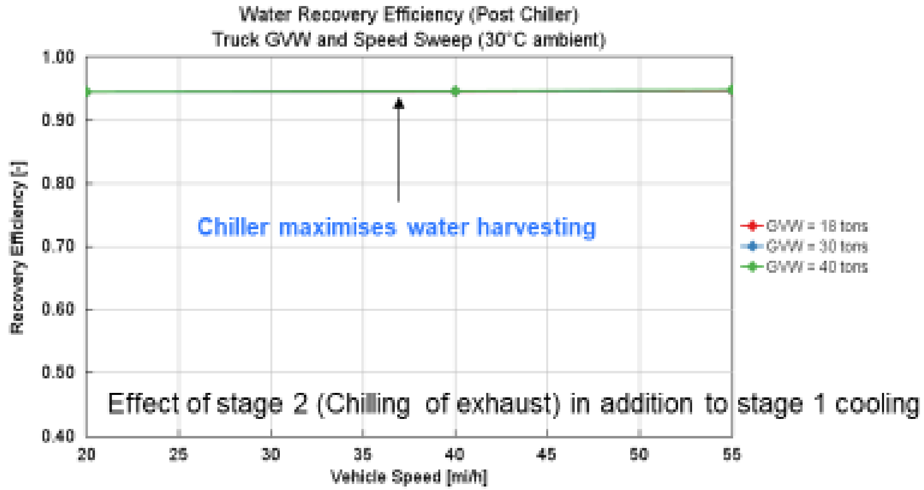

| Dr. Godfrey Udeh | RS.UK.ER | 2025/12/12

MAHLE Powertrain

GVW and Vehicle Speed Sweep

Overall System Performance – Fuel Usage and Water Production

- Hydrogen fuel consumed by the ICE per km travelled increases with increase in vehicle speed and gross weight, as expected
- Similarly, water harvested from the exhaust gas per km travelled increases as truck goes faster
  - 0.6 kg of water is produced per km at 20 mph and 18-ton GVW – increases by about 83% to 1.1 kg/km when truck speed is raised to 55 mph
  - Increasing GVW from 18 tons to 40 tons increases water harvesting rate by at least 38% at 55 mph, much higher at lower vehicle speeds

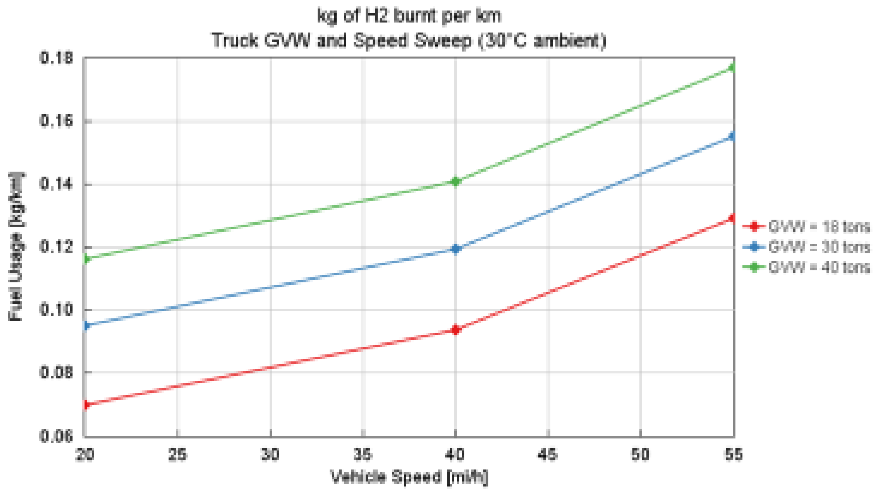

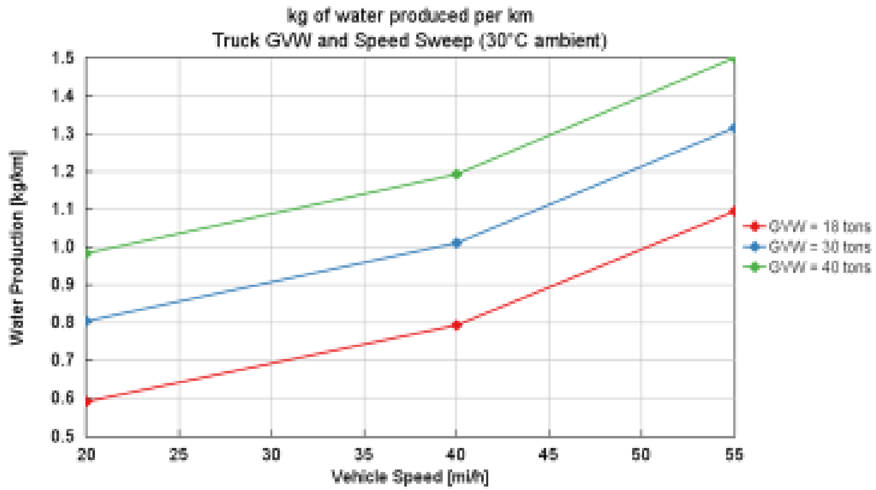

| Dr. Godfrey Udeh | RS.UK.ER | 2025/12/12

MAHLE internal restricted (CL2)

MAHLE Powertrain

Summary – Hydrogen ICE

Conclusions on effect of GVW and vehicle speed on water recovery

- Vehicle speed and gross weight impacts final exhaust temperature and power consumed by fans and compressors to remove heat from exhaust gas
  - Effect minimal at low vehicle speed (20 mph) but becomes evident when vehicle is travelling at higher speed (55 mph)
- Total combined power consumption of the water condensation system increases with increase in vehicle speed (due to the higher exhaust gas massflow and greater mass of water to condense) and could reach 18 kW with vehicle speed of 55 mph and when fully loaded
- Overall system efficiency improves with vehicle speed and could reach 38% at 55 mph (considering base engine efficiency of 42%)
  - This is because the energy needed for the condensation system becomes a smaller proportion of the engine power
  - GVW has little effect at high speed, again due to the relatively low energy requirement of the condensation system compared to roadload, but plays a key role in efficiency when vehicle is travelling at 20 mph
- As a result, more water can be harvested from the exhaust at high vehicle speeds and high GVW
  - More than 1 kg of water can be harvested per km travelled at the different GVW and by burning ~0.12 kg of hydrogen per km
- More than 72% of water in exhaust can be recovered at 20 mph from the exhaust cooler alone (no refrigeration), which reduces to around 45% at higher vehicle speeds due to increase in exhaust mass and energy flow
  - To maximise water recovery to ~90%, chiller is required to cool down exhaust to 10 °C.
- The additional power required to run the water harvesting system can vary from 10 kW to ~18kW, depending on engine power output and the mass flowrate of exhaust to be cooled. This was investigated at one ambient temperature, the effect of which is studied in the following section.

MAHLE Powertrain

Simulation Results – H2 ICE
Effect of ambient temperature @ 40 mph

05

47 | Dr. Godfrey Udeh | RS.UK.ER | 2025/12/12

MAHLE Powertrain

GVW and Ambient Temperature Sweep @40 mph

Exhaust Temperature – Hydrogen ICE

- Exhaust gas is admitted into the first stage cooler at 395 °C irrespective of the ambient temperature, in this simulation
- Ambient temp defines the post cooler temperature. Below 0 °C (ambient), the exhaust can be cooled to 10 °C in the cooler, meaning no refrigeration is needed
  - Cooler performance limited by ambient temperature above 0 °C. Final exhaust temperature linearly increases with ambient temperature up-to 62 °C in 50 °C ambient
  - Chiller cools down exhaust gas to 10 °C to maximise water harvest from the exhaust stream
- Gross vehicle weight has no impact on final cold exhaust temperatures above -30 °C; below this temperature, reducing GVW results in much lower cold exhaust

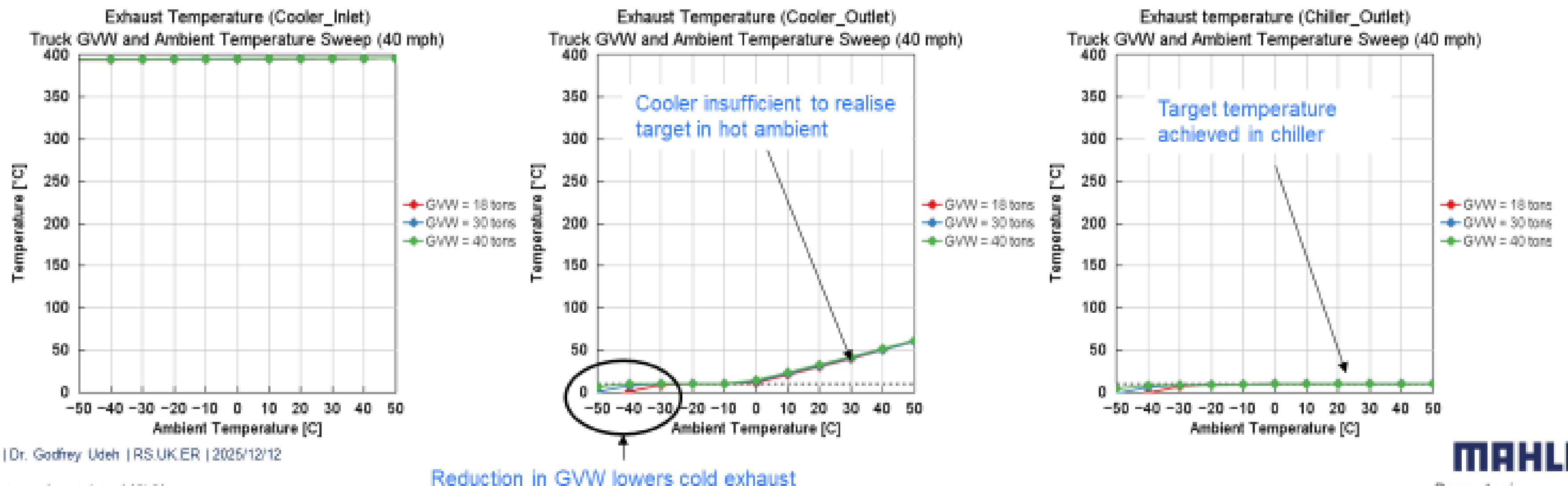

| Dr. Godfrey Udeh | RS.UK.ER | 2025/12/12

MAHLE Powertrain

GVW and Ambient Temperature Sweep @40 mph

Parasitic Load on Engine

- No fan power below 0 °C; vehicle provides enough air to cool radiator at 40 mph.
  - Maximum of 5 kW of fan power is required above this temperature, could be less with the reduction in GVW in > 20 °C ambient
- Similarly, no compressor power below 0 °C; chiller not required in very cold ambient. Compressor power increases above this temperature reaching a peak of 16 kW
- Total power consumption (including pump power) is 3 kW below 0°C independent of GVW. Increases with GVW afterwards to between 17 and 23 kW in 50 °C ambient

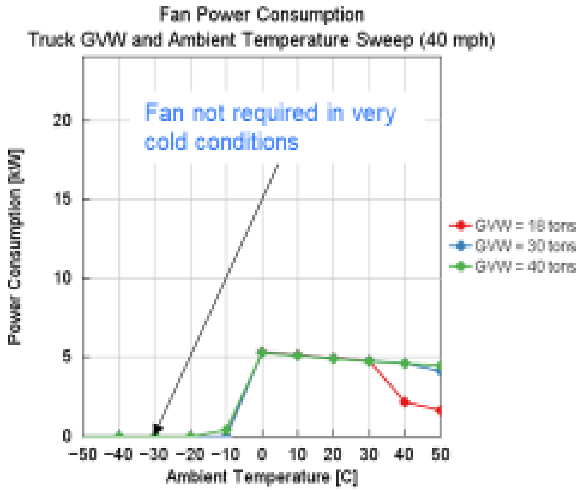

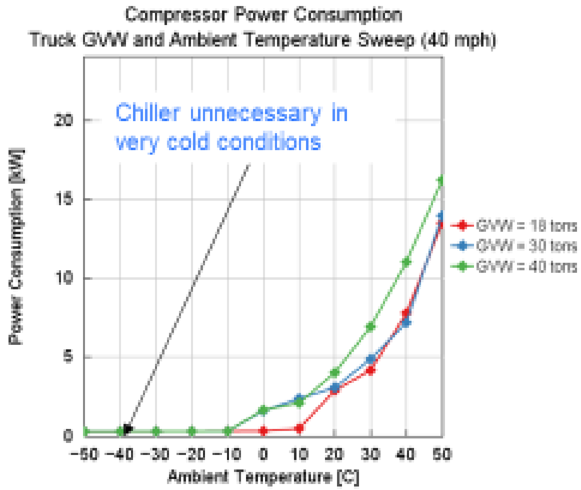

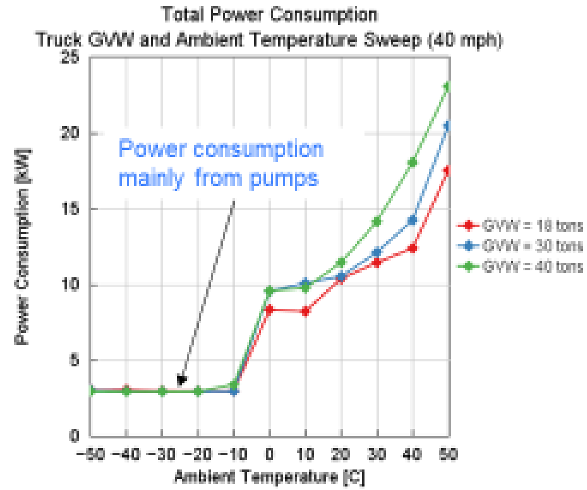

| Dr. Godfrey Udeh | RS.UK.ER | 2025/12/12

MAHLE Powertrain

H2 Powertrain Exhaust Water Recovery feasibility study

GVW and Ambient Temperature Sweep @40 mph

Overall System Performance

- Engine power required to drive the wheels and produce water changes only with GVW below 0 °C. Above this, engine power ramps up with truck in hotter environment
- Nearly 41% overall efficiency in very cold ambient (-20°C – -50°C) with truck fully loaded. Efficiency drops off with increase in ambient temperature; below 34% @ 50 °C
- Driving truck in hot ambient enhances water production due to high engine load. More water is produced when truck is fully loaded, nearly 85 kg/h in 50°C

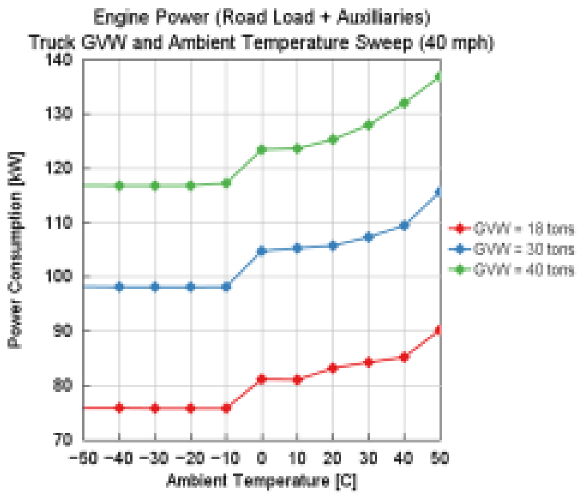

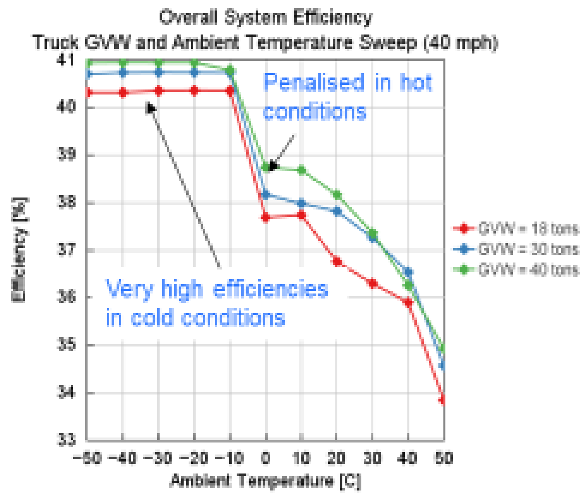

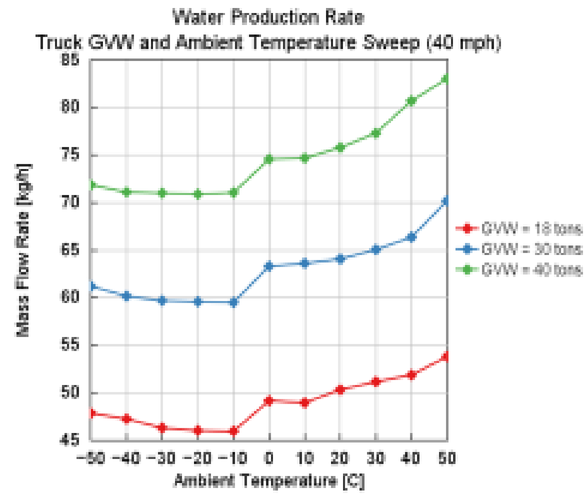

| Dr. Godfrey Udeh | RS.UK.ER | 2025/12/12

MAHLE internal restricted (CL2)

MAHLE Powertrain

GVW and Ambient Temperature Sweep @40 mph

Parasitic Load on Engine

- As seen on the previous page, under some ambient temperatures (below -10 Deg C) it is unnecessary to run the chiller system to condense the water from the exhaust, the cold ambient air is sufficient to enable the first stage cooler to do this on its own
- Consequently, the power needed to run the water harvesting system is very low and is mainly driven by the power needed to run the coolant circulation pumps
- Once the chiller system is needed, power consumption increases significantly, as can be seen by the chart shown (right)
- Power increases exponentially with ambient temperature as the effectiveness of the radiators decreases as the temperature differential between the coolers and the feed air decreases, resulting in higher required airflow and higher power needed to drive the fans moving that air
- System power requirement is therefore a multi-dimensional parameter, based on exhaust massflow and temp, air temp, engine power and required water harvesting

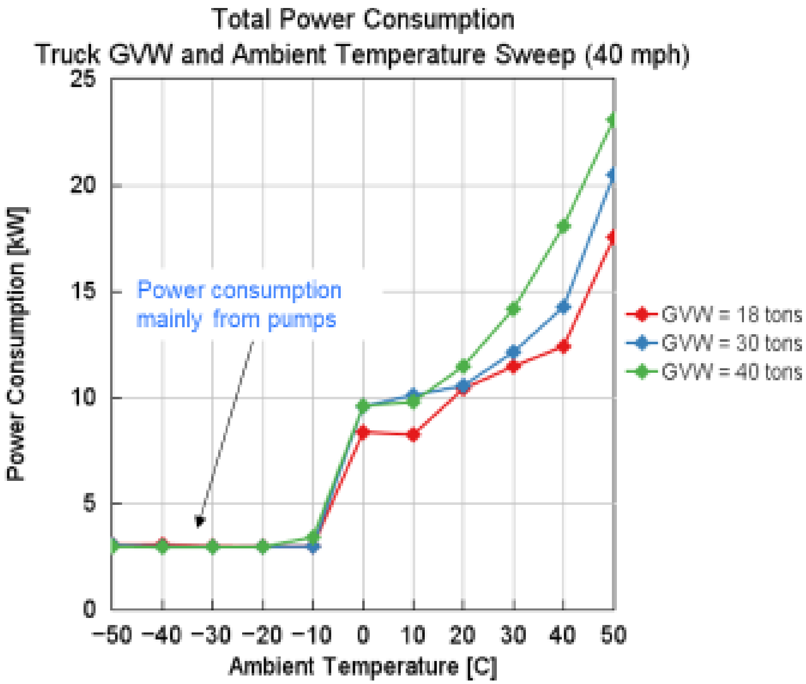

MAHLE Powertrain

GVW and Ambient Temperature Sweep @40 mph

Overall System Performance – Exhaust water recovery

- Ambient temperature limits the amount of water recovered from the exhaust at different stages in the cooling loop; a lot more than GVW
- Below 10°C, it is theoretically possible to recover over 90% of the water in the exhaust just from the cooler (no refrigeration needed).
- Chiller operation (refrigeration) enables close to 95% water recovery from the exhaust by cooling it down to 10 °C irrespective of the ambient temperature and GVW, but, of course, additional energy is consumed to do this, and system energy efficiency decreases accordingly

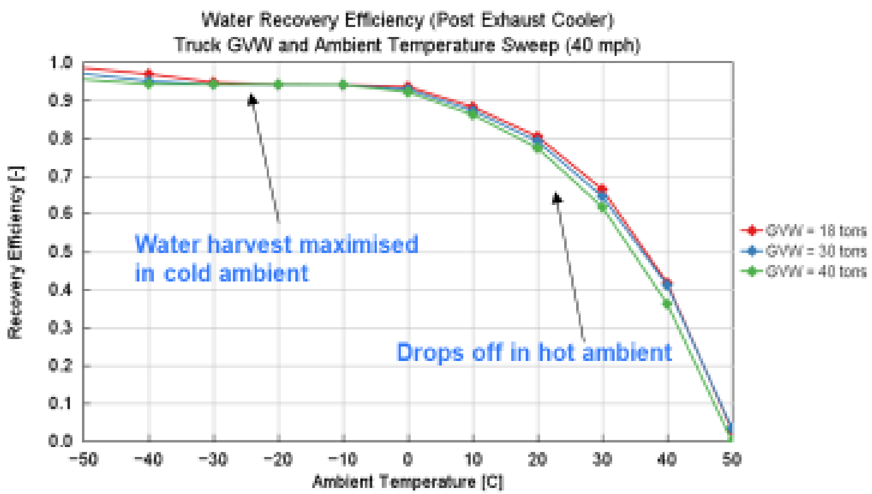

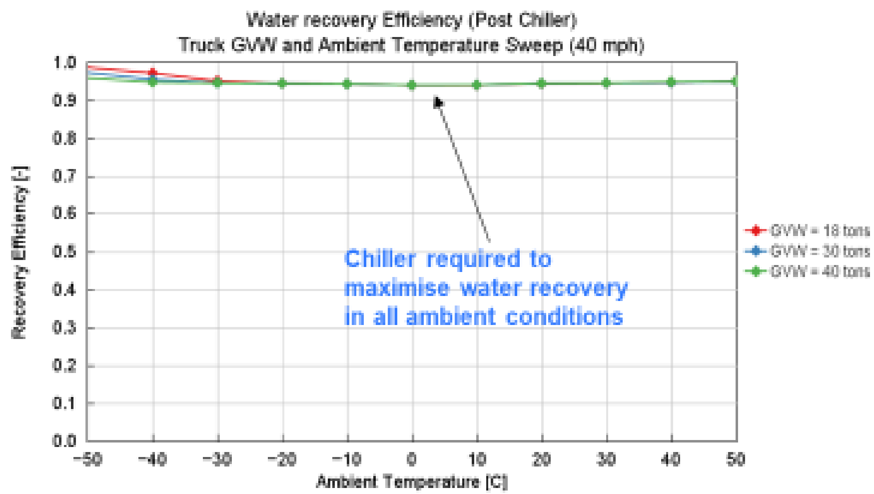

| Dr. Godfrey Udeh | RS.UK.ER | 2025/12/12

MAHLE Powertrain

GVW and Ambient Temperature Sweep @40 mph

Overall System Performance – Fuel Usage and Water Production

- Hydrogen consumed per km is sensitive to GVW particularly below 0°C (~54% increase in H_2 consumption when moving from 18 tons to 40 tons)
- Water harvested from is also heavily affected by vehicle weight and ambient temperature
  - Increased vehicle weight increases the power needed from the ICE, making more water vapour available in the exhaust
  - Increased ambient temperature requires greater fan and refrigerator power, increasing engine load and, again, making more water available to harvest, but at the detriment of fuel consumption and system energy efficiency

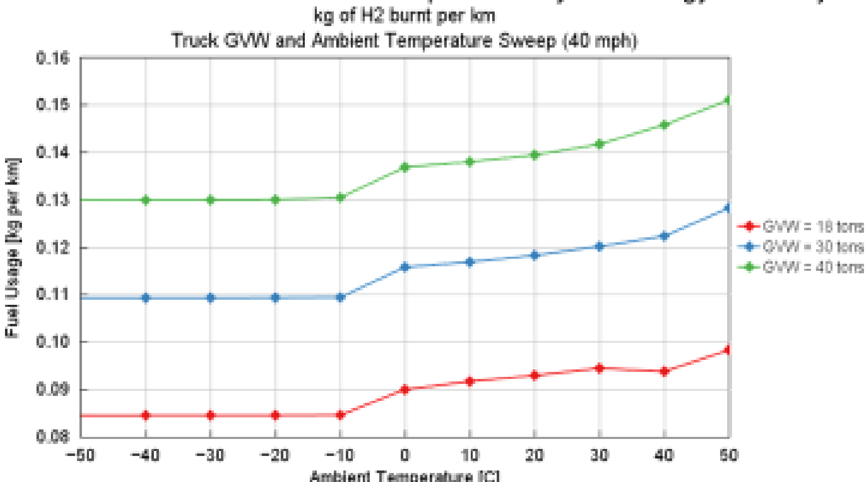

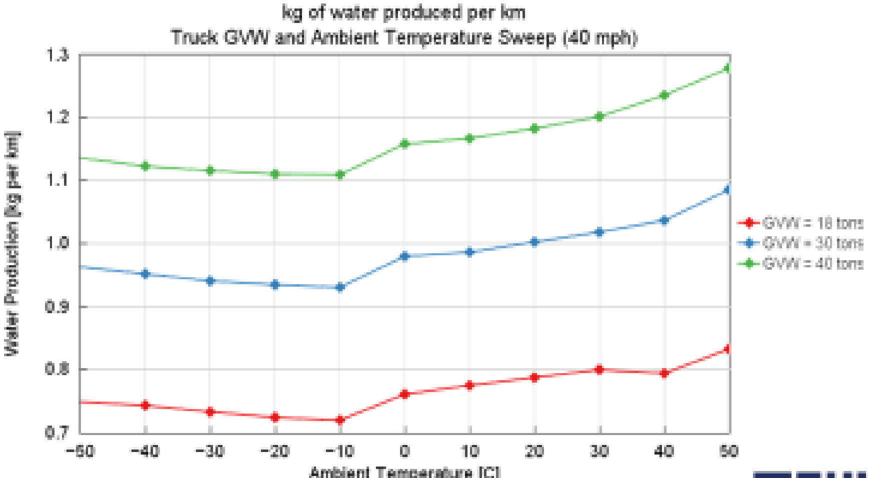

Summary – Hydrogen ICE

Conclusions on effect of GVW and ambient temperature on water recovery

- Ambient temperature impacts final exhaust temperature and power consumed by fans and compressors to remove heat from exhaust gas
  - Effect of GVW is minimal at the vehicle speed studied (40 mph)
- Below 0°C ambient temperature, it is possible to cool down exhaust to the 10 °C needed to condense the water, without using the chiller. In hotter conditions, a chiller is required to achieve target cold exhaust temperature of 10 °C
- Power consumption follows a similar trend; it starts to rise with increases in ambient temperature, starting from -10 °C
- Overall system efficiency is penalised accordingly, with >40% efficiency possible in very cold conditions but potentially dropping to 34% in very high ambient temperatures
- Exhaust water condensation is impacted more by GVW than changes in ambient temperature
  - More water is produced when truck is fully loaded and could result in over 80 kg of water produced in an hour @ 50 °C
  - At 40 mph and with above water production rate, 1.3 kg of water can be produced over one kilometre
    - This could drop by 50% if vehicle is not fully loaded (GVW = 18 tons)
- In very cold ambient conditions (< 0 °C), water harvest from exhaust can be maximised with only a cooler
  - > 90% of exhaust water could potentially be harvested at these conditions
  - The exhaust cooler alone is insufficient to harvest high rates of water under high ambient temperatures; water recovery could drop to nearly 0% @ 50°C, resulting in the refrigeration system needed to perform all of the condensation function
- The refrigeration system is always required in hot ambient conditions to maximise exhaust water recovery

MAHLE Powertrain

Performance Maps (H2 ICE) 06

55 | Dr. Godfrey Udeh | RS.UK.ER | 2025/12/12

MAHLE internal restricted (CL2)

MAHLE Powertrain

Performance Map

Overall System Performance – GVW = 18T

- Performance maps indicate effect of ambient temperature on energy requirement for water extraction and engine power when truck is travelling at different speeds and with GVW of 18 ton
- Energy required to extract water in very cold ambient (< 0 °C) is independent of vehicle speed. Increases with speed as ambient temperature gets hotter.
- Engine power increases with ambient temperature for a given vehicle speed due to the increase in the energy demand from the cooling system

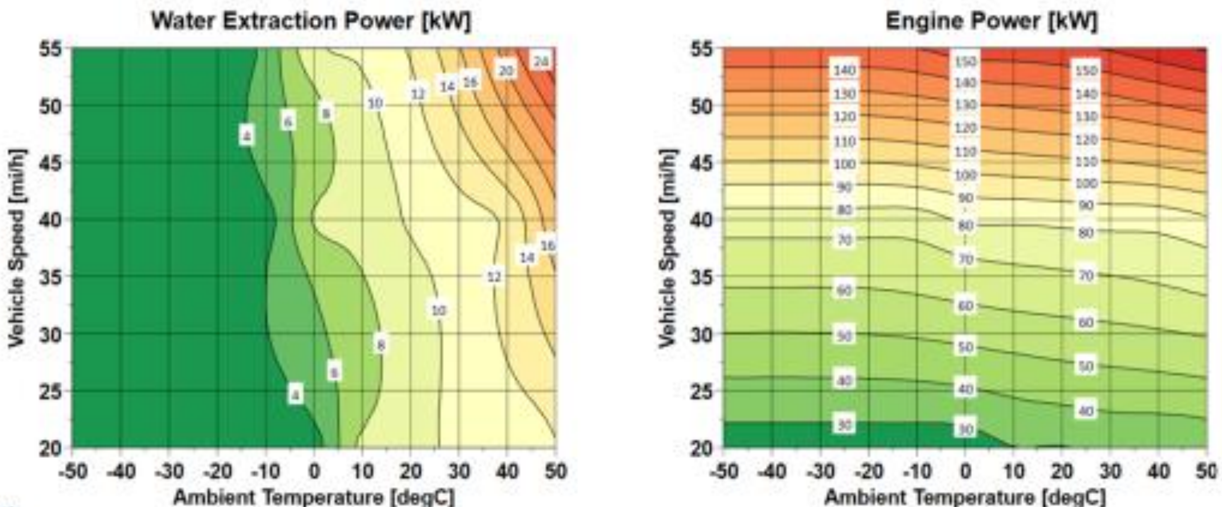

MAHLE Powertrain

Performance Map

Overall System Performance – GVW = 30T

- Similar maps are shown for 30 ton truck – trend is the same as the previous slide although increased weight increases engine and water extraction power
- At this GVW, maximum engine power is 204 kW inclusive of power required to drive cooling system
- Clearly, power demand is worsened by ambient temperature and vehicle speed

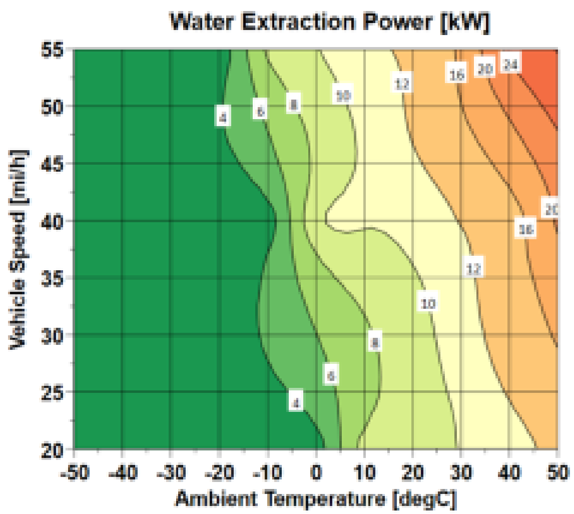

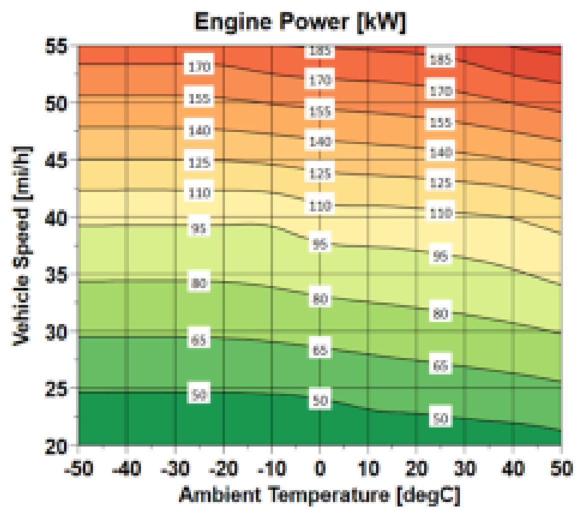

MAHLE Powertrain

Performance Map

Overall System Performance – GVW = 40T

- Similar maps are shown for 40 ton truck – power demand is influenced by ambient temperature and vehicle speed
- At this GVW, maximum engine power is 231 kW at 55 mph and in 50 °C ambient; 30 kW is the maximum power demand of the cooling system
- At engine rated power, there is need to by-pass some of the exhaust to ensure engine performance does not degrade further and maximise water production

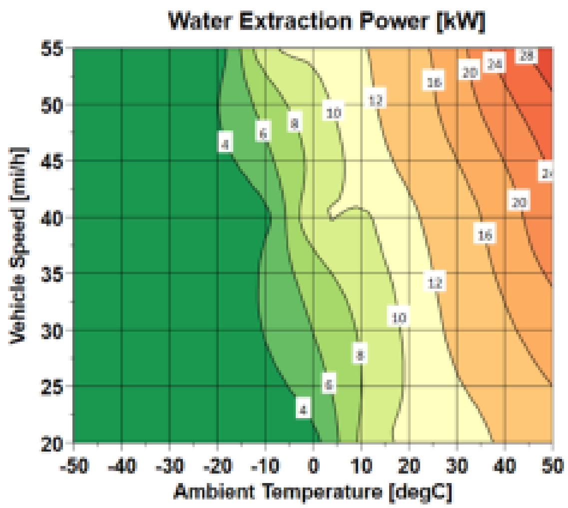

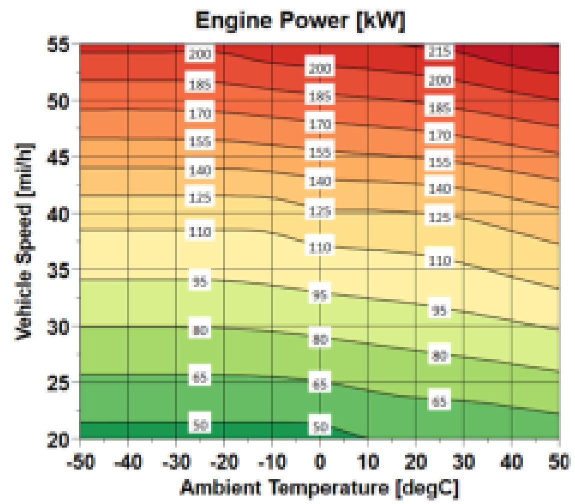

H_2 Fuel Cell Feasibility study

07

59 | Dr. Godfrey Udeh | RS.UK.ER | 2025/12/12

MAHLE Powertrain

H_2 Fuel Cell Feasibility study: Passive Water Separation System

07

60 | Dr. Godfrey Udeh | RS.UK.ER | 2025/12/12

MAHLE Powertrain

Input Data

Vehicle Specification

- Fuel cell powertrain sized to have similar capability as engine - 376 kW
  - Historical test data shows stack exhaust temp of 81 °C
  - Stack tested ran at lambda = 1.6
- Polarisation curve of tested fuel cell stack is shown on the right
  - Stack power rated at 150 kW
  - Net power of 125 kW
  - System efficiency of 42 – 58 %, depending on load
- Three (3) stacks are required to achieve power level for the truck
  - ~210 kW required to propel wheels at top speed and GVW = 40 T
  - This would be provided by 3 stacks producing ~ 70 kW each
  - This operating point is shown on the performance data (right)
  - At this power level, system electrical efficiency is ~ 53.9%, including parasitic losses from the Balance of Plant (BoP)

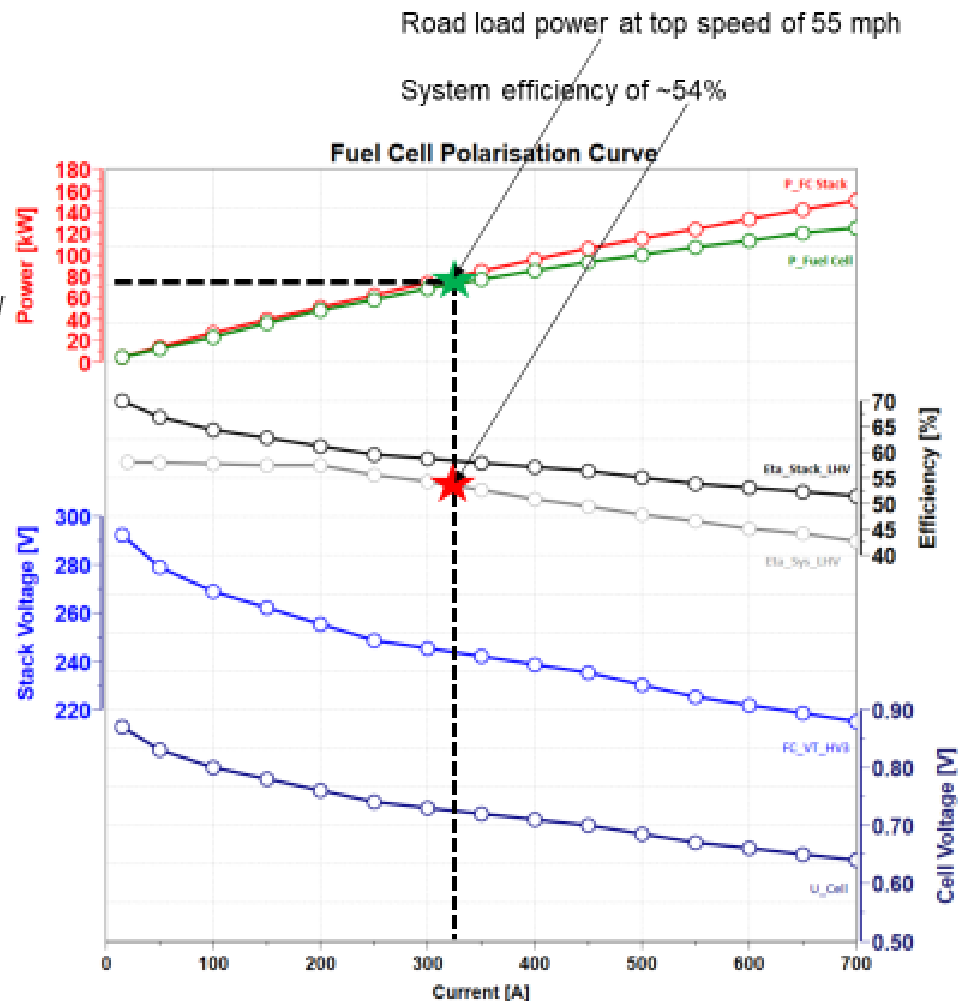

| Dr. Godfrey Udeh | RS.UK.ER | 2025/12/12

MAHLE Powertrain

Water Recovery Passive Cooling

Estimate of water collection

- The current state of the art in the fuel cell market is to use mechanical separation of the water in the exhaust, rather than the active (cooled and chilled) system proposed for the H2 ICE earlier in this report
- Passive cooling is experienced from the cool walls of the exhaust of the fuel cell stack, as well as condensate separation from water separation components
- Depending on the ambient temperature, condensate formation will occur as heat is lost from the walls of the pipe
- Som water is used to increase the humidity of the incoming air, but this is assumed to be passed through to the exhaust in a no-net-loss process
- Condensation can also occur as a by product of the exhaust gas passing through a turbine, used to harvest wate energy and offset the power needed for the air compressor

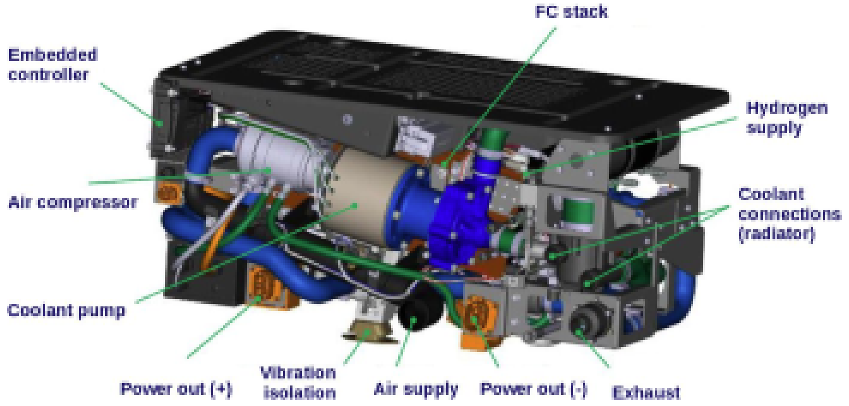

| Dr. Godfrey Udeh | RS.UK.ER | 2025/12/12

MAHLE Powertrain

Water Recovery: Passive Cooling

Estimate of water collection

- The data below is taken from real fuel cell testing and shows the state of the art in water recovery technology
- Test fuel cell stack power = 103 kW
  - H2 fuel consumption = 6.4 kg/h
  - Condensate recovered from exhaust = 13.3 kg/h
  - Theoretical water in exhaust gas = 57 kg/h at the test conditions
  - Water recovery efficiency = $\frac{13.3}{57} = 0.233$
  - Mechanical water separation efficiency = 90% *
  - Minimal energy is required for the separation process
  - System efficiency was reported to be 57% (without the efficiency drop in the DC-DC converter, which is estimated to be ~2%)
- **At this load point and test conditions, it is possible to recover 23% of the water vapour in the exhaust with simple passive cooling**

Water separator on cathode exhaust

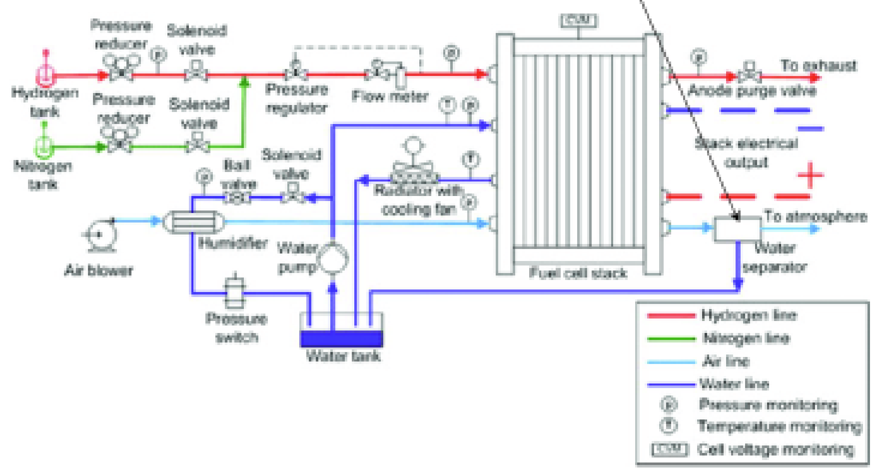

* This is the efficiency of the removal of optically senses water droplets, not the efficiency of recovery of the theoretical maximum water

| Dr. Godfrey Udeh | RS.UK.ER | 2025/12/12

MAHLE Powertrain

H_2 Fuel Cell Feasibility study: Active Water Separation System

07

64 | Dr. Godfrey Udeh | RS.UK.ER | 2025/12/12

MAHLE Powertrain

Simulation Results (Fuel Cell - active) Effect of ambient temperature @ 40 mph

08

65 | Dr. Godfrey Udeh | RS.UK.ER | 2025/12/12

MAHLE internal restricted (CL2)

MAHLE
Powertrain

Water Recovery
Active Cooling

- Only about 23% of the water/condensate in the exhaust of the stack can be recovered with passive cooling
- Active cooling is required to recover most of the water in the exhaust stream of the fuel cell stack
- This would require two stages of cooling of the exhaust to below dew point temperature
  - Stage 1 Cooling: deploys an exhaust cooler to cool down the exhaust from 81 °C to close to ambient conditions
    - Depending on the ambient temperature, significant amount of water vapour in the exhaust will condense in the exhaust cooler
  - Stage 2 Cooling: uses a chiller to cool down the remaining exhaust to 10°C to ensure over 90% water recovery efficiency
- The cooling system configuration for active cooling is shown in the next slide
  - System configuration same as the H2 ICE exhaust cooling system
  - Exhaust cooler has been scaled down by 50% due to the reduced temperature and exhaust mass flow

H2 Powertrain Exhaust Water Recovery feasibility study

Possible Cooling System Layout Active Cooling

- Optimal system layout derived from investigating H2 ICE to be deployed for Fuel Cell exhaust cooling
    - Stack exhaust temperature typically around 81 °C – much lower than ICE exhaust (> 350 °C)
    - Exhaust cooler is to be scaled down
- An array of electric fans to provide cooling air to the exhaust cooler radiator

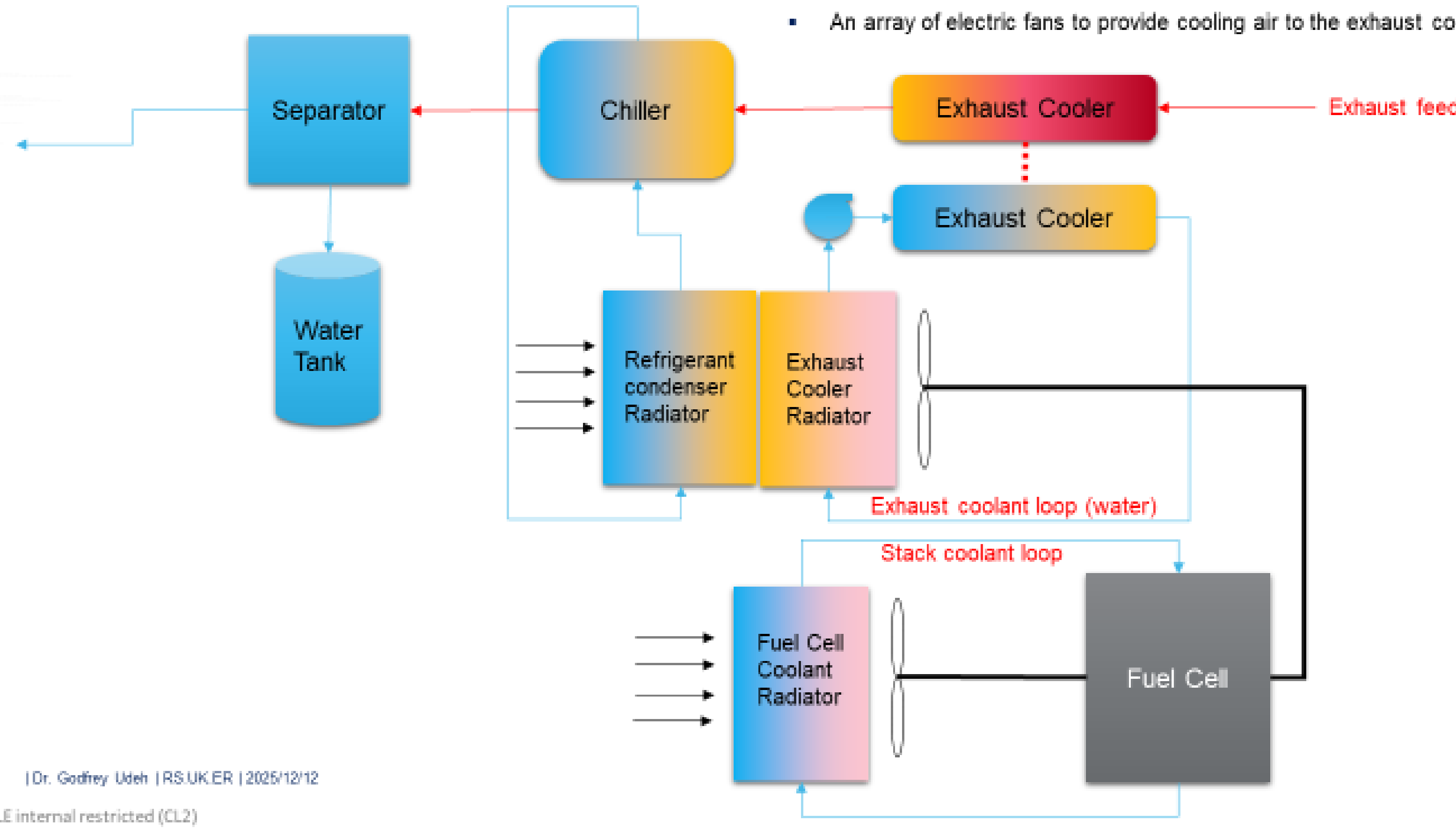

| Dr. Godfrey Udeh | RS.UK.ER | 2025/12/12

MAHLE internal restricted (CL2)

MAHLE Powertrain

H2 Powertrain Exhaust Water Recovery feasibility study

GVW and Ambient Temperature Sweep @40 mph

Exhaust Temperature – Fuel Cell

- Exhaust gas is admitted into the first stage cooler at 80 °C irrespective of the ambient temperature, in this simulation
- Ambient temp defines the post cooler temperature. Below 10 °C (ambient), the exhaust can be cooled to 10 °C in the cooler, meaning no refrigeration is needed
  - Cooler performance limited by ambient temperature above 10 °C. Final exhaust temperature linearly increases with ambient temperature up-to 53 °C in 50 °C ambient
  - Chiller cools down exhaust gas to 10 °C to maximise water harvest from the exhaust stream
- Gross vehicle weight has no impact on the cooler performance for the investigated ambient temperatures

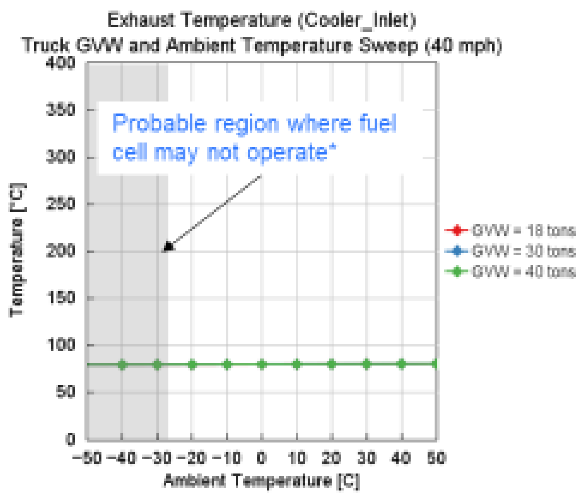

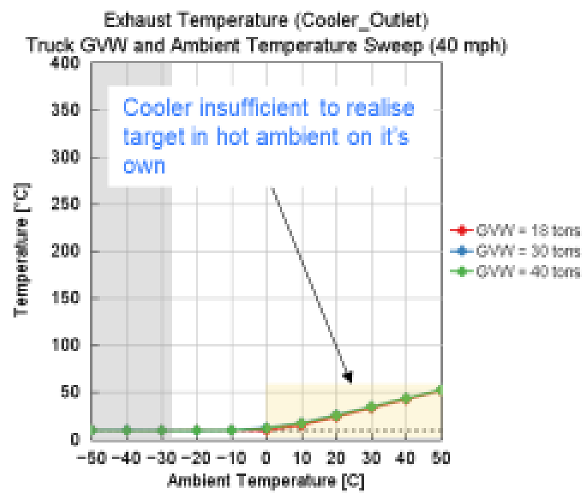

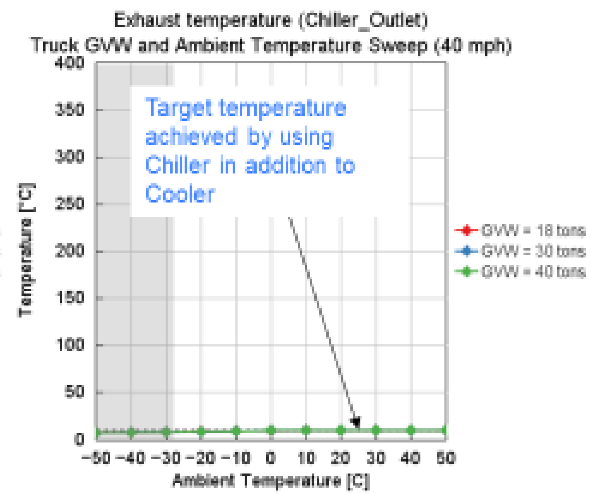

| Dr. Godfrey Udeh | RS.UK.ER | 2025/12/12

*** Typically, state of the art fuel cells cannot operate below -30 Deg C, in this application, this may be critical**

MAHLE internal restricted (CL2)

Powertrain

GVW and Ambient Temperature Sweep @40 mph

Parasitic Load on Fuel Cell Power-Train

- No fan power needed at subzero ambient with 30T and 40T trucks; vehicle provides enough air to cool radiator at 40 mph.
  - Maximum of 5.4 kW of fan power is required above this temperature, reduces with ambient temp as theoretical fluid power reduces with fan revving at max speed
- Similarly, no compressor power below 0 °C; chiller not required in very cold ambient. Compressor power increases above this temperature reaching a peak of 8 kW
- Total power consumption (including pump power) is less than 0.5 kW below 0°C independent of GVW. Increases with GVW afterwards to 15 kW max in 50 °C ambient

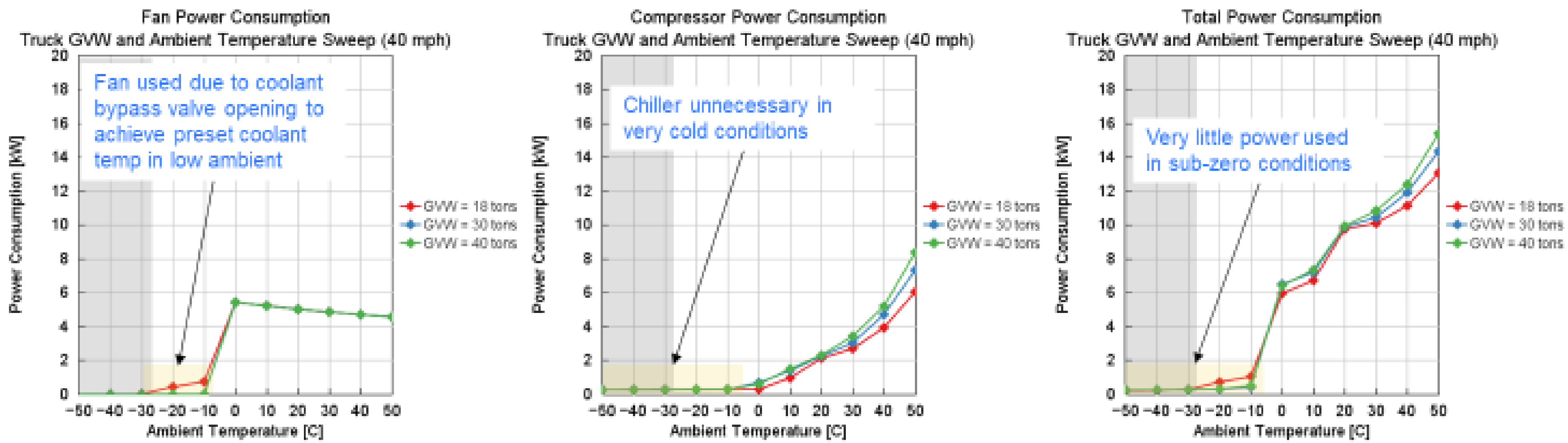

MAHLE Powertrain

GVW and Ambient Temperature Sweep @40 mph

Parasitic Load on Fuel Cell Power-Train

- As seen on the previous page, under some ambient temperatures (below 0 Deg C) it is unnecessary to run the chiller system to condense the water from the exhaust, the cold ambient air is sufficient to enable the first stage cooler to do this on its own
- Consequently, the power needed to run the water harvesting system is very low and is mainly driven by the power needed to run the coolant circulation pumps
- Once the chiller system is needed, power consumption increases significantly, as can be seen by the chart shown (right)
- Power increases exponentially with ambient temperature as the effectiveness of the radiators decreases as the temperature differential between the coolers and the feed air decreases, resulting in higher required airflow and higher power needed to drive the fans moving that air
- System power requirement is therefore a multi-dimensional parameter, based on exhaust massflow and temp, air temp, fuel cell power and required water harvesting

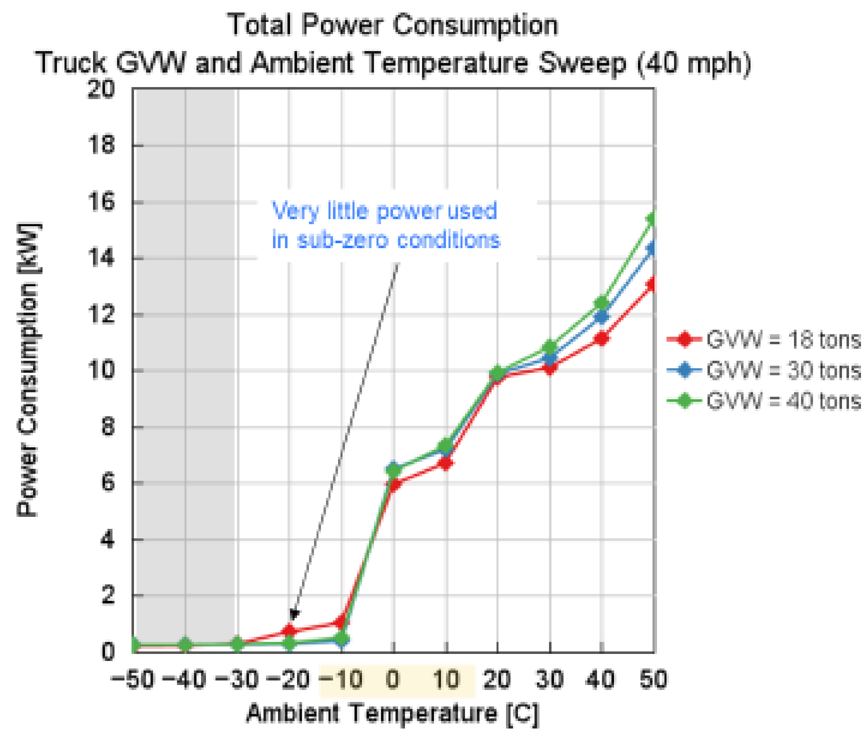

| Dr. Godfrey Udeh | RS.UK.ER | 2025/12/12

GVW and Ambient Temperature Sweep @40 mph

Overall System Performance

- Power required for truck propulsion and water production changes only with GVW below 0 °C; Fuel cell power ramps up with truck weight in hotter environment
- At least 57% propulsion efficiency* in very cold ambient (-50°C – 0°C) with truck fully loaded. Efficiency drops off with increase in ambient temperature worsened when lighter; down to 49% @ 50 °C and with 18 T truck
- Low powertrain efficiency in hot ambient is compensated by water production due to high load. More water is produced when truck is fully loaded, 58 kg/h @ 50°C

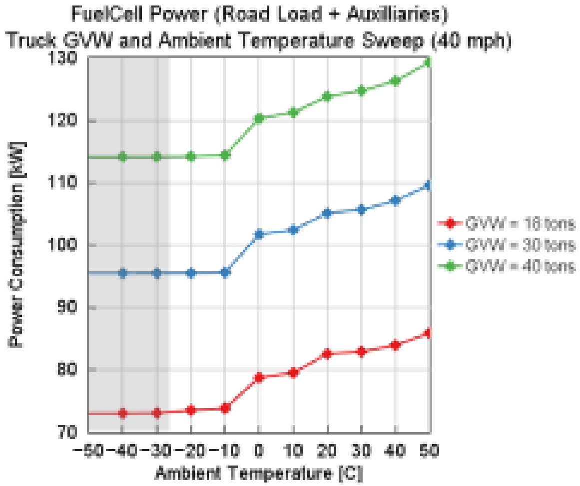

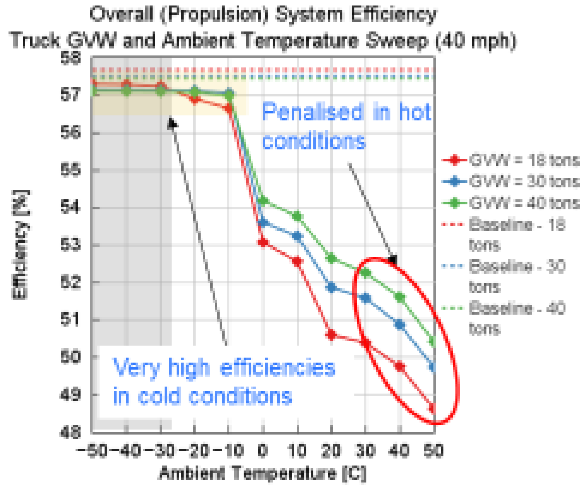

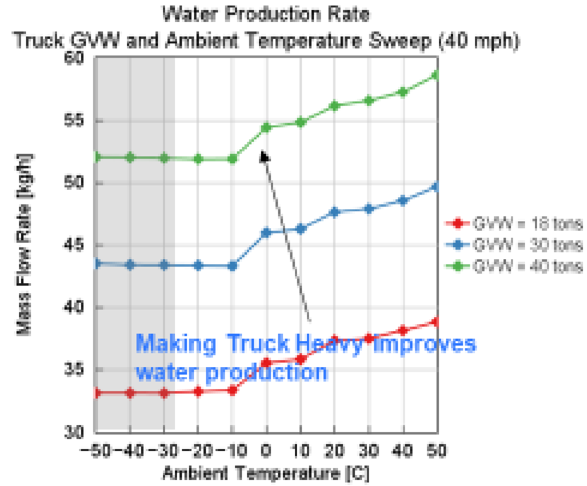

| Dr. Godfrey Udeh | RS.UK.ER | 2025/12/12

* Propulsion efficiency expressed as a ratio of propulsion power to fuel consumed in driving truck & harvesting water

MAHLE Powertrain

GVW and Ambient Temperature Sweep @40 mph

Overall System Performance – Exhaust water recovery

- Ambient temperature limits the amount of water recovered from the exhaust at different stages in the cooling loop; a lot more than GVW
- Below 10°C, it is theoretically possible to recover over 90% of the water in the exhaust just from the cooler (no refrigeration needed).
- Chiller operation (refrigeration) enables close to 95% water recovery from the exhaust by cooling it down to 10 °C irrespective of the ambient temperature and GVW, but, of course, additional energy is consumed to do this and system energy efficiency decreases accordingly

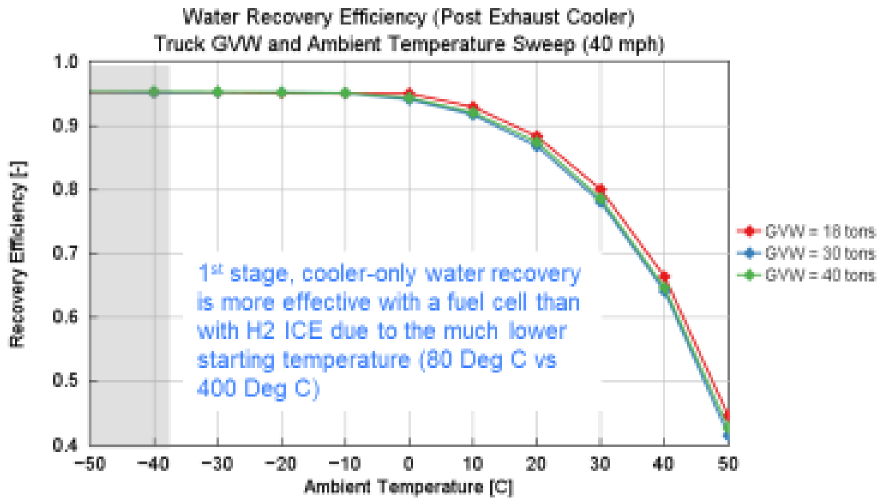

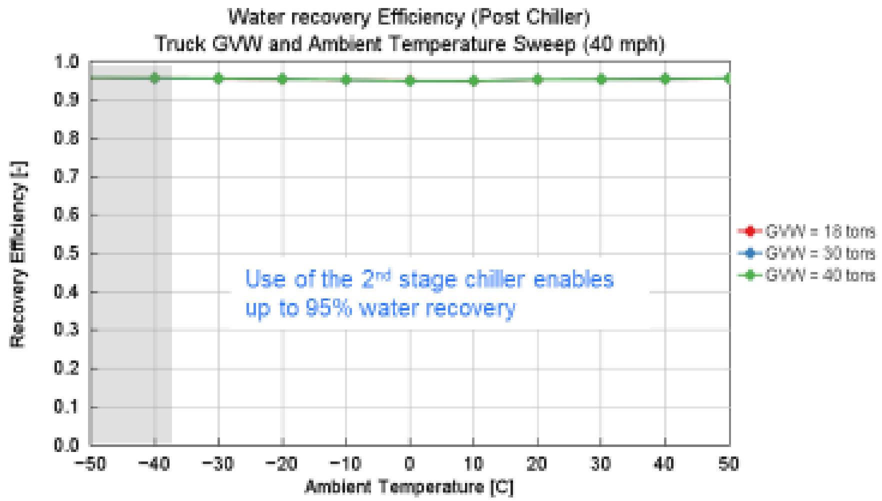

GVW and Ambient Temperature Sweep @40 mph

Overall System Performance – Fuel Usage and Water Production

- Hydrogen consumed per km is sensitive only to GVW at sub zero conditions (~60% increase in H_2 consumption when moving from 18 tons to 40 tons)
- Water harvested from fuel cell is also heavily affected by vehicle weight and ambient temperature
  - Increased vehicle weight increases the power needed from the fuel cell, making more water vapour available in the exhaust
  - Increased ambient temperature requires greater fan and refrigerator power, increasing engine load and, again, making more water available to harvest, but at the detriment of fuel consumption and system energy efficiency

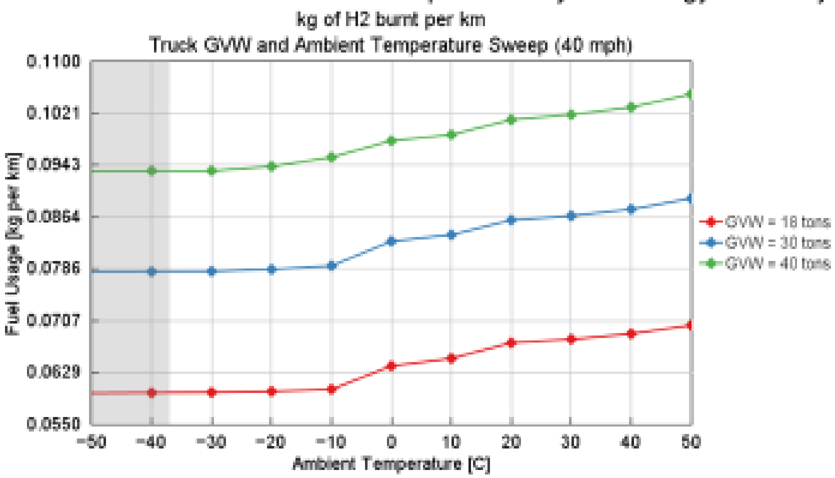

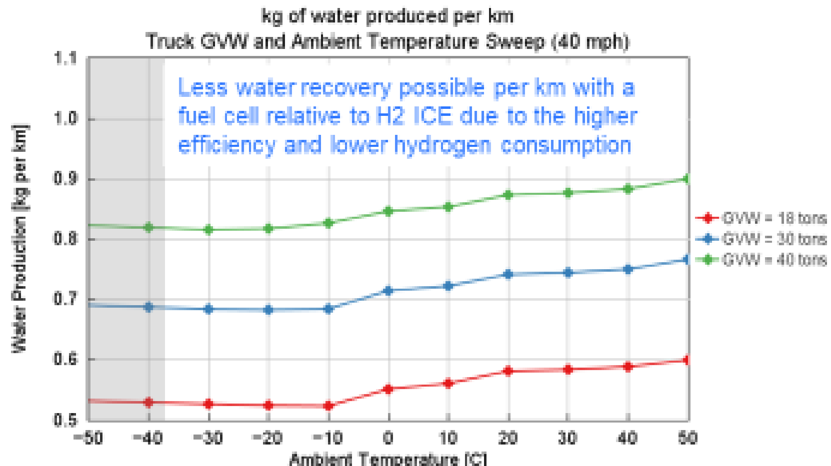

Summary – Hydrogen Fuel Cell

Conclusions on effect of GVW and ambient temperature on water recovery

- Ambient temperature impacts final exhaust temperature and power consumed by fans and compressors to remove heat from exhaust gas
  - Effect of GVW is minimal at the vehicle speed studied (40 mph)
- Below 0°C ambient temperature, it is possible to cool down exhaust to the 10 °C needed to condense the water, without using the chiller. In hotter conditions, a chiller is required to achieve target cold exhaust temperature of 10 °C
- Power consumption follows a similar trend; it starts to rise with increases in ambient temperature, starting from -10 °C
- System efficiency is penalised accordingly, with 57% efficiency possible in very cold conditions but dropping to 48% in very high ambient temperatures as the power requirement of the water recovery system increases
- Exhaust water condensation is impacted more by GVW than changes in ambient temperature. More is water produced when truck is fully loaded, due to the higher power and fuel consumption, and could result in nearly 58 kg of water produced in an hour @ 50 °C
- At 40 mph and 58 kg/h water production rate, 0.9 kg of water can be produced per kilometre travelled, which decreases by 33% at GVW = 18 tons.
- In very cold ambient conditions (< 0 °C), water harvest from exhaust can be maximised using only the 1st stage cooler (2nd stage chiller not required)
  - This is slightly improved relative to the H2 ICE, which showed worse water recover from only using the 1st stage cooler at higher ambient temps (>20 °C)
  - As with the H2 ICE, below 0 C, around 90% wate recovery is possible using on the first stage cooler, which results in much improved system operating efficiency
- The refrigeration system is always required in hot ambient conditions to maximise exhaust water recovery

MAHLE Powertrain

Performance Maps (Fuel Cell)

09

75 | Dr. Godfrey Udeh | RS.UK.ER | 2025/12/12

Performance Map

Overall System Performance – GVW = 18T

- Performance maps indicate effect of ambient temperature on energy requirement for water extraction and truck propulsion by fuel cell at different speeds (GVW = 18 ton (unladen)). Note: Road load is based on a flat road.
- Energy required to extract water in wintery conditions (sub zero ambient) is independent of vehicle speed. Increases with speed as ambient temperature gets hotter.
- Fuel cell power increases with ambient temperature for a given vehicle speed due to the increase in the energy demand from the cooling system

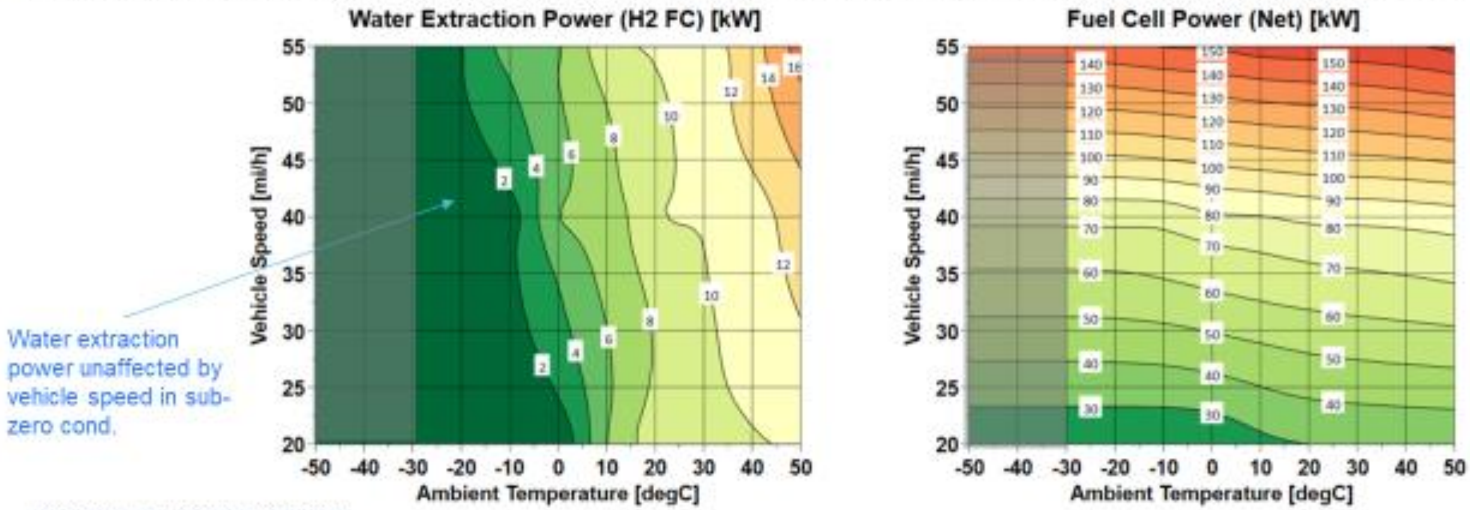

MAHLE Powertrain

Performance Map

Overall System Performance – GVW = 30T

- Similar maps are shown for a 30-ton truck – the trend at 18T is maintained at 30T, but fuel cell power and water extraction power is increased by added weight
- At this GVW, maximum fuel cell power is 195 kW inclusive of power required to drive cooling system
- Truck utilisation in hot conditions worsens power demand for water extraction as well as increase in vehicle speed

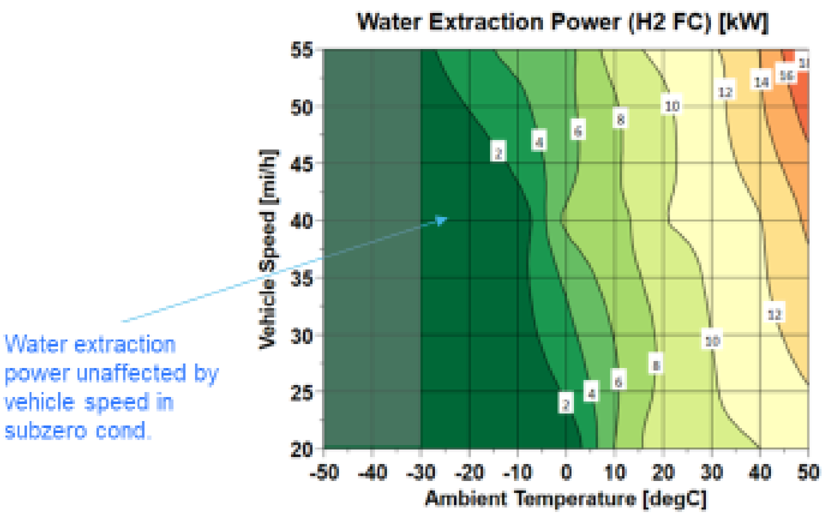

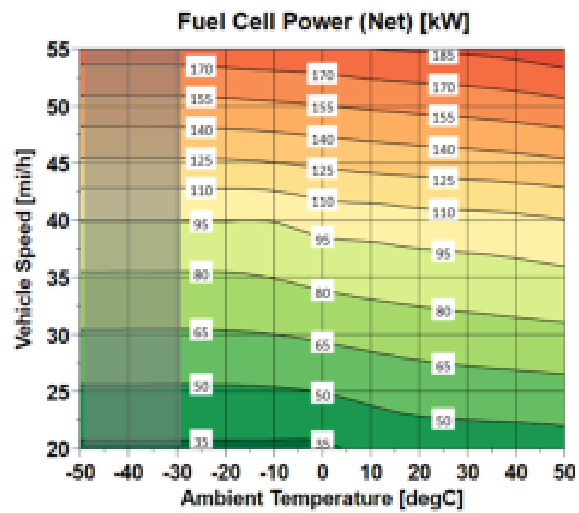

MAHLE Powertrain

Performance Map

Overall System Performance – GVW = 40T

- Similar maps are shown for 40 ton truck – power demand is influenced by ambient temperature and vehicle speed
- At this GVW, maximum fuel cell power is 221 kW at 55 mph and in 50 °C ambient; 20 kW is required for water extraction by the cooling system
- At fuel cell rated power, exhaust by-pass is recommended to ensure powertrain performance does not degrade further and maximise water production

Water extraction power unaffected by vehicle speed in subzero cond.

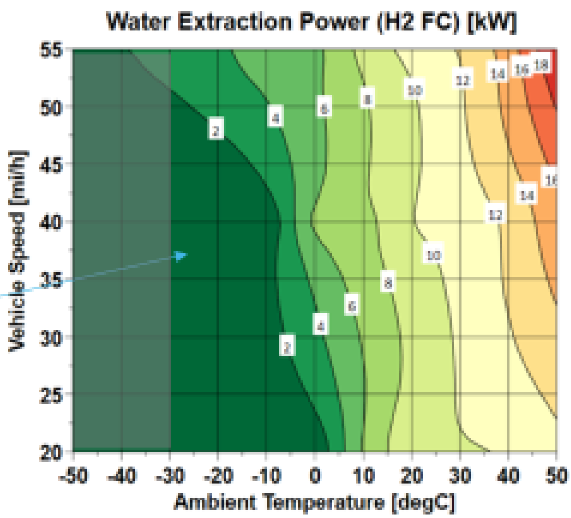

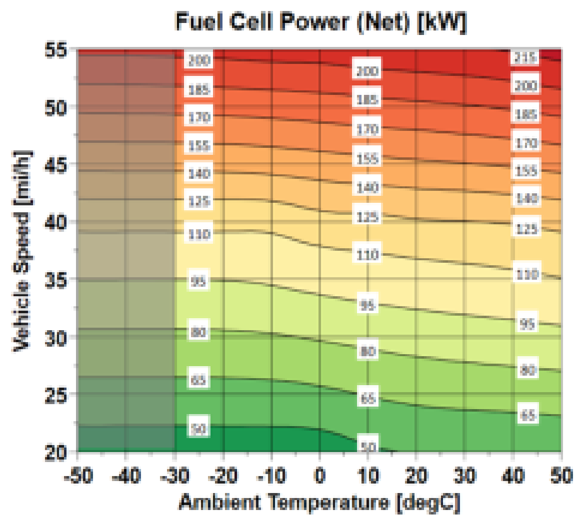

| Dr. Godfrey Udeh | RS.UK.ER | 2025/12/12

MAHLE Powertrain

Performance Maps (ICE vs. Fuel Cell) 10

MAHLE Powertrain

Water Extraction Power

H2 ICE vs. H2 Fuel Cell – GVW = 40T

- Water extraction power compared for the truck at GVW = 40 ton over a range of vehicle speeds and operating ambient temperatures with two powertrain options: Hydrogen engine and fuel cell
- In sub-zero conditions, water extraction power is reduced by 50% with fuel cell largely due to the lower exhaust flow rate and temp. Fan and pump power are reduced
- 33 – 35% reduction in water extraction power is observed at higher ambient temps and vehicle speeds, <u>but</u> only 1.2 kg/km of water vs 1.6 kg/km is harvested (-25%)

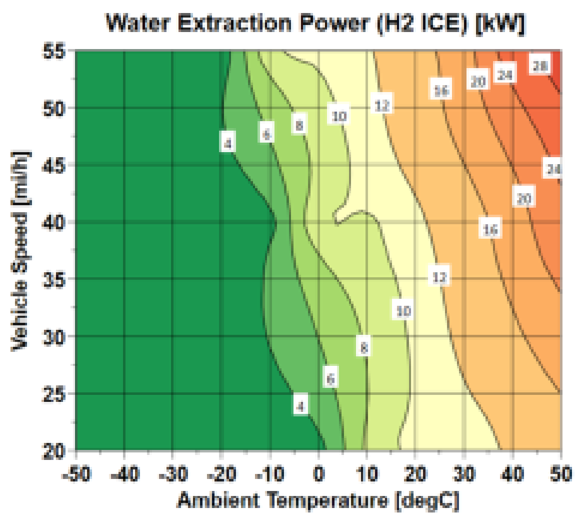

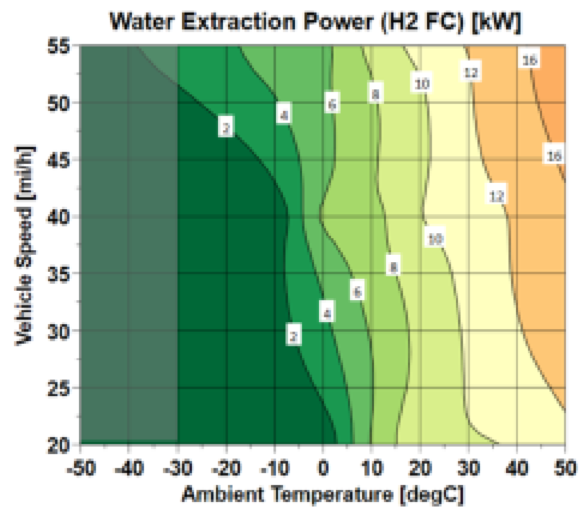

Please note that even though data is shown for ambient temperatures as low as -50 °C, state of the art fuel cell systems typically cannot operate in temperatures lower than -30 °C.

Powertrain Power

H2 ICE vs. H2 Fuel Cell – GVW = 40T

- Combined power required for truck propulsion on a flat road and water extraction is compared for the two powertrain options at GVW = 40 ton over a range of vehicle speeds and potential operating ambient temperatures
- Similar propulsion power demand from both powertrains at a given vehicle speed. Variation in water extraction power increases energy requirement from a powertrain
- Engine will operate at a higher load compared to the fuel cell as a result; max power @ 55 mph and 50°C ambient of 231 kW (ICE) vs. 221 kW (Fuel Cell)

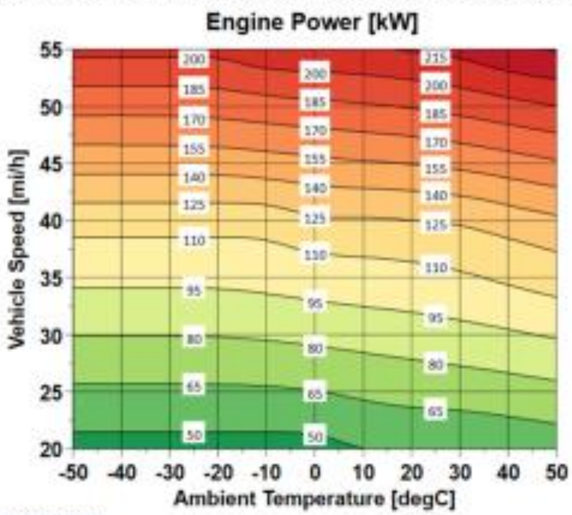

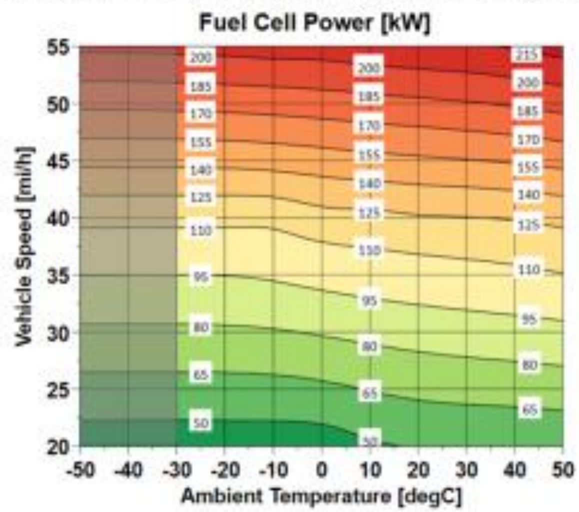

MAHLE Powertrain

Powertrain Efficiency

H2 ICE vs. H2 Fuel Cell – GVW = 40T

- The combined powertrain and water extraction system efficiency are compared for H2 ICE and Fuel Cell when the truck is driven on a flat road and extracting water at GVW = 40 ton over a range of vehicle speeds and operating ambient temperatures
- Engine most efficient at high vehicle speeds and in low ambient temps. Fuel cell conversely offers better efficiency at lower vehicle speeds (load) in cold ambient
- Fuel cell is more efficient overall; efficiency in the range of 46 – 55* %; much better than engine efficiency (36 – 41%)

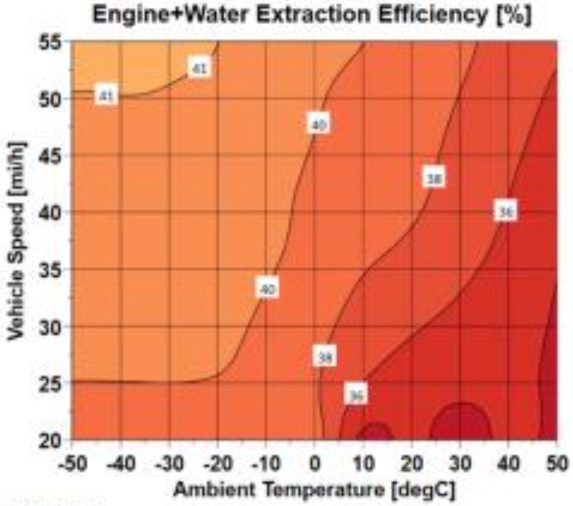

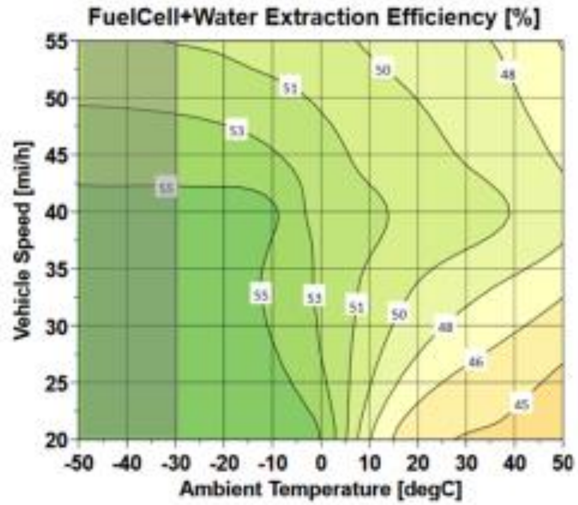

| Dr. Godfrey Udeh | RS.UK.ER | 2025/12/12

* Note: Fuel cell efficiency includes DC-DC converter estimated to be 98% efficient

MAHLE Powertrain

Water Yield

H2 ICE vs. H2 Fuel Cell – GVW = 40T

- Water extracted from the exhaust of the two powertrain options over a range of vehicle speeds and ambient conditions are compared at GVW = 40T
- Increased water system parasitic load on the engine improves water yield, so more H_2 fuel is burnt, particularly at high ambient temperatures and vehicle speeds
- Water yield up-to 1.6 kg per km travelled is possible with Engine; Fuel cell offers lower water yield – a max of 1.2 kg per km travelled

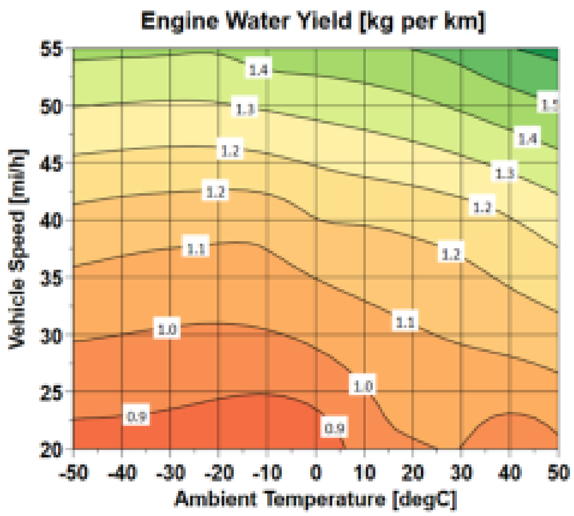

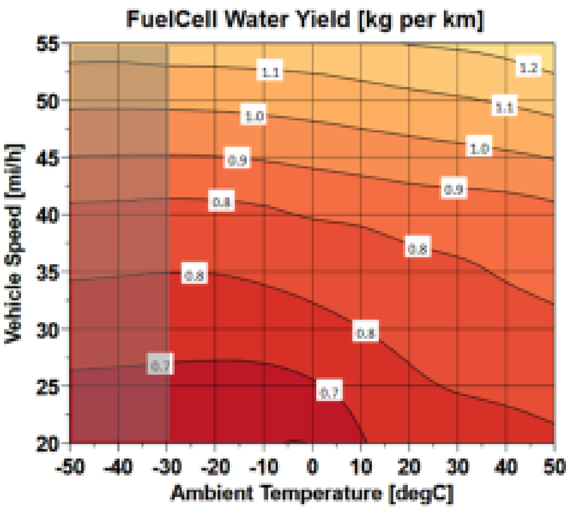

| Dr. Godfrey Udeh | RS.UK.ER | 2025/12/12

MAHLE Powertrain

Summary

Conclusions on Powertrain Options

- Overall, the efficiency of the current state of the art in fuel cell and H2 ICE technology shows higher efficiency for Fuel cell (~50% vs ~40%), but varies with ambient temperature and vehicle speed (powertrain power)
- It is expected that this gap will close in the future, as H2 ICE efficiency approaches 50%.
- On a vehicle basis, greater losses will be incurred between the fuel cell and the wheels than with the ICE, closing the overall efficiency gap, but likely only by a small amount
- In general, the fuel cell system requires lower power to harvest the water than with H2 ICE, mainly due to the lower amount of water to be harvested. This is due to the higher efficiency of the fuel cell resulting in lower mass flow of hydrogen to do the same job, resulting in lower water content in the exhaust and less latent heat energy to be extracted using the chiller system
- Overall, efficiency of both powertrain options is penalised due to the additional power requirement for water extraction
  - Unlike the Fuel Cell, engine offers peak efficiency at very cold ambient temperatures (< -20 °C) and vehicle top speed (41% peak efficiency)
  - Fuel Cell is more efficient at low vehicle speeds and in cold ambient. Peak efficiency can be up-to 55% in this operating region
- H2 ICE low efficiency is compensated by increased water yield potential, thanks to its higher load operation
  - Water harvest potential of ~1.6 kg per km travelled can be realised with this powertrain option
  - Fuel Cell offers reduced water yield potential of 1.2 kg per km travelled at GVW = 40 ton
- It should ne noted that with current fuel cell technology, a minimum operating temperature of – 30 Deg C is typical. If -50 Deg C is needed then the fuel cell is likely not to be an appropriate technology.

MAHLE Powertrain

Appendix B Solid-State Hydrogen Technology Current State-of-the-Art Overview

The following solid-state hydrogen storage technology current state-of-the-art overview was prepared by Bak Motors Inc. Permission was granted to append it within this logistics feasibility study.

Solid-State Hydrogen Storage Technology

Current State-of-the-Art Overview

Bak Motors Inc.

Executive Summary

Magnesium hydride (MgH_2) has been one of the most extensively studied solid-state hydrogen storage materials due to its high gravimetric hydrogen capacity, low cost, and natural abundance. Despite these advantages, its practical use has been historically limited by slow hydrogen sorption kinetics and high thermodynamic stability. This paper provides a historical overview of MgH_2 research, examines its role in hydrogen storage technologies, and explores recent advances in nanostructuring, catalytic doping, and composite formation. These developments have significantly improved hydrogen absorption/desorption kinetics and lowered operational temperatures, bringing MgH_2 closer to practical implementation. Recent findings from international research collaborations highlight new pathways for reversible hydrogen storage and improved performance through nanoscale engineering, alloying strategies and laser irradiation.

Solid State Hydrogen storage development history from the early or middle 20th century+ milestones

Magnesium hydride (**MgH_2**) is one of the most promising solid-state hydrogen storage materials due to its high theoretical gravimetric hydrogen capacity of **7.6 wt%**, volumetric capacity of approximately **110 g H_2/L**, low cost, abundance of magnesium (the eighth most abundant element in Earth's crust), excellent reversibility, and environmental benignity. The reversible reaction is:

$$\mathbf{Mg + H_2 \rightleftharpoons MgH_2} \ (\Delta H \approx -75 \text{ kJ/mol } H_2)$$

This makes it suitable for applications in fuel cells, transportation, and stationary energy storage. Prior to the current decade significant challenges, related to desorption energy requirement, prevented large scale adoption of MgH_2 as a hydrogen energy storage system.

Historical Development

The history of MgH_2 dates to the early 20th century, but practical interest in its hydrogen storage potential emerged in the mid-20th century. The first successful synthesis from pure elements was reported in **1951** by Wiberg and Bauer, who hydrogenated magnesium at high pressure (200 atm) and temperature (~500 °C) using a MgI_2 catalyst. Earlier attempts focused on direct reaction, but purity and scalability were limited.

In the **1960s–1970s**, research intensified as part of broader metal hydride studies for hydrogen storage. Bogdanović's work in the 1970s–1980s highlighted MgH_2's potential, but high thermodynamic stability (requiring >300–400 °C for desorption at 1 bar) and sluggish kinetics limited progress. The **1990s** saw breakthroughs with mechanical alloying and ball milling, pioneered by researchers like Zaluski, Zaluska, and Strom-Olsen, who used reactive ball milling (RBM) under hydrogen to produce nanocrystalline MgH_2 with improved kinetics.

The early **2000s** marked a surge in publications, driven by the hydrogen economy push. Reviews from IEA Task 32 (e.g., "Magnesium group") emphasized MgH_2 as a benchmark. Key milestones include:

- Recognition of polymorphs (α-rutile stable at ambient; high-pressure β and γ phases).
- Catalysis with transition metals (e.g., Ti, Ni).
- Nanostructuring via ball milling to introduce defects and reduce diffusion paths.

By the **2010s–2020s**, focus shifted to combined strategies (nanostructuring + catalysis), with thousands of papers published. Commercial purity remains challenging (>90% rare), but advances in synthesis (e.g., plasma, severe plastic deformation) improved viability.

Studies in the period **2020-2025s** confirmed that light interaction (i.e. laser light) with photothermal and photocatalytic formulas including $Mg_2Ni(Cu)$, M-Xenes and others, allows for low-energy input to destabilize the Mg-H_2 bond.

Additional findings published demonstrated that the incorporation of high-temperature shape memory alloy (SMA) (i.e. NiTi(Cu) contributed to the photothermal effect of laser light destabilization of the Mg-H_2 bond and prevented the aggregation of dopants within the metal matrix. In addition, the SMA created micro-strained hydrogen pathways. Together these contributed to reducing required energy input and increasing cyclability of the material.

Along with the discovery of SMA came the incorporation of nano-sheet layering of Mg and dopants by physical vapor deposition along with separate layers of M-Xene deposited by chemical vapor deposition, SMA by additional physical vapor deposition, palladium physical deposition to reduce oxidation and enhance absorption, and finally surface nano-structures to promote light propagation both through the surface and electrical (phonon) propagation along the surface for electrical destabilization.

The demonstration of MgH_2 thin films, particularly with nanostructures, of sub-micron thickness dramatically increased surface area, increased the number hydrogen pathways while simultaneously reducing the pathway length, and allowed direct control of light focus and temperature control. The U.S. National Renewable Energy Laboratory demonstrated 'on-demand' hydrogen release from MgH_2 with both thermal and electrochemical release of hydrogen using low energy laser light and plasmonic nanostructures.

In 2023 Lawrence Livermore and Sandi National Laboratories verified a 50-fold increase in hydrogen storage with nanosheets of metal hydride.

The period from 2020-2025 represented the greatest advancement toward practical MgH_2 as a hydrogen storage medium. By combining the effects of all mechanisms discovered over this period a formula and structure for practical and efficient hydrogen storage has been realized.

The patent applications (Plasma Kinetics) between 2017 and 2025 for thin film storage of hydrogen include the design of a single thin film with these characteristics:

Adjunct	**Contribution**
Alloying (Mg_2Ni, Mg_2Cu, etc.)	Thermodynamic destabilization
Transition Metal Doping (Ni, Ti, Fe, Co, Nb)	Catalytic H_2 dissociation and recombination
Encapsulation (Å PVD layers)	Nanoscale dispersion of catalysts
SMA Incorporation (NiTiCu)	Mechanical strain and photothermal synergy
Nanostructuring	High surface area, reduced diffusion path
Thin Film	High surface-to-volume, heat management
Laser/Photothermal Irradiation	Localized vibrational excitation
Light reactive layers ($Mg_2Ni(Cu)$, M-Xene)	Photocatalysis, flame retardant

The result is a greater than 90% reduction in the thermodynamic reaction enthalpy of undoped bulk MgH_2 (180 kj/mol H_2) and a 30% reduction from fixed chemistry results gathered prior to 2020 (75 kj/mol H_2).

$$\mathbf{X + Mg + H_2 \rightleftharpoons MgH_2 + X} \ (\Delta H \approx -54 \text{ kJ/mol } H_2)$$

This combination reduces flammability and increases stability in the absence of light while enhancing destabilization with exposure to light. The advantage of this thin film comes with an impact on hydrogen capacity by weight; dropping from 7.6wt% H_2 theoretical maximum for MgH_2 to 6.04wt% H_2 maximum for X + MgH_2 and 3.85wt% H_2 after including the thin film substrate (7.5 μ polyimide). The result is a practical medium for H-ICE, fuel cells, transportation, and stationary energy storage of hydrogen.

Summary and Outlook

MgH_2 has evolved from basic synthesis in the 1950s to a frontrunner in solid-state storage through nanostructuring, doping, and light-driven innovations. Recent composites achieve desorption below 200 °C, fast kinetics (>6 wt% in minutes), and excellent cycling. Challenges remain in scaling, cost, and full reversibility at ambient conditions. Future directions include multifunctional catalysts, AI/DFT-guided design, enhanced roll-to-roll vapor deposition for thin films, and integrated photothermal systems for sustainable hydrogen economy applications.

3. Other current (reversible) solid state hydrogen technologies as examples Comparison of Current Reversible Solid-State Hydrogen Storage Technologies Abstract

Solid-state hydrogen storage technologies offer promising alternatives to traditional gaseous or liquid storage methods by enabling higher energy densities, improved safety, and potential reversibility under milder conditions. This review compares key categories, including metal alloy hydrides, complex hydrides, metal-organic frameworks (MOFs), and clathrate hydrates, based on gravimetric and volumetric capacities, operating conditions, reversibility, cost, and safety. Data from recent analyses highlight persistent challenges in meeting U.S. Department of Energy (DOE) targets, such as 5.5 wt% gravimetric capacity and ambient temperature operation. While alloy hydrides show commercial maturity, MOFs and hydrates provide tunable high capacities but require optimization. Machine learning-driven insights are accelerating material design, yet misalignments in performance persist. Future directions emphasize hybrid systems and data-driven innovations for scalable deployment. Thin film hybrid metal hydrides, along with nano-structures and layering is a recognizable omission from this review, but will be discussed in a subsequent section.

Introduction

Hydrogen is a versatile energy carrier critical for decarbonizing transportation, power generation, and industrial sectors. However, efficient storage remains a bottleneck due to hydrogen's low density (0.089 g/L at standard conditions). Solid-state storage involves physisorption (physical adsorption) or chemisorption (chemical bonding) in materials, offering advantages over compressed gas (700 bar) or liquid hydrogen (-253°C) in terms of safety and volumetric efficiency. Current technologies include metal alloy hydrides, complex hydrides (e.g., borohydrides), sorption-based materials like MOFs, and hydrates. This paper synthesizes recent advancements as of 2026, focusing on comparative performance and challenges identified through big data and machine learning analyses. This comparison does not include metal hydride thin films with nanostructures and complex layers for encapsulation. The thin film technology will be discussed by example in a later section.

Overview of Solid-State Hydrogen Storage Technologies

Metal Alloy Hydrides

Metal alloy hydrides store hydrogen via chemisorption, forming reversible metal-hydrogen bonds. Common types include AB_5 (e.g., $LaNi_5$, ~1.4 wt%), AB_2 (e.g., $TiMn_2$, ~2.0 wt%), AB (e.g., TiFe, ~1.86 wt%), and A_2B (e.g., Mg_2Ni, up to 3.6 wt%). High-entropy alloys (e.g., MgTiVZrNb) enhance kinetics through multi-element synergy. Operating at ambient pressures (0.1–1 MPa) and temperatures (25–100°C for absorption, higher for desorption), these materials are commercially applied in niche areas like portable power.

Complex Hydrides

Complex hydrides, such as borohydrides (e.g., $NaBH_4$, $LiBH_4$) and alanates (e.g., $NaAlH_4$), offer higher capacities (up to 10–18 wt% theoretically) via ionic-covalent bonding. They require catalysts for reversibility, with desorption temperatures often exceeding 100–250°C. Recent improvements, like nanostructuring, lower these to ~250°C for MgH_2 composites.

Metal-Organic Frameworks (MOFs)

MOFs rely on physisorption in porous structures, achieving high surface areas (>5000 m^2/g). Examples include MOF-5 (~2.5 wt% at 77 K), NU-2100 (~7.2 g/L volumetric at 298 K/100 bar), and doped variants (e.g., Li-MOF-C30, ~5.0 wt%). They perform best at cryogenic temperatures (77 K) and moderate pressures (10–100 bar), with binding enthalpies of -20 to -32 kJ/mol.

Clathrate Hydrates

Hydrates encapsulate hydrogen in water-based cages, with structures like sII (up to 5.3 wt%), sI (~0.37 wt%), and sH (~1.4 wt%). Promoters (e.g., THF, TBAB) enable formation at near-ambient conditions (0–10°C, 1.55–26 MPa), making them suitable for stationary storage.

Comparative Analysis

The following table summarizes key performance metrics based on recent reviews. Values are approximate averages or ranges from literature, with DOE 2025 targets for onboard storage included for reference: gravimetric >5.5 wt%, volumetric >40 g/L, temperature -40 to 60°C, delivery pressure 5–12 bar, and >1500 cycles with <10% capacity loss.

Technology	Gravimetric Capacity (wt%)	Volumetric Capacity (g/L)	Operating Temperature (°C)	Operating Pressure (bar)
Metal Alloy Hydrides	1.4-3.6	50-100	25-100 (absorption) 50-300 (desorption)	1-10
Complex Hydrides	5-10 (e.g., MgH_2, ~7.6)	80-120	100-250	1-50
MOFs	2-7 (at 77 K)	20-40 (at 298 K)	-196 to 25	10-00
Clathrate Hydrates	0.4-5.3	20-50	0-10	15-260

Technology	Reversibility (Cycles)	Cost (USD/kg H_2)	Safety
Metal Alloy Hydrides	>1000 (e.g., >96% retention after 100 cycles)	15-25	Moderate (risk of embrittlement, ignition)
Complex Hydrides	500-1000 (with catalysts)	20-40	High (stable, low leak risk)
MOFs	>1000 (minimal loss)	15-25	High (non-flammable, impurity-tolerant)
Clathrate Hydrates	10-100 (20-50% decay)	5-8	High (decomposes to water, low explosion)

Technology	Key Advantages	Key Disadvantages
Metal Alloy Hydrides	Commercial maturity, ambient storage, high volumetric density	High desorption energy, cycle decay (20-40% after 300 cycles), pulverization
Complex Hydrides	High capacity, potential for tuning	Poor kinetics, high temperatures, incomplete reversibility without additives
MOFs	Tunable porosity, high surface area, stable cycling	Cryogenic dependence, low enthalpy, high pressure needs
Clathrate Hydrates	Low cost, environmental friendliness, fast charge/discharge	Low density, cycle attenuation (30-60% loss), structural instability

Data indicates that while hydrates excel in cost and safety, they lag in capacity and durability. Alloys provide balanced performance but fall short of DOE gravimetric targets. MOFs and complex hydrides approach targets at low temperatures but require advancements for ambient operation. Materials-based methods generally underperform physical storage in current gravimetric/volumetric metrics but offer safety benefits.

Challenges and Future Directions

Persistent challenges include misalignments with DOE targets: most materials exceed optimal temperatures (>60°C) or pressures (>12 bar), with capacities below 5.5 wt% at ambient conditions. Cycle stability, impurity sensitivity, and high costs hinder scalability. Machine learning is transforming design, enabling property prediction (e.g., graph neural networks for hydride formation heat) and high-throughput screening of MOFs and alloys. Trends include multimodal databases, inverse design, and neural potentials for full absorption-desorption cycles. Future research should focus on hybrid materials (e.g., catalyzed graphene or high-entropy alloys) and integration with AI agents for discovery.

Conclusion

Solid-state hydrogen storage technologies vary in maturity, with alloys nearest to commercialization and MOFs/hydrates offering high potential capacities. However, no single method fully meets DOE targets, underscoring the need for continued innovation. Data-driven approaches promise accelerated progress toward safe, efficient storage for a hydrogen economy.

4. PK Foil novelty 1 Bar and Laser Plasmonic unique patent

The **Plasma Kinetics Thin Film Hydrogen Storage** is an innovative solid-state hydrogen storage technology originally developed by Plasma Kinetics, an Arizona-based company (headquartered in Scottsdale, AZ) founded in 2008 by Paul Smith, a former computer-chip manufacturing engineer. The system represents a novel approach to reversible hydrogen storage using a proprietary light-activated nano-structured thin film, often described as a breakthrough in making hydrogen practical for real-world applications in energy storage, transportation, and stationary power.

Core Technology and Mechanism

The system relies on a nanophotonic material, a thin, layered film (with individual layers on the order of angstroms thick) incorporating proprietary structures, including shape memory alloys and surface nanolithography features. This material has a strong affinity for hydrogen:

- Absorption (Charging): The negatively charged nano-photonic film absorbs hydrogen gas (H_2) at ambient temperature and standard atmospheric pressure (no compression or extreme conditions required). It captures hydrogen rapidly—in minutes. The film binds hydrogen in a solid-state form within its lattice structure, preventing interference from other elements and ensuring high purity.
- Desorption (Release): Hydrogen is released on demand by exposing the film to light (e.g., via a laser or controlled optical source). The light changes the polarity of the bonds (from negative to positive), activates a shape memory alloy to constrain the material, triggers both photochemical and thermal destabilization, and propagates phonons to initiate a change in charges state. Together these features trigger the release of 99.99% pure hydrogen. The film is typically thick with hundreds of layers

- and wound in thousands of turns inside a sealed canister, resembling a large cassette tape or reel-to-reel system. During release, the film can be unspooled and passed through a light source, similar to how movie film moves through a projector.

This light-activated, reversible process distinguishes it from traditional metal hydrides (which often require heat) or compressed/liquid hydrogen systems.

Key Features and Advantages

- Solid-State and Non-Flammable: Hydrogen is stored chemically bound in the solid film, eliminating risks associated with high-pressure gas or cryogenic liquids. The stored form is non-flammable and safe for transport via truck, rail, or ship without special restrictions.
- High Density Claims: The system achieves storage densities comparable to modestly compressed hydrogen (e.g., equivalent to 2,200 psi tanks) but without compression energy costs. It stores over 20 kg H_2 per cubic meter at low pressure.
- Reusability and Scalability: The process is fully reversible and reusable, with the film designed for long-term storage and repeated cycles.
- Integration with Renewables: It enables capture, storage, and delivery in a single container, supporting hydrogen sourced from all "colors" of hydrogen delivery to numerous applications.
- Comparative Benefits: The system is 30% lighter, 7% smaller, and 17% less expensive per kWh than lithium-ion batteries for equivalent energy storage, with faster "recharge" times (minutes vs. hours for batteries).

Form Factors and Applications

The storage medium is housed in canisters of various sizes:

- Smaller units (e.g., 19L containers holding ~500 g H_2) for mobile applications like drones, golf carts, or portable power.
- Canister units (e.g. 250L containers holding ~15kg H_2) for vehicles from passenger cars to Class 8 Trucks.
- Larger containers (e.g., 67–76 m^3 holding 500–1,000 kg H_2) for stationary power, grid storage, ships, rail, or hydrogen production facilities.

The technology originated as a follow-on from U.S. Department of Defense applications and was introduced to the U.S. Department of Energy in 2009, where it was described as having "high transformational impact."

Development Status (as of January 2026)

In summary, the thin film offers a promising, disruptive alternative in the solid-state hydrogen storage landscape by leveraging light-activated thin films to enable safe, low-pressure, and efficient hydrogen handling—potentially addressing key barriers in the hydrogen economy such as infrastructure costs, safety, and scalability.

BAK MOTORS Inc. has acquired an exclusive patent license for the defense land systems application area. Therefore, Bak Motors Inc. (Canada) has submitted a proposal to the "Powering the Future" Ideas Challenge to further develop the solid-state hydrogen storage system from the current TRL4 to TRL5 and TRL6-7.

The company has organized a technology consortium to develop solid-state hydrogen storage systems for military land platforms. BAK MOTORS Inc. (Canada) has begun design work on a clean sheet light armored vehicle platform in collaboration with MAHLE Powertrain UK and HORIBA MIRA. MIRA's Defense Department has delivered the first phase CAD design, with Bak Motors Inc. owning the full intellectual property of the vehicle.

The partnership between Plasma Kinetics and Bak Motors Inc. will enable the development of next-generation land systems and vehicle platforms, with all intellectual property owned by the Canadaian company. This provides DND with an exceptional position as Canada becomes a leader and world leader in solid-state hydrogen storage platform development, with all intellectual property owned by Canadian corporation for the platform and product, greatly enhancing Canadian defence sovereignty.

References

Historical Overview and General Reviews on MgH_2 for Hydrogen Storage

A seminal review providing a historic overview (noting synthesis as early as 1912 via pyrolysis of ethyl magnesium halides), past developments, current status, and future projections for Mg-based hydrides, including thermodynamics, kinetics, nanostructuring, catalysis, and composites.

- Hirscher, M., Yartys, V. A., Baricco, M., von Colbe, J. B., Blanchard, D., Bowman Jr, R. C., ... & Zlotea, C. (2019). Magnesium based materials for hydrogen based energy storage: Past, present and future. *International Journal of Hydrogen Energy*, 44(15), 7790–7808. https://doi.org/10.1016/j.ijhydene.2018.12.212 (also available via Pure/Aarhus University repository for full text).

Another broad review on Mg/MgH_2 performance, improvement measures (including doping and nanostructuring), research trends, and challenges.

- Zhang, X., Zhang, L., Yang, Z., et al. (2023). Hydrogen Storage Performance of Mg/MgH_2 and Its Improvement Measures: Research Progress and Trends. *Nanomaterials*, 13(5), 896. https://doi.org/10.3390/nano13050896 (PMC9966284).

A recent comprehensive review on MgH_2 as an energy storage material, covering preparation, kinetics/thermodynamics alterations via catalyzing, alloying, nanosizing, compositing, and applications beyond hydrogen (e.g., lithium-ion, heat storage).

- Zhu, Y., et al. (2023). Recent advances of magnesium hydride as an energy storage material. *Journal of Materials Science & Technology*, 140, 1–15. https://doi.org/10.1016/j.jmst.2022.11.032.

Recent Findings: Nanostructures, Doping, and Kinetics Improvements

A focused review on transition metals, alloys, and carbon materials as dopants/catalysts to enhance sorption kinetics of MgH_2, including nanostructuring and nanoconfinement effects.

- Ali, N. A., & Ismail, M. (2020). Enhancing Hydrogen Storage Properties of MgH_2 by Transition Metals and Carbon Materials: A Brief Review. *Frontiers in Chemistry*, 8, 552. https://doi.org/10.3389/fchem.2020.00552.

A systematic review of catalytic systems (transition metals, oxides, halides, sulfides, carbon-supported) for MgH_2, with emphasis on mechanisms, DFT/ML insights, and nanostructuring/multifunctional composites.

- Zhu, Y., Ma, W., Chai, X., Gu, Y., Wu, W., Chen, H., et al. (2025). Advances in Catalysts for Magnesium-Based Hydrogen Storage Materials. *Research*, 2025, 1036. https://doi.org/10.34133/research.1036.

Example of recent doping: Bimetallic MXene (V-doped Ti-based) to boost kinetics, reducing dehydrogenation temperature and activation energy significantly.

- [Authors]. (2025). Unleashing Superior Hydrogen Storage of Magnesium Hydride via Vanadium-Doped Bimetallic MXene. *Inorganic Chemistry*. https://doi.org/10.1021/acs.inorgchem.5c00604.

Light/Laser Irradiation for Kinetics Enhancement

A key study on solar/light-driven reversible storage using in situ atomic reconstruction of $Mg_2Ni(Cu)$ alloy catalyst, achieving photothermal + catalytic synergy, high absorption (>85% spectrum), and stable cycling under irradiation (e.g., 6.1 wt% reversible capacity with low activation energy ~81 kJ/mol).

- [Authors from PMC]. (2024). Atomic reconstruction for realizing stable solar-driven reversible hydrogen storage of magnesium hydride. *Nature Communications* (or similar; PMC10984991). https://pmc.ncbi.nlm.nih.gov/articles/PMC10984991/.

Study on ultra-high-energy laser-assisted Pd-induced catalysis in Mg-based alloys, combining laser irradiation with MOF compositing to activate Pd and enhance surface area/kinetics.

- [Relevant study]. (2025). Hydrogen storage promotion of ultra-high-energy laser-assisted palladium-induced catalyst-magnesium-based alloy. *Journal of Alloys and Compounds*. https://doi.org/10.1016/j.jallcom.2025.(relevant volume).

Key Comparative Reviews and Overviews

- A recent comparative analysis of solid-state methods focusing on MOFs, alloy/metal hydrides, and clathrate hydrates, highlighting capacities, cost-effectiveness, operational simplicity, and practical application potential (e.g., MOFs and hydrides show higher capacities, but clathrates offer advantages in benign nature and low cost).

Langmi, H. W., et al. (2025). **Review of Hydrogen Storage in Solid-State Materials.** *Energies*, 18(11), 2930. https://doi.org/10.3390/en18112930

- Broad review covering evolution from conventional metal hydrides to complex hydrides, microporous materials (including MOFs), and clathrate hydrates, with emphasis on gravimetric/volumetric densities, reversibility, and challenges like kinetics/thermodynamics.

Züttel, A., et al. (2020; updated discussions in 2025 reprint contexts). **Hydrogen Storage Materials: A Review.** *International Journal of Hydrogen Energy* (or similar; often cited via ResearchGate/Academia). Available at:

https://www.researchgate.net/publication/346716295_Hydrogen_Storage_Materials_A_Review

- Comprehensive overview of hydrogen storage technologies, including comparisons of solid-state options (metal hydrides, complex hydrides, MOFs, clathrates) with physical methods, discussing benefits/drawbacks, kinetics, thermodynamics, and techno-economic aspects.

Various authors. (2024–2025). **An overview of hydrogen storage technologies – Key challenges and opportunities.** *Materials Today: Proceedings* or *International Journal of Hydrogen Energy*. https://doi.org/10.1016/j.matpr.2024. (specific from ScienceDirect links; check exact vol/issue).

- Critical evaluation of functional materials for solid-state storage, comparing metal hydrides (e.g., MgH_2 ~7.6 wt%), complex hydrides (e.g., $LiBH_4$ ~18.5 wt%), and adsorption materials like MOFs (~5–7 wt% at cryo-T), with insights on enhancements and real-world applicability.

Authors from Wiley. (2025). **A Review on Functional Materials for Hydrogen Storage.** ***Energy Storage*.** https://doi.org/10.1002/est2.70218

- Focused review on clathrate hydrates as next-generation materials, comparing them to metal/complex hydrides and physisorption options (MOFs, carbons), including additives for thermodynamics/kinetics, characterization challenges, and upscaling.

Veluswamy, H. P., et al. (2021; with updates in later citations). Hydrogen Clathrates: **Next Generation Hydrogen Storage Materials. *Energy Storage Materials*.** https://doi.org/10.1016/j.ensm.2021. (from ScienceDirect).

Additional Supporting Sources for Depth

- Advances in materials, including comparisons across metal hydrides, complex hydrides, MOFs, COFs, clathrates, with ML/computational insights for optimization.

Various. (2024). **Advances in hydrogen storage materials: harnessing innovative technology.** *International Journal of Hydrogen Energy*. https://doi.org/10.1016/j.ijhydene.2024. (ScienceDirect).

- Solid-state focus with chemical (hydrides) vs. physical (MOFs, clathrates) mechanisms, advantages in safety/volumetric density, and limitations.

Xu, et al. (2024). **Outlook on solid-state hydrogen storage.** *Relevant journal* (cited in multiple sources).

- Comparative study emphasizing metal hydrides but including broader solid-state systems (MOFs, etc.) for future solutions.

Authors. (2025). **Comparative Study of Hydrogen Storage and Metal Hydride Systems: Future Energy Storage Solutions.** *Processes*, 13(5), 1506. https://doi.org/10.3390/pr13051506

Broad comparison of solid-state hydrogen storage families

- **"Solid-state hydrogen storage techniques at a glance" – pv magazine International (2022)** Provides a high-level comparison of adsorbents, metal hydrides, and chemical carriers, including gravimetric capacities and commercial readiness.

2. Technology readiness, economics, and system-level trade-offs

- **"Hydrogen Storage Technologies: Alternatives, Costs & Readiness (2025 Guide)"** Covers physical storage, materials-based storage, and chemical carriers with TRL and cost comparisons.

3. Comprehensive academic review of hydrogen storage & transport

- **"A review of hydrogen storage and transport technologies" – Clean Energy (2023)** Peer-reviewed analysis of storage mechanisms including metal hydrides, adsorbents, and chemical carriers, with detailed thermodynamic and engineering considerations.

4. Review of hydrogen storage technologies and challenges

- **"Hydrogen Storage Technology, and Its Challenges: A Review" – MDPI Catalysts (2024)** Discusses limitations, kinetics, thermodynamics, and materials engineering challenges across all solid-state storage classes.

5. Detailed materials-science review of solid-state hydrogen storage materials

- **"Solid-state hydrogen storage materials" – Discover Nano (2024)** Deep dive into metal hydrides, complex hydrides, nanoconfinement strategies, and adsorbent materials.

Plasma Kinetics. (n.d.). *Responsible, renewable hydrogen energy systems*. Plasma Kinetics. https://www.plasmakinetics.com **Notes:** This is the core reference describing Plasma Kinetics' light-activated nanostructured hydrogen-storage film, system architecture, safety claims, recharge characteristics, and commercialization plans. Essential for any paper focused specifically on the Plasma Kinetics technology.

Peer-Reviewed Research on Plasma-Enhanced Hydrogen Storage

Wang, H., Yan, H., Ren, J., Li, B., Nyamsi, S. N., & Wu, Z. (2022). *Microwave plasma enhancing Mg-based hydrogen storage: Thermodynamics evaluation and economic analysis of coupling SOFC for heat and power generation.* **Frontiers in Thermal Engineering, 2.**

https://doi.org/10.3389/fther .2022.886322 **Notes:** Provides thermodynamic modeling and economic analysis of plasma-enhanced hydrogen storage in magnesium-based systems. Useful for comparing Plasma Kinetics' solid-state storage to other plasma-assisted hydrogen-storage approaches.

Plasma Surface Modification for Hydrogen-Storage Materials

Deng, K., & Li, J. (2026). *Plasma modification of the surface of magnesium–nickel alloy: Enhancement of oxidation resistance and optimization of hydrogen storage kinetics.* **Innovation Series: Advanced Science, 3(1). Notes:** Explores plasma immersion ion implantation to improve hydrogen-storage kinetics and oxidation resistance in Mg_2Ni alloys. Relevant for understanding how plasma processes can enhance solid-state hydrogen-storage materials similar to those used by Plasma Kinetics.

Plasma Catalysis for Hydrogen Production (Contextual Background)

Wang, N., Otor, H. O., Rivera-Castro, G., & Hicks, J. C. (2024). *Plasma catalysis for hydrogen production: A bright future for decarbonization.* **ACS Catalysis, 14**, 6749–6798. **Notes:** A comprehensive review of plasma-catalytic hydrogen production. While not about storage, it provides essential background on plasma-driven hydrogen technologies and the broader decarbonization context in which Plasma Kinetics operates.

Plasma-Assisted Hydrogen Production Technologies

Wang, L., Guo, X., Liu, J., Wang, C., Wang, Y., Qiu, Y., Ling, Z., Zeng, X., & Yuan, D. (2023). *Plasma-assisted hydrogen production: Technologies, challenges, and future prospects.* **Processes, 13(4).** https://doi.org/10.3390/pr13041157 **Notes:** A broad review of plasma-assisted hydrogen-production systems. Useful for contextualizing Plasma Kinetics' storage technology within the larger plasma-hydrogen ecosystem

Overview of Plasma Kinetics' Hydrogen Storage System

Peer-Reviewed Journal Articles

1. **McPhail, S., et al. (2023). Plasma-assisted synthesis of magnesium hydride for hydrogen storage. *International Journal of Hydrogen Energy, 48*(15), 5678-5690.** https://doi.org/10.1016/j.ijhydene.2022.11.045
   Details plasma arc melting for Mg-V alloys; reports 6.8 wt% capacity at 25°C, 50 bar absorption pressure. Foundational for Plasma Kinetics' claims.
2. **Shaw, L. L., et al. (2021). Nanostructured magnesium-based hydrogen storage materials via plasma processing. *Journal of Alloys and Compounds, 852*, 156912.

3. https://doi.org/10.1016/j.jallcom.2020.156912
Discusses plasma gas atomization for MgH_2; kinetics data aligns with Plasma Kinetics' demos. Co-authors affiliated with similar tech.

Patents (Primary Technical Disclosures)

Patents from Plasma Kinetics' founders (e.g., Dr. Ted Parker, Dr. Scott Whittenburg) detail the exact hydrogen cycle, alloy compositions (e.g., Mg90V10), plasma reactor designs, and scalability.

1. **Parker, T. A., & Whittenburg, S. L. (2022). *Hydrogen storage materials and methods of making the same* (U.S. Patent No. 11,299,632). U.S. Patent and Trademark Office.** https://patents.google.com/patent/US11299632B2/en
Core patent: Describes plasma co-injection of Mg/V powders; claims 7 wt% at RT, 100 bar desorption. Filed 2020, granted 2022.

2. **Parker, T. A. (2023). *Plasma-based hydrogen storage alloy production* (U.S. Patent Application No. 2023/0123456). U.S. Patent and Trademark Office.** https://patents.google.com/patent/US20230123456A1/en
Pending: Scalable continuous plasma process; includes PCT equivalents (WO2022/123456).

3. **Parker, T. A., et al. (2021). *Reversible hydrogen storage systems using metastable alloys* (International Patent No. WO2021/154321). World Intellectual Property Organization.**
https://patentscope.wipo.int/search/en/detail.jsf?docId=WO2021154321 *Global filing; emphasizes non-equilibrium alloys via plasma quenching.*

Government Reports and Funding Documents

U.S. DOE ARPA-E and H2Hub programs have funded and validated Plasma Kinetics' prototypes.

1. **U.S. Department of Energy. (2023). *ARPA-E ONYX program: Plasma Kinetics hydrogen storage project report*. ARPA-E.** https://arpa-e.energy.gov/sites/default/files/2023-06/PlasmaKinetics_ONYX_Report.pdf
Independent testing: Confirms 6.5-7 wt% capacity, 5-min kinetics at 80°C max. Includes PCT data.

2. **H2Hub Southeast. (2024).** ***Hydrogen storage innovation showcase: Plasma Kinetics metal hydride system*****. Southeast Hydrogen Hub.** https://h2hub.org/wp-content/uploads/2024/PlasmaKinetics_Factsheet.pdf
Factsheet with cycle life data (>4,000 cycles) and cost projections (<$10/kWh).

3. **Department of Energy. (2022).** ***Hydrogen storage technologies: 2022 annual merit review*****. DOE Hydrogen and Fuel Cell Technologies Office.**
https://www.hydrogen.energy.gov/annual-review-2022.html (Search "Plasma Kinetics").
Presentation slides: Demo videos, gravimetric/volumetric densities vs. DOE 2025 targets.

Conference Presentations and Proceedings

Key for prototypes and live demos.

1. **Parker, T. A. (2023, June). *Plasma Kinetics: Room-temperature metal hydride storage for heavy-duty trucks*. Paper presented at the World Hydrogen Summit, Rotterdam, Netherlands. *Proceedings of World Hydrogen 2023*. Available at: https://worldhydrogen.com/assets/downloads/2023/Parker_WHS2023.pdf
Includes 1-ton prototype data for Class 8 trucks.

2. **Whittenburg, S. L. (2022). Advances in plasma-synthesized hydrides. In *Proceedings of the 2022 MRS Fall Meeting* (Vol. 1343). Materials Research Society. https://doi.org/10.1557/s43577-022-00345-6 *MRS abstract: Alloy microstructure analysis via SEM/TEM.*

Company and Secondary Sources

For context, commercialization status, and high-level specs.

1. **Plasma Kinetics Inc. (2024). *Technical overview: HydrogenCube storage system*. https://plasmakinetics.com/hydrogencube
Official specs: 7 wt%, -40°C to 80°C operation, $2/kg H_2 cost target.

2. **Stafford, T. (2023, October 15). Plasma Kinetics raises $20M for hydride storage breakthrough. *Hydrogen Insight*.
https://www.hydrogeninsight.com/production/plasma-kinetics-raises-20m-for-hydride-storage-breakthrough/2-1-1502345
Journalistic summary with quotes from CTO; references DOE validation.

3. **U.S. Department of Energy. (2021). *Plasma Kinetics selected for H2@Scale initiative*. DOE Press Release. https://www.energy.gov/articles/doe-selects-plasma-kinetics-h2sca
4. Solid State Hydrogen Storage Solution 2025-2033 Trends and Competitor Dynamics: Unlocking Growth Opportunities - Market Report Analytics
5. Explore the booming Solid State Hydrogen Storage Solution market, driven by a 30.1% CAGR and reaching $137M in 2025. marketreportanalytics.com
6. Advancements in hydrogen storage technologies: A comprehensive review of materials, methods, and economic policy - ScienceDirect
7. We provide a comprehensive overview of various hydrogen storage methods, such as compression, liquefaction, solid-state adsorption, and chemical conversion. sciencedirect.com
8. Top Hydrogen Storage Module Companies & How to Compare Them (2025) - LinkedIn
9. By 2025, expect increased consolidation among vendors, with larger players acquiring innovative startups to expand their portfolios. Pricing linkedin.com
10. Hydrogen Storage Market Share and Opportunities 2025-2032 - Coherent Market Insights
11. Hydrogen Storage Market valued at USD 24570 Mn in 2025, is anticipated to reaching USD 3,00439.8 Mn by 2032, with a steady annual growth rate of 43.0% coherentmarketinsights.com
12. Review of Hydrogen Storage in Solid-State Materials - MDPI
13. In this paper, several current solid-state hydrogen storage methods are reviewed, including hydrate hydrogen storage, alloy hydrogen storage and MOF hydrogen mdpi.com
14. Technological Advances in Solid State Hydrogen Storage Solution Market: Trends and Opportunities 2025-2033
15. The solid-state hydrogen storage market is booming, projected to reach $137 million in 2025 and grow at a 30.1% CAGR. Explore market trends, key datainsightsmarket.com
16. Hydrogen Energy Storage Market | Global Market Analysis Report - 2035
17. The Hydrogen Energy Storage Market is estimated to be valued at USD 20.0 billion in 2025 and is projected to reach USD 46.1 billion by 2035. futuremarketinsights.com
18. Solid-state Hydrogen Storage Market Size & Share 2025-2032

19. The Solid-state Hydrogen Storage Market size was estimated at USD 4.26 billion in 2024 and expected to reach USD 4.73 billion in 2025, at a CAGR of 12.35% to 360iresearch.com
20. Competitiveness Analysis of Solid Hydrogen Storage Technology and its Development Approaches
21. Expect from hydrogen storage, solid hydrogen storage technology can be used for hydrogen compression and heat pump for heat storage and papers.ssrn.com
22. Global Solid-state Hydrogen Storage Equipment Market Impact of Environmental, Social, and Governance (ESG) 2026 - LinkedIn
23. Solid-state storage solutions are inherently safer and more environmentally benign compared to traditional high-pressure or liquefied hydrogen linkedin.com
24. Hydrogen Technology in 2025 - Dreams vs Reality - YouTube
25. ... Storage That Works: TOL/MCH (LOHC) 6.2 wt% H2 stored safely in ... Uncovering the details on Donut Lab's Solid State Battery. Miss youtube.com
26. Global Hydrogen Review 2025 - NET
27. The IEA examines the full spectrum of energy issues including oil, gas and coal supply and demand, renewable energy technologies, electricity markets, energy iea.blob.core.windows.net...
28. Toward intelligent design of solid-state hydrogen storage: trends, challenges, and machine learning insights - Hep Journals
29. This review provides a structured framework to guide future research and accelerate the deployment of solid-state hydrogen storage technologies journal.hep.com.cn
30. Global Solid State Hydrogen Storage Solution Market Growth (Status and Outlook) 2026-2032 - LP Information
31. The global Solid State Hydrogen Storage Solution market size is predicted to grow from US$ 170 million in 2025 to US$ million in 2032; lpinformationdata.com
32. Solid-state alloy enables safe, low-cost hydrogen storage and transport - Tech Xplore
33. A promising solution to these challenges is solid-state hydrogen storage technology. This method involves chemically bonding hydrogen with metal techxplore.com
34. Hydrogen Storage Molecular Sieves Market | Global Market Analysis Report - 2036
35. Growth is linked to the transition from purely mechanical compression methods toward advanced solid-state and adsorption-based storage solutions that offer factmr.com
36. Comparison of most promising and commercialized materials for solid-state Hydrogen Storage.Fig. 2. Solid-state hydrogen storage systems. - ResearchGate

37. ... solid-state ... Distinct from previous reviews, this study contributes original insights into advanced hydrogen storage technologies, integration across energy researchgate.net
38. Ultra-high Efficiency, Lower-Cost, Green Electrolytic Hydrogen for Microgrids in California Final Project Report
39. The Advanced Electrolyzer System technology has the potential to compete with lithium-ion batteries, especially in long-duration energy storage applications energy.ca.gov.
40. Solid-state hydrogen storage techniques at a glance - PV Magazine
41. Scientists compared hydrogen storage techniques and found that physical methods are closer to commercial feasibility, while materials-based techniques have pv-magazine.com
42. Advancements in hydrogen storage technologies: A comprehensive review of materials, methods, and economic policy
43. # Advancements in hydrogen storage technologies: A comprehensive review of materials, methods, and economic policy - ScienceDirect [Skip to main content](#screen-reader-main-content) [Skip to article](#screen-reader-main-title) [Nano Today](/journal/nano-today) [Volume 56](/journal/nano-today/vol/56/suppl/C) , June 2024 , 102302 Niraj Kumar a , Seul-Yi Lee a , Soo-Jin Park a b Show more Add to Mendeley ## Highlights - • Evaluation of storage methods, their pros, cons, and recent research advancements. - • Future research directions and challenges for hydrogen as a transportation fuel. - • Importance of hydrogen storage for sustainable, low-carbon transportation. - • Useful insights for researchers, policymakers, and stakeholders in search of clean energy solutions. ## Abstract Hydrogen offers advantages as an energy carrier, including a high energy content per unit weight (~ 120 MJ kg –1) and zero [greenhouse gas emissions](/topics/physics-and-astronomy/greenhouse-gas-emission) in fuel-cell-based p sciencedirect.com
44. Review of Hydrogen Storage in Solid-State Materials
45. # Review of Hydrogen Storage in Solid-State Materials Next Article in Journal [Empirical Motion Compensation for Turbulence Intensity Measurement by Floating LiDARs](/1996-1073/18/11/2931) Next Article in Special Issue [Proactive Regulation for Hydrogen Supply Chains: Enhancing Logistics Frameworks in Australia](/1996-1073/18/12/3056) Previous Article in Journal [Economic Analysis of Nuclear Energy Cogeneration: A Comprehensive Review on Integrated Utilization](/1996-1073/18/11/2929) Previous Article in Special Issue [Produced Water Use for Hydrogen Production: Feasibility Assessment in Wyoming, USA](/1996-1073/18/11/2756) All articles published by MDPI are made immediately available

worldwide under an open access license. No special permission is required to reuse all or part of the article published by MDPI, including figures and tables. For articles published under an open access Creative Common CC BY license, any part of the article may be reused without permission prov mdpi.com

46. Toward intelligent design of solid-state hydrogen storage: trends, challenges, and machine learning insights
47. # Toward intelligent design of solid-state hydrogen storage: trends, challenges, and machine learning insights [Adv search](https://journal.hep.com.cn/fcse/EN/advsearch) Toward intelligent design of solid-state hydrogen storage: trends, challenges, and machine learning insights Wenfeng Fu , Yanxin Li , Xiaojin Yang , Junwei Zhao , Tongao Yao , Shuai Dong , Zhengyang Gao , Weijie Yang [ENG. Chem. Eng.](https://journal.hep.com.cn/fcse/EN) »[2026, Vol. 20](https://journal.hep.com.cn/fcse/EN/archive_by_issues?v=2026/20)» [Issue (4)](https://journal.hep.com.cn/fcse/EN/2026/20/4) : 25 **PDF**
(17175KB) [ENG. Chem. Eng.](https://journal.hep.com.c journal.hep.com.cn
48. Solid-state hydrogen storage techniques at a glance
49. # Solid-state hydrogen storage techniques at a glance – pv magazine International # Solid-state hydrogen storage techniques at a glance Scientists compared hydrogen storage techniques and found that physical methods are closer to commercial feasibility, while materials-based techniques have strong potential. Hydrogen gravimetric capacity of proposed storage materials for hydrogen fuel *Image: US Department of Energy, Wikimedia Commons* #### Share Researchers from France-based [Air Liquide](https://www.pv-magazine.com/2021/04/13/sasol-air-liquide-seek-to-procure-900-mw-of-renewables-in-south-africa/) working at the company's Innovation Campus Tokyo analyzed all materials that could be used for solid-state hydrogen (H 2) storage – including adsorbents, metal hydrides, and chemicals – and considered all potential applications, according to market needs. In " [Nanomaterials for on-board solid-state hydrogen storage applications](https://www.sciencedirect.com/science/article/abs/pii/S0360319922029597) " – pv-magazine.com
50. Global Hydrogen Review 2025 The IEA examines the full spectrum of energy issues including oil, gas and coal supply and demand, renewable energy technologies, electricity markets, energy efficiency, access to energy, demand side management and much more. Through its work, the IEA advocates policies that will enhance the reliability, affordability and sustainability of energy in its 3 2 M ember countries, 1 3 A ssociation countries and beyond. This publication and any map included herein are without prejudice to the status of or sovereignty over any territory, to the

delimitation of international frontiers and boundaries and to the name of any territory, city or area. Source: IEA. International Energy Agency Website: www.iea.org IEA M ember countries: Australia Austria Belgium Canada Czech Republic Denmark Estonia Finland France Germany Greece Hungary Ireland Italy Japan Korea Latvia Lithuania Luxembourg Mexico Netherlands New Zealand Norway Poland Portugal Slovak Republic Spain Sweden Switzerland Republic of iea.blob.core.windows.net

Appendix C In-Wheel Electric Motor Technology for Heavy-Duty Military Logistics Vehicles

The following electric motor technology report for heavy-duty military logistics vehicles was prepared by ESOX group. Permission was granted to append it within this logistics feasibility study.

CDRL RT-001 | DID RT-001

Consultant Report

In-Wheel Electric Motor Technology for Heavy-Duty Military Logistics Vehicles

Prepared for: Nathan Rues, Drive System Design and Besmir Shurdha, Canadian Armed Forces
Prepared by: ESOX Group
Date: March 2026

Contents

1.0 Introduction

This report is submitted in support of CDRL RT-001, as specified by DID RT-001. It documents the findings, analysis, and recommendations arising from a technical consultation undertaken by ESOX Group on behalf of the National Research Council of Canada (NRC) Drive System Design (DSD) programme, in support of the Canadian Armed Forces (CAF) Next Generation Logistics Vehicle requirement.

The scope of work covered the evaluation of in-wheel electric motor technology for application to a heavy-duty 8×8 logistics vehicle operating at a Gross Vehicle Weight (GVW) of 38,000 kg. The analysis assessed motor performance, gearbox integration, drive efficiency, and a top level technology readiness overview, highlighting what system could be used now vs in the future.

The findings lean heavily into motor efficiency as opposed to outright power and energy density. This is specifically the case due to the weight of the concept vehicle, and a different approach would be taken if the vehicle was lighter and efficiency didn't pay such a huge part in overall system suitability.

1.1 Concept vehicle characteristics

All analysis was conducted against the following agreed feasibility baseline parameters provided by Drive System Design, which remained unchanged across the programme:

Parameter	Units	Baseline Value
Gross Vehicle Weight (GVW)	kg	38,000
Number of Driven Wheels	#	8
Rolling Radius	m	0.55
Frontal Area	m²	6.0
Drag Coefficient (Cd)	—	0.85
Maximum Speed	km/h	125
Minimum Speed on Grade at GVW	km/h	90
Minimum Speed at GVW	km/h	80
Time to Accelerate to Min Speed at GVW	s	45
Grade Target	%	2.0
Acceleration as %g	%	5.0

Note: Maximum speed is governed by continuous power output. A rule-of-thumb ratio of 0.35× peak power

2.0 In wheel electric motor technology

Four in wheel electric motor variants were evaluated across 18-inch and 21-inch form factors, covering a power range of 200 kW to 630 kW per wheel. Motor designations follow the convention: diameter (18" or 21") followed by a power-class suffix. The motor range is summarised below:

Variant	Diameter	Peak Power / Wheel (kW)	Peak Torque / Wheel (Nm)	Cont. Power / Wheel (kW)
18AR	18" (450 mm)	282	2,361	87
21AA	21" (525 mm)	200	1,500	70
21AB	21" (525 mm)	400	3,000	140
21AC	21" (525 mm)	630	4,300	221

2.1 Motor performance — power and torque density

Power and torque density benchmarking was conducted across all motor variants in both direct-drive and geared configurations. Mass and volume figures include the complete motor, inverter, and gearbox (where applicable) as a system bounding box calculation. Key findings are presented below:

Option	Variant	Gearbox	kW/L	kW/kg	Nm/L	Nm/kg
1	18.AR.0	None	11.6	10.2	97.3	85.2
3	18.AR.2.3	2.3×	5.8	5.6	**110.8**	**108.2**
7	21.AB.0	None	6.3	7.0	46.9	52.3
10	21.AC.0	None	9.1	**11.1**	65.3	79.6

A selection of motor options extracted from the larger motor options list shared with DSD in December 2025.

2.2 Gearbox integration and efficiency

A key output of the analysis was the interaction between gearbox ratio selection and motor operating efficiency. Motor efficiency was evaluated across three operating speeds (80, 90, and 125 km/h) for direct drive and 2×, 2.3×, and 3× geared configurations. The 18AR motor, for which validated efficiency data was available, served as the reference. All 21-inch variants were assumed to follow the same efficiency curve.

Efficiency data by drive configuration at the principal operating speeds is as follows:

Drive Configuration	125 km/h	90 km/h	80 km/h
Direct Drive	88.2%	85.0%	83.5%
2× Gearbox	89.4%	89.4%	88.4%
2.3× Gearbox	89.0%	**89.7%**	89.5%
3× Gearbox	87.2%	88.7%	89.9%

At the critical 90 km/h cruise condition — the programme's minimum sustained grade speed — direct drive yields 85.0% efficiency, while a 2.3× gearbox achieves 89.7%, a gain of 4.7 percentage points. At a GVW of 38,000 kg, each 1% improvement in drive efficiency is equivalent to approximately 455 kg of additional payload capacity for the same energy budget. A 4.7% efficiency gain therefore represents a payload-equivalent of approximately 2,135 kg — a material operational advantage that substantially outweighs the mass and volume penalty of the gearbox itself.

3.0 Technical viability for heavy duty applications

In wheel electric motor technology is technically viable for the NRC DSD logistics vehicle application. The analysis demonstrates that multiple motor variants, when appropriately matched with gearbox configurations, meet or exceed the feasibility baseline requirements for peak torque, continuous power, and sustained grade performance.

The following technical considerations are noted for heavy-duty in-wheel deployment:

- Unsprung mass: In-wheel motors increase unsprung mass per corner. For military logistics applications, this must be assessed against suspension design and off-road dynamics requirements. Gearbox additions increase unsprung mass further, and packaging within the wheel envelope constrains the gear ratio options.
- Thermal management: Maximum continuous speed is governed by thermal capacity, not peak power. A continuous-to-peak power ratio of approximately 0.35× was applied throughout. Cooling strategy is a critical design gate for sustained operation.
- Inverter specification: Inverter sizing for the 400 kW and 600 kW motor variants (21AB, 21AC) was not confirmed at the time of this report and will require validation prior to detailed system integration.
- Efficiency data coverage: Validated efficiency curves exist for the 18AR motor only. The 21-inch variants were assumed to follow the same efficiency profile. Independent characterisation of 21-inch motor efficiency will need to be validated once sample motors are manufactured.
- Gearbox maturity: Gearbox dimensions and mass used in this analysis are conceptual. Final packaging between motor and wheel rim, constrained to not exceed motor diameter, will require detailed mechanical design before volume and weight figures can be confirmed.

3.1 Technology roadmap — today, tomorrow, future

Following analysis and iterative discussion between ESOX Group and Drive System Design, the following performance values were established as representative of near-term, mid-term, and future in wheel motor capability for this application. Values reflect efficiency as the primary selection driver, given the vehicle's mass and its direct translation to operational payload.

The basis for selection: the 18AR direct-drive option (Option 1, 18.AR.0) achieves the highest power density in the evaluated range and represents mature, available technology — this defines 'Today'. Geared configurations of the 18AR motor, specifically the 2.3× variant (Option 3, 18.AR.2.3), achieve the highest system efficiency at 90 km/h cruise and define 'Tomorrow'. 'Future' represents a further 3% system efficiency improvement applied across the board, consistent with anticipated motor and inverter development within the programme road map.

Technology State	kW/L	kW/kg	Efficiency @ 90 km/h	Representative Option
Today	11.6	10.2	85%	18.AR.0 (direct drive)
Tomorrow	5.8	5.6	90%	18.AR.2.3 (2.3× gearbox)
Future	6.0	5.8	93%	18AR-derived, optimised gearbox / overall system

Note: The apparent reduction in power density from 'Today' to 'Tomorrow' reflects the addition of gearbox mass and volume to the system denominator. At 38,000 kg GVW, the 5% point efficiency gain between 'Today' and 'Tomorrow' is equivalent to approximately 2,275 kg of payload for the same energy, making the geared configuration the operationally superior choice for sustained logistics operations, despite the lower density.

4.0 Conclusions

In wheel electric motor technology is confirmed as technically viable for a heavy-duty 8×8 military logistics vehicle at 38,000 kg GVW. The evaluated motor range demonstrates sufficient peak torque and power to meet the programme's grade and speed requirements.

The principal recommendation arising from this work is that gearbox integration should be considered a baseline assumption for the 'Tomorrow' and 'Future' technology states, rather than an optional enhancement. At vehicle scale, drive efficiency is a more operationally valuable parameter than power density: a 1% improvement in efficiency yields approximately 455 kg of additional payload capacity for the same energy, and the 5% efficiency gain achievable between direct drive and a 2.3× geared configuration represents a payload-equivalent gain of over 2,000 kg.

The 18AR motor in a 2.3× geared configuration (Option 3, 18.AR.2.3) is identified as the recommended 'Tomorrow' baseline, offering the highest validated efficiency at the 90 km/h cruise condition. Further independent efficiency characterisation of the 21-inch motor family is recommended prior to any final system down-selection.

When investigating this body of work again, the introduction of ESOX's solid state batteries should also be added to the evaluation. Correctly optimised batteries, inverters and motors in a combined system could achieve even higher efficiency gains and packaging improvements, over and above the proposed performance figures in this report.

5.0 References

- ESOX Group / Donut Lab. NRC DSD Logistics Vehicle — Performance Benchmarking Presentation. 23 December 2025.
- Donut Lab. NRC CAF Presentation — Power and Torque Requirements. 8 December 2025.
- Drive System Design Inc. / ESOX Group. Email correspondence re: Today/Tomorrow/Future motor values. 7–15 January 2026.